ISSN 0003–26

ANALYTICA CHIMICA ACTA

International monthly devoted to all branches of analytical chemistry
Revue mensuelle internationale consacrée à tous les domaines de la chimie analytique
Internationale Monatsschrift für alle Gebiete der analytischen Chemie

ELSEVIER SCIENTIFIC PUBLISHING COMPANY

AMSTERDAM

Anal. Chim. Acta, Vol. 85, 219–432, September 1976

Published monthly

Completing Volume 85

ANALYTICA CHIMICA ACTA

Publication Schedule for 1976

Vol. 81, No. 1	January 1976	
Vol. 81, No. 2	February 1976	**(completing Vol. 81)**
Vol. 82, No. 1	March 1976	
Vol. 82, No. 2	April 1976	**(completing Vol. 82)**
Vol. 83	May 1976	**(complete in one issue)**
Vol. 84, No. 1	June 1976	
Vol. 84, No. 2	July 1976	**(completing Vol. 84)**
Vol. 85, No. 1	August 1976	
Vol. 85, No. 2	September 1976	**(completing Vol. 85)**
Vol. 86	October 1976	**(complete in one issue)**
Vol. 87, No. 1	November 1976	
Vol. 87, No. 2	December 1976	**(completing Vol. 87)**

Subscription price for 1976 (covering November '75/December '76, Vols 80–87): Dfl. 840.00 plus Dfl. 96.00 postage. Subscribers in the U.S.A. and Canada receive their copies by airmail. Additional charges for airmail to other countries are available on request. For advertising rates apply to the publishers.

Subscriptions should be sent to:
Elsevier Scientific Publishing Company, P.O. Box 211, Amsterdam, The Netherlands.

GENERAL INFORMATION

Languages

Papers will be published in English, French or German.

Detailed information

Authors should consult Vol. 73, p. 435 for detailed instructions. Reprints of this information are obtainable from Dr. Macdonald or from: Elsevier Editorial Services Ltd., Mayfield House, 256 Banbury Road, Oxford (Great Britain)

Submission of papers

Papers should be sent to:

Prof. Philip W. West,
Coates Chemical Laboratories,
College of Chemistry and Physics,
Louisiana State University,
Baton Rouge 3,
La. 70803 (U.S.A.)

or to:

Dr. A.M.G. Macdonald,
Department of Chemistry,
The University,
P.O. Box 363
Birmingham B15 2TT (Great Britain)

Reprints

Fifty reprints will be supplied free of charge. Additional reprints (minimum 100) can be ordered at quoted prices. They must be ordered on order forms which are sent together with the proofs.

Chromatography of Steroids

by E. HEFTMANN

JOURNAL OF CHROMATOGRAPHY LIBRARY, Vol. 8

1976. about 225 pages
US $34.75/Dfl. 90.00
ISBN 0-444-41441-X

Written by one of the pioneers in the field, this is the only complete and up-to-date book on steroid chromatography currently available.
Although some theory is included, it is mainly a laboratory handbook, arranged according to the steroids analyzed as well as according to the methods used. The subject index, along with extensive tables of *R* values and a list of requisite chemicals, permits the reader to select appropriate procedures, many of which are described in detail. The bibliography covers 1200 of the most important articles published on this subject since 1964.

CONTENTS: 1. Introduction. 2. Liquid column chromatography. 3. Paper and thin-layer chromatography. 4. Gas chromatography. 5. Relations between structure and chromatographic mobility. 6. Sterols. 7. Bile acids and alcohols. 8. Estrogens. 9. Androstane derivatives. 10. Pregnane derivatives. 11. Corticosteroids. 12. Miscellaneous steroid hormones. 13. Vitamins D. 14. Molting hormones. 15. Steroid sapogenins and alkaloids. 16. Cardenolides and bufadienolides. Subject index.

ELSEVIER SCIENTIFIC PUBLISHING COMPANY
P.O. Box 211, Amsterdam,
The Netherlands

Distributor in the U.S.A. and Canada:
ELSEVIER/NORTH-HOLLAND, INC.,
52 Vanderbilt Ave., New York, N.Y. 10017

The Dutch guilder price is definitive.
US $ prices are subject to exchange rate fluctuations.

9E

Chemical Derivatization in Liquid Chromatography

by J.F. LAWRENCE *and* R.W. FREI

JOURNAL OF CHROMATOGRAPHY LIBRARY, Vol. 7

1976 viii + 214 pages
US $34.50/Dfl. 90.00
ISBN 0-444-41429-0

This book is intended for all investigators concerned with the use of physical separation techniques for solving complex analytical problems. It is the first publication to provide a comprehensive account of modern derivatization in liquid chromatography with special emphasis on the practical aspects. Many examples are given in sufficient detail to permit the worker to reproduce a method without resorting to the original literature. Thus, the book will be particularly useful on the bench top of the laboratory, as well as in practically-oriented courses.

CONTENTS: INTRODUCTION: Pre-separation techniques. Post-separation techniques. BACKGROUND: Chromatographic principles. Spectrometry. Direct measurements from solid surfaces. Further reading. INSTRUMENTATION: TLC equipment. HPLC equipment. Further reading. APPLICATIONS: UV-visible derivatization. Fluorimetric derivatization. Radiochemical derivatization. Derivatization and mass spectrometry. Subject index.

ELSEVIER SCIENTIFIC PUBLISHING COMPANY
P.O. Box 211, Amsterdam,
The Netherlands

Distributor in the U.S.A. and Canada:
ELSEVIER/NORTH-HOLLAND INC.,
52 Vanderbilt Ave., New York., N.Y. 10017

The Dutch guilder price is definitive.
US $ prices are subject to exchange rate fluctuations.

The Science of the Total Environment

an international journal for scientific research into the environment and its relationship with man

Editors: **E.I. HAMILTON,** Plymouth, England
J.L. MONKMAN, Ottawa, Canada
P.W. WEST, Baton Rouge, La., U.S.A.

Since The Science of the Total Environment was established in 1972, it has been accepted with increasing interest by scientists concerned with environmental problems. As a result, it has grown from a quarterly to a bi-monthly journal. Although the scope of the journal is broad, particular emphasis is given to those topics involving environmental chemistry.

1976 - Volumes 5 and 6
Subscription price: US $67.95/Dfl. 170.00 (including postage).
Please address your request for specimen copies to: Dr. A.B. Dempster, P.O. Box 330, Amsterdam, The Netherlands

A selection of publications:

The carcinogenicity of Dieldrin
S.S. Epstein (Cleveland, Ohio, U.S.A.)

Detailed evaluation of three chemiluminescent ozone monitors
W.J. Findlay, G. Dowd and N. Quickert (Ottawa, Canada)

Some recent thinking on the future carbonate system of the sea
P. Moller and P.P. Parekh (Berlin, G.F.R.)

Environmental and food contamination with PCB's in Japan
K. Fujiwara (Kyoto, Japan)

Sulfuric acid aerosol
V. Dharmarajan, R.L. Thomas, R.F. Maddalone and P.W. West (Baton Rouge, La., U.S.A.)

Experimental data and critical review of the occurrence of hexachlorobenzene in the Italian environment
V. Leoni and S.U. D'Arca (Rome, Italy)

Reactions in the aqueous environment of low molecular weight organic molecules
M.C. Goldberg (Denver, Colo., U.S.A.)

The chemical elements and environmental chemistry - Strategies and tactics
E.I. Hamilton (Plymouth, England)

The inhibition of photochemical smog. V. Products of the diethylhydroxylamine inhibited reaction
L. Stockburger, B.K.T. Sie and J. Heicklen (University Park, Pa., U.S.A.)

Trace element concentrations in higher fungi
A.R. Byrne, L. Kosta and V. Ravnik (Ljubljana, Yugoslavia)

Journals are automatically sent by air to the U.S.A. and Canada at no extra cost, and to Japan. Australia and New Zealand with a small additional postal charge

ELSEVIER SCIENTIFIC PUBLISHING COMPANY
P.O. Box 211, Amsterdam, The Netherlands
The Dutch guilder price is definitive. US $ prices are subject to exchange rate fluctuations.

5351E

Isotachophoresis

Theory, Instrumentation and Applications

by F.M. EVERAERTS, J.L. BECKERS *and* TH. P.E.M. VERHEGGEN.

JOURNAL OF CHROMATOGRAPHY LIBRARY, Vol. 6

1976 xiv + 418 pages
US $61.50/Dfl. 160.00
ISBN 0-444-41430-4

This book is the only text currently available providing full information on the new separation technique known as Isotachophoresis, which competes with liquid and gas chromatography. All kinds of ionic materials can be separated and several classes of components can be analysed in quick succession as a proper rinsing of the equipment is all that is needed between separations. The various chapters of the book can be referred to more or less independently by scientists interested in fundamental aspects, by researchers intending to construct an instrument and by workers mainly concerned with analytical aspects.

CONTENTS: 1. Historical review. THEORY: 2. Principles of electrophoretic techniques. 3. Concept of mobility. 4. Mathematical model for isotachophoresis. 5. Choice of electrolyte systems. INSTRUMENTATION: 6. Detection systems. 7. Instrumentation. APPLICATIONS: 8. Introduction. 9. Practical aspects. 10. Quantitative aspects. 11. Separation of cationic species in aqueous solutions. 12. Separation of anionic species in aqueous solutions. 13. Amino acids, peptides and proteins. 14. Separation of nucleotides in aqueous systems. 15. Enzymatic reactions. 16. Separations in non-aqueous systems. 17. Counter flow of electrolyte. APPENDICES: A. Simplified model of moving-boundary electrophoresis for the measurement of effective mobilities. B. Diameter of the narrow-bore tube, applied for separation. C. Literature. Symbols and abbreviations. Subject index.

ELSEVIER SCIENTIFIC PUBLISHING COMPANY
P.O. Box 211, Amsterdam,
The Netherlands

Distributor in the U.S.A. and Canada
ELSEVIER/NORTH-HOLLAND, INC.,
52 Vanderbilt Ave., New York, N.Y. 10017

The Dutch guilder price is definitive.
US $ prices are subject to exchange rate fluctuations.

7E

Instrumental Liquid Chromatography

A practical manual on high-performance liquid chromatographic methods

by **N.A. PARRIS**

JOURNAL OF CHROMATOGRAPHY LIBRARY, Vol. 5.

1976 x+329 pages. US $38.50/Dfl. 100.00
ISBN 0-444-41427-4

Available texts on liquid chromatography have tended to emphasize the developments in the theoretical understanding of the technique and methodology or to list numerous applications, complete with experimental details. The present work is intended to bridge the gap between these two treatments by providing, with the minimum of theory, a practical guide to the use of the technique for the development of separations. The material is based largely on practical experience and high-lights details which may have important operational value for laboratory workers. Information regarding the usefulness of available equipment and column packings is given, together with chapters devoted to the methodology of each separation method. Applications of liquid chromatography are described with reference to the potential of the technique for qualitative, quantitative and trace analysis as well as for preparative applications. Numerous applications from the literature are tabulated and cross-referenced to sections concerned with the optimisation procedures of the particular methods. In addition, many of the figures have been drawn from hitherto unpublished work. Although written primarily for workers currently involved with the application or the development of liquid chromatographic methods, the book will also be of value to those who seek to establish whether methods for their particular interests have been reported or seem feasible.

ELSEVIER SCIENTIFIC PUBLISHING COMPANY
P.O. Box 211, Amsterdam,
The Netherlands

Distributor in the U.S.A. and Canada:
ELSEVIER/NORTH-HOLLAND INC.,
52 Vanderbilt Ave., New York., N.Y. 10017

The Dutch guilder price is definitive.
US $ prices are subject to exchange rate fluctuations.

1933 E

Analytica Chimica Acta, 85 (1976) 219—230

THE SPECTROPHOTOMETRIC DETERMINATION OF ARSENIC IN SEA WATER, POTABLE WATER AND EFFLUENTS

M. G. HAYWOOD and J. P. RILEY

Department of Oceanography, The University, P.O. Box 147, Liverpool L69 3BX (England)

(Received 16th March 1976)

SUMMARY

Procedures are described for the determination of arsenic in sea water, potable waters and effluents. The sample is treated with sodium borohydride added at a controlled rate. The arsine evolved is absorbed in a solution of iodine and the resultant arsenate ion is determined photometrically by a molybdenum blue method. The time required for a complete analysis is about 90 min, but of this only 15 min is operator time. For sea water the range, standard deviation, and detection limit are 1—4 $\mu g\, l^{-1}$, 1.4 % and 0.14 $\mu g\, l^{-1}$, respectively; for potable waters they are 0—800 $\mu g\, l^{-1}$, about 1 % (at 20 $\mu g\, l^{-1}$ level) and 0.5 $\mu g\, l^{-1}$, respectively. Silver and copper cause serious interference at levels of 0.5 $mg\, l^{-1}$, and nickel, cadmium and bismuth interfere at concentrations of a few tens of $mg\, l^{-1}$; however, these elements can be removed either by preliminary extraction with a solution of dithizone in chloroform or by ion exchange. Arsenic present in organo-arsenic compounds is not directly determinable, but can be rendered reactive either by photolysis with ultraviolet radiation or by oxidation with permanganate or nitric—sulphuric acid mixture. Arsenic(V) can be determined separately from total inorganic arsenic after extracting arsenic(III) as its pyrrolidine dithiocarbamate into chloroform.

The very low concentration of arsenic in sea water renders its determination difficult. Although most workers prefer to preconcentrate arsenic before determining it, Johnson [1] and Johnson and Pilson [2] have described a direct photometric molybdenum blue method for its determination in which correction must be applied for the usually dominant effect of phosphate. Preconcentration methods have included coprecipitation with iron(III) hydroxide [3—5], co-crystallization with thionalide [6, 7] and evolution as arsine, for which most early workers used the Gutzeit method [8—10]; however, this technique is not satisfactory for the determination of low levels of arsenic as arsenic cannot be evolved quantitatively, and it is also difficult to obtain sufficiently low reagent blanks. Sodium borohydride has many advantages over zinc and mineral acid for the reduction to arsine, and has been employed by several workers (usually in conjunction with atomic absorption spectrometry) [11—19]. Its advantages include the greatly increased speed and efficiency of arsine evolution and the very low reagent blank obtainable. Equipment is now available commercially in which the arsine evolved is collected in a reservoir and subsequently decomposed, atomized and determined

by atomic absorption spectrometry. However, experience with such a unit showed that reproducibility was generally poor (± 10—15 %, see also Caldwell et al. [20]) and that the sensitivity was nearly an order of magnitude too poor for the analysis of sea water.

The only workers who appear to have applied the borohydride reduction technique to sea water are Braman et al. [13], who carried out the subsequent determination by discharge emission spectrometry. However, the levels of arsenic found (in samples from Tampa Bay, Florida) were an order of magnitude greater than those currently accepted for sea water and the precision of their data was not indicated. An examination of the data in the literature suggested that neither emission nor atomic absorption spectrometry has sufficient sensitivity to allow evolved arsenic to be determined with adequate precision at its normal level in sea water (1—2 $\mu g\ l^{-1}$). It was therefore decided to investigate the possibility of evolving arsenic with borohydride, trapping it and determining it colorimetrically, since a suitably sensitive arseno—molybdenum blue photometric procedure was available [6]. Preliminary tests showed that arsine could be absorbed quantitatively in a solution of iodine in potassium iodide; the absorbent also oxidizes the element to the pentavalent state required for colorimetry. In the published techniques for arsine evolution, the borohydride is added in one increment, either as a pellet or in solution. This leads to very rapid and short-lived hydrogen evolution, and under these conditions it proved impossible to absorb arsine quantitatively in the iodine—iodide solution. This difficulty was overcome by adding borohydride solution gradually to the acidified sample by means of a peristaltic pump; gas evolution then took place at a controlled rate and the evolution and absorption of arsine was almost quantitative (> 98.5 %). This procedure was therefore adopted for the analysis of sea water and subsequently it was adapted slightly for the examination of potable and waste waters. Although the method is somewhat slower in operation than the evolution—atomic absorption spectrometric technique, it may be of value to laboratories which require greater precision, or which lack the specialized a.a.s. equipment needed.

EXPERIMENTAL

Apparatus

The apparatus used for the evolution of arsine is shown diagrammatically in Fig. 1. Sodium borohydride solution was delivered from the reservoir (A) via a manifold (B) to a Watson—Marlow Type HR peristaltic pump (C) fitted with Acidflex tubing which served to inject the reagent at a controlled rate into the 250-ml evolution flask (D) mounted at an angle of ca. 35° on a stand. The evolved hydrogen, along with entrained arsine, was passed through the jet (E) (bore 0.05 mm) into the absorption tube (F) (calibrated at a volume of 2.5 ml) containing iodine solution. Multichannel operation of the peristaltic pump enabled up to 6 evolutions to be carried out simultaneously.

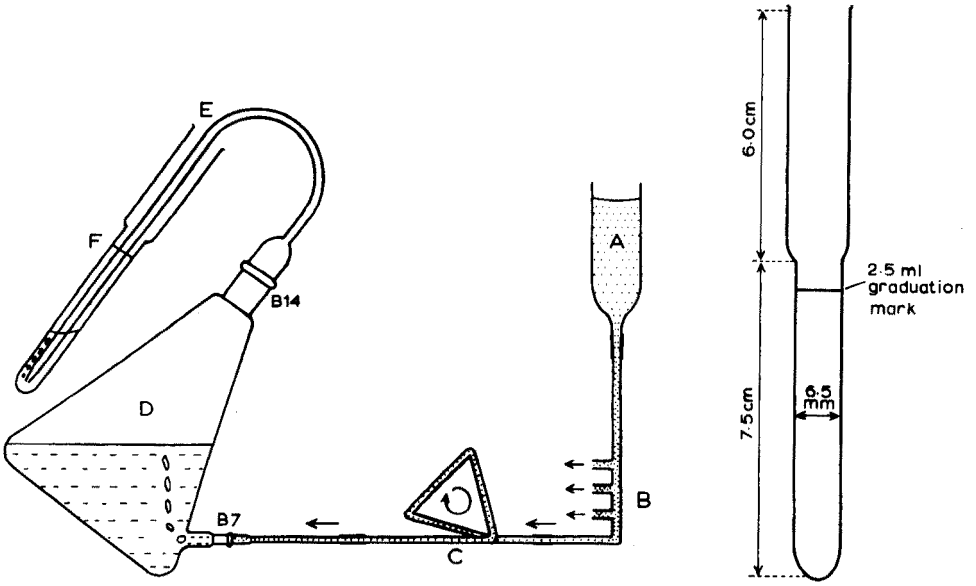

Fig. 1. Apparatus for the evolution and trapping of arsenic. The dimensions of the absorption tube F are given in the inset.

A Unicam SP 500 spectrophotometer fitted with 40-mm glass microcuvettes was used.

All glassware was cleaned initially by soaking in 18 M sulphuric acid overnight.

Reagents and standards

Sodium borohydride solution. Dissolve 25 g of powdered sodium borohydride in 100 ml of distilled water, and filter through a retentive filter paper into a conical flask. To purify the solution add 2 g of calcium hydroxide, loosely close the flask with a bulb stopper and warm to 75 °C in a water bath for 20 min; under these conditions a small proportion of the borohydride decomposes rapidly, thus removing traces of arsenic as arsine. Cool the solution to room temperature, filter through a retentive filter paper and dilute to 250 ml with water. This solution should be replaced after 2 d as it decomposes slowly.

Absorption solution. Dissolve 0.25 g of iodine in a solution of 0.4 g of potassium iodide in 5 ml of water and dilute to 100 ml with water. Store the solution in a well-stoppered bottle; it is stable indefinitely.

Ammonium molybdate solution, 4.8 % (w/v). Dissolve 4.8 g of ammonium molybdate in 60 ml of water and dilute to 100 ml with distilled water. Store

the solution in a polyethylene bottle; reject if it becomes discoloured, or if a precipitate forms.

Ascorbic acid solution, 1.76 % (w/v). Prepare in redistilled water and store at 0 °C. Reject when it becomes yellow.

Potassium antimonyl tartrate solution (1 mg Sb ml^{-1}). Use a 0.274 % (w/v) solution in distilled water.

Mixed reagent. Mix 10 ml of 2.5 M sulphuric acid, 3 ml of ammonium molybdate solution, 1.0 ml of potassium antimonyl tartrate solution and 6 ml of ascorbic acid solution. The reagent should be used within 1 h of preparation as it is unstable.

Cation-exchange column for removal of heavy metals. Digest Zerolit 225 ion-exchange resin (52—100 mesh) on a water bath at 80 °C with excess of 6 M hydrochloric acid. After 1 h pour off the acid and wash the resin several times with distilled water. Place a wad of silica wool at the bottom of a 5 cm × 0.8 cm^2 ion-exchange column and fill the column with about 5 ml of the resin. (Glass wool should not be used for supporting the resin since it tends to retain arsenic.) Convert the resin to the sodium form by passing 50 ml of 1 M sodium chloride through it. Finally, wash the column with 50 ml of distilled water. After use, the column can be regenerated by washing with 50 ml of 1 M hydrochloric acid and then reconverting to the sodium form.

Standard arsenic solution. Prepare from reagent-grade arsenic(III) oxide a stock solution containing 100 μg As ml^{-1}. Prepare working standards (0.1 μg As ml^{-1}) as required since they tend to be unstable.

Arsenic-free sea water. Purify 1 l of sea water by passing it through an ion-exchange column (i.d., 1 cm) packed with a 5-cm bed of hydrous zirconium oxide (Bio-rad HZO-1; 100-200 mesh) treated previously with 50 ml of 2 M sodium hydroxide and then washed free from alkali. After use the column can be regenerated, but as this causes some deterioration in the performance of the packing it is recommended that regeneration should not be carried out with alkali more than 10 times.

Determination of total inorganic arsenic in sea water

Place 150 ml of the filtered (0.45 μm) sea-water sample in the evolution flask and add 5 ml each of 2.5 M sulphuric acid and 2 % (w/v) EDTA (di-sodium salt) solution. Replace the flask on its stand and fit the head and delivery tube. Pipette 1.2 ml of the I_2—KI absorption solution and 0.2 ml of 4.2 % (w/v) sodium hydrogen carbonate solution into an absorption tube. Insert the delivery tube so that its jet is close to the bottom of the absorption tube. Secure the absorption tube to the flask with a rubber band. With the

peristaltic pump add sodium borohydride solution at a rate of 15 ml h^{-1}. After 1 h lower the absorption tube and rinse the tip of the delivery tube into it with 0.2—0.3 ml of water. Add 0.5 ml of mixed reagent and dilute to 2.5 ml with distilled water. Mix thoroughly, preferably in an ultrasonic bath, to release the carbon dioxide liberated from the hydrogen carbonate in the absorption solution. After 30 min, measure the absorbance of the solution at 866 nm in a 40-mm microcuvette. Determine the reagent blank in the same way but substitute 150 ml of arsenic-free sea water for the sample; the absorbance of the blank is normally about 0.025. Calibrate the method in the same manner with 150-ml aliquots of arsenic-free sea water to which 1.0 and 2.0-ml increments of standard arsenic solution have been added (corresponding to 0.1 and 0.2 μg As, respectively).

Determination of arsenic(V) in sea water

Place 150 ml of the sample in a separating funnel and add 2 ml of 2.5 M sulphuric acid and 4 ml of freshly prepared 1 % (w/v) ammonium pyrrolidine dithiocarbamate (APDC) solution. Extract the APDC—As(III) complex by shaking for 2 min with two 5-ml aliquots of chloroform. Transfer the aqueous phase to a conical flask, cover with a bulb stopper and boil gently for 20 min to decompose the excess of APDC. Cool the solution and determine arsenic(V) as described above. Carry out a blank in the same manner, but substitute 150 ml of arsenic-free sea water for the sample. Calibrate the method similarly with 150-ml aliquots of arsenic-free sea water spiked with 1.0 and 2.0-ml increments of standard arsenic solution (corresponding to 0.10 and 0.2 μg As).

Determination of total arsenic in sea water

To determine total arsenic in sea water, adjust the pH to about 6, and irradiate the sample for 2 h in a fused silica tube at ca. 60 °C at a distance of 15 cm from a 1-kW, medium-pressure, mercury lamp. After the irradiation, dilute to the original volume and continue the analysis as described above for total inorganic arsenic.

Determination of total inorganic arsenic in potable water

Place 50 ml of the filtered water sample in an evolution flask and add 5 ml of 2.5 M sulphuric acid and 5 ml of 2 % EDTA (disodium salt) solution. Continue the analysis as described for sea water with the exception that the sodium borohydride solution should be added at a rate of 10 ml h^{-1}. Determine the blank in the same way with 50 ml of distilled water instead of the sample; the absorbance of the blank is normally ca. 0.025. Calibrate the method similarly with distilled water spiked with 2 and 4-ml increments of standard arsenic solution (corresponding to 0.2 and 0.4 μg As, respectively), and then diluted to a total volume of 50 ml.

Determination of total arsenic in potable and natural waters containing less than 0.1 mg l^{-1} of heavy metals

Place 50 ml of the sample in a 250-ml conical flask and add 5 ml of 2.5 M sulphuric acid and 25 ml of aqueous 1.0 M potassium permanganate solution (0.632 % w/v). Close the flask loosely with a bulb stopper and heat on a boiling water bath for 8 h. If necessary add further permanganate solution to maintain an excess in the solution. After cooling, slowly add, with shaking, 10 % hydroxylammonium chloride solution until the permanganate colour is just discharged. Transfer the solution to an evolution flask, add 5 ml of 2 % EDTA solution, and continue the analysis as described in the previous paragraph. Carry out blank determinations and standardizations in the same manner with 50-ml aliquots of distilled water alone and spiked with 0.4 μg of arsenic, respectively.

Determination of arsenic in effluents or natural waters containing more than 0.1 mg l^{-1} of heavy metals

Place 50 ml of the sample in a polytetrafluoroethylene beaker and evaporate to about 10 ml on a hot plate. Cool and add, cautiously, 2 ml of concentrated nitric acid and 1 ml of concentrated sulphuric acid. Continue the evaporation until dense white fumes of sulphur trioxide begin to be evolved. After cooling, take up the residue in 25 ml of distilled water. When the concentration of heavy metals in the original sample exceeds 0.1 mg l^{-1} these elements must be removed before proceeding to the evolution stage; this can be achieved in two ways:

(i) Place the solution of the residue in a separatory funnel and adjust to pH 7—8 by cautious addition of 2 M ammonia solution. Extract the solution with 10 ml of a 0.05 % solution of dithizone in chloroform. If necessary, readjust to pH 7—8. Repeat the extraction with further aliquots of dithizone solution until the organic phase remains green. Wash the aqueous phase with 10 ml of chloroform and dilute it to 50.0 ml with distilled water. Reject the extracts and washings. This procedure is satisfactory up to a total heavy metal concentration of about 25 mg l^{-1}.

(ii) Alternatively, adjust the solution of the residue to pH 3.0—3.5 by careful addition of 2 M ammonia solution. Pass the solution through a column of Zerolit 225 (Na^+ form) and wash the column with four 5-ml aliquots of distilled water. Combine the percolate and washings and dilute to 50.0 ml with distilled water. This procedure can be used for a total heavy metal concentration of up to 2 g l^{-1}.

Transfer a suitable volume of the solution ($\leqslant$ 1 μg As) to an evolution flask, dilute to 50 ml with distilled water, and continue the analysis as described for the determination of inorganic arsenic in potable waters. Carry out blank determinations and calibrations through the whole procedure with 50-ml aliquots of distilled water and distilled water spiked with 0.4 μg As, respectively.

RESULTS AND DISCUSSION

Sea water

The precision of the method was tested by carrying out replicate analyses (10) on 150-ml aliquots of two sea-water samples from the Irish Sea. Average arsenic concentrations of 2.63 ± 0.05 and 2.49 ± 0.05 $\mu g\ l^{-1}$ were found; thus the average relative standard deviation was 1.4 %. Replicate (10) determinations of the reagent blank were performed with arsenic-free sea water and showed a standard deviation of ± 0.035 μg As l^{-1}; this implies a detection limit of 0.14 μg As l^{-1} if this is assumed to be four times the standard deviation. The recovery of arsenic was checked by analyzing 150-ml aliquots of arsenic-free sea water which had been spiked with known amounts of arsenic(V). The results of these experiments (Table 1) show that there is a linear relationship between absorbance and arsenic concentration and that arsenic could be recovered from sea water with an average efficiency of 98.0 % at levels of 1.3—6.6 $\mu g\ l^{-1}$. Analogous experiments in which arsenic(III) was used gave similar recoveries.

Determination of the As(III) : As(V) ratio in sea water

Although purely thermodynamic considerations suggest that arsenic should exist in oxic sea waters practically entirely in the pentavalent state, equilibrium rarely appears to be attained, probably because of the existence of biologically mediated reduction processes. For this reason, the arsenic in most of these waters exists to an appreciable extent in the trivalent state, and indeed, As(III) : As(V) ratios as high as 1:1 have been found in a number of instances [21]. It is of considerable interest to the oceanographer to study the extent to which the ratio varies in the sea and to relate this to the microbiological activity and redox potential of the water. The experimental evaluation of the ratio is a matter of difficulty. Johnson and Pilson [2] have attempted to determine it by a photometric procedure; however, since this depends on measurement of the differences between three large absorbances it lacks precision. Braman et al. [13] have claimed that they can differentiate between the two oxidation states of arsenic by its behaviour with sodium borohydride, arsenic(III) being reduced to arsine at pH 4—9, whereas arsenic(V) is not. However, we were unable to confirm this observation. We

TABLE 1

Recovery of arsenic(V) from spiked samples of arsenic-free sea water (150 ml)

As added (μg)	0.200	0.300	0.400	0.600	0.800	1.000
Absorbance per $\mu g\ l^{-1}$	0.063_6	0.063_4	0.064_3	0.063_5	0.063_0	0.063_8
As found (μg)	0.196	0.294	0.396	0.586	0.778	0.985
Recovery (%)	98.1	97.8[a]	99.1	97.9	97.2	98.5

[a]Average for 10 determinations; range 96.0—99.2 %, standard deviation ± 1.35 %.

have found that arsenic(III) can be separated from arsenic(V), even at levels of 2 $\mu g\ l^{-1}$, by extracting it as the pyrrolidine dithiocarbamate with chloroform. This technique was applied to samples of sea water spiked with As(V) and As(III) as described in the experimental section and it was found (Table 2) that arsenic(V) could be satisfactorily determined in the presence of arsenic(III).

Potable water

The relationship between absorbance and arsenic(V) concentration in distilled water medium was investigated by the method described for potable waters. A linear relationship was closely adhered to for arsenic concentrations in the range 10—800 $\mu g\ l^{-1}$; for measurements of 50—800 μg As l^{-1}, the solutions were diluted to an appropriate final volume, and the absorbances normalized. Deviation from linearity at higher arsenic concentrations almost certainly resulted from the use of insufficient absorption reagent to trap the arsine completely. In contrast to the observations of Braman et al. [13], no difference was found between the evolution behaviour of arsenic(III) and arsenic(V). The reproducibility and precision of the method was tested by performing replicate (8) analyses on 50-ml aliquots of distilled water spiked at three different levels with arsenic(V). Over the range 4—40 μg As l^{-1}, the relative standard deviation was 0.6—1.1 % and the average arsenic recovery was 98.7 % (Table 3). The detection limit of the method was assessed by making replicate (10) measurements of the reagent blank. The standard deviation (s) of these was 0.13 $\mu g\ l^{-1}$; this corresponds to a detection limit ($4s$) of 0.5 $\mu g\ l^{-1}$.

TABLE 2

Determination of arsenic(V) in sea water[a]

As^{3+} added (μg)	1.000	1.000	0.000	0.000	1.000	1.000	1.000	1.000
As^{5+} added (μg)	0.000	0.000	1.000	1.000	1.000	1.000	1.000	1.000
As found (μg)	0.018	0.015	0.979	0.985	0.990	0.980	0.976	1.032

[a]150-ml aliquots extracted with APDC in chloroform before the evolution and determination of arsenic.

TABLE 3

Replicate (8) determinations of arsenic(V) in spiked samples of distilled water

Arsenic concentration ($\mu g\ l^{-1}$)	4.0	20.0	40.0
Recovery range (%)	96.5—99.6	97.9—99.1	99.0—100.5
Average recovery (%)	98.1	98.6	99.5
Relative standard deviation (%)	1.0_5	0.5_8	0.6_1

Interferences

Smith [22] has shown that many elements (e.g. Ni, Au, Ag, Cu, platinum metals) interfere in the determination of arsenic by reduction to arsine by borohydride followed by atomic absorption using an $Ar—H_2$ flame. Belcher et al. [23] have shown that the interference of many of these elements in a similar molecular emission cavity analysis method can be eliminated by complexing them with EDTA before the evolution of arsine. However, very little information is available about the interference of other elements and substances in the evolution stage itself. For this reason, the effect of a variety of likely interfering anions, cations and organic solvents on the determination of 20 μg As l^{-1} was examined (Tables 4 and 5). Alkali and alkaline earth elements, chloride and sulphate were not included in this investigation since they caused no interference at their normal concentrations in sea water.

The survey showed that no significant interference was produced by up to 250 mg l^{-1} of iron(III), lead, manganese(II) and chromium(III). Despite the addition of EDTA [23], silver and copper caused serious interference in the evolution stage even at levels of 500 μg l^{-1}. Interference from nickel, bismuth,

TABLE 4

Effect of various cations on the recovery of 20 μg As l^{-1} from 50-ml aliquots of distilled water

Cation	Recovery (%)			
	0.5 mg l^{-1}	2.5 mg l^{-1}	50 mg l^{-1}	250 mg l^{-1}
—	98.7	98.7	98.7	98.7
Ag^{+}	69.4	47.7	10.2	6.7
Bi^{3+}	98.1	99.9	78.7	67.3
Cd^{2+}	99.5	98.4	93.1	64.4
Cr^{3+}	99.1	98.3	99.1	97.9
Co^{2+}	97.9	97.9	98.1	52.5
Cu^{2+}	91.2	80.3	9.2	5.3
Fe^{3+}	99.1	98.1	98.3	96.9
Ge^{4+}	99.5	98.6	100.5	107.4
Hg^{2+}	97.6	97.5	97.9	95.5
Mn^{2+}	98.3	99.3	98.6	96.9[a]
Mo^{6+}	98.8	98.0	97.0[b]	—
Ni^{2+}	99.5	99.5	12.7	5.8
Pb^{2+}	99.5	98.3	98.4	98.6
Sb^{3+}	100.9	100.9	—[c]	—[c]
Se^{4+}	79.2	67.8	—[d]	—[d]
Sn^{2+}	99.5	95.1	50.0	35.4
Zn^{2+}	99.1	98.5	98.5	98.9

[a]A recovery of 98.2 % was obtained at a manganese concentration of 1000 mg l^{-1}.
[b]Final solution had a yellowish-green colour instead of the usual faint blue colour.
[c]White turbidity in final solution.
[d]Elemental selenium precipitated in final solution

TABLE 5

Effect of various anions and other substances on the determination of 20 μg As l^{-1} from 50-ml aliquots of distilled water (Concentrations of species (in mg l^{-1}) are shown in parentheses)

Species	Recovery (%)			
—	98.7	98.7	98.7	98.7
ClO_3^-	99.5 (0.5)	96.8 (2.5)	96.8 (50)	92.6 (250)
NO_3^-	98.9 (40)	98.2 (200)	98.2 ($4 \cdot 10^3$)	98.2 ($2 \cdot 10^4$)
PO_4^{3-}	97.2 (1.0)	99.5 (5.0)	100.9 (100)	102.5 (500)
SiO_4^{4-}	99.9 (0.4)	98.8 (4.0)	99.9 (40)	97.9 (100)
Chloroform	99.5 (4.0)	98.9 (20)	99.0 (400)	98.8 (2000)
Methanol	98.1 (2.0)	98.7 (10)	98.6 (200)	88.1 (1000)
Sodium dodecyl sulphate	97.9 (0.5)	98.4 (2.5)	101.7 (50)	—[a]

[a]Evolution stage vitiated by froth.

tin and cadmium became significant at concentrations above 2.5 mg l^{-1}, and that from cobalt at concentrations above 50 mg l^{-1}. These elements could be satisfactorily removed up to levels of at least 50 mg l^{-1} by extraction with a solution of dithizone in chloroform or at higher concentrations (1000 mg l^{-1}) by adsorption onto a strongly acidic cation exchanger (see Experimental and Table 6).

Selenium(IV) causes serious interference even at the 0.5 mg l^{-1} level; during the evolution stage it is reduced to hydrogen selenide and is subsequently precipitated in the elemental form by the ascorbic acid in the chromogenic reagent. Germanium causes slight positive interference at the 250 mg l^{-1} level, presumably because it is volatilized as germane and subsequently converted to a germanium molybdenum blue complex. Although both nitrate and chlorate have been said to interfere, nitrate caused no interference at a level of

TABLE 6

Removal of interfering metals in determination of arsenic (50-ml samples)

Dithizone extraction					
Cation	Ag^+	Co^{2+}	Cu^{2+}	Ni^{2+}	Bi^{3+}
Concn. (mg l^{-1})	50	50	50	50	50
As added (μg l^{-1})	20.0	20.0	20.0	20.0	20.0
As found	19.7	20.0	19.7	19.6	19.6
Cation exchange with Zerolit 225					
Cation	Ag^+	Co^{2+}	Cu^{2+}	Ni^{2+}	Sn^{2+}
Concn. (mg l^{-1})	1250	1250	1000	1250	1250
Concn. after ion exchange (μg l^{-1})	<10	<10	<10	<10	<100
As added (μg l^{-1})	5.0	5.0	5.0	5.0	5.0
As found (μg l^{-1})	4.9	4.9	4.7	4.9	4.7

20 g NO_3^- l^{-1}; however, chlorate significantly inhibited arsine evolution at a level of 250 mg ClO_3^- l^{-1}. Levels of antimony in excess of 2.5 mg l^{-1} led to the development of a turbidity which interfered in the photometric measurement.

Destruction of organo-arsenic compounds

Many species of micro-organisms can convert inorganic arsenic compounds to organic derivatives, the presence of which has been detected in cultures of marine organisms grown in arsenic-enriched media [21]. However, it is uncertain, despite the observations of Gorgy et al. [10], and the finding of traces of methyl arsenic and arsonic acids by Braman and Foreback [24], whether sea water contains significant proportions of organo-arsenic compounds. Armstrong and Tibbitts [25] have shown that the dissolved organic-phosphorus in sea water can be photolyzed to orthophosphate by irradiation with an intense source of ultraviolet radiation. It appeared that this technique might also be of value for the breakdown and subsequent indirect determination of organo-arsenic compounds. Tests carried out by the procedure described in the Experimental section demonstrated that arsenic could be recovered quantitatively (> 98 %) from tetraphenylarsonium chloride (—C—As linkage), and from a number of aromatic arsonic acids (—C—O—As linkages). This irradiation technique can also be applied to potable waters, provided that they do not contain significant amounts of substances which absorb ultraviolet radiation, e.g. humic acids. For strongly absorbing samples and effluents it is necessary to oxidize organic arsenic compounds chemically. For potable waters this can be achieved by digesting the acidified sample overnight at 100 °C with an excess of potassium permanganate. When the oxidation conditions described in the experimental section were employed, practically quantitative recoveries (> 98 %) of arsenic were obtained from tetraphenylarsonium chloride, 1-(*o*-arsono-phenylazo)-2-naphthol-3,6-disulphuric acid and *o*-arsonophenylazo-*p*-dimethylaminobenzene. For effluents, it is preferable to oxidize the organic arsenic compounds by evaporating the sample to fuming with a mixture of nitric and sulphuric acids, as described by Caldwell et al. [20], but reducing the amount of sulphuric acid used by a factor of 10 to minimize the reagent blank. Evaporations carried out in this way gave almost quantitative (> 98 %) recoveries of inorganic arsenic(III) and of the three organic arsenic compounds mentioned above.

REFERENCES

1 D. L. Johnson, Environ. Sci. Technol., 5 (1971) 411.
2 D. L. Johnson and M. E. Q. Pilson, J. Mar. Res., 30 (1972) 140.
3 M. Ishibashi, T. Shigematsu and Y. Nishikawa, Rec. Oceanogr. Works Jpn., 5 (1960) 66.
4 K. Sugawara, Prepr. Reg. Symp. Phys. Oceanogr. Tokyo, 1955.
5 A. I. Ryabinin and A. S. Romanov, Geokhimiya, (1973) 257.
6 J. E. Portmann and J. P. Riley, Anal. Chim. Acta, 31 (1964) 509.
7 S. Gohda, Bull. Chem. Soc. Jpn., 45 (1972) 1704.
8 N. W. Rakestraw and F. B. Lutz, Woods Hole Biol. Bull., 65 (1933) 397.

9 E. G. Young, D. G. Smith and W. M. Langille, J. Fish. Res. Board Can., 16 (1959) 7.
10 S. Gorgy, D. L. Fox and N. W. Rakestraw, J. Mar. Res., 7 (1948) 22.
11 F. J. Schmidt and J. L. Royer, Anal. Lett., 6 (1973) 17.
12 E. N. Pollock and S. J. West, At. Absorpt. Newsl., 12 (1973) 6.
13 R. S. Braman, L. L. Justen and C. C. Foreback, Anal. Chem., 44 (1972) 2195.
14 F. J. Fernandez, At. Absorpt. Newsl., 12 (1973) 93.
15 J. C. Van Loon, Anal. Lett., 7 (1974) 505.
16 T. Maruta, Anal. Chim. Acta, 77 (1975) 37.
17 D. C. Manning, At. Absorpt. Newsl., 10 (1971) 123.
18 H. C. Freeman, At. Absorpt. Newsl., 13 (1974) 75.
19 K. C. Thompson, Analyst (London), 99 (1974) 595.
20 J. S. Caldwell, R. J. Lishka and E. F. McFarren, J. Am. Water Works Assoc., 65 (1973) 731.
21 M. G. Haywood, Ph.D. Thesis, University of Liverpool, 1976.
22 A. E. Smith, Analyst (London), 100 (1975) 300.
23 R. Belcher, S. L. Bogdanski, E. Henden and A. Townshend, Analyst (London), 100 (1975) 522.
24 R. S. Braman and G. C. Foreback, Science, 182 (1973) 1249.
25 F. A. J. Armstrong and S. Tibbitts, J. Mar. Biol. Assoc. U.K., 48 (1968) 143.

Analytica Chimica Acta, 85 (1976) 231—239

DOSAGE DES MÉTAUX LOURDS DANS LE PLANCTON PAR SPECTROMÉTRIE D'ABSORPTION ATOMIQUE SANS FLAMME

R. MACHIROUX et J. C. DUPONT

Laboratoire de Chimie analytique, Université de Liège au Sart Tilman, B-4000 Liège (Belgique)

(Reçu le 2 mars 1976)

RÉSUMÉ

Le dosage du cuivre dans le plancton peut se réaliser de différentes manières: analyse directe du solide, mise en solution après calcination à basse température, mise en solution par les acides. A certaines conditions un bon accord est observé entre les valeurs obtenues. Le cas du chrome paraît plus complexe en ce sens que cet élément peut donner lieu à des phénomènes de rétention ou de volatilisation qui perturbent l'analyse.

SUMMARY

The application of flameless atomic absorption spectrometry to the determination of copper and chromium in plankton is discussed. Three modes are examined: (a) direct analysis of powdered samples; (b) analysis in solution after dry ashing; (c) analysis after wet dissolution. For copper, results obtained by these methods are generally in good agreement. The case of chromium is more complex; there are large discrepancies between the results. Results for iron, manganese, nickel and cobalt are also described.

De nombreuses techniques analytiques ont été appliquées à l'analyse du plancton marin et du plancton d'eau douce. Relevons, parmi elles, la spectrographie d'émission [1, 2], utilisée pour l'analyse de tests de foraminifères, la spectrophotométrie d'absorption dans le visible [3—5] et la fluorescence-x [6]. L'analyse par activation neutronique [7, 8], la chronoampérométrie par redissolution anodique [9] et enfin la spectrophotométrie d'absorption atomique [10, 11] ont également contribué à résoudre le problème du dosage des métaux lourds dans le plancton. Outre les alcalins et les alcalino-terreux, un grand nombre de métaux lourds ont été déterminés: Fe, Mn, Cu, Ni, Zn, Ag, Cd, Pb, Hg [3] auxquels il faut ajouter V, Co [11], I, Br, As [7].

En ce qui nous concerne, nous avons travaillé en liaison avec Gillain [9] et nous nous sommes intéressés, en ordre principal, au dosage du cuivre et du chrome et, accessoirement, du Fe, Mn, Co, Ni dans le plancton de la mer du Nord. Nous avons essayé de mettre au point une méthode d'analyse directe du plancton à l'état solide. Pas la suite nous nous sommes intéressés à deux techniques de mise en solution du plancton.

PARTIE EXPÉRIMENTALE

Appareillage, reactifs et solutions

Nous avons utilisé un spectrophotomètre d'absorption atomique Perkin-Elmer 303 équipé d'une lampe multiélémentaire Intensitron 303-6103 et d'un atomiseur à tube de graphite HGA 72. Les calcinations à basse température ont été faites dans un calcinateur LTA Trapelo (LFE Corporation).

Autant que possible, nous avons utilisé les acides Merck Suprapur (HCl, HNO_3, H_2SO_4, HF) ou, à défaut, les acides Baker p.a. Les solutions-étalons ont été préparées à partir des métaux purs (Fe, Co, Cu) ou de sels p.a. (K_2CrO_4; $(NH_4)_2SO_4 \cdot MnSO_4 \cdot 6H_2O$; $(NH_4)_2SO_4 \cdot NiSO_4 \cdot 6H_2O$). Toutes les solutions ont été réalisées au moyen d'eau déminéralisée, bidistillée dans un distillateur en quartz.

Afin d'éviter les dilutions intermédiaires, les prélèvements de solution-étalon ont été effectués au moyen de micropipettes Pipetman Gilson P20 (0—20 μl) et P200 (0—200 μl).

Conditions d'atomisation

Nous avons adopté les programmes d'atomisation repris ci-dessous: pour tous les éléments, phase 1: 10 s à 110 °C; phase 2: 15 s à 850 °C; et phase 4: 5 s à 2700 °C.

Nous avons remarqué une importante interférence du fer à l'endroit de la raie 240,7 nm du cobalt, qui est la raie généralement utilisée. En effet, le fer possède une raie atomique à 240,7229 nm [12]. Cette interférence est éliminée en utilisant la raie 241,2 nm du Co. Elle possède des caractéristiques spectrales voisines de celles de la 240,7 nm et est utilisée le même domaine de concentration [13].

Préparation du plancton

La méthode de collection a été décrite par Gillain [9]. Le plancton est recueilli dans un filet aux mailles de 400 μm. La récolte est lavée à l'eau distillée. Le plancton est lyophilisé puis le résidu sec est broyé mécaniquement au mortier d'agate pendant 30 min à ± 100 tours/min. La poudre obtenue est conservée dans des flacons hermétiques de manière à minimiser l'adsorption de vapeur d'eau atmosphérique.

Dans ces échantillons, nous avons tenté de doser le cuivre et le chrome selon les modalités suivantes: (a) introduction directe du solide dans l'atomiseur; (b) calcination à basse température puis reprise par HCl Suprapur; ou (c) mise en solution HNO_3—H_2SO_4—H_2O_2—HF.

Toutes les mises au point préliminaires ont été faites sur le dosage du cuivre.

Analyse directe du solide

Programme d'atomisation. Nous avons adopté le programme d'atomisation suivant: phase 1: 100 °C (10 s); phase 2: 700 °C (10 s); phase 3: 2400 °C

TABLEAU 1

Eléments	λ (nm)	Programme	Phase 3 (5 s)
Co	241,2	—	2400°
Cr	357,9	7 → 1660°	2600°
Cu	324,7	—	2400°
Fe	248,8	8 → 2200°	2540°
Mn	403,1	—	2400°
Ni	232,0	—	2600°

(5 s); phase 4: 2800 °C (10 s). Pour limiter les effets perturbateurs de NaCl, nous avons fait précéder la phase d'atomisation (no. 3) d'un traitement à température programmée: T initiale, 700 °C; 3 ΔT: 270 °C min^{-1}; T finale, 1930 °C.

La Fig. 1(a) montre un exemple de courbe d'absorption du plancton en fonction de la température. On y remarque, au voisinage de 1500 °C, un pic d'absorption qui correspond à la volatilisation de NaCl. La température finale de 1930 °C représente le meilleur compromis entre l'élimination complète de NaCl et la réduction des pertes de $CuCl_2$ (T_S = 1400 °C). Au moment de l'atomisation, apparaît un important signal qui se superpose au signal du cuivre et qui provient de l'absorption due à la silice présente dans le plancton. Cette absorption parasite a pu être éliminée en injectant dans le four 50 µl de HF. La silice s'élimine alors sous forme de SiF_4 (Fig. 1b).

Homogénéisation. Pour cette étude, nous avons choisi un échantillon contenant 33,5 p.p.m. Cu [9, 14], teneur rapportée au poids de matière sèche. Nous avons introduit dans les flacons à échantillon deux billes de verre

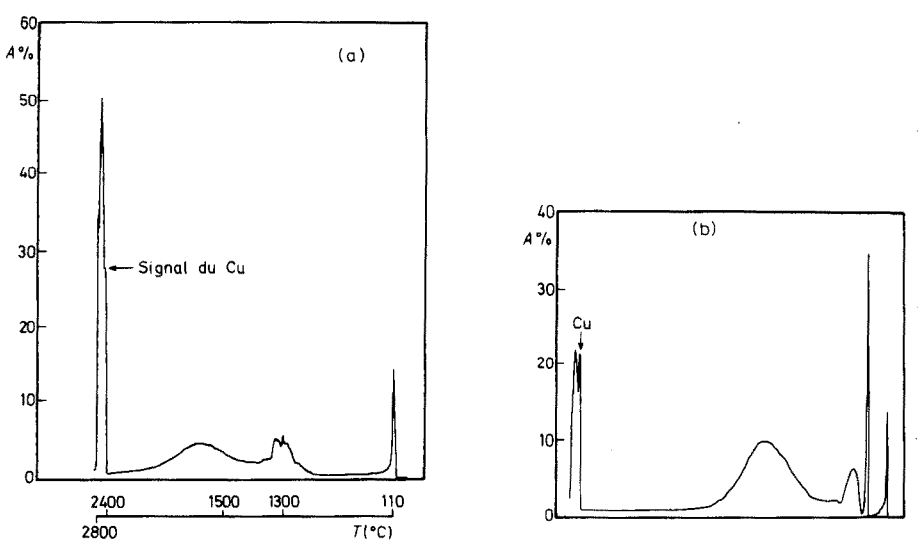

Fig. 1(a) Courbe d'absorption du plancton. (b) Effet de HF.

de 10 mm de diamètre. Les flacons ont été placés sur une roue à godets et maintenus en rotation pendant des temps variables. Nous avons ensuite pesé six échantillons de ±1 mg sur lesquels nous avons mesuré le signal d'atomisation du cuivre. Nous avons alors déterminé l'évolution en fonction du temps du σ_A coefficient de variation calculé sur les six mesures d'absorbance. Pour permettre la comparaison des résultats, nous avons dû tenir compte des différences de taille des échantillons en rapportant, par calcul, toutes les absorbances à 1 mg de matière, avant le calcul du σ_A. Cette interpolation nous paraît justifiée par les faibles différences de taille des échantillons, et l'excellente linéarité du graphique de l'absorption du cuivre en fonction de la quantité injectée. La Figure 2 donne un exemple des courbes obtenues. La valeur de σ_A atteint un minimum au bout de 3 h d'agitation; temps audelà duquel σ_A se remet à croître. Ce phénomène est probablement causé par des entraînements mécaniques au cours des traitements thermiques précédant l'atomisation.

Étalonnage. Nous avons utilisé la méthode d'étalonnage par encadrement au moyen de solutions de cuivre(II) 0.1 M en HCl. Les étalons, accompagnés de 50 µl HF ont subi les mêmes cycles d'atomisation que le plancton. Nous avons, par ailleurs, examiné les possibilités de la méthode des ajouts. En outre, nous avons tenté d'établir des droites d'étalonnage au moyen d'échantillons connus. Les résultats enregistrés se sont révélés peu encourageants.

Dosage du cuivre. Le Tableau 2 rassemble les teneurs en cuivre mesurées sur 10 échantillons. Les colonnes a.s.v. et a.a.s. reprennent les valeurs trouvées après mise en solution, respectivement par redissolution anodique [9] et spectrophotométrie d'absorption atomique sans flamme [14].D'une manière générale, il existe un accord satisfaisant entre les trois séries de valeurs. On ne remarque aucune déviation systématique, qui pourrait faire penser soit à un effet de matrice, soit à une perte de cuivre. Les valeurs de

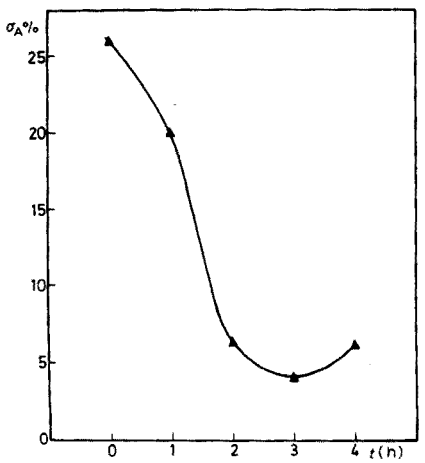

Fig. 2. Variation de σ_A en fonction du temps d'homogénéisation.

TABLEAU 2

Teneurs en cuivre (μg Cu g^{-1} de matière sêche)

No.	A.s.v.	A.a.s.	Nos valeurs[a]	σ_A (%)
401	67	72	85,5	9
402	72	67	83	7
406	126	305	147	14
410	11	51	54	4
411	—	33,5	32	7
413	173	120	170	15
416	24	28	28	7
417	45	30	46	4
419	30	49	31	6
3	13	—	16	15

[a]La moyenne de 6 mesures.

σ_A s'étagent entre 4 et 15 % et, à une exception près, les dispersions les plus fortes sont observées pour les teneurs les plus élevées. Cette observation nous parait devoir être rapportée aux entraînements mécaniques auxquels nous avons fait allusion plus haut.

Sur la base de ces mesures, nous avons tenté d'estimer la limite de dosage du cuivre. Compte tenu que la masse de plancton ne peut dépasser 2 mg et que 97 % du sont cuivre sont perdus par volatilisation, la limite de dosage peut être estimée à environ 0.2 μg g^{-1}. La durée totale de l'analyse d'un échantillon (6 prises de 1 mg) se situe entre 1.5 et 2 h.

Dosage du chrome. Nous avons appliqué, au dosage du chrome, le mode opératoire de l'analyse du cuivre. La température d'atomisation a été portée à 2600 °C, et les absorbances ont été mesurées à 357,9 nm. La calibration a été effectuée au moyen d'une solution aqueuse de K_2CrO_4, 0,1 M en HCl.

Comme nous ne disposions d'aucune valeur de comparaison, nous avons également dosé le chrome du plancton par a.a.s. après calcination à basse température et reprise du résidu par HCl 12 M et après mise en solution sulfonitrique. Pour cette raison, nous détaillerons les résultats obtenus sur le solide dans un prochain paragraphe.

Analyse par voie humide

Analyse après calcination dans l'oxygène activé. Les échantillons (300—500 mg) ont été calcinés 24 h à une puissance de 300 W (100—200 °C) sous 1 mm de mercure. Le résidu est repris par 3 ml de HCl 12 M Suprapur. La silice a été éliminée par filtration et le filtrat a été amené à 100 ml en ballon jaugé. Les solutions ont été analysées directement par la technique des ajouts standard. Comme nous ne disposions pas de correcteur-D_2, les valeurs excessives des teneurs en cuivre (Tableau 3 col. 5) nous ont contraints à pratiquer une

TABLEAU 3

Teneurs en cuivre ($\mu g\ g^{-1}$)

No.	A.s.v.	A.a.s.	A.a.s. (sol)	Calcination O_2		Dissolution
				Sans extr.	Avec extr.	Extraction
401	67	72	85,5	1720	70	86
406	126	305	147	3320	129	139
410	11	51	54	2810	49	45
411	—	33,5	32	2530	71	36
413	173	120	170	2180	117	125
419	30	49	31	2635	34	36

extraction par l'APDC à pH 4.5, dans la méthylisobutylcétone. En faisant abstraction des valeurs de la colonne 5, on retrouve une bonne concordance entre les valeurs obtenues en suivant des modalités différentes.

Dans le cas du chrome, la situation se présente moins favorable (Tableau 4). Les analyses après calcination dans l'oxygène activé et après dissolution par les acides ont été réalisées directement sur la solution sans extraction. Contrairement à ce que l'on aurait pu attendre après l'analyse du cuivre (Tableau 3, col. 5), les teneurs mesurées sont nettement inférieures aux résultats obtenus sur le solide.

A cette discordance, nous voyons deux raisons principales. Nous avons pu observer des pertes de chrome très importantes pendant la calcination. En présence de NaCl, dans nos conditions de calcination, 71 % du Cr(VI) et 46 % du Cr(III) sont perdus. Nous pensons que le chrome se volatilise sous forme de CrO_2Cl_2 (T_{eb}: 117 °C) qui se formerait par action de l'oxygène activé, en présence de chlorures. En outre, nous avons également constaté que le résidu de silice retenait des quantités importantes de chrome (Tableau 4, col. 4), rétention qui n'a pas été observée pour le cuivre.

Mise en solution par les acides. Pour maîtriser les difficultés recontrées dans l'analyse du chrome, nous avons procédé à la dissolution suivante. L'échantillon (0.2 g) est traité au bain-marie par 2 ml de H_2SO_4 18 M Suprapur en capsule de platine. Après élimination des chlorures, on ajoute 10 ml de HNO_3 14 M. On porte à l'ébulliton pendant 30 min et on termine l'oxydation par 1 ml de perhydrol. On fait réduire le volume puis, en fin d'évaporation, on ajoute 3 ml de HF et on évapore à fumées blanches. Le résidu est repris par 10 ml de HCl fumant et amené à 100 ml.

Le cuivre a été analysé après extraction par l'APDC; le chrome a pu être dosé directement sur les solutions acides.

Les résultats sont repris dans les Tableaux 3 et 4.

TABLEAU 4

Teneurs en chrome ($\mu g\ g^{-1}$)

No.	A.a.s. (sol)	A.a.s. (calcin)	Anal. rés. SiO_2[a]	Dissol. acides
401	59	18	9,8	63,7
402	83	40	7,5	58,0
406	52	18	6,5	50,6
407	265	88,5	10,0	59,0
410	193	94	8,9	55,8
411	55	25	4,5	—
413	46	13	6,8	—
414	50	25	—	—
416	54	—	—	—
417	55	—	—	—
419	285	—	—	64,6
3	177	—	—	73,8

[a]Les teneurs sont ramenées au poids initial de plancton et non au poids de résidu.

DISCUSSION

Cas du cuivre

D'après le Tableau 3, on peut se rendre compte qu'il existe un accord assez satisfaisant entre les différentes valeurs expérimentales (col. 5 excepté). Les divergences qui subsistent traduisent, à notre sens, le caractère essentiellement hétérogène du plancton. Pour vaincre cette hétérogénéité, on pourrait croire qu'il suffit d'augmenter la taille de l'échantillon. On n'observe cependant pas un meilleur accord entre les valeurs des colonnes 2, 3, 6 et 7, valeurs pour lesquelles le poids d'échantillon varie de 0.3 à 0.5 g. Il s'agit plutôt d'une dispersion liée à la constitution zoologique du plancton.

Les résultats de la colonne 5 ont été obtenus sans extraction: leurs valeurs élevées semblent bien signifier que les sels présents en solution donnent lieu à une intense absorption non sélective. L'effet bénéfique de l'extraction confirme cette hypothèse.

Cas du chrome

Nous n'avons pas retrouvé, dans le cas du chrome, l'accord entre les teneurs trouvées à l'état solide et en solution. Les valeurs élevées de la colonne 2 (Tableau 4) peuvent témoigner de l'existence d'une absorption parasite dont nous nous expliquons mal l'origine. On voit malaisément les raisons qui justifient les différences observées. Il se pourrait que le chrome se trouvant partiellement sous forme de Cr (VI), des pertes se produisent lors de la mise en solution sulfonitrique.

La comparaison des teneurs en chrome mesurées après des traitements préliminaires différents fait clairement ressortir l'importance de cette phase

de l'analyse. En particulier, la calcination à basse température doit être utilisée avec grande circonspection. La volatilité de certains composés halogénés d'éléments, comme Fe, As, Ge, Sb, Sn, Se, Te, risque d'entraîner de fortes erreurs par défaut. En ce qui concerne le Cd, le Cu, le Pb et le Zn, Gillain [9] s'est livré à deux vérifications: (a) l'expérience montre que ces éléments sont récupérés quantitativement après calcination au LTA; (b) le résidu de silice ne contient aucun de ces éléments. Par contre, dans le cas du chrome, nous avons observé une rétention importante par le précipité de silice.

En définitive, bien que l'analyse directe du solide soit sujette à certaines difficultés, comme le montrent les écarts entre les résultats du Tableau 4 (col. 2 et 5), elle est cependant très susceptible de fournir rapidement et sans grande complication expérimentale un ordre de grandeur de la concentration, au moins pour certains éléments peu volatils.

Toutefois, lorsqu'on recherche une valeur plus exacte, il est indispensable de recourir à la mise en solution par les acides. La présence d'acide fluorhydrique nous paraît indispensable pour éliminer les phénomènes de rétention signalés pour le chrome, tout comme il est souhaitable de recourir à une extraction par l'APDC pour supprimer l'effet perturbateur des sels, au moment de l'atomisation. Cette extraction permet d'ailleurs d'étendre aisément l'analyse à d'autres éléments (Co, Ni, Fe, Mn • • •) et de réaliser aisément une préconcentration des éléments de basse teneur. A titre d'exemple le Tableau 5 rassemble les résultats obtenus en Co, Fe, Mn et Ni après dissolution par les acides sans extraction (Fe, Mn) et après préconcentration par l'APDC (Co, Ni).

Nos résultats s'intègrent bien dans les estimations de Fujita et Yamamoto [3] qui situent les teneurs en fer entre 500 et 11000 p.p.m. et en Mn entre 30 et 200 p.p.m. Le Ni est également en accord avec les valeurs limites citées par Martin et Knauer [10]. Ces derniers auteurs n'ont pu doser le Co, leur limite de détection se situant au voisinage de 1 p.p.m.

CONCLUSION

La versatilité de l'atomiseur à tube de graphite permet de réaliser le dosage de nombreux métaux lourds dans le plancton, à des niveaux de concentration très différents. Ce dosage peut se pratiquer à l'état solide moyennant les

TABLEAU 5

Concentrations en Fe, Mn, Co, Ni ($\mu g\ g^{-1}$)

No.	Fe	Mn	Co	Ni
3	4540	92,3	0,37	4,45
401	11700	316	0,54	6,7
410	5810	135	0,46	5,7
419	4140	169	0,70	6,6

restrictions que nous avons émises. En solution, il est possible de tirer parti des possibilités de l'extraction liquide—liquide pour préconcentrer les éléments de basse teneur et pour éliminer les effets perturbateurs sans cependant que cela soit absolument indispensable (cas du Fe, Mn, etc.).

Nous assurons le Professeur G. Duyckaerts de toute notre gratitude pour l'intérêt et la sollicitude qu'il a bien voulu nous manifester au cours de ce travail. Nous remercions Monsieur G. Gillain qui a assuré la récolte et la préparation des échantillons de plancton. Nous remercions également le F.N.R.S. et le C.I.P.S. dont le soutien financier, nous a permis de réaliser ce travail.

BIBLIOGRAPHIE

1 J. P. Riley, J. Mar. Biol. Assoc., 51 (1971) 63.
2 N. V. Belgaeva, Okeanologiya, 13 (1973) 303.
3 T. Fujita et T. Yamamoto, Nippon Kagaku Zasshi, 90 (1969) 680.
4 C. Valuchevicius et R. Jurevicius, Liet TSR, Aukst. Mokyklu. Mosklo. Darb. Chem. Techn., 12 (1970) 6772.
5 R. Jurevicius et K. Blazis, Okeanologiya, 12 (1972) 349.
6 F. C. Young et M. L. Roush, Int. J. Appl. Radia. Isotop., 24 (1973) 153.
7 G. Lunde, Int. Rev. Ges. Hydrobiol., 52 (1967) 265.
8 M. Merlini, O. Ravera et C. Bigliocca, Euratom Contrib., no. 420.
9 G. Gillain, Prog. Natl. sur l'Env. Phys. et Biol. Tech. Rept., 1973.
10 G. H. Martin et G. A. Knauer, Geochim et Cosmochim. Acta, 37 (1973) 1639.
11 D. A. Segar et J. L. Gillio, Int. J. Env. Anal. Chem., 2 (1973) 291.
12 W. R. Brode, Chemical Spectroscopy, 2e edition, Wiley, New York, 1947.
13 M. Pinta, Spectrométrie d'Absorption Atomique, Masson, Paris, 1971.
14 D. Janssens, communication personnelle.

Analytica Chimica Acta, 85 (1976) 241—251

THE DETERMINATION OF CATIONIC SURFACTANTS IN THE PRESENCE OF ANIONIC SURFACTANT IN BIODEGRADATION TEST LIQUORS

J. WATERS

Unilever Research Port Sunlight Laboratory, Port Sunlight, Wirral, Merseyside L62 4XN (England)

W. KUPFER

Hoechst AG, 6230 Frankfurt (Main) 80 (West Germany)

(Received 3rd March 1976)

SUMMARY

A method is described for the determination of cationic surfactants in biodegradation test liquors and effluents containing anionic surfactant and other components which interfere with existing colorimetric procedures. The cationic surfactant is concentrated by evaporation of the aqueous sample and separated from the resulting residue by solvent extraction as an ion-association compound. The extract is treated under non-aqueous conditions on Bio-Rad AG 1-X2 resin in the chloride form to remove interfering anionic components. The isolated cationic surfactant is determined colorimetrically as its disulphine blue ion-association compound, extractable into chloroform. The recovery of added cationic surfactants from biodegradation test liquors is generally better than 95 %, and concentrations in the range 0.1—10 mg l^{-1} can be determined. The method is suitable for biodegradability test studies where control liquors are available, e.g. OECD Screen and Confirmatory tests. In environmental samples, materials other than cationic surfactant may respond to disulphine blue and these limit severely the application of the procedure.

There is no suitable analytical method for the determination of the biodegradability of cationic surfactants in the presence of anionic surfactants or in complex media where other anionic interferences occur. However, colorimetric procedures exist for determining low levels of quaternary ammonium cationic surfactants in biodegradation test liquors, such as those recommended by the Organisation for Economic Co-operation and Development [1], in the absence of anionic surfactant and other anionic interferences. These procedures are all based on the reaction of the cationic surfactant with an intensely coloured anionic dye material (e.g. Orange II [2], bromothymol blue [3], bromophenol blue [4], and picric acid [5]) to form solvent-extractable ion-association compounds. However, when cationic surfactants must be determined under more realistic conditions in the presence of anionic surfactants, these simple procedures fail because the anionic surfactant interacts more strongly with the cationic surfactant than does the anionic dye reagent.

This paper describes a novel analytical method which eliminates the interference of anionic surfactant and other anionic components in the colorimetric determination of cationic surfactant (0.1—10 mg l^{-1}) in biodegradation test liquors. The cationic surfactant is separated from a test sample as the stable ion-association compound before the interfering anionic components are removed by a non-aqueous anion-exchange step. The isolated cationic surfactant is then determined colorimetrically as its ion-association compound with disulphine blue.

EXPERIMENTAL

Reagents

Standard cationic solutions (100 mg l^{-1} and 10 mg l^{-1}). Prepare these in distilled water. Cetyltrimethylammonium chloride (CTMAC) is a useful reference surfactant.

Disulphine blue VN 150 (Acid Blue 1; C.I. 42045; 1.3 · 10^{-3} M). Dissolve 0.16 g of disulphine blue (ICI Ltd.) in 20 ml of 10 % (v/v) ethanol in water. Transfer to a 250-ml graduated flask and make up to volume with distilled water.

Buffer solution, pH 5. Adjust 2 M sodium acetate to pH 5 with 2 M acetic acid.

Alkylbenzene sulphonate (ABS) solution (1000 mg l^{-1}). Use an ABS such as Marlon A 350 (Hüls) in distilled water.

The cationic surfactant solution (1000 mg l^{-1}) for pre-conditioning the resin contained cetyltrimethylammonium chloride in methanol.

Chloroform and methanol were of analytical-reagent grade.

Apparatus

The extraction device described by Taylor and Fryer [6] was used to transfer the chloroform extracts from the centrifuge tube to the optical cell.

Ion-exchange columns of conventional design (10-mm i.d., 250-mm long) were made with a Quickfit joint to take a 250-ml separating funnel as a solvent reservoir. The anion-exchange resin was Bio-Rad AG1-X2 (50—100 mesh, chloride form).

A Unicam SP 1800 spectrophotometer was used with matched 10-mm glass optical cells.

Procedures

Preparation of anion-exchanger columns. Fill the columns one-third full with methanol, plug the lower constriction above the tap with a small wad

of cotton wool and slurry 12 ml of wet resin into each column with methanol. Remove any gas bubbles from the resin bed and plug the top of the column with a small pad of cotton wool. Pre-condition the resin column to cationic surfactant by passing 10 ml of the CTMAC solution in methanol at a rate of 2 ml min^{-1}. Wash the resin columns by passing 600 ml of methanol at a rate of 2—3 ml min^{-1}. Run a column blank to determine whether any cationic material remains in the resin bed. Continue to wash the resin bed until the column blank is similar to the reagent blank for the colorimetric step.

Separation and concentration of cationic surfactant. Take a volume of unfiltered test liquor containing 50—1000 μg of cationic surfactant and evaporate to dryness. The volume of the sample should preferably not exceed 200 ml. A volume of control solution equivalent to that taken for the test determination is also evaporated to dryness. If the samples contain little or no anionic surfactant, add alkylbenzene sulphonate to make the concentration of anionic surfactant up to 20 mg l^{-1}. This aids the recovery of cationic surfactant.

Break up the sample residue thoroughly with a glass rod and extract it with 20 ml of boiling methanol. Filter the cationic extract through a small cotton wool pad plugged into a filter funnel and collect the filtrate in a 250-ml beaker. Wash the pad with 10 ml of cold methanol. Repeat the extraction with two further 20-ml portions of boiling methanol. Finally wash the extraction beaker, pad, and filter funnel with 20 ml of cold methanol. Evaporate the combined extracts to dryness.

Ion-exchange removal of anionic interferences. Dissolve the cationic residue in 10 ml of methanol, using a glass rod to break up any residue, and place the whole extract on top of a prepared ion-exchange column. Pass the sample through the resin bed at a rate of less than 1 ml min^{-1}, and collect the eluate in a 250-ml beaker. Use a further two 10-ml portions of methanol to ensure quantitative transfer of the sample to the column. Wash the sample through the column with 100 ml of methanol at a rate of 2—3 ml min^{-1}. Evaporate the column eluate to dryness.

Wash the columns with a further 150 ml of methanol after each separation and before re-using. The capacity of the resin bed is such that a column can be used 5—10 times.

Colorimetric determination of cationic surfactant. Redissolve the cationic surfactant residue from the ion-exchange separation in 20 ml of boiling water-saturated chloroform and transfer to a graduated flask. The volume of the flask is chosen so that a 10-ml aliquot of the final solution contains 5—50 μg of cationic material. Use a further portion of hot solvent and several portions of cold solvent to wash the beaker and make the solution up to the appropriate volume. For residues that are sticky and insoluble in chloroform, a small measured volume of methanol (e.g. 2.5 ml) is used

initially to dissolve the extract before the further addition of 15 ml of cold water-saturated chloroform (which generally results in precipitation of material). A similar washing procedure to that used above resulted in quantitative recovery of cationic surfactant. The final chloroform solution should contain no more than 2.5 % (v/v) of methanol.

Pipette 2.5 ml of 2 M acetate buffer pH 5 and 1 ml of disulphine blue reagent into a 40-ml conical centrifuge tube previously conditioned to reagents and cationic surfactant, and add 15 ml of distilled water. Pipette 10 ml of the chloroform sample solution into the tube. Stir the contents of the tube vigorously for 90 s by high-speed stirrer, so that the two layers are completely mixed. Centrifuge for 30 s to separate the layers. For the methanol—chloroform sample solutions, which are generally cloudy in appearance, more prolonged centrifuging is required to obtain clear colorimetric extracts. Attach a teat to the short arm of the extraction device. Introduce the long arm through the aqueous layer into the chloroform layer, maintaining a slight positive pressure on the teat to produce a slow stream of air bubbles. Secure the bung in the mouth of the centrifuge tube and then remove the teat. Transfer the chloroform extract directly to a glass 10-mm optical cell (previously conditioned with a disulphine blue—cationic chloroform solution) by applying pressure with the syringe via the needle. Wash the cell once with the extract and then immediately measure the absorbance of the extract at 628 nm against a chloroform reference.

After use, wash the centrifuge tubes several times with distilled water. Wash the extraction device and optical cells with methanol followed by chloroform at the end of a series of determinations.

Determine the amount of cationic surfactant in the sample by reference to a previously prepared calibration graph. Calculate the concentration of cationic surfactant in a test liquor (C mg l^{-1}) from the expression $C = N \times V_1 / 10 \times V_2$, where N is the actual number of micrograms of cationic surfactant in 10-ml aliquot of the test liquor chloroform solution after subtraction of the control liquor value, V_1 is the total volume of the chloroform solution, and V_2 is the volume of the aqueous sample taken for analysis.

Preparation of calibration graph. By burette, add 0, 1, 2, 3, 4 and 5 ml (0—50 μg) of the 10 mg l^{-1} cationic surfactant solution into a series of 40-ml centrifuge tubes and make up the volume to 15 ml with distilled water. Add 2.5 ml of pH 5 acetate buffer, 1 ml of disulphine blue reagent, and 10 ml of chloroform (or an appropriate methanol—chloroform solvent mixture) and proceed with the colorimetric estimation as indicated above. Construct a calibration graph of absorbance against the concentration (μg) of cationic surfactant.

SCOPE OF METHOD

Disulphine blue colorimetric determination of cationic surfactant

Disulphine blue VN 150, a pH indicator dye (pk_a 2.63), was chosen on the basis of its high sensitivity (molar absorptivity 96,200 at 640 nm in water). Biswas and Mandal [7] have indicated that only the base form of the dye forms chloroform-extractable 1:1 stoichiometric compounds with cationic surfactants from both neutral and acidic solutions. In this study, the wavelength of maximum absorption for all the disulphine blue—cationic compounds examined was at 628 nm in chloroform.

Extraction conditions. The extractability of the disulphine blue—distearyldimethylammonium compound into chloroform was studied. The effect of the number of chloroform partitions, pH of the aqueous phase, and the stirring time on the extraction are shown in Table 1. A single chloroform extraction (10 ml) results in virtually quantitative removal of cationic surfactant from strongly and weakly acidic disulphine blue solutions when the stirring time is 90 s. A shorter stirring time, e.g. 30 s, results in incomplete extraction irrespective of whether single or multiple chloroform partitions are used. Accordingly, a single extraction technique with the extraction device described by Taylor and Fryer [6] was chosen for all subsequent work.

Efficient extraction of all the commercially important cationic surfactants examined was obtained with the single extraction technique when a 10-fold or greater excess of disulphine blue reagent (1 ml of $1.3 \cdot 10^{-3}$ M solution) and a working pH of 5 (2.5 ml of 2 M acetate buffer) were used.

TABLE 1

The effect of the number of partitions, pH of aqueous phase and stirring time on the extractability of the distearyldimethylammonium compound
(Aqueous phases contained 50 μg of DSDMAC and a 10-fold molar excess of disulphine blue)

No. of partitions (vol.)	Stirring time (s)	pH of Aqueous phase	% Extracted
1 (10 ml)	30	1—2	75.8
1 (10 ml)	90		97.1
3 (3 ml)[a]	30		81.6
3 (3 ml)[a]	90		99.4
5 (2 ml)	30		85.4
5 (2 ml)	90		100.0
1 (10 ml)	30	5	81.8
1 (10 ml)	90		97.2
3 (3 ml)[a]	90		98.3
5 (2 ml)	90		100.0

[a]Extracts made up to 10 ml.

Calibrations and precision. Linear Beer's Law plots were obtained over the range 5—50 μg for all the long-chain alkyl cationic surfactants examined. In some instances, however, the calibrations showed a tendency to intersect the concentration axis rather than pass through the origin; this was attributed to the adsorption of a small amount of cationic surfactant on to the extraction apparatus, and conditioning of the equipment to reagents and samples minimized the effect. Calibrations were identical regardless of whether the cationic standards were prepared in water or chloroform.

The estimated limit of detection of the disulphine blue reaction is about 1 μg of cetyltrimethylammonium chloride (CTMAC) or distearyldimethylammonium chloride (DSDMAC); the response of 1 μg of cationic surfactant is equivalent to the size of the average reagent blank, (0.02 absorbance in 10-mm cell).

Inorganic nutrient solution and synthetic sewage containing no anionic surfactant (i.e. the two feedstock liquors recommended by the Organisation for Economic Co-operation and Development [1] for use in the OECD Screen and Confirmatory tests, respectively, for the biodegradability of anionic surfactants) do not affect the response of cationic surfactant to disulphine blue; the responses are identical to those in distilled water. For all three liquors, standard deviations of ±1—2 % were obtained for determinations carried out at the 50 μg level of DSDMAC.

Relationships between alkyl chain length and disulphine blue response. The responses of a range of even-numbered alkyl chain cationic surfactants of the alkyltrimethylammonium series (C_6, C_8, C_{10}, C_{12}, C_{14} and C_{16}) and the dialkyldimethylammonium series (C_8, C_{10}, C_{12}, C_{16} and C_{18}) to disulphine blue were determined. In the former series, decyltrimethylammonium chloride is only partially extractable as its disulphine blue compound, whilst the octyltrimethylammonium compound is slightly extracted and the dodecyltrimethylammonium compound almost completely extracted. Members of the latter series are all extractable. On this basis, the commercially important cationic surfactants should generally respond to the disulphine blue reaction.

Colour stability of extracts. The absorbance of disulphine blue chloroform extracts decreases on standing in the measuring compartment of the spectrophotometer. The effect of increased temperature on the extract and the adsorption of disulphine blue—cationic compounds on to the walls of the optical cell may cause this drop in absorbance. However, the readings are consistent when the extracts are measured immediately in pre-conditioned cells. Quartz optical cells are not recommended because of their high substantivity for disulphine blue—cationic compounds.

Removal of anionic interferences by ion exchange

Mixtures of cationic, anionic, non-ionic and ampholytic surfactants have been separated on a macro-scale for identification purposes by means of anion- and cation-exchange resins and non-aqueous solvent systems [8]. In the work described here, a similar approach successfully removed the interference of anionic components, particularly anionic surfactants, in the determination of low levels of cationic surfactant in biodegradation test liquors. With non-aqueous elution, the normally strong association that exists in water between the cationic surfactant and anionics is decreased sufficiently for an anion-exchange resin to bind the anionic components selectively.

The most effective combination of anion-exchange resin and non-aqueous solvent was Bio-Rad AG1-X2 resin and methanol. This combination gave high recoveries of cationic surfactant and the column blanks were only slightly larger than the reagent blank for the colorimetric step alone. Occasional low recoveries were observed when small quantities of cationic surfactant were passed through freshly prepared columns. This was attributed to adsorption of cationic surfactant; pre-conditioning of the resin with cationic surfactant eliminated such losses.

The recovery of DSDMAC (100—1000 μg) and CTMAC (65—1000 μg) from methanolic solutions containing anionic surfactant in various molar excesses was examined. The results obtained are given in Table 2. The recoveries of both materials are high and independent of the molar excess of anionic surfactant and the resin form (chloride and hydroxide).

Concentration and separation of cationic surfactant in biodegradation test liquors

Both solid—liquid and liquid—liquid solvent extraction techniques were examined for concentrating and separating the cationic surfactant from extraneous materials in samples before the ion-exchange step. The former technique gave the highest recoveries of cationic surfactant. Accordingly, samples were evaporated to dryness before extraction.

Several solvents were investigated for their ability to extract cationic surfactants as their ion-association compounds; hot methanol and chloroform gave complete extraction of pure, solid cationic—anionic surfactant compounds. Both solvents were tested for their ability to extract cationic surfactant (DSDMAC and CTMAC) from the residues of OECD nutrient and synthetic sewage solutions containing excess of anionic surfactant. Table 3 shows the recoveries obtained. Methanol is clearly superior to chloroform for recovering cationic surfactant quantitatively from the test liquors. However, for real sewage sample residues, methanol extracts many other components together with the cationic surfactant; this lowers the overall efficiency of the ion-exchange separation and interferes with the colorimetric step. For such samples chloroform extraction of the residue (or the residue obtained from an initial methanol extraction) gives acceptable recoveries of cationic surfactant and reduces possible interference.

TABLE 2

Recovery of cationic surfactant in the presence of excess of anionic surfactant

Compound	Amount taken (μg)	Molar ratio cationic:anionic	Resin form	% Recovery
CTMAC	65	1:1	OH^-	101.0
	65	1:5	OH^-	94.0
	500	1:3	OH^-	99.0
	500	1:3	OH^-	97.8
	1000	1:4	Cl^-	99.8
	1000	1:4	Cl^-	98.8
DSDMAC	100	1:3	Cl^-	94.0
	100	1:3	Cl^-	98.6
	300	1:5	Cl^-	97.0
	300	1:5	Cl^-	100.0
	1000	1:4	Cl^-	96.7
	1000	1:4	Cl^-	95.7

TABLE 3

Influence of extractant on recovery of cationic surfactant from nutrient solution and synthetic sewage residues

Compound	Amount taken (μg)	Molar ratio cationic:anionic	Extractant	% Recovery
Nutrient solution[a]				
DSDMAC	100	1:10	Methanol	98.2
				94.9
			Chloroform	88.3
				93.3
CTMAC	65	1:10	Methanol	94.8
				96.0
			Chloroform	86.0
				75.5
Synthetic sewage[b]				
DSDMAC	250	1:6	Methanol	94.6
				96.4
			Chloroform	82.6
				81.5

[a]Three extractions with boiling solvent; 100-ml samples.
[b]50-ml samples.

The highly substantive cationic surfactants should be more readily recoverable from samples in the form of their uncharged ion-association compounds. For this purpose, additional anionic surfactant is added to effluent samples containing little or none of this component to ensure the highest possible recoveries of cationic surfactant. Typically, 20 mg l^{-1} of ABS is added to such samples.

Interferences

The disulphine blue reaction is not specific for synthetic cationic surfactants in biodegradation test liquors. Any long-chain amines [7] and other compounds that can be protonated in weakly acidic conditions, or which contain a quaternary nitrogen group, may also form extractable disulphine blue compounds that can interfere. For example, the OECD synthetic sewage, which contains no added cationic surfactant, gave a measurable apparent cationic level (see Results). Therefore, control liquors are generally required to correct for low levels of other materials that are reactive to disulphine blue before the actual cationic surfactant content of the test liquor can be determined. For waste and surface water samples, the levels of natural substances that react with disulphine blue are likely to be so high that the procedure cannot be used for monitoring their cationic surfactant contents. The use of alternative colorimetric extraction conditions has not resulted in the elimination of these interferences.

RESULTS

The recovery of cationic surfactants was assessed in the presence of excess of anionic surfactant from nutrient solution and synthetic sewage.

Nutrient solution

Recoveries obtained for repeated determinations on solutions containing 1.0 mg l^{-1} and 0.65 mg l^{-1} of DSDMAC and CTMAC, respectively, and various excesses of anionic surfactant are shown in Table 4. On average, 95 % of the DSDMAC and CTMAC was recovered. Table 4 also shows that recoveries for both surfactants are virtually quantitative at the 5.0 mg l^{-1} level. Nutrient control determinations are invariably small.

Synthetic sewage

Table 5 shows that high recoveries were obtained for repeated determinations on 5.0 mg l^{-1} solutions of DSDMAC and CTMAC; both water-saturated chloroform and 2.5 % (v/v) methanol—chloroform were used to redissolve the final ion-exchange residues. However, the methanol—chloroform solvent mixture gives significantly higher recoveries of cationic surfactant from the ion-exchange residues than water-saturated chloroform. An apparent disadvantage of this system is that it gives cloudy solutions which require more prolonged centrifuging to produce clear colorimetric extracts. Control values

TABLE 4

Recovery of cationic surfactant from nutrient solution

Compound	Amount taken (mg l^{-1})	Molar ratio cationic:anionic	% Recovery
DSDMAC	1.0	1:1	100.9
		1:1	92.6
		1:5	95.9
		1:5	97.3
		1:10	98.2
		1:10	94.9
			Av. 96.6
CTMAC	0.65	1:1	88.7
		1:1	90.2
		1:5	90.2
		1:5	97.7
		1:10	94.8
		1:10	96.6
			Av. 93.1
Control	0.05[a]		
DSDMAC	5.0	1:4	102.8
			99.8
CTMAC	5.0	1:4	99.8
			98.8
Control	0.01[a]		

[a]Expressed as mg l^{-1} DSDMAC.

TABLE 5

Recovery of cationic surfactant from synthetic sewage

Compound	Amount taken (mg l^{-1})	Molar ratio cationic:anionic	% Recovery	
			Water-saturated chloroform	Methanol—chloroform
CTMAC	5.0	1:3	95.7	103.6
			94.6	106.3
			97.6	107.0
			97.6	108.1
			95.1	
DSDMAC	5.0	1:3	91.8	98.3
			91.8	98.3
			95.6	102.9
			94.3	104.8
Control	0.3[a]			

[a]Expressed as mg l^{-1} DSDMAC.

for the synthetic sewage are significantly larger than for the nutrient solutions, indicating the presence of species that react with disulphine blue (e.g. peptone, beef extract).

REFERENCES

1 Pollution by Detergents. Determination of the Biodegradability of Anionic Synthetic Surface-Active Agents, Organisation for Economic Co-operation and Development, Paris, 1972.
2 G. V. Scott, Anal. Chem., 40 (1968) 768.
3 M. E. Auerbach, Anal. Chem., 15 (1943) 492.
4 M. E. Auerbach, Anal. Chem., 16 (1944) 739.
5 I. Sheiham and T. A. Pinfold, Analyst (London), 94 (1969) 387.
6 C. G. Taylor and B. Fryer, Analyst (London), 94 (1969) 1106.
7 H. K. Biswas and B. M. Mandal, Anal. Chem., 44 (1972) 1636.
8 D. M. Gabriel and J. Mulley, in J. Cross (Ed.), Surfactant Science Series, Anionic Surfactants—Analytical Chemistry, Marcel Dekker, New York, Chap. 3, in preparation.

Analytica Chimica Acta, 85 (1976) 253—259

DETERMINATION OF NITROGEN IN SOLUTION BY GAS-PHASE MOLECULAR ABSORPTION SPECTROMETRY

M. S. CRESSER

Soil Science Department, Aberdeen University, Old Aberdeen, AB9 2UE (Scotland)

(Received 29th March 1976)

SUMMARY

Measurement of the molecular absorbance at 201 nm of the ammonia gas displaced from strongly alkaline solutions containing ammonium ions provides a rapid, sensitive and selective method for the determination of nitrogen. A simple apparatus based on an atomic absorption spectrometer is described. The method can be applied to the determination of the nitrogen content of soil and plant samples.

The characteristic u.v. absorption spectrum of gaseous ammonia has been recognized for many years [1, 2], and absorption spectrometry has been used [3—5] to monitor the ammonia concentration in air. However, no attempt appears to have been made to determine the ammonium content of solutions by measuring the u.v. absorbance of ammonia gas displaced from alkaline solutions. The results of a preliminary investigation of the feasibility of this technique are reported below.

Preliminary studies

The u.v. absorption spectrum of ammonia in a 10-mm silica cell above ca. 0.2 ml of diluted ammonia solution (diluted to give a suitable absorption signal at 201 nm) was plotted between 195 and 225 nm on a Cary-Varian model 118 double-beam spectrophotometer (Fig. 1).

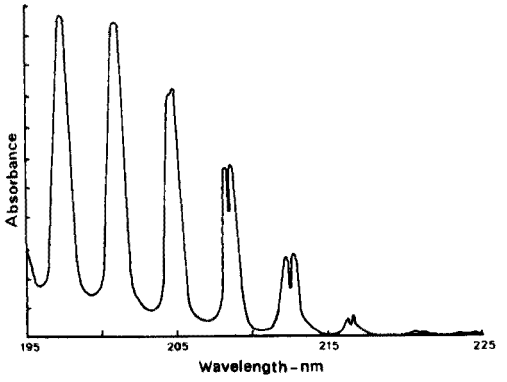

Fig. 1. Absorption spectrum of ammonia gas in a 10-mm cell.

An attempt was made to determine ammonia from the dissociation of ammonium sulphate in a cool flame by measurement of the ammonia absorbance at 201 nm. The ammonium sulphate solutions were nebulized directly into a 100-mm argon—hydrogen—entrained air flame; a Shandon Southern A3400 atomic absorption spectrometer was used with a hydrogen continuum hollow-cathode lamp source. Although linear calibration plots were obtained, the sensitivity was too poor to have any practical value. It was therefore decided to investigate the use of an unheated 500-mm path-length absorption cell, with gaseous ammonia displaced from the alkaline sample solution by a slow flow of air passing through the cell. Analytically useful signals were observed from 20 μg N ml^{-1} solutions, but the precision was initially poor. This was attributed to adsorption of ammonia and slow desorption by and from condensed droplets at the end of the absorption cell. When the 500-mm cell was replaced by a 530-mm condenser, with steam passing through the outer jacket in place of cooling water, this problem was eliminated.

EXPERIMENTAL

Instrumentation

A schematic representation of the apparatus finally used is shown in Fig. 2. Light from an Activion hydrogen hollow-cathode lamp, operated in the d.c. mode, was focussed with a 100-mm focal length silica lens to pass as a narrow beam through the centre of the condenser onto the entrance slit of the monochromator of a Unicam SP900A spectrometer. The output from the spectrometer amplifier was passed to a Bryans 29000 series chart recorder. The zero and photomultiplier e.h.t. controls were adjusted to give true transmittance readings of 0 and 100 %.

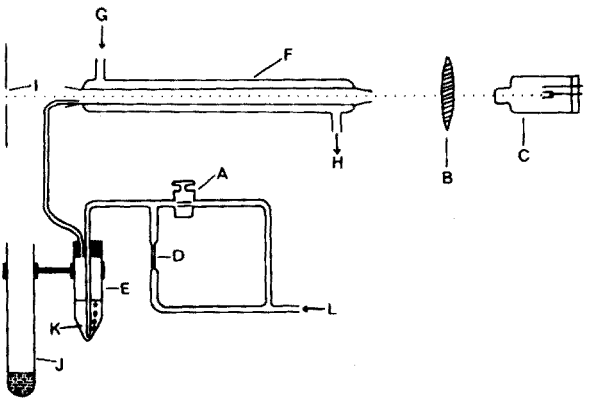

Fig. 2. Schematic representation of apparatus. A, tap; B, silica lens; C, hollow-cathode lamp; D, capillary constriction; E, centrifuge tube; F, condenser; G, steam inlet; H, steam outlet; I, monochromator entrance slit; J, tube containing acid for flushing period; K, sample; L, air inlet.

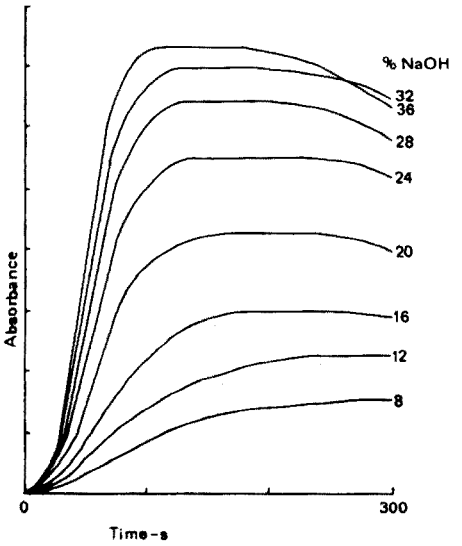

Fig. 3. Effect of sodium hydroxide concentration on absorbance vs. time characteristics.

Effect of sodium hydroxide concentration and temperature

The effect of final sodium hydroxide concentration on absorbance—time plots at an air flow-rate of 150 ml min^{-1} is shown in Fig. 3. Both the rate of evolution of ammonia and the magnitude of the resulting absorption maximum increased with the sodium hydroxide concentration. The rate at which bubbles passed through the sample solution was too rapid for the air to come to equilibrium with the ammonia gas. The peak absorption was therefore found to increase with decreasing air flow-rate over the range 100—2000 ml min^{-1}, and with the depth of solution (at constant NH_3 and NaOH concentrations) through which the air bubbles passed.

The heat of dilution of the stronger sodium hydroxide solutions used caused a small but noticeable increase in the temperature of the samples. The effect of temperature during the flushing stage on the sensitivity of the determination was therefore investigated. Aliquots of 50 μg N ml^{-1} solution (4 ml, as ammonium sulphate) were added to aliquots (20 ml) of 40 % sodium hydroxide solution in a set of identical rigid plastic centrifuge tubes. The tubes were immediately tightly stoppered, shaken, and placed in duplicate in a series of thermostat tanks set at different temperatures for at least 30 min, to allow the attainment of thermal equilibrium. The ammonia gas was then displaced in the normal way. The results obtained are shown in Fig. 4.

Three conclusions may be drawn from these results. Firstly, to obtain good precision at typical laboratory temperatures, storage of samples for an adequate period in a thermostat tank is advisable. Secondly, the effect of the heat of dilution of sodium hydroxide must contribute to some extent to the

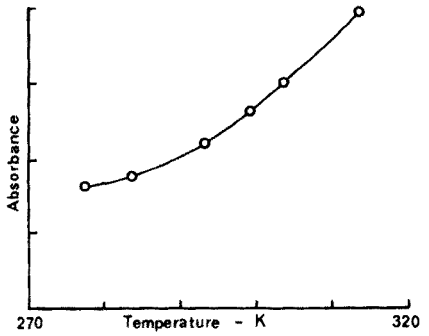

Fig. 4. Effect of temperature on absorbance.

strong dependence of the absorbance of ammonia on sodium hydroxide concentration shown in Fig. 3. Finally, when strongly acidic Kjeldahl digests are to be analysed, the heat of neutralization of the acid, which might be consumed to varying extents by various sample types, would make the use of a thermostat bath essential for samples of diverse composition such as soils.

When the effect of final sodium hydroxide concentration was studied after incorporation of a temperature control step (30 min at 303 K), it was found that the rate of evolution of ammonia increased slightly, particularly at low sodium hydroxide concentrations. Although the absorbance—time plots were generally similar to those shown in Fig. 3, the plots for 36 % and 32 % NaOH were virtually identical, and the dependence on sodium hydroxide concentration was less pronounced.

The effect of employing acid sample solutions is shown in Fig. 5; 50 μg N ml^{-1} solutions were prepared in 0—20 % (v/v) sulphuric acid, aliquots of each (4 ml) were added to aliquots of sodium hydroxide solution (20 ml, 40 %), and the absorbance of the displaced ammonia was measured with and without the thermostatting step. In the absence of any temperature control, the heat of neutral-

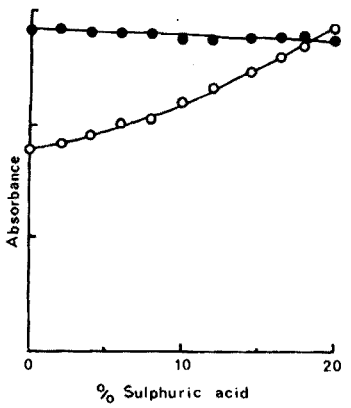

Fig. 5. Effect of sulphuric acid concentration of samples in the thermostatted (•) and non-thermostatted (○) modes.

ization effect was stronger than the effect of the decrease in sodium hydroxide concentration caused by neutralization of the sulphuric acid, and the absorbance increased quite sharply with acid concentration. However, when temperature control was used, only a very slight neutralization effect was observed.

Sequential analysis

When a centrifuge tube is used as a reaction cell, a lower limit upon the useful air flow-rate is imposed by the time required for each sample. At 150 ml min^{-1}, the sample throughput rate was limited to ca. 20 per hour, even at final sodium hydroxide concentrations exceeding 30 %. The analysis rate was improved to some extent by using the by-pass flushing system shown in Fig. 2, which reduced the time required between samples to flush ammonia out of the system; further improvement could be obtained by thermostatting pre-mixed samples at higher temperature.

In the proposed method, the required aliquots of sample and sodium hydroxide solutions are mixed in a clean, dry centrifuge tube; the sample thus prepared may be used immediately, or, if thermostatting is necessary, the tube is tightly stoppered and placed in a thermostat tank for at least 30 min. Tap A is closed, and the bung and glass delivery tube are inserted to a carefully reproduced depth into tube E with the air inlet tube centralized. Once the peak absorbance signal has been recorded, the delivery tube and bung are removed, dried externally with a clean tissue, and inserted in a longer tube containing ca. 2 ml of 6 M sulphuric acid, so that the bottom of the delivery tube is at least 10 mm above the surface of the acid. This prevents small splashes of alkaline solution containing ammonia from causing zero drift between analyses. Tap A is opened, and the absorption cell is flushed at a flow rate of about 1 l min^{-1}.

RESULTS AND DISCUSSION

The method used for the digestion of plant material in this laboratory for nitrogen determination [6] yields acid digests containing less than 6 % sulphuric acid and perchloric acid. The method used for soils yields acid digests containing up to 12 % sulphuric acid, together with K_2SO_4, $CuSO_4$, and selenium. The presence of perchloric acid or selenium, K_2SO_4 and $CuSO_4$ was shown to have no detectable effect on the determination when synthetic standard solutions containing appropriate amounts of acid were tested. Since 2-ml aliquots of sample solution may be used, rather than the 4-ml aliquots used to obtain the data shown in Fig. 5, these correspond in effect to 3 % and 6 % sulphuric acid relative to this Figure. The effects of acid loss during digestion, either by volatilization or chemical reaction, should therefore be small. It is fortuitous that where acid loss is particularly high for soils with a very high organic matter content, the content of nitrogen is often particularly high, and a smaller aliquot of sample solution may be used, together with the

TABLE 1

Comparison of the proposed method and the conventional distillation—titration techniques for soil and plant nitrogen determination

Sample	% N[a]	
	Distillation—titration	Proposed method
Soil		
Tillycorthie grass—sandy loam	0.257	0.260[b]
Keith limestone—silty loam + grit	0.037	0.038[b]
Peat	1.22	1.22[c]
Ythan silt—silty loam	0.795	0.800[b]
Craibstone—sandy loam	0.303	0.301[b]
Cruden Bay clay—clay loam	0.195	0.195[b]
Plant		
Kale	4.31	4.25[b]
Barley	2.00	2.03[b]
Wheatings	2.91	2.90[b]
Spruce needles	1.25	1.23[b]
Pine needles	1.38	1.38[b]
Freeze-dried rye grass	2.08	2.10[b]
Freeze-dried rye grass	2.93	2.96[b]
Freeze-dried rye grass	4.53	4.58[b]

[a] Mean of duplicate determinations on single digests. [b] 2-ml sample + 20 ml of 40 % NaOH. [c] 0.5-ml sample + 1.5-ml reagent blank + 20 ml of 40 % NaOH.

TABLE 2

Precision of proposed method at various nitrogen levels

N concn. (μg ml^{-1})	Absorbance		s_r[a] (%)
	Range	Mean[a]	
10.0	0.086—0.094	0.090	3.0
20.0	0.178—0.188	0.182	1.6
30.0	0.267—0.280	0.275	1.6
40.0	0.360—0.374	0.366	1.2
50.0	0.449—0.469	0.460	1.2

[a] Based on 10 determinations.

addition of an appropriate amount of reagent blank. Standard solutions are prepared in every instance by the addition of aliquots of stock ammonium sulphate solution to the appropriate digest blanks before dilution to volume.

The proposed method was tested on a range of soil and plant samples. Duplicate aliquots of digest were analysed by the proposed method and by conventional distillation—titration techniques; the results obtained are shown in Table 1. To obtain an indication of the precision attainable, ten replicate

4-ml aliquots of each of a range of standard solutions were analysed; 20-ml aliquots of sodium hydroxide solution (40 %) were used, and samples were stored for 30 min at 303 K in every instance. The variation in precision with concentration is shown in Table 2.

The results obtained in this preliminary investigation indicate that gas-phase molecular absorption spectrometry is a rapid, sensitive and selective method for the determination of ammonium-nitrogen in solution and total nitrogen in a wide range of sample types. The procedure and apparatus requirements are simple if an atomic absorption spectrometer is available.

The author is indebted to Mrs. E. Haw for assistance with some of the experimental work, to P. Isaacson for plotting the spectrum, and to the Science Research Council for financial support.

REFERENCES

1 E. Tannenbaum, E. M. Coffin and A. J. Harrison, J. Chem. Phys., 21 (1953) 311.
2 F. A. Gunther, J. H. Barkely, M. J. Kolbezen, R. C. Blinn and E. A. Staggs, Anal. Chem., 28 (1956) 1985.
3 M. J. Kolbezen, J. W. Eckert and C. W. Wilson, Anal. Chem., 36 (1964) 593.
4 F. A. Gunther, R. C. Blinn, M. J. Kolbezen, R. A. Conkin and C. M. Wilson, J. Agric. Food Chem., 7 (1959) 496.
5 F. A. Gunther, R. C. Blinn, M. J. Kolbezen, C. W. Wilson and R. A. Conkin, Anal. Chem., 30 (1958) 1089.
6 T. Batey, M. S. Cresser and I. R. Willett, Anal. Chim. Acta, 69 (1974) 484.

Analytica Chimica Acta, 85 (1976) 261—276

A CALCIUM-SENSITIVE MICROELECTRODE SUITABLE FOR INTRACELLULAR MEASUREMENT OF CALCIUM(II) ACTIVITY

H. M. BROWN, J. P. PEMBERTON and J. D. OWEN

Department of Physiology, University of Utah Medical Center, Salt Lake City, Utah 84132 (U.S.A.)

(Received 16th December 1975)

SUMMARY

A calcium-selective microelectrode with a 1-μm diameter tip suitable for impaling single neurons has been developed. The electroactive material is di[*p*-(1,1,3,3-tetramethylbutyl)phenyl]phosphoric acid (t-HDOPP). The selectivity coefficients are about $5 \cdot 10^{-7}$ for $k_{Ca,K}$, $1—4 \cdot 10^{-7}$ for $k_{Ca,Na}$, and 10^{-3} for $k_{Ca,Mg}$. Values reported previously for other calcium-selective electrodes based on long-chain phenylphosphoric acids are given for comparison. The calcium-selective microelectrodes have a linear response in 0.2 M KCl solutions over the range $10^{-2}—10^{-6}$ M $CaCl_2$; 10^{-7} and 10^{-8} M $CaCl_2$ solutions containing 0.2 M KCl can be detected but the response is not linear.

A calcium(II)-sensitive microelectrode for the assay of calcium(II) activity in the presence of high potassium activity should be useful in many different applications, and would be clearly of value to the cellular physiologist, since it would provide another tool to study the involvement of calcium(II) in several vital cellular functions where it plays an important and direct role, e.g. muscle contraction [1], the visual transduction process [2], and induction of ion permeability changes in nerve cell membranes [3].

Several calcium-sensitive electrodes of different types have been reported [4—9], and some of these innovations are available commercially [10—12]; however, all of them are unsuitable for intracellular measurement of calcium activity since they are (a) too large, or (b) insufficiently sensitive, or (c) inadequately selective for calcium over other cations, especially K^+ and Mg^{2+}, both of which occur in substantial amounts inside cells. Orme [13] has reported on a microelectrode incorporating the Orion calcium(II) ion-exchanger [6] that meets criterion (a) but is unsuited for intracellular measurement because of criteria (b) and (c).

Recent developments in calcium(II)-selective macroelectrodes, particularly by Moody et al. [7] and Růžička et al. [9], prompted us to design and develop a microelectrode that would meet the criteria mentioned above. The microelectrode described here consists of a glass micropipette plugged at the tip by an inert plastic matrix containing an organophosphorus acid, its calcium salt, and a mediator of low dielectric constant. An especial effort

was made to establish the optimal ratio of these constituents since Griffiths et al. [8] have stressed the importance of this in the performance of their macroelectrodes. The electrode developed is sufficiently small at the tip (1—2.5 μm) to be useful for assays in very small volumes (down to 10 nl). Many of the larger nerve, muscle and sensory cells are of this order. By comparison a 200-μl sample is required for small-volume analysis with the Orion flow-through calcium electrode [10] and another instrument using a different principle for assay of calcium(II) requires a sample volume of 5 μl. The present electrode has a linear slope of 20—23 mV/pCa over the range 10^{-1}—10^{-6} M Ca^{2+} in the presence of 0.2 M K^+ and is sensitive to Ca^{2+} beyond 10^{-8} M Ca^{2+} even in 0.2 M K^+. Preliminary studies with single muscle and nerve cells indicate that the value of intracellular calcium activity obtained with these electrodes is in good agreement with values obtained by other means.

EXPERIMENTAL

Materials

A 70 %—30 % (w/w) mixture of the di- and monoesters of octylphenyl acid phosphate was obtained from Pfaltz & Bauer. The chemical names and abbreviations for the di- and monoesters in the mixture are di-[*p*-(1,1,3,3-tetramethylbutyl)phenyl] phosphoric acid (t-HDOPP; I), and mono-[*p*-(1,1,3,3-tetramethylbutyl)phenyl] phosphoric acid (t-H_2MOPP; II).

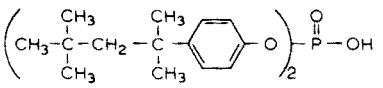

(I)

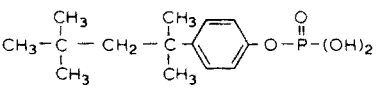

(II)

The abbreviated names are consistent with the codes for similar compounds used by Růžička et al. [9]; our t (for tertiary octyl) is used to differentiate between the straight-chain di-[*p*-(n-octyl)phenyl] phosphoric acid (HDOPP) used by Růžička et al. [9] and the branched compound used in the electrode described here. The commercial ester mixture was treated by the method of Růžička et al. [9] to obtain the diester. For future discussion the diester will be called the acid. Some of the acid was converted to the calcium salt (the salt) by precipitation from an ethanolic solution of the acid, aqueous $CaCl_2$ and NaOH. The precipitate formed was filtered and dried. Di-(n-octyl) phenylphosphonate (the mediator; III; DOPP-n; Aldrich Chemicals) was used as received.

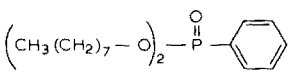

(III)

Electrode preparation

The sensor was prepared by combining the salt and the acid in a 1:2 molar ratio. The mediator was then combined with the sensor in a 10:1 (w/w) ratio. Polyvinylchloride (PVC; Breon S 110-10, B. P. Chemicals International) [8] was added in various weight-percents to determine the optimum ratio for a particular electrode size as described under Results. The mixture was allowed to dissolve in 6 ml of tetrahydrofuran (THF) for 1—2 h. Pyrex capillary tubing (1 mm i.d.) was pulled on a micropipette puller (Industrial Science Assoc., Ridgewood, New York) to obtain electrodes with tip sizes of 1.0 and 2.5 μm. For each tip size, the ratio of PVC to acid-salt-mediator was found to be crucial to obtain functioning microelectrodes. The electrode tips were silanized by dipping them in a 3 % (v/v) solution of tri-n-butyl-chlorosilane (Columbia Organic) in 1-chloronaphthalene (Eastman) and baked in an oven for 10 min at 250 °C, as described by Walker [14]. The solvent (THF) was allowed to evaporate for 20—30 min leaving a sturdy membrane 75—100 μm in thickness at the tip of the electrode. The electrode was then filled with a 0.1 M $CaCl_2$ internal filling solution. These details are shown schematically in Fig. 1. The salt bridge to the Ag/AgCl reference electrode was a 3 M KCl-filled pipette with a tip size of 50—100 μm. The electrochemical cell for measurements was

$$\text{Ag/AgCl} \mid \text{0.1 M } CaCl_2 \mid \text{Membrane} \mid Ca^{2+} \text{ sample} \parallel \text{3 M KCl} \mid \text{AgCl/Ag}$$

The indicator half-cell was led off to a varactor bridge amplifier (input impedance: 10^{14} ohms) and the reference half-cell was at the midpoint of the power supply of the varactor bridge which was the system reference potential. The potential difference between the indicator and reference

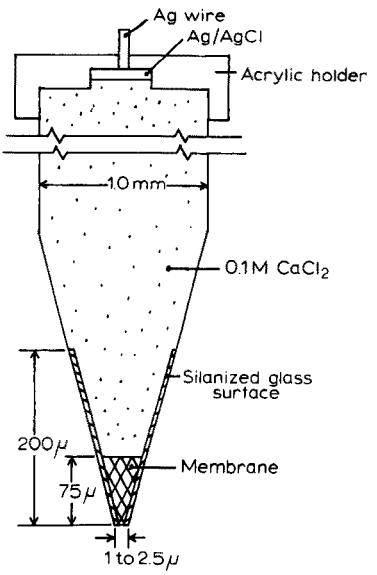

Fig. 1. Construction features of the calcium-sensitive microelectrode.

electrodes was displayed on a digital voltmeter; the time course of the potential changes was displayed on a conventional chart recorder. Measurements of hydrogen ion interference were made with a standard X-Y recorder in conjunction with a Corning 470651 glass electrode and Model 110 pH meter.

Electrode calibration and selectivity

Calibrating solutions. Calibrating solutions were buffered to pH 7.26 with Tris/Tris-HCl (50 mM) except when the effects of pH on the electrode performance were evaluated. This pH (7.26) is within the range (7.0—7.4) measured in single cells [15]. A further prerequisite for the standard calibrating solutions was that they all contained 0.2 M K^+ since this is the maximum concentration encountered in most intracellular investigations. An advantage of using a high background potassium concentration is that all of the calibrating solutions are at the same ionic strength (with the exception of the 0.1 M Ca^{2+} solution) and the calcium activities should remain relatively constant in each test solution. Also changes in the junction potentials at the electrode/solution interface are minimized and plots of e.m.f. vs calcium concentration should yield the same slopes as those obtained for pure solutions.

It was found by spectrophotometric measurements with murexide, that accurate calcium(II) solutions much below 10^{-5} M Ca^{2+} could not be prepared from our laboratory water since the water itself contained about 10^{-6} M Ca^{2+}. Therefore, two sets of solutions were used routinely for calibrating procedures. The first set was used to cover the range of 10^{-1}—10^{-5} M calcium(II) by serial dilution of a 0.1 M $CaCl_2$ solution containing 0.2 M KCl and 50 mM Tris buffer with a solution containing 0.2 M KCl and the buffer. The second set of solutions were buffered to the appropriate pCa with the calcium—ligand systems EDTA (ethylenediaminetetracetic acid), EGTA (ethyleneglycol-bis-(β-amino ethyl ether)N,N′-tetraacetic acid), or NTA (nitrilotriacetic acid). These calcium buffers were made up to contain a final concentration of 0.2 M K^+, and Tris was used to buffer the pH. The EDTA complex formation constant (K) used to compute the calcium concentration of the EDTA buffers at pH 7.26 was $\log K_{CaEDTA} = 10.7$ [16].

The calibrating solutions were checked empirically with potassium-selective ion-exchanger electrodes and the measured values were all within about 5 % of one another. The computed potassium activity of the solutions was about 0.70 which is in close agreement with published values of a 0.2 M KCl solution. This value was used in Fig. 6 to obtain estimates of calcium activity in artificial salines.

Electrode conditioning and selectivity measurements. Each electrode was preconditioned by soaking at least overnight in a pCa 5 solution with 0.2 M KCl

(pH 7.26). The time for pre-conditioning could be reduced to a few hours by soaking in a pCa 3 solution of $CaCl_2$ and 0.2 M KCl. The calibrating procedure commenced by equilibrating the electrode in the solution with the lowest Ca^{2+} value, then to the highest value and then in decade steps back to the lower concentrations. The selectivity coefficients, $k_{Ca,i}$, where i represents a monovalent interfering species (K^+, Na^+ and H^+) were evaluated by the mixed solution method [7]; magnesium(II) interference was evaluated by both the mixed solution and separate solutions methods [7]. Estimates of calcium(II) in two artificial salines containing different amounts of calcium were obtained graphically.

RESULTS

Electrode calibration

The following data were obtained from electrodes with a 2.5-μm tip size and 22 % PVC. The influence of tip size and PVC ratios on electrode performance are described later.

Figure 2(A) shows changes of the electrode potential over seven decades of calcium(II) concentration; each solution contained 200 mM KCl and was buffered to pH 7.26. In panel 1, the electrode was in the $2 \cdot 10^{-8}$ M Ca^{2+} (EDTA) solution; the electrode potential was −57 mV. A change in the Ca^{2+} concentration to 10^{-1} M produced a rapid change in the electrode potential to + 100 mV about 30 s after the solution was changed, and then a slower change of about +10 mV over the next 5 min, after which the potential remained stable. In panel 2, the input was momentarily grounded (0-mV) while the solution was changed to one containing 10^{-2} M Ca^{2+}. After this change, the input was once again connected to the electrode (arrow); the potential in this solution was stable within 1 min. Panels 3—8 show potential changes to successive ten-fold changes in calcium concentration. With each decade change in calcium concentration the potential change was 22—23 mV which is in close agreement with the initial total change for approximately seven decades (22 mV/decade). The final electrode voltage in the $2 \cdot 10^{-8}$ M Ca^{2+} solution was within 3 mV of the original value obtained an hour earlier. Figure 2(B) shows the relation between electrode potential and the logarithmic calcium(II) concentration; the relationship for this particular electrode is reasonably linear over the full range, with a slope of 23 mV/decade.

Interfering ions

Potassium. The performance of the microelectrode in environments containing low Ca^{2+} and high K^+ concentrations was of particular interest. This presented some problems, since calcium(II) buffers are required to provide low calcium(II) concentrations, and the conventional method of establishing selectivity coefficients with different interferents is to compare electrode behavior in solutions containing only the primary ion and solutions

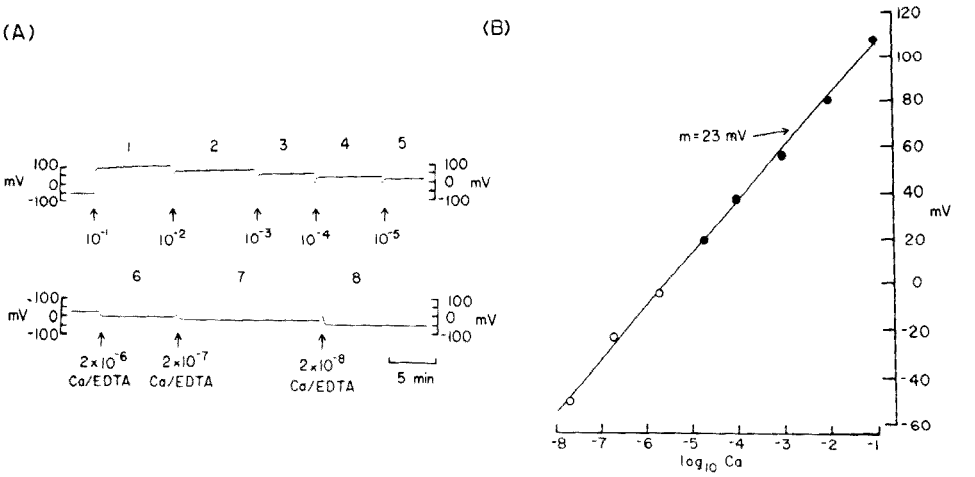

Fig. 2.
(A): Potential changes of a Ca^{2+} microelectrode from changes of Ca^{2+} concentration over the range 10^{-1}—$2 \cdot 10^{-8}$ M; 200 mM K^+ was present in all solutions. In panel 1, the solution was exchanged by washing without grounding the amplifier input whereas the input was grounded (0 mV) between changes of solution in each of the other panels.
(B): Relation between electrode potential and the logarithm of the Ca^{2+} concentration. Data obtained from Fig. 2(A). The straight line represents a rate of 23 mV/pCa. •$CaCl_2$ + 200 mM KCl with serial dilutions. ○ $CaCl_2$ + EDTA + 200 mM KCl.

containing the interferent and primary ion. A baseline at lower calcium(II) concentrations was required so that it could be established that any changes in the calibration curves in the presence of interferent were due to selectivity rather than sensitivity. For this purpose, the e.m.f. of six individual electrodes was measured in solutions containing only $CaCl_2$ (plus Tris buffer), solutions containing 50 mM KCl and 10^{-1}—10^{-5} M Ca^{2+} and Ca/EDTA solutions ($2 \cdot 10^{-6}$—$2 \cdot 10^{-8}$ M Ca^{2+}) containing 50 mM K^+. Data were also obtained over the same calcium range with solutions containing 200 mM K^+. The calibrating procedure required 6—8 h for each electrode. The protocol used was as follows. The solutions containing 0.2 M K^+ were used as the "standards" since they were of primary interest. The electrode was returned to a standard containing a certain calcium concentration and the e.m.f. checked after each exposure to the test solutions containing 50 mM K^+ or no potassium. For example, the data points shown in Fig. 3(A) at 10^{-1} M Ca^{2+} were obtained by first exposing the electrode to the 10^{-1} M Ca^{2+}—0.2 M K^+ solution (•); then the e.m.f. was obtained in the K^+-free solution (○), then back to the 0.2 M K^+ solution, then to the 50 mM K^+ solution (△) back to the 0.2 M K^+ solution and so on. This procedure was repeated at each calcium concentration. If the electrode e.m.f. varied by more than 1—2 mV in any standard solution (0.2 M K^+) that preceded or followed a particular test solution, the entire run was conducted again. The average e.m.f. from six electrodes examined in this

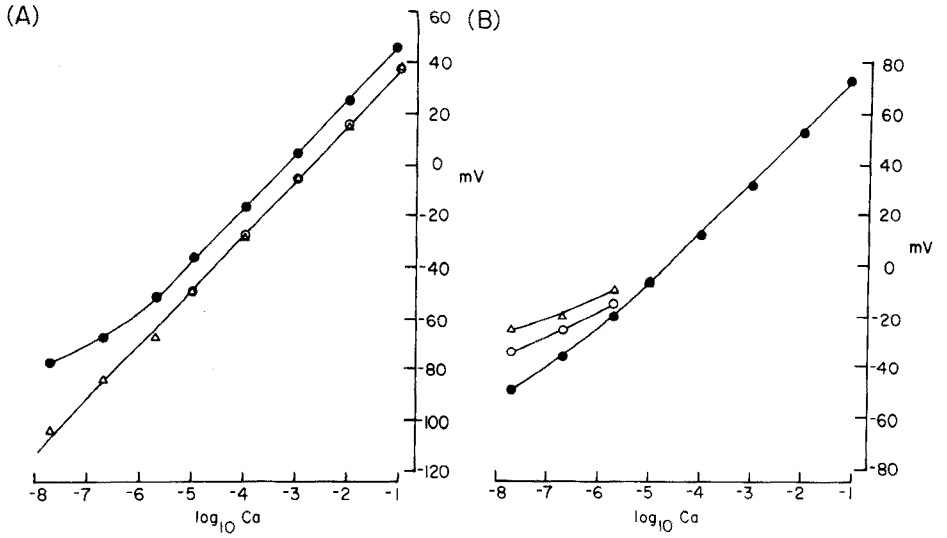

Fig. 3. Potassium interference.
(A): The average e.m.f. from six electrodes calibrated in solutions containing only $CaCl_2$ (○), Ca^{2+} solutions containing 50 mM K^+ (△), and Ca^{2+} solutions containing 200 mM K^+ (●). Note that the slopes are parallel for each potassium concentration down to $2 \cdot 10^{-6}$ M Ca^{2+}.
(B): Average e.m.f. of another group of four electrodes in Ca^{2+} solutions containing 200 mM K^+ (●), 500 mM K^+ (○), and 1000 mM K^+ (△).

way is shown in Fig. 3(A). In solutions containing only the primary ion or low K^+ (50 mM), the average electrode response appears linear (21.5 mV/decade) down to $2 \cdot 10^{-8}$ M Ca^{2+}. Background 200 mM K^+ did not affect the slope down to $2 \cdot 10^{-6}$ M Ca^{2+}, but at lower concentrations, the response deviated. Nevertheless, between pCa 7 and 8 at 200 mM K^+, the electrode response remained substantial (10—11 mV). This plot also shows that increasing the ionic strength produces a shift of the electrode potential (+ 10 mV), though the slope remains unchanged. Two electrodes in the group did not show this shift, and it is not known whether this was due to the calcium-sensitive electrode, the reference electrode, or both. However, the results provide a basis for maintenance of the ionic strength at a relatively constant level in evaluation of electrode performance.

Table 1 shows the mean difference in e.m.f. between 50 mM K^+ and 200 mM K^+ solutions at low calcium concentrations for this group of electrodes. For this analysis, the ionic strength effect was corrected for individual electrodes by shifting each point by the deviation observed at 10^{-1} M Ca^{2+}. Student's *t*-test was used to determine which differences were statistically significant. As expected from the small standard deviation of the differences and the mean differences shown in Fig. 3(A), 200 mM K^+ produces a significant effect only at the two lower calcium levels; down to $2.5 \cdot 10^{-6}$ M Ca^{2+}, the

TABLE 1

t-Tests of differences between electrode potentials in solutions containing 200 mM and 50 mM K^+ ($n = 6$)

$[Ca^{2+}]$ (M)	$\bar{y} \pm s$ (mV)[a]	t[b]	S[c]
$1 \cdot 10^{-5}$	0.3 ± 1.63	0.5	—
$2 \cdot 10^{-6}$	0.83 ± 3.25	0.6	—
$2 \cdot 10^{-7}$	8.5 ± 2.2	9.6	*
$2 \cdot 10^{-8}$	16 ± 2.3	17.2	*

[a]Mean difference ± standard deviation. [b]Paired comparisons. [c]*Indicates significant at 0.025 level in 2-tailed tests.

electrode response remained substantially the same in 50 mM or 200 mM potassium.

Table 2 summarizes the selectivity coefficients obtained for individual electrodes in this group. The $k_{Ca,K}$ values obtained were $2—5 \cdot 10^{-7}$; the average $k_{Ca,K}$ value was $4.5 \cdot 10^{-7}$.

Another group of four electrodes was used to evaluate the effect of still higher potassium concentrations. The protocol was the same as that described above, i.e., the electrode was exposed to the standard 200 mM K^+ solutions before and after each exposure to the 500 mM K^+ or 1000 mM K^+ solutions. The relation between the average electrode e.m.f. and Ca^{2+} concentration is shown in Fig. 3(B). The measurements from each electrode were shifted by an appropriate amount to correct for ionic strength effects observed at 10^{-1} M Ca^{2+}. This produced essentially coincident curves down to 10^{-5} M Ca^{2+}. At lower calcium concentrations, the electrode potential became systematically more positive as the background K^+ was increased. However, even in the presence of 1 M K^+, the potential change was about 10 mV for pCa 6—7 and 5 mV for pCa 7—8. Table 3 summarizes the differences in electrode potentials in 0.2, 0.5 and 1.0 M K^+ from this group of electrodes at the lower calcium concentrations. Increasing the potassium concentration from 0.2 to 0.5 M produced a significant positive shift of the electrode e.m.f. at the two lower levels of calcium concentration, but on increasing the potassium from 0.5 M to 1.0 M, there was no statistical difference in e.m.f. This is attributable to smaller differences in e.m.f. for the change 0.5 to 1.0 M K^+ than for 0.2 to 0.5 M K^+.

Table 2 summarizes the selectivity coefficients calculated for individual electrodes in this group at each background potassium concentration. The individual selectivity coefficients were comparable to those obtained from the other group at 0.2 M K^+, although the coefficients tended to increase slightly at 1 M K^+. The coefficients range from $2 \cdot 10^{-7}$ (at 0.2 M KCl) to $7 \cdot 10^{-7}$ (at 1.0 M KCl).

TABLE 2

Selectivity coefficients ($k_{Ca,K}$)[a] for individual electrodes determined from mixed solutions

Electrode	Concentration of interferent (K^+)			
	0.2 M[b]	0.2 M[c]	0.5 M[c]	1.0 M[c]
1	$2.0 \cdot 10^{-7}$	$1.4 \cdot 10^{-7}$	$4 \cdot 10^{-7}$	$7 \cdot 10^{-7}$
2	$2.5 \cdot 10^{-7}$	$1.4 \cdot 10^{-6}$	$1.6 \cdot 10^{-6}$	$4 \cdot 10^{-7}$
3	$2.5 \cdot 10^{-7}$	$<10^{-7}$	$3 \cdot 10^{-7}$	$3 \cdot 10^{-7}$
4	$2.5 \cdot 10^{-7}$	$<10^{-7}$	$4 \cdot 10^{-7}$	$7 \cdot 10^{-7}$
5	$2.5 \cdot 10^{-7}$			
6	$5 \cdot 10^{-7}$			

[a]From $k = [Ca]/[i]^{z/z}$. $\Delta V = 18$ mV. [b]Electrodes from Fig. 3(A). [c]Electrodes from Fig. 3(B).

TABLE 3

t-Tests of differences between electrode potentials in solutions containing 1000 mM, 500 mM and 200 mM ($n = 4$)

[Ca] (M)	(0.5 M − 0.2 M) $\bar{y} \pm s$ (mV)[a]	t[b]	S[c]	(1.0 M − 0.5 K) $\bar{y} \pm s$ (mV)[a]	t[b]	S[c]
$2 \cdot 10^{-6}$	4.3 ± 4.4	1.95	—	3.0 ± 3.6	1.44	—
$2 \cdot 10^{-7}$	9.5 ± 1.7	11.0	*	4.3 ± 4.5	1.66	—
$2 \cdot 10^{-8}$	16.8 ± 4.4	7.57	*	5.3 ± 5	1.8	—

[a]Mean difference ± standard deviation. [b]Paired comparisons. [c]*Indicates significant at 0.025 level in 2-tailed tests.

Sodium. Similar experiments were conducted to investigate interference from sodium ion. Sodium affects the electrode in much the same way as potassium, and the selectivity coefficients of individual electrodes are in the same range. Data obtained with 200 mM Na^+ instead of K^+ produced curves similar to those shown in Fig. 3(A). At the lower calcium concentrations the shift of the electrode potential increased as the sodium ion concentration was increased as in Fig. 3(B). These shifts (corrected for ionic strength) allowed estimates of the selectivity coefficients; four electrodes yielded $k_{Ca,Na}$ values ranging from $<1 \cdot 10^{-7}$ to $4 \cdot 10^{-7}$. There was no evidence that the selectivities were concentration-dependent.

Magnesium. Figure 4(A) shows the mean e.m.f. ± standard deviation of four different electrodes standardized in solutions of calcium(II) or magnesium(II) containing 0.2 M KCl. For purposes of comparison, the e.m.f. values of each electrode were normalized to + 60 mV in the 10^{-1} M Ca^{2+} solution. The e.m.f. in 10^{-1} M Mg^{2+} solution was about 65 mV more negative than in 10^{-1} M Ca^{2+} solution. The change in e.m.f. over the decade 10^{-1}—10^{-2} M Mg^{2+} was

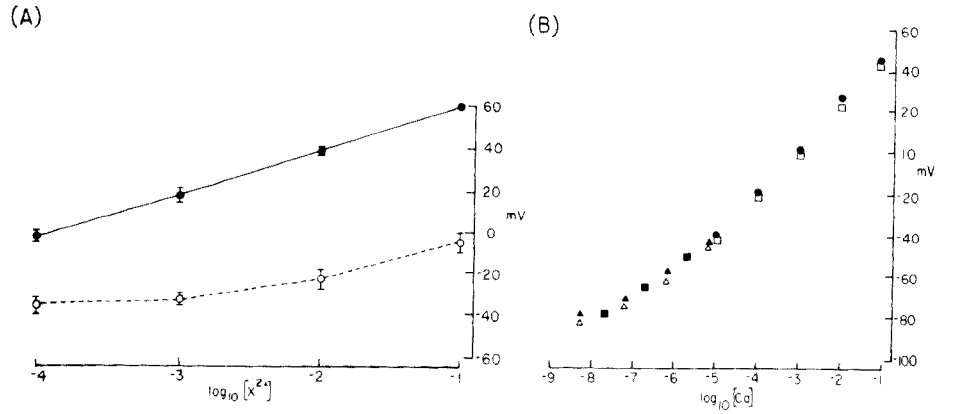

Fig. 4. Magnesium interference.
(A): Mean (± s.d.) of four electrodes calibrated in $CaCl_2$ (•), and $MgCl_2$ (○); all solutions contained 200 mM KCl. Data from individual electrodes were normalized to + 60 mV in the 0.1 M $CaCl_2$ solutions.
(B): Electrode response in Ca^{2+} solutions containing a constant background of 200 mM K^+ (•, ▪), and 200 mM K^+ plus 2 mM Mg^{2+} (□, △). (•) $CaCl_2$. (▪, □) Ca—EDTA. (▲, △) Ca—EGTA. The electrode response remained virtually unchanged in the presence of 2 mM Mg^{2+}.

substantial, but was small at lower concentrations, e.g. 3 mV for 10^{-3}—10^{-4} M Mg^{2+}. The same electrodes showed slopes of 21 mV/decade for calcium(II). The selectivity coefficient $k_{Ca,Mg}$ calculated from these average data was $1.4 \cdot 10^{-3}$ from the difference in potential at 10^{-1} M, and $5.3 \cdot 10^{-2}$ at 10^{-4} M. When calculated from the ratio of the activities at the same potential (—4 mV), the $k_{Ca,Mg}$ value was $1.4 \cdot 10^{-3}$. Values are tabulated for six separate electrodes in Table 4.

The range of values obtained from separate electrodes by the different methods was quite broad, i.e., from 10^{-2} to $3 \cdot 10^{-4}$. The higher values are anomalous in that they were obtained at a concentration (10^{-4} M) where the electrode responds very well to calcium yet negligibly to magnesium(II). Two separate lines of evidence indicate that $k_{Ca,Mg}$ is less than 10^{-3} and for some electrodes may be ca. 10^{-5}. The specification for the magnesium chloride used to make the stock solutions indicated that a 0.1 M solution would contain $2.5 \cdot 10^{-6}$ M Ca^{2+}. The potential drop of the electrodes from 10^{-1} M $CaCl_2$ to 10^{-1} M $MgCl_2$ would put the calcium concentration in the magnesium solutions at pCa 4—5 (Fig. 4). However, the potential difference of about 30 % of the electrodes calibrated under conditions shown in Fig. 4 was great enough to reach the pCa 5—6 region; under these conditions extrapolation of the calcium calibration curve produced an intersection with the magnesium curve between pCa 5 and 6. This evidence is indirect but is substantiated by experiments in which the calcium concentration was varied in the presence of a constant background of Mg^{2+} and K^+ (Fig. 4(B)). Data from an electrode demonstrating little interference from Mg^{2+} is shown. By comparing the e.m.f. values in solutions with and without magnesium (both

TABLE 4

Selectivity coefficients for individual electrodes determined from separate solutions of $CaCl_2$ and $MgCl_2$ in the presence of 200 mM KCl

Electrode	Selectivity coefficients		
	1[a]	2[b]	3[c]
1	$3 \cdot 10^{-2}$	$5.7 \cdot 10^{-4}$	*[d]
2	$1.5 \cdot 10^{-2}$	$5.7 \cdot 10^{-4}$	$1.25 \cdot 10^{-3}$
3	—	$3 \cdot 10^{-4}$	*[d]
4	$1 \cdot 10^{-2}$	$4 \cdot 10^{-3}$	$4.5 \cdot 10^{-3}$
5	$2.6 \cdot 10^{-2}$	$1.4 \cdot 10^{-3}$	$1.4 \cdot 10^{-3}$
6	$1.2 \cdot 10^{-2}$	$1.7 \cdot 10^{-3}$	$2 \cdot 10^{-3}$

[a]From difference of potential at 10^{-4} M. [b]From difference of potential at 10^{-1} M. [c]From ratio of concentrations at the same electrode potential. [d]No potential overlap in Mg^{2+} and Ca^{2+} solutions.

with 200 mM K^+) it can be seen that the limit of detection for calcium in the sub-micromolar range remains very good even in the presence of millimolar magnesium(II). Some other electrodes showed different behavior in these complex solutions (2 mM Mg^{2+} plus 200 mM K^+): the slope was augmented in high Ca^{2+} (10^{-1}—10^{-4} M) but depressed in lower Ca^{2+} concentrations, and the limit of detection was not less than 10^{-6} M. At present we have no explanation for these differences.

Hydrogen. The potential changes at different values of pH are shown in Fig. 5. The electrodes were calibrated before these tests from 10^{-1}—$2 \cdot 10^{-8}$ M Ca^{2+} in the presence of 200 mM K^+. The input from the electrode was then applied to the y-axis of an x—y point plotter and pH was monitored on the x-axis. The solutions were made basic with potassium hydroxide, and then progressively acidified with hydrochloric acid. The electrodes would not recalibrate after exposure to solutions outside the pH range 3—10. Figure 5 shows that the electrode response at constant calcium concentrations of 10^{-2}—10^{-4} M remains stable (within 1—2 mV) from pH 9 to pH 5; the pH range was extended as the calcium concentrations were increased. But at all calcium concentrations the behavior of the electrodes indicated a preference for hydrogen ion over calcium(II). The characteristic "dip" that precedes the positive potential change at low pH that has been observed in several other calcium electrodes [6—9] was not observed with the present electrode.

Complex solutions

Estimates of the calcium activity in two artificial physiological salines [17, 18] with salt compositions similar to sea water were obtained to ascertain whether or not reasonable values of calcium activity could be obtained after

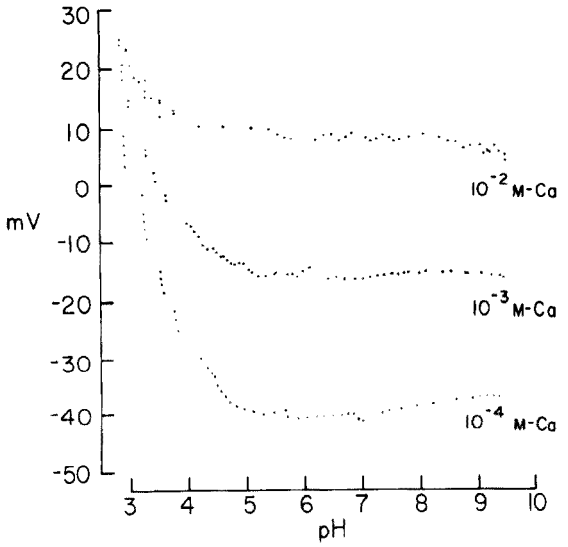

Fig. 5. Hydrogen ion interference. Change in response to a decrease in pH from 9.5 to 3 at three different Ca^{2+} concentrations is noted. The electrode was recalibrated between each pH run.

the electrode had been calibrated in calcium solutions containing 200 mM K^+ The composition of these salines is shown in Table 5. These salines are commonly used in conjunction with certain molluscan neurones (*Aplysia*) and crustacean neurons (barnacles) and are designated ASW and NBS respectively. Data in Fig. 6 were plotted with the activity coefficient for a solution of 0.2 M KCl (0.72), except for data obtained in the solution containing 0.1 M $CaCl_2$ and 0.2 M KCl. In the latter case, an activity coefficient of 0.6 was used based on empirical estimates of the reduction of chloride activity in solutions containing known amounts of $CaCl_2$ [19]. After calibration of the electrodes in standard solutions containing 0.2 M K^+, the e.m.f. was measured in one or both of the artificial salines. Both contained essentially the same amount of NaCl (ca. 0.5 M) and KCl (ca. 10 mM) but ASW contained half as much calcium as NBS (10 vs. 20 mM) and about four times as much magnesium. The e.m.f. values from different electrodes in the 10 mM Ca^{2+}—50 mM Mg^{2+} saline are indicated by (○) in the top five curves of Fig. 6. The range of a_{Ca} obtained was from 5—7 mM; the mean a_{Ca} was 5.8 ± 0.76 mM. This average value yields an activity coefficient of 0.58. The saline containing 20 mM Ca^{2+} and 12 mM Mg^{2+} yielded the potentials represented by (△) which are superimposed on the appropriate calibration curve. The range of a_{Ca} from these curves was 8.5—10.5 mM with a mean value of 9.5 ± 0.94 mM. The average value yields an activity coefficient of 0.48 for this saline. The activity coefficient of a pure solution of 0.5 M NaCl is 0.6 and it has been found empirically [19] that the addition of divalent cations in the amounts stated above can depress the chloride activity in a

TABLE 5

Composition (in mmol) of two artificial salines used in *Aplysia* (ASW) and barnacle (NBS) studies

	ASW	NBS
NaCl	494	462
KCl_2	10	8
$CaCl_2$	10	20
$MgCl_2$	20	12
$MgSO_4$	30	0
Tris/Tris HCl pH 7.65	10	10

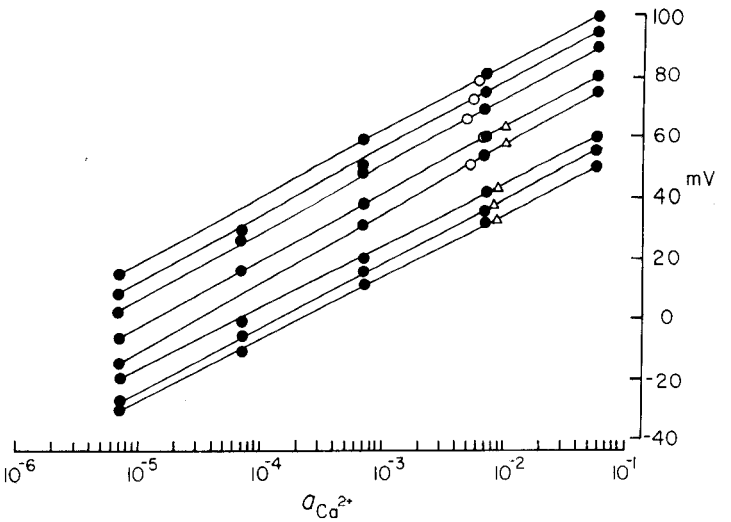

Fig. 6. Estimates of calcium activity from eight separate electrodes in two physiological salines containing different concentrations of Ca^{2+}: ○ = 10 mM, △ = 20 mM.

0.5 M NaCl solution to about 0.5, which is in good agreement with the values obtained.

Influence of tip size and PVC ratios on electrode performance

It was found for a given microelectrode tip size that the PVC and the sensor material ratio (w/w) can be a variable influencing electrode performance. In general, raising the amount of PVC above 22 % (w/w) tended to depress the slope of the calibration graph; above 28 % PVC, the sensitivity was also reduced. As tip size was reduced, some reduction in PVC was needed to maintain good electrode performance. Reduction of the tip size from 2.5 μm to 1.0 μm in two different groups of electrodes reduced the slope from about 22 to about 19 mV/decade. The slopes of the calibration lines of another group of electrodes with 1-μm tips but with reduced PVC (10 %),

were similar to the larger tipped electrodes. Alternatively, the 1-μm tips of electrodes containing 22 % PVC could be carefully broken back on a microforge to 2.5 μm so that the usual 22 mV slope was obtained. Other versions of the sensor and different ratios of PVC to sensor/mediator which show promise of enhancing the performance of electrodes with tip sizes of 1 μm without sacrificing the other characteristics described above are under study.

Other approaches to a calcium microelectrode

A miniaturized electrode of the type described by Bloch et al. [5] was made; the electrode response was good in pure solutions of $CaCl_2$ but minimal to calcium(II) changes in the presence of 0.1 M K^+. Variations of the paraffin electrode [20] were also made, with different but equally disappointing results; these electrodes could only be made with an extremely low yield and the slopes were low (10—12 mV), though some showed promise of measuring low calcium values in the presence of high potassium concentrations. Another approach attempted was to introduce the calcium ionophore 23187 (Lilly) into a PVC membrane. This approach was promising but still fell short of the electrode described above. The performance of one of these electrodes is shown in Fig. 7; the electrode was calibrated in calcium solutions containing 0.2 M K^+. For 10^{-1}—10^{-4} M Ca^{2+}, the potential change ranged from 26 to 20 mV/decade, but below 10^{-4} M Ca^{2+} the slope was greatly diminished and there was no change below 10^{-6} M Ca^{2+}. Tetraphenylborate was also introduced into the membrane since this substance has been reported to enhance the performance of some other calcium(II) systems [21]. The electrode performance was basically the same as depicted in Fig. 7.

DISCUSSION

The miniature calcium(II)-selective electrode described here possesses selectivity and sensitivity characteristics that make it potentially suitable for intracellular measurement of calcium(II). The electrode has several advantages over others made here. It is easy to build, small, and sufficiently sensitive and selective to calcium(II) to be of utility for low-level measurements in the presence of high levels of potassium and moderately high levels of magnesium ions. The time course of the potential change in response to a change in calcium concentration is comparable to that of the macroelectrodes described by Moody et al. [7] and Růžička et al. [9]. But the selectivity and sensitivity of the present microelectrode appear to be superior to both of these macroelectrodes. The slope of the present electrodes (ca. 22 mV/dpCa) is somewhat less than that obtained with the macroelectrodes (29 mV/pCa); preliminary studies indicate that this is not due entirely to the process of miniaturization. This disadvantage is compensated for by the sensitivity of the electrode which has a useful range down to $1 \cdot 10^{-8}$ M Ca^{2+} even in the presence of 0.2 M K^+ and 2 mM Mg^{2+}.

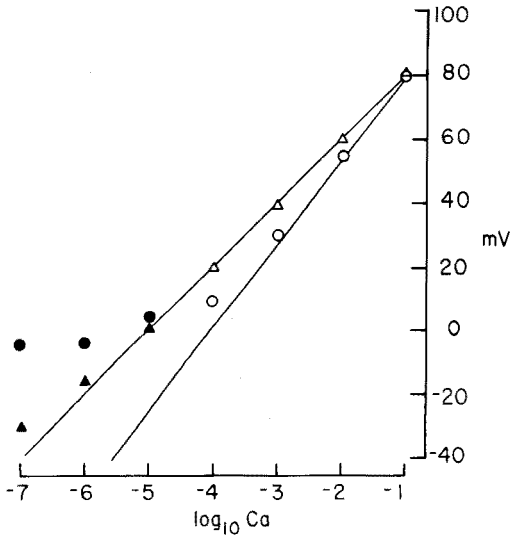

Fig. 7. Comparison of the performance of a calcium(II)-ionophore microelectrode (○) with the calcium(II) electrode described herein (△). Both electrodes contained 20 % PVC and had 2-μm diameter tips. All solutions contained 200 mM K^+. Darkened symbols correspond to NTA solutions.

Selectivities for the present electrode were measured in the same way as those reported for other calcium-sensitive electrodes so that results from this study could be readily compared. In general, the range of $k_{Ca,Mg}$ is similar to that obtained for some macroelectrodes. Moody et al. [7] reported somewhat lower selectivity coefficients ($1.3 \cdot 10^{-1}$—$5.3 \cdot 10^{-3}$) when the difference in potential in separate solutions was used for the calculation. The values for the present electrode are $4 \cdot 10^{-3}$—$3 \cdot 10^{-4}$, with the same method in the same concentration range. Růžička et al. [9] reported $2.5 \cdot 10^{-4}$ for the value of $k_{Ca,Mg}$ by the separate solution method, but details of the method were not given. Quite different values can be obtained depending on the method of computation (cf. Table 4) as emphasized by Moody et al. [7]. Two additional methods were used to estimate $k_{Ca,Mg}$. One is shown in Fig. 4(B) and the other involved reciprocal dilutions of Ca^{2+} and Mg^{2+} at constant ionic strength; these produced values of $k_{Ca,Mg}$ that were consistently between $1 \cdot 10^{-4}$ and $1 \cdot 10^{-3}$. These values are consistent with the values shown in Table 4 and are considered to be the best estimates of $k_{Ca,Mg}$ for the electrodes examined in the present study.

Na^+ and K^+ selectivities were evaluated on previously reported calcium electrodes, which contained different sensing materials by the mixed solution method, which was also used here. Růžička et al. [9] reported values of $6.3 \cdot 10^{-6}$ and $2 \cdot 10^{-6}$ for Na^+ and K^+, respectively; Moody et al. [7] reported values of $6.7 \cdot 10^{-5}$ for Na^+ and $2.2 \cdot 10^{-5}$ for K^+. Generally, K^+ and Na^+ appeared to affect the performance of the present electrode in much

the same way, i.e., the values of $k_{Ca,Na}$ were in the same range as those obtained for K^+ (Table 2). The best single estimate of these values based on the average data is about $5 \cdot 10^{-7}$.

Preliminary experiments involving penetration of muscle cells (100-μm diameter) from the barnacle *B. eburneus* and large ganglion cells (500 μm) from *Aplysia californica* with these calcium microelectrodes have been conducted. The range of the free calcium(II) concentration obtained from these impalements is 10^{-6}—10^{-7} M. This is in good agreement with values obtained by other investigators who used less direct methods.

This work was supported in part by Utah Heart Grant 2531 and NIH Grant EY 00762 from the National Eye Institute. The careful technical assistance of Toni Gillett, and the help of Sharon Edde in preparing the manuscript, are gratefully acknowledged. We also thank Dr. G. J. Moody for the sample of PVC and Eli Lilly for providing ionophore A23187.

REFERENCES

1 S. Ebashi and M. Endo, Prog. Biophys. Mol. Biol., 18 (1968) 123.
2 W. A. Hagins, Annu. Rev. Biophys. Bioeng., 1 (1972) 131.
3 R. W. Meech, Comp. Biochem. Physiol., 42 A, (1972) 493; J. Physiol., 237 (1974) 259.
4 H. J. C. Tendeloo and A. Krips, Rec. Trav. Chim., 77 (1958) 406, 678.
5 R. Bloch, A. Shatkay and H. A. Saroff, Biophys. J., 7 (1967) 865.
6 J. W. Ross, Science, 156 (1967) 1378.
7 G. J. Moody, R. B. Oke and J. D. R. Thomas, Analyst (London), 95 (1970) 910.
8 G. H. Griffiths, G. J. Moody and J. D. R. Thomas, Analyst (London), 97 (1972) 420.
9 J. Růžička, E. H. Hansen and J. C. Tjell, Anal.Chim. Acta, 67 (1973) 155.
10 Orion Instrument, Inc., Calcium Ion Selective Electrode Model 92-20.
11 Corning Scientific Instruments, Calcium Ion Electrode Model 476041.
12 Philips Analytical Equipment, Liquid Membrane Calcium Electrode IS560-Ca.
13 F. W. Orme, Glass Microelectrodes, Ed. Lavallee et al., Wiley New York, 1969.
14 J. L. Walker, Anal. Chem., 43 (1971) 89A.
15 P. C. Caldwell, J. Physiol. (London), 124 (1957) 1P.
16 J. Bjerrum, G. Schwarzenbach and L. G. Sillen, Stability Constants, Part 1: Organic Ligands, The Chemical Society, London, 1957 p. 90.
17 G. Hoyle and T. Smyth, Comp. Biochem. Physiol., 10 (1963) 291.
18 F. R. Hayes and D. Pelluet, J. Mar. Biol. Ass., (U.K.), 26 (1947) 580.
19 J. H. Saunders and H. M. Brown, (in preparation).
20 H. J. C. Tendeloo and F. J. Van der Voort, Rec. Trav. Chim. Pays-Bas, 70 (1960) 639.
21 W. E. Morf, D. Ammann and W. Simon, Chimia, 28 (1974) 64.

Analytica Chimica Acta, 85 (1976) 277—285

AN ACTIVATED ENZYME ELECTRODE FOR CREATININE

M. MEYERHOFF and G. A. RECHNITZ

Department of Chemistry, State University of New York, Buffalo, New York 14214 (U.S.A.)

(Received 18th January 1976)

SUMMARY

A highly selective enzyme electrode for creatinine, based on tripolyphosphate-activated creatininase enzyme, is described and evaluated. Kinetic studies comparing purified creatininase enzyme in the activated and non-activated forms show that the activation mechanism involves an increase in V_{max} but no change in K_m. The analytical effect of enzyme activation is to extend the sensitivity of the electrode to lower limits and to improve the response slope of calibration curves. As a result, this activated creatininase enzyme electrode shows promise as a sensor for urine and serum samples.

New developments in the area of enzyme electrodes have been discussed at length in recent publications [1—4]. The application of gas-sensing electrodes as components for these substrate probes, has proven to be advantageous over previously used ion-selective electrodes [1, 2, 5], although problems of sensitivity and stability still limit the clinical use of such sensors.

Commonly, workers have studied effects of pH, temperature, ionic strength, etc., as means of optimizing response characteristics of enzyme electrodes [6—8]. In most investigations, improved response is attributed to optimizing the activity of the immobilized enzyme; however, such gains may be made at the expense of the internal sensing electrode because optimum conditions for enzyme activity and electrode response will seldom be identical.

In this paper, a new approach to this problem is proposed via the use of enzyme activators to improve electrode response. Moreover, the mechanism of the activation process is evaluated in terms of enzyme kinetics (e.g. V_{max}, the maximum rate of reaction at saturated substrate levels, and K_m, the Michaelis—Menten constant) as related to the steady-state behavior of the overall electrode system [9].

This study uses the enzyme creatininase (creatinine iminohydrolase, EC 3.5.4.2.1), which specifically catalyzes the conversion of creatinine to ammonia and *N*-methylhydantoin. Szulmajster [10] purified and studied the characteristics of this enzyme isolated from *Clostridium*, while Thompson and Rechnitz [11] showed the possible application of the enzyme to

creatinine determinations, using a gas-sensing ammonia electrode to measure ammonia production after in vitro incubation for several hours. The commonly employed colorimetric method for creatinine is subject to many interferences [12], and further work on more selective methods, both enzymatic and colorimetric, has been the focus of recent papers [13—15].

The present paper describes a new enzyme electrode for creatinine, which has improved dynamic response and stability through the use of a tripolyphosphate activator and of concentrated enzyme [16]. The electrode is free from creatine, urea, or arginine interference and is useful for analyses in urine and serum samples.

EXPERIMENTAL

Apparatus

The creatinine electrode was prepared by immobilizing creatininase enzyme on an Orion model 95-10 ammonia gas-sensing electrode. Potential measurements were recorded with a Beckman model 1055 pH/mV recorder. All studies were carried out with a 100-ml thermostated cell at 27 ± 0.5 °C. Electrode response measurements in physiological samples and kinetic studies were carried out in 10- and 5-ml thermostated cells, respectively.

Spectrophotometric determinations of enzyme activity were performed with a Beckman model BD-G grating spectrophotometer according to the Beckman microbic assay procedure [17].

All pH values were measured with a Corning combination pH electrode and Corning model 12 pH meter. Mathematical treatment of experimental data and construction of calibration curves were done with a Hewlett-Packard model 9100-A calculator and plotter.

Reagents

Analytical-grade reagents were used to prepare all buffers. Creatinine (Sigma Chemical Company) was recrystallized. To prevent slow hydrolysis of creatinine to creatine at room temperature [18], all creatinine standards and urine standards were stored at 4 °C. Sodium tripolyphosphate ($Na_5P_3O_{10}$) was obtained from Pflautz and Bauer, Inc.

Tris-phosphate buffers (0.15 M and 0.025 M; pH 8.50) were prepared by mixing the proper ratio of tris(hydroxymethyl)amino methane and sodium dihydrogen phosphate monohydrate. Activated buffer solutions, pH 8.50, with the following compositions were also prepared: 0.02 M tris-phosphate—10^{-2} M sodium tripolyphosphate—10^{-4} M EDTA, and 0.06 M tris-phosphate—$3 \cdot 10^{-2}$ M sodium tripolyphosphate— $3 \cdot 10^{-4}$ EDTA. The more concentrated activation solution was used in all urine and serum studies.

Hycel urine controls (Fischer Scientific) and Calibrate serum controls (Armour Pharmaceutical Co.) were reconstituted according to manufacturers' directions. Removal of interfering ammonium ions in urine samples was achieved by using a 1-cm × 10-cm column containing cation exchanger (Baker ANGC-101).

Enzyme purification and concentration

One unit of enzyme is defined as the amount catalyzing the hydrolysis of 1 micromole of creatinine per min at 37 °C and pH 8.5.

The enzyme creatininase (Beckman Microbics, Inc.) has been shown to be in crude form containing various other ammonia-producing enzymes including urease and arginase [11], as well as a considerable amount of creatininase amidohydrolase [19]. To purify the enzyme, the procedures outlined by others [10, 11], were followed except that, in order to obtain more concentrated pure enzyme, the total volume of eluting salt gradient was reduced to 40 ml, and the columns of DEAE-52 used had a larger (ca. 400 mg) protein capacity.

The crude enzyme before purification was dialyzed in a Dow dialysis minibeaker (cellulose hollow fibers, 7-ml capacity). Preliminary crude solutions were prepared by diluting 1 g of lyophilized enzyme with 5 ml of 0.025 M tris-phosphate buffer. Enzyme purification was performed on DEAE-52 microgranular anion-exchange cellulose (Whatman, Inc.); the columns used were 25-ml disposable syringes (2 cm × 10 cm). Fractions (1.5 ml) of eluent were collected at a flow rate of 0.25 ml min^{-1} at 4 °C. A Technicon sampler was used in place of a fraction collector, and creatininase activity was measured in a Technicon Autoanalyzer, which was set up as shown in Fig. 1. The Orion flow-through ammonia electrode measures the amount of ammonia produced after each fraction is allowed to incubate at 37 °C and pH 8.5 with 10^{-2} M creatinine solution for 30 min, and then quenched with 0.1 M NaOH. The change in potential for each fraction is proportional to the activity of pure enzyme in that fraction. This technique offers an advantage over those methods previously employed [10, 11] in that only those fractions containing creatininase will be detected while others containing creatinine amidohydrolase will not yield a response. The colorimetric method, being an indirect one based on creatinine consumption, cannot differentiate between the two enzymes. The three or four fractions containing the highest enzyme concentration (typically 0.05—0.1 units ml^{-1}) were joined and stored in the cold room.

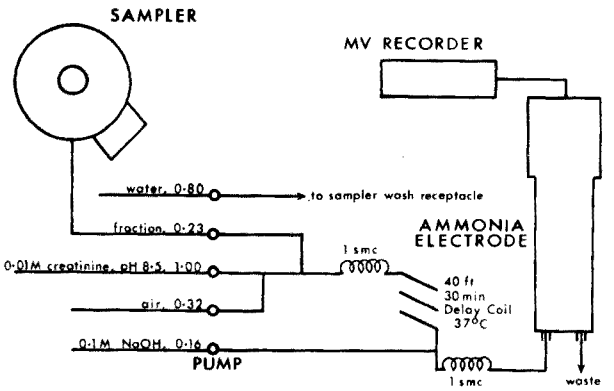

Fig. 1. Autoanalyzer set-up for enzyme fraction analysis.

Starting with 52 units of crude enzyme, the purification procedure was repeated five times using 400 mg of protein and a fresh anion-exchange column each time. The 52 units refers to Beckman's assay of the crude enzyme. This is a false high value owing to the detection of the amido-hydrolase by the colorimetric assay method.

The resulting purified enzyme, about 30 ml, was concentrated by a molecular filtration process [16]. The pure enzyme solution was passed through a PSED Pellicon molecular filter (25,000 molecular weight cutoff) at 4 °C under 50 p.s.i. of nitrogen gas pressure over a 12-h period. At the end of that period, about 1 ml of enzyme solution with a specific activity of 2.9 units ml^{-1} remained. All creatinine electrodes were prepared from this enzyme solution which was stored at 4 °C for several months with no significant loss of activity.

Electrode preparation

The creatinine electrode was assembled by the general technique demonstrated for the urea electrode [5]. In this case, 15 μl of enzyme solution was placed between the cellophane dialysis membrane and the gas-permeable membrane of the ammonia electrode. Differences in starting potentials and slopes of freshly prepared electrodes can be attributed to many irreproducible factors in electrode preparation (i.e. uniformity of enzyme layer, pressure of internal pH electrode on membrane surface, etc.). For maximum activation to occur, the electrode was preconditioned for 1 h in 0.02 M tris-activator buffer. Between runs and overnight, the electrode was left in the same activator solution.

Procedure for urine and serum calibration curves

Additions of standard creatinine to diluted aliquots of Hycel urine control (100 mg/100 ml) were made to produce urine standards with a range of creatinine concentrations ($5 \cdot 10^{-4}$ M—$2 \cdot 10^{-2}$ M). Portions (5 ml) of the standards were passed through an appropriately conditioned cation-exchange column and washed with two 5-ml portions of deionized water. The more concentrated activation buffer (8 ml) was added to the effluent and then final dilution to 25 ml was made with deionized water. Critical adjustment of pH to exactly 8.50 was made on each standard by using microvolumes (1—3 μl/25 ml) of 10 M NaOH.

A serum calibration curve was prepared by adding concentrated activation buffer to the Calibrate serum control (1.00 mg/100 ml) to gain a (2 + 1) dilution of the original serum creatinine level. Electrode response after continuous additions of standard creatinine to the serum solution was recorded.

Procedure for kinetic studies

The ammonia gas-sensing electrode was used to measure initial rates of reaction at various substrate concentrations by the method outlined earlier

[20]. In the case of activation, the enzyme was first dialyzed against 0.02 M tris-phosphate—10^{-2} M sodium tripolyphosphate—10^{-4} M EDTA for 2 h. All measurements were made at 27 °C, with 25 μl of enzyme in 1 ml of substrate solution.

RESULTS AND DISCUSSION

Preliminary work with the crude enzyme indicated that the extremely low enzyme activity would greatly limit the sensitivity and stability of this electrode. Furthermore, upon purification, a large net loss of activity [11] as well as dilution of the enzyme would present further difficulties. These problems were eliminated in part by the molecular filtration process used to concentrate the pure enzyme.

Figure 2 shows a typical calibration curve for an electrode based on purified but unactivated enzyme in 0.15 M tris-phosphate buffer, pH 8.50, at 27 °C. The electrode responds in a linear fashion over a concentration range of $4.2 \cdot 10^{-4}$—$8.9 \cdot 10^{-3}$ M creatinine with a slope of 44.4 mV per concentration decade. Loss of enzyme activity over a period of 4 d is quite evident as seen in Fig. 3. This instability was expected in view of preliminary work with the crude enzyme and other previous work [11].

Despite the instability, it was surprising that fairly good response could be obtained with such low enzyme concentrations. Previous enzyme electrodes [5, 8] based on this ammonia sensor, have used much higher enzyme concentrations, e.g. 60—150 units ml^{-1}, to obtain similar response. The apparent explanation is that at pH 8.5, which is the optimum for creatininase activity [10], the ammonium—ammonia equilibrium is favorable to the response of the ammonia electrode [21].

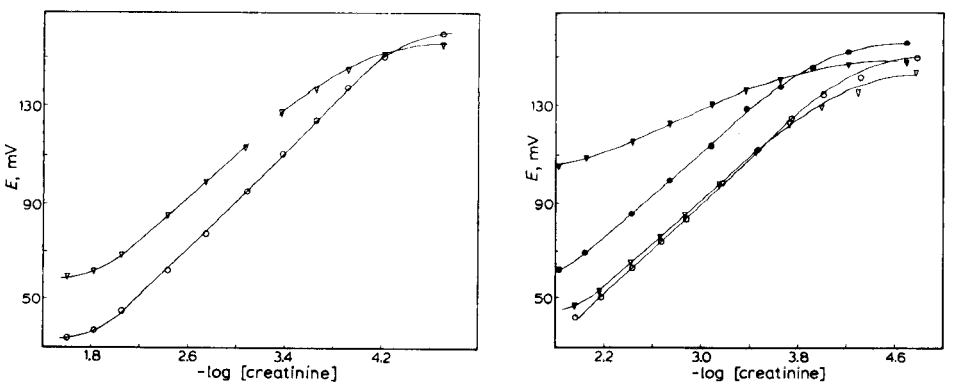

Fig. 2. Calibration curves of the creatinine electrode under non-activated (△) and activated (○) conditions.

Fig. 3. Stability of creatinine electrode on 1st (●) and 4th (▲) days, non-activated; 1st (○) and 4th (△) days, activated.

Though the electrode responded reasonably well over a short period of time, its lack of stability and sensitivity would limit analytical application. Attempts to improve its response and stability by varying ionic strength and temperature proved unsuccessful. After one run at 37 °C, the electrode exhibited little or no response, probably because of denaturation of the enzyme.

Szulmajster [10] studied the effect of various inorganic ions as possible activators and inhibitors for creatininase enzyme, and found high enzyme activation by phosphates with an activity increase of about 300 % for polyphosphates, a finding typical for deaminases [22]. Divalent cations lower enzyme activity, but their effect can be overcome by the addition of EDTA.

The enzyme electrode was therefore conditioned for 1 h in a solution of 0.02 M tris-phosphate—10^{-2} M sodium tripolyphosphate—10^{-4} M EDTA, pH 8.50, before use. Figure 2 shows the resulting calibration curve when additions of standard creatinine are made to the activated buffer solution at 27 °C. The response shown is for the same electrode on the same day, after one run in the non-activated form. It can be seen that the linear calibration is extended down to $7 \cdot 10^{-5}$ M and the slope increased to 49.4 mV per concentration decade (correlation coeff. = 0.9995). It should be noted that the curve is shifted to a more negative potential which corresponds to a higher ammonia concentration at a given substrate level. Freshly prepared, activated electrodes exhibit slopes in the range of 45—55 mV/decade depending upon preparation variables.

Response times for the activated electrode depend on substrate concentration. Below $5 \cdot 10^{-3}$ M, typical response times are in the range of 6—10 min. Above $5 \cdot 10^{-3}$ M response times are between 2—5 min. Only a slight improvement in response times is noted over the unactivated electrode.

Figure 3 also shows the improved stability of the activated electrode over a 4-day period; the electrode loses only 1.5 mV in its slope, and absolute potentials over the linear portion do not vary by more than 3 mV. Some slight loss in the length of the linear portion of the calibration curve can be seen, and is due to a small loss of enzyme activity. On the 5th or 6th day, the electrode potentials show a considerable shift and the slope tends to decrease. However, the electrode is still usable even on the 8th day.

Selectivity of the activated creatinine electrode is shown in Fig. 4. The electrode exhibits no response to arginine, urea, or creatine, and normal response to creatinine in the presence of all three species (equimolar concentrations of each). This indicates that acceptable purification of the crude enzyme was accomplished, and future use of the electrode in physiological samples is feasible.

The observed activation effects can be explained in terms of enzyme kinetics and the steady-state behavior of layered enzyme electrodes. Racine and Mindt [23] have derived equations which depict the kinetics of a model system similar to the present one, where the enzyme is held on the electrode

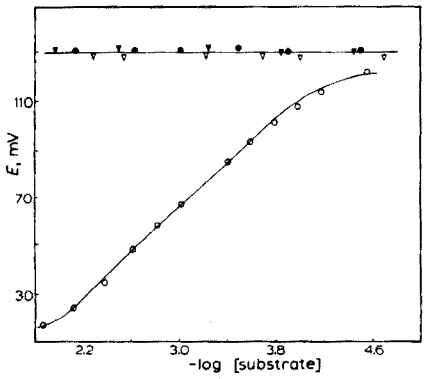

Fig. 4. Selectivity of creatinine electrode on additions of standard creatine (△), arginine (▲), urea (●), and creatinine (○).

by means of a semipermeable membrane. Since permeability of the cellophane membrane is small, the diffusion of the substrate through the membrane is the rate-limiting step. Therefore, the concentration of substrate within the enzyme layer at the steady-state is considerably less than the concentration in the bulk solution and smaller than the K_m value of the enzyme [23, 24]. This criterion allows for a linear response of many enzyme electrodes [23]. At the steady state, the concentration of ammonia being sensed by the inner electrode remains constant and, therefore, the rate of ammonia production by the enzyme is equal to the rate of diffusion of the ammonia from the enzyme layer. The rate of ammonia production will, of course, be the same as the rate of substrate consumption. Racine and Mindt's expression for this rate shows a direct proportionality to enzyme concentration and an inverse relation to the K_m value of the enzyme substrate complex. The concentration of ammonia in the enzyme layer, at a given bulk substrate concentration, is therefore determined by these enzyme parameters. Activation serves to increase the effective enzyme concentration.

Activation of the enzyme—substrate system can take two possible forms [9]. In one case, the maximum velocity (V_{max}) of the enzymatic reaction at saturated substrate level is increased (i.e. increased activity). A second type of enzyme activation can occur when the K_m value of the enzyme is lowered, but V_{max} remains unchanged. A combination of both these processes is also possible.

In an attempt to elucidate the origin of the observed effect, kinetic studies of the enzyme reactions were undertaken and are displayed by means of the Eadie—Hofstee plots [9, 20] shown in Fig. 5. Curve A was obtained with pure enzyme which was dialyzed for 2 h vs. 0.15 M tris-phosphate buffer, pH 8.50. This represents the non-activated enzyme and the K_m value determined from the slope is $4.4 \cdot 10^{-3}$ M. The maximum velocity, V_{max}, of

the enzyme reaction expressed in ΔmV per unit time, was 36 mV min^{-1} for the non-activated enzyme. The activated form of the same enzyme preparation, yields (Curve B) an increase in V_{max} to 91 mV min^{-1} but little change in the K_m value (i.e. $4.2 \cdot 10^{-3}$ M).

It can therefore be concluded that the increased sensitivity range and response slope of the activated enzyme electrode is due only to an increase in V_{max}. Increased stability of the activated electrode can be attributed, in part, to the increased enzyme activity [24] and to the stabilizing effect of EDTA [5].

The activated enzyme electrode was tested under physiological conditions to show possible future applications in clinical chemistry. Curve A in Fig. 6 shows the electrode response to urine standards prepared from Hycel urine control. The electrode slope is 52.8 mV/decade over a concentration range of $5.2 \cdot 10^{-4}$ M—$9.6 \cdot 10^{-3}$ M (correlation coeff. = 0.9992). Pretreatment of each sample through a cation-exchange column is necessary to remove high levels of interfering ammonia present in urine [25, 26]. After a (1 + 4) dilution during pretreatment of urine samples, normal and most abnormal urine creatinine values [25] fall well within the linear range of the activated electrode. Slopes obtained in urine standards are comparable to those obtained in creatinine standards (45—55 mV/decade).

Curve B of Fig. 6 shows the electrode response in serum. The lower slope of 29.0 mV/decade indicates that the high viscosity and presence of high protein concentrations in serum may reduce the diffusion rate of substrate through the cellophane membrane [23]. Although not linear in the normal range of serum creatinine ($5 \cdot 10^{-5}$ M—$1 \cdot 10^{-4}$ M [25]), the electrode could provide a semi-quantitative screening test for abnormally high serum creatinine values with minimal pretreatment, since the serum ammonia level is too low [26] to present an interference.

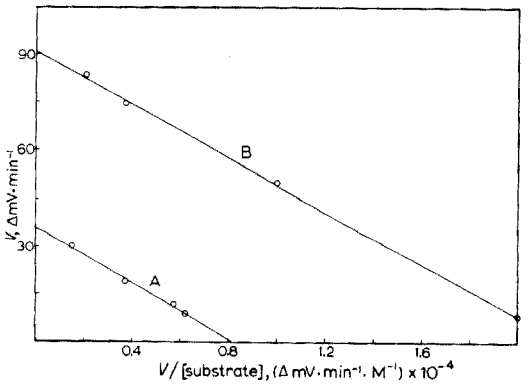

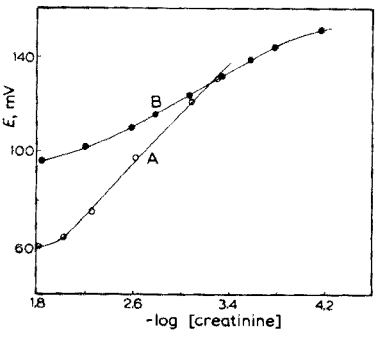

Fig. 5. Eadie—Hofstee plots of non-activated (Curve A) and activated (Curve B) creatininase enzyme kinetics.

Fig. 6. Calibration curves for creatinine in urine (Curve A) and serum (Curve B) standards.

We thank the National Institutes of Health for support of this research.

REFERENCES

1 G. J. Moody and J. D. R. Thomas, Analyst (London), 100 (1975) 609.
2 G. A. Rechnitz, Science, 190 (1975) 234.
3 G. A. Rechnitz, Chem. Eng. News, 53(4) (1975) 29.
4 G. A. Rechnitz, Am. Lab., 6(2) (1974) 13.
5 D. S. Papastathopoulos and G. A. Rechnitz, Anal. Chim. Acta, 79 (1975) 17.
6 M. Nanjo and G. G. Guilbault, Anal. Chem., 46 (1974) 1769.
7 T. Anfalt, A. Granoli and D. Jagner, Anal. Lett., 6 (1973) 969.
8 D. S. Papastathopoulos and G. A. Rechnitz, Anal. Chem., 48 (1976) 862.
9 A. L. Lehninger, Biochemistry, Worth Publishers, New York, 1975.
10 J. Szulmajster, Biochim. Biophys. Acta, 30 (1958) 154.
11 H. Thompson and G. A. Rechnitz, Anal. Chem., 46 (1974) 246.
12 J. T. Clarke, Clin. Chem., 7 (1961) 271.
13 G. A. Moss, R. J. L. Bondar and D. M. Buzzelli, Clin. Chem., 21 (1975) 1422.
14 J. Romeo, Lab. Med., 6(8) (1975) 18.
15 G. Ceriotti, Clin. Biochem., 2 (1974) 1122.
16 Molecular Filtration, Publication AR 801, Millipore Corp., Bedford, Mass., 1974.
17 Product Catalog, Beckman Instruments, Inc., Microbic operations, Carlsbad, Cal., 1974.
18 G. Edger and H. E. Shiver, J. Am. Chem. Soc., 47 (1925) 1179.
19 K. L. Donovan, Beckman Microbics Operations, Carlsbad, Calif., private communication, 1975.
20 R. L. Llenado and G. A. Rechnitz, Anal. Chem., 44 (1972) 486, 1366.
21 Instruction Manual for Ammonia Electrode, Orion Research, Inc. Cambridge, Mass., 1972.
22 J. P. Greenstein and F. M. Lenthardt, Arch. Biochem., 17 (1948) 105.
23 P. Racine and W. Mindt, Exp. Suppl., 18 (1971) 525.
24 G. G. Guilbault, Pure Appl. Chem., 25(9) (1971) 727.
25 R. J. Henry, Clinical Chemistry; Principles and Technics, Hoober Medical Div., Harper and Row, New York, 1968.
26 CRC Handbook of Clinical Laboratory Data, 2nd edn., CRC, Cleveland, 1968.

Analytica Chimica Acta, 85 (1976) 287—293

AN AUTOMATIC POTENTIOMETRIC ANALYZER FOR ATMOSPHERIC HYDROGEN FLUORIDE DETERMINATIONS

MARCO MASCINI

Istituto di Chimica Analitica- Universita di Roma, 00185 Roma (Italy)

(Received 6th January 1976)

SUMMARY

An automatic potentiometric analyzer for the determination of atmospheric hydrogen fluoride is described. Hydrogen fluoride is collected from the air, which is pumped at 25 l min^{-1}, in a thin layer of sodium carbonate in a spiral absorber, and measured every hour by washing the absorber with a citrate buffer and measuring the fluoride with a fluoride-selective electrode. The analytically useful range is 0.1—15 μg HF m^{-3}.

The concentration of hydrogen fluoride in the atmosphere generally ranges from 0.1 to 15 μg m^{-3}. Hydrogen fluoride is emitted into the atmosphere from industrial plants which produce aluminium, phosphate fertilizers, glass, ceramics, steel, etc. Vegetation and animals are affected by fluoride pollution, and it is known that even very low concentrations (0.2 μg m^{-3}) can damage certain sensitive vegetation [1, 2]. The damage depends also on the "point value", i.e., the maximum concentration attained during a short period, and regulations in various states specify short periods of measurement. Generally, owing to the low concentrations of fluoride in urban and even industrial air, determinations are limited to 24 h and refer to total fluoride. However, there is a definite need for methods of measuring the concentration of gaseous hydrogen fluoride, which is much more toxic than particulate fluoride, for short periods and on a continuous basis, so that pollution can be correlated with industrial activity and atmospheric conditions such as wind, humidity, the presence of other pollutants, etc.

In the automatic apparatus described in this paper, hydrogen fluoride is collected from the air on a solid support and is measured after one hour of sampling, with a fluoride-selective electrode. The fluoride monitor collects the air through a large filter warmed at about 80 °C; this filter, which is impregnated with citric acid, allows the gaseous fluoride and gaseous fluoride adsorbed on particulate matter to pass through, but retains particulate fluoride [3, 4]. The range measurable with the apparatus is 0.1 to 15 μg m^{-3}.

Principle of operation

Air aspirated with a high-capacity vacuum pump (1.5 $m^3 h^{-1}$) passes through a spiral glass tube covered with a thin layer of strong sodium carbonate solution which fixes the hydrogen fluoride. Each hour, the glass tube is washed with a known volume of citrate solution (5 ml), the fluoride being dissolved; the solution is collected in an analysis cell, in which the fluoride concentration is measured with a fluoride-selective electrode and a reference electrode. The electrode potential is recorded and expressed as the average fluoride concentration in the air ($\mu g\ m^{-3}$) during the previous hour. Then a thin layer of sodium carbonate is deposited on the glass tube, and aspiration of air continues for the next hour.

The hydrogen fluoride is concentrated $3 \cdot 10^5$-fold from air in the aqueous solution. This allows a concentration of 10^{-6} M fluoride to be achieved in the solution when the average hydrogen fluoride concentration is 0.1 $\mu g\ m^{-3}$. This concentration is considered to be the detection limit of the apparatus.

EXPERIMENTAL

Design of the analyzer

Figure 1 shows design of the apparatus. The air passes first through a miniature centrifugal dust separator (cyclone), and through a filter where particulate matter is separated. Then from the spiral glass tube where hydrogen fluoride is fixed on sodium carbonate, the air passes through an electrically operated valve V7 to a second cyclone where the absorption solution residues are collected, and through a needle valve to a flow meter and a suction pump.

The citrate solution which dissolves the fluoride collected each hour flows

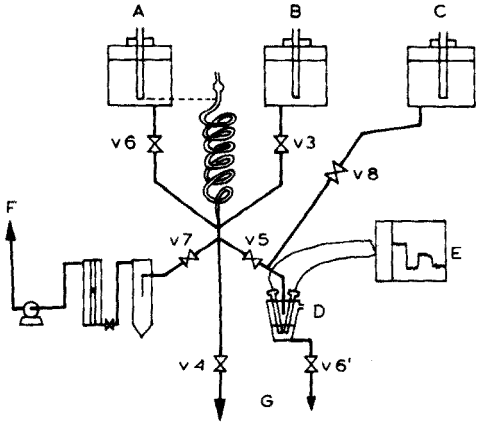

Fig. 1. Design of the analyzer. A. Sodium citrate reservoir. B. Sodium carbonate reservoir. C. Sodium fluoride reservoir. D. Analysis cell. E. Potentiometric recorder. F. Gas exit. G. Waste.

into the spiral glass tube by gravity when the valve V6 is open and valve V7 is closed to stop the flow of air. The level of the inlet tube in the citrate reservoir regulates the volume of solution delivered (5 ml). The citrate solution remains in the tube for 90 s and then passes through valve V5 to the analysis cell. The spiral glass tube is then filled with sodium carbonate solution through V3, by gravity, and after a fixed time (30 s) this solution flows to waste through valve V4. The thin layer of solution remaining on the glass is enough to fix the hydrogen fluoride from the atmosphere for the next hour. The cycle then ends and air is again aspirated by opening valve V7. The operation of the valves is regulated by a timer-programmer with cams and switches, and the entire cycle lasts for 2 min.

During the sampling time, the electrodes are calibrated with a standard solution of sodium fluoride to check the potential value. The standard solution replaces the citrate solution in the cell through valve V8 and is passed to waste through valve V6'.

Separation of hydrogen fluoride. The first centrifugal dust separator and the filter allow hydrogen fluoride to be separated from particulate matter. Three forms of fluoride occur in the atmosphere: fluorine-containing gases,

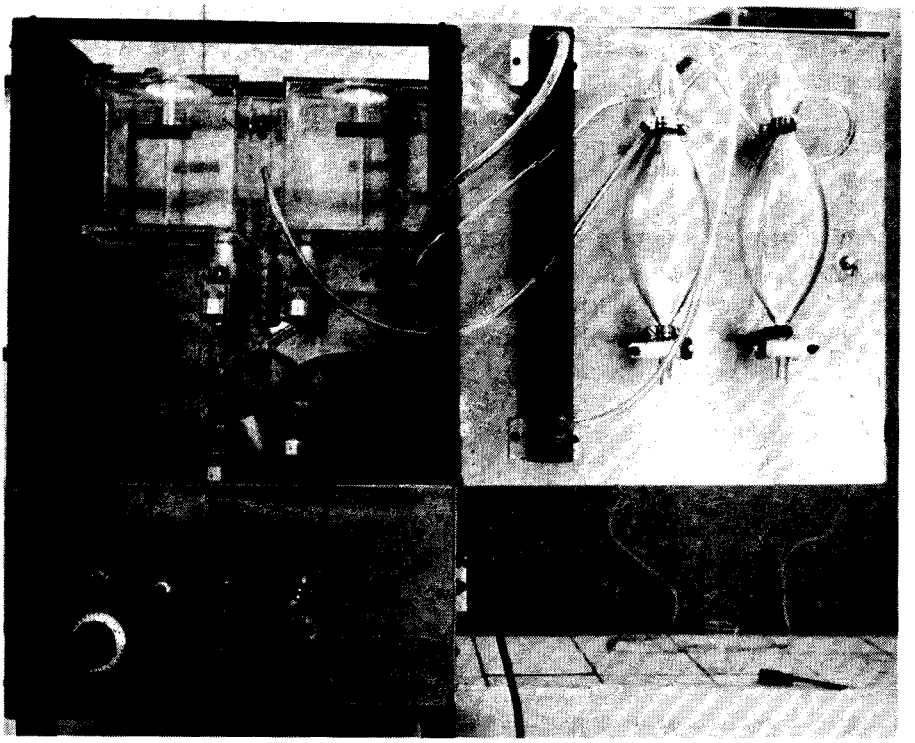

Fig. 2. The hydrogen fluoride analyzer.

fluoride particulates (NaF, AlF_3, cryolite, etc.) and gaseous fluoride adsorbed on particulates. It was proved that filters wetted with citric acid solution retain the fluoride particulates while releasing adsorbed fluoride. Heating is useful when air with high humidity is aspirated.

The filter paper used was Whatman No. 41 but any other similar paper is suitable. The size is large enough (12.5-cm diameter) to ensure that variations in the pressure drop do not occur for a week. The paper is soaked in 0.1 M citric acid solution, dried at 105 °C, and then placed in a suitable stainless-steel holder heated through a Variac control. Once a week, the filter is replaced. The size of the filter selected depends to some extent on the average size and amount of particulate matter in the atmosphere.

Spiral absorber. The spiral absorber is made from a 1-m length of glass tubing (2.5 mm internal diameter). The dimensions were selected to provide total recovery of fluoride, a low total volume to be filled with citrate solution (5 ml) and a low pressure drop in the tube during aspiration of air. These needs are conflicting, so that a compromise must be made.

Valves and pumping system. The solenoid valves chosen (Sirai type L143H1, Milan, Italy) have plastic bodies to prevent reactions with chemicals and to ensure high efficiency in continuous operation.

The excess of liquid in the spiral absorber is drained off when air is admitted; the excess is collected in a second centrifugal separator, which prevents entry of liquid to the flow meter. A needle valve is used to adjust the air flow to 25 l min^{-1}. The suction pump is of the membrane type, with teflon collars, suitable for continuous operation.

Solutions

All solutions are enough for 30 days of continuous use.

Sodium citrate solution. Dissolve 142.8 g of trisodium citrate in 1500 ml of distilled water, adjust the pH to about 6 with concentrated hydrochloric acid (about 30 ml) and dilute to 4 l.

Sodium carbonate solution. Dissolve 120 g of sodium carbonate in water and dilute to 4 l.

Standard fluoride solutions. Prepare a sodium citrate solution as above, but before the final dilution, add sufficient sodium fluoride to give a final concentration of $5 \cdot 10^{-5}$ M.

Analysis cell and electrodes

The design of the analysis cell (D) is shown in Fig. 1. The electrodes are an Orion model 90-01 fluoride-selective electrode and a saturated calomel reference electrode. The solution is not stirred; the response time of the

electrode under such conditions for fluoride concentrations of 10^{-4}—10^{-6} M is several minutes.

Measurements are made by means of an amplifier connected to a recorder or a printer, which alternatively gives the value for the standard solution and that for the sample solution. The value for the sample solution is converted by means of a calibration curve or table to the average hydrogen fluoride content in the atmosphere.

The solutions are passed to waste in a large container which is emptied once in a month.

Timer

The different functions of the apparatus, opening of the different solenoid valves and printing of the results are operated with one programmer-timer (Crouzet 88.645).

The cycle is as follows. During the period 0—58 min, air is aspirated through the spiral absorber. In the period 58—60 min, the airflow is stopped; the solution in the analysis cell flows to waste; citrate solution enters the spiral absorber, dissolves fluoride and passes to the analysis cell; sodium carbonate solution enters the spiral absorber and flows to waste, leaving a thin layer on the coil. On the 60th minute, air is admitted through the spiral absorber. On the 70th minute, the printer prints the electrode potential value for the sample; solution from the analysis cell passes to waste; standard fluoride solution enters the analysis cell, and the printer prints the potential value.

RESULTS

The efficiency of the recovery was tested by comparison with a conventional unit which had two absorbers containing 0.025 M sodium hydroxide in series, placed in parallel with the potentiometric analyzer. Air was bubbled through the absorbers at the rate of 2 l min^{-1}, and the experiment was continued for at least 70 h to collect enough fluoride in the bubblers. The solutions were analyzed by the usual TISAB procedure.

Some experiments were carried out in an aluminium factory in the north of Italy where the mean content of hydrogen fluoride in the atmosphere is around 5 $\mu g\ m^{-3}$. Some results in the range 10—50 $\mu g\ m^{-3}$ were obtained by using a standard atmosphere which was prepared by evaporation of a 1 % hydrogen fluoride solution.

The results (Fig. 3) showed that with atmospheric concentrations higher than 10 $\mu g\ m^{-3}$ the spiral absorbing system is no longer suitable. The use of a longer spiral glass tube (2 m), and even the use of glass beads in the spiral glass tube to give greater surface contact, did not improve the efficiency of the collection. These results agree with the efficiencies reported earlier for another hydrogen fluoride analyzer [5].

The analyzer was operated near an aluminium reduction plant for several

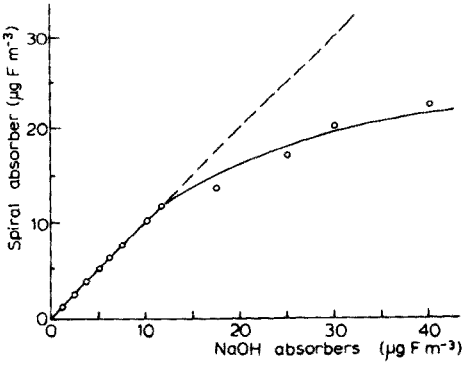

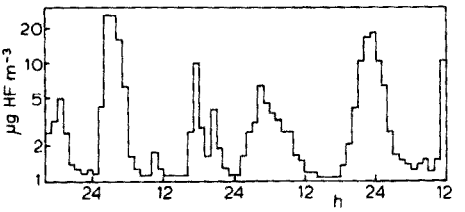

Fig. 3. Efficiency of recovery of the spiral absorber compared to conventional NaOH absorbers.

Fig. 4. Results obtained in field testing.

months; the graph obtained for a short period is shown in Fig. 4. Table 1 summarizes the results obtained during the period November 1974—March 1975.

DISCUSSION

In the last ten years, much work on the reliability of fluoride-selective electrodes has been published, and in most official methods for the determination of atmospheric fluoride [6, 7], the procedure with the lanthanum fluoride electrode is recommended. In the present work, this electrode was therefore used as a reference, and attention was focussed on sampling and on field work with the assembled analyzer.

Reports on damage by fluoride to vegetation, animals and humans [1, 2] indicate a value in the range 0.2—2.0 $\mu g\ m^{-3}$ as the air quality standard [8]. Analysis in this range is therefore necessary for environmental study and control. In the first apparatus developed here [9], the limit of detection was about 10 $\mu g\ m^{-3}$; this limit was set by the unsatisfactory concentration ratio

TABLE 1

Atmospheric hydrogen fluoride concentrations (in $\mu g\ m^{-3}$) measured near an aluminium reduction plant

	Nov.	Dec.	Jan.	Feb.	March
Monthly mean concn.	2.4	0.9	1.1	2.3	6.1
Daily maximum concn.	6.1	2.4	2.1	5.2	11.5
Hourly maximum concn.	11.0	6.2	5.5	15.0	24.0

between the air bubbling in a liquid and the volume of the liquid. Practical problems arise when the bubbling rate exceeds 2 l min^{-1}, and this limits the concentration of hydrogen fluoride from the atmosphere into aqueous solutions. The principle of solid contact was then investigated, and the results obtained are encouraging because the analytically useful range fits the environmental range for hydrogen fluoride.

In many environmental studies and in the regulations for environmental control, there is a discrepancy between the injurious rôle of fluoride and its determination. Gaseous fluorides are considered toxic, whereas particulate fluorides may be regarded as harmful or beneficial [2]; but regulations are usually concerned with the determination of total fluoride or, in some cases, of water-soluble fluoride, i.e. a relative index [10]. The sampling system in the analyzer described here is such that only gaseous fluoride is absorbed.

The response of the analyzer is semi-continuous; the hourly response obtained represents the mean content of the atmosphere for the previous hour. Such results on a daily basis seem entirely adequate for environmental study and control. The reliability and ruggedness of the analyzer are of importance. During the tests in the aluminium factory, the instrument was in continuous use for a period of six months, and stopped only twice because of breakage at the air pump.

The apparatus could be adapted to measure other pollutants like hydrogen bromide or hydrogen chloride by changing the ion-selective electrode and the dissolving solution. Studies in this direction are currently in progress.

REFERENCES

1 A. C. Hill, J. Air Pollut. Contr. Ass., 19 (1969) 331.
2 R. G. Bond and C. P. Straub (Eds.), Handbook of Environmental Control, Vol. 1, C.R.C. Press, Cleveland, 1972.
3 T. Okita, K. Kaneda, T. Yanaka and R. Sugai, Atmos. Environ., 8 (1974) 927.
4 G. W. Israel, Atmos. Environ., 8 (1974) 159.
5 T. Okita and M. Mori, 64th Ann. Meeting Air Pollut. Contr. Assoc. Atlantic City, N.J., 1971.
6 Italian law: "Legge 13 July 1965 no. 615", Gazz. Uff., June 1971.
7 Development of Methods for Sampling and Analysis of Particulate and Gaseous Fluorides from Stationary Sources, A. D. Little, Cambridge, Mass., Nov. 1972.
8 World's Air Quality Management Standards, Environ. Prot. Agency (U.S.) Publ., EPA-650/9-75-001 a.
9 M. Mascini, A. Liberti, Gazz. Chim. Ital., 103 (1973) 989.
10 G. B. Morgan, U.S. Public Health Service Publication 1960.

Analytica Chimica Acta, 85 (1976) 295—300

ASSAY OF CHOLINESTERASE IN AN ELECTRODE SYSTEM WITH AN IMMOBILIZED SUBSTRATE

G. G. GUILBAULT and A. IWASE

Department of Chemistry, University of New Orleans, New Orleans, Louisiana 70122 (U.S.A.)

(Received 19th February 1976)

SUMMARY

A rapid, simple method for the measurement of cholinesterase based on an immobilized acetylcholine substrate is described. Each assay requires only 3 min and the immobilized substrate can be used for 10 assays with excellent results; the substrate can then be renewed easily and quickly. The precision obtained (2.5 %) is the same as that possible with the soluble substrate system.

Several methods of assay for cholinesterase based on detection of the increase in hydrogen ion during the enzymatic reaction have been reported [1—3]. Recently, a rapid method for the measurement of cholinesterase was developed by Guilbault and Gibson [4], who were able to analyze 40 samples per hour in an automated system. This method was based on the observation that under certain conditions an enzymatic reaction can result in a linear change of pH with time.

In this paper, the concept of the use of an immobilized substrate for assay of enzyme activity with a hydrogen-ion electrode is reported. It is easy to design a reaction cell for use with an immobilized substrate, and it was found possible to use an immobilized substrate system for electroanalytical measurement of the cholinesterase by means of the following reaction:

$$[CH_3CO_2CH_2CH_2N^+(CH_3)_3]_R + H_2O \rightleftharpoons CH_3COO^- + H^+ + [HOCH_2CH_2N^+(CH_3)_3]_R$$

where subscript R indicates the resin phase used to insolubilize (immobilize) the substrate.

EXPERIMENTAL

Immobilization of substrate

Acetylcholine chloride (2 g; Calbiochem Co., Calif.) and a cation-exchange resin (1 g; Na^+ form; Dowex 50, 200 mesh, or Amberlite IRC-50, 20—50

mesh) were added to about 0.5 ml of 2 mM Tris buffer solution (pH 8.10), and the slurry was mixed well. The mixture was filtered on a glass filter, and washed three times with the same buffer solution. This immobilized substrate was kept in a refrigerator until use.

Reagents

Tris buffer, pH 8.10—8.15, 2 mM, was prepared fresh daily from tris-(hydroxymethyl)aminomethane (Sigma, St. Louis). Sodium chloride was added to insure a constant ionic strength (μ) and to stabilize the electrode response. The cholinesterase enzyme (Worthington Biochemical Co., Freehold, N.J.; 5 U/mg) was dissolved in redistilled water (10 U/100 μl).

Apparatus

A Corning Digital 110 pH meter or a Beckman Research pH meter was combined with a Heath operational amplifier system. pH—time curves were recorded with a Heath recorder adjusted so that 0.1 pH unit corresponded to 6.5 cm on the paper.

The two reaction cells (Fig. 1) were constructed from polyethylene beakers (diameter, 2 cm; height, 3 cm) with tightly fitting lids. Holes were made in the lid so that a flat-tipped glass electrode [5] (Radiometer E 5036/0; ca. 12 mm^2 area) and glass tube A could be placed in it. An additional hole B was used for the addition of a sample with a micropipette. The immobilized substrate was placed between layers of nylon cloth (Nylon 677-74) and secured by rubber O-rings. For cell 1, 100 mg of immobilized substrate on Amberlite IRC-50, and for cell 2, 1 g of immobilized substrate on Dowex 50, were used.

Teflon-coated magnetic bars were used to stir all solutions.

Procedures

To a reaction cell, was added 3.0 ml of Tris buffer. When a steady pH reading was observed, 100 μl of the enzyme sample was rapidly added and

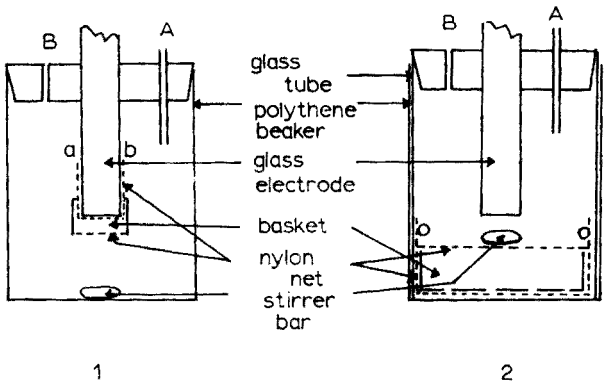

Fig. 1. Reaction cells used. For description, see text.

the pH change was recorded for ca. 2 min. All experiments were conducted at room temperature (23 °C). The immobilized substrate (reaction cell 2) could be used 10 times, and then an easy renewal of the substrate resin was effected.

Some results were obtained in an atmosphere of nitrogen (see below).

RESULTS AND DISCUSSION

The two different reaction cells are shown in Fig. 1. Cell 1 is a self-contained "substrate" electrode, with the immobilized substrate directly on the surface of the glass electrode, kept in place by nylon net in a "basket". Configuration 2 uses the immobilized enzyme held in a nylon net "basket" at the bottom of the cell, with the electrode then free to measure H^+ ions. Some typical pH—time curves obtained with those cells, and no cholinesterase added are shown in Fig. 2. No change in pH was observed with cell 2, but with cell 1, a increase in initial pH was observed, with a leveling after about 8—10 min.

Some typical rate curves obtained with cells 1 and 2 upon addition of cholinesterase are shown in Fig. 3. Curve 1 represents the rate curve upon addition of 0.5 units of cholinesterase obtained with the reaction cell 1 in 2 mM Tris buffer (pH 8.10, μ = 0.01). Curves 2 and 3 show the rate curves after addition of 0.5 and 0.25 units of cholinesterase, and were obtained with reaction cell 2 in 2 mM Tris buffer. Under these conditions, the enzymatic reaction yields a linear change of pH with time. In the case of cell 2, it was necessary to wash with distilled water three times before each use.

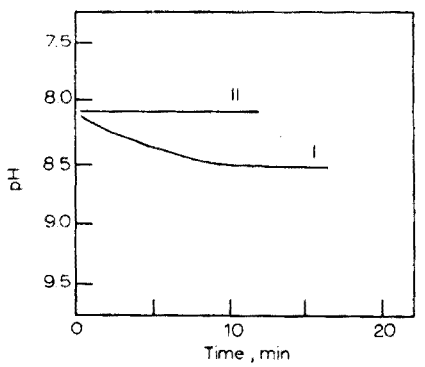

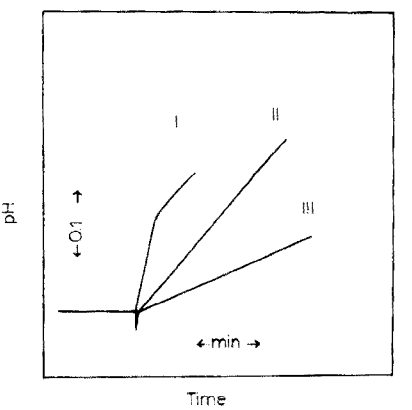

Fig. 2. Spontaneous pH—time curves obtained in 3.0 ml of 2 mM Tris buffer pH 8.15, μ = 0.01. I. Reaction Cell 1. II. Reaction Cell 2.

Fig. 3. Rate curves obtained on addition of 100 μl of enzyme sample to 3.0 ml of 2 mM Tris buffer (pH 8.10, μ = 0.01). I. 0.50 units cholinesterase, Cell 1. II. 0.50 units cholinesterase, Cell 2. III. 0.25 units cholinesterase, Cell 2.

The effect of pH, ionic strength and buffer concentration

Figure 4 shows the pH profile for the reaction rate of 0.5 units of cholinesterase, in the 2 mM Tris buffer solution, containing 0.01 M NaCl, the pH of which was adjusted from 7.5 to 8.5 by adding 0.1 M hydrochloric acid. It is clear that the reaction rate is constant over the range pH 7.8—8.3 in both cases.

The rate curves were measured in reaction cell 2 under the same conditions as for Fig. 4 at pH 8.18, except for the ionic strength used. An ideal reaction curve was not obtained in reaction cell 1, at varying concentrations of sodium chloride (0.02—0.06 M). Figure 5 shows the plot of the reaction rate against the square root of the ionic strength. An approximately straight line with a slope of —0.4 was obtained. The reaction rate decreased as the concentration of sodium chloride increased; this can be attributed to the decrease in activity of the substrate on the resin phase.

The rate curves were then measured under the same conditions as Fig. 4 at pH 8.10, except for the use of varying concentrations of Tris buffer from 2 to 8 mM. In both cell 1 and cell 2, the region of linearity of the rate curves decreased as the concentration of Tris buffer increased. Consequently, the concentration of buffer must be limited, because of this lowering of sensitivity to hydrogen ion. Good results were obtained with 2 mM Tris buffer.

The effect of enzyme concentrations

Figure 6 illustrates some calibration plots obtained. The sensitivity of the immobilized substrate method with cell 1 was found to be higher than that of the cell 2. Unfortunately, cell 1 is inefficient. For cell 2, the sensitivity was found to be the same as that of the soluble substrate method, and the

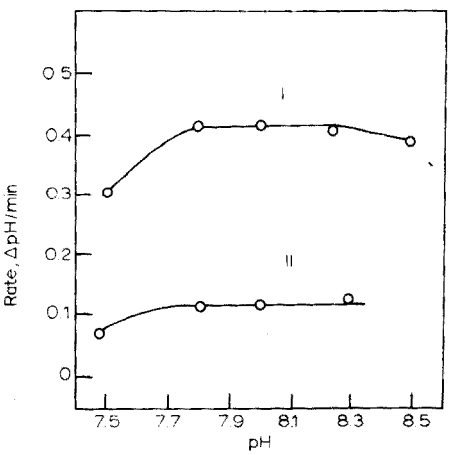

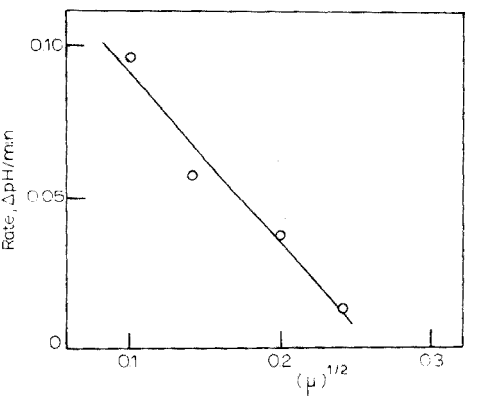

Fig. 4. Effect of pH on the rate of addition of 0.50 units of cholinesterase to 3.0 ml of 2 mM Tris buffer, μ = 0.01. I. Cell 1. II. Cell 2.

Fig. 5. Effect of ionic strength on the rate in cell 2 at pH 8.15. Same conditions as Fig. 4.

method is easy to run. A linear plot was obtained in the enzyme concentration range 0.025—1.0 units per 100 μl sample. In the range above 1.0 units, the reproducibility of the rate curves was not good, probably because the reaction rate was too fast. The rate curve with cell 2, even with the closed system (no nitrogen), was the same as that obtained in nitrogen.

The relationship between the reaction rate obtained with a particular system and the number of runs is given in Fig. 7. As shown for cell 2, for a 0.5-unit cholinesterase sample, the same reading was obtained for 10 assays, followed by a slight decrease up to 18 assays. At point R of curve 2, the resin was renewed by passing a 10 % acetylcholine chloride solution through it; good results were then obtained, as is shown by Curve III of Fig. 7. However, after another 10 assays, another regeneration was necessary. Only a few minutes are required to renew the resin. Hence, this method is useful as a practical assay device, although it does have one weak point, in that the kinetic data are affected quite sensitively by variations in the ionic strength.

Conclusions

Compared to the mobile substrate system described previously [4] for cholinesterase assay, this type of approach with cell 2 has some advantages: it is fast (3 min per assay) and easy to perform. An immobilized substrate can be prepared easily from acetylcholine chloride and the sodium form of a cation resin, and used for a number of repetitive assays.

Cell 1 suffers from a continuous loss of substrate after 2—3 runs, and hence with this configuration the substrate layer must be renewed after each run.

The financial assistance of the General Medicine Division, National Institute of Health, Grant No. GM 17268, is gratefully acknowledged.

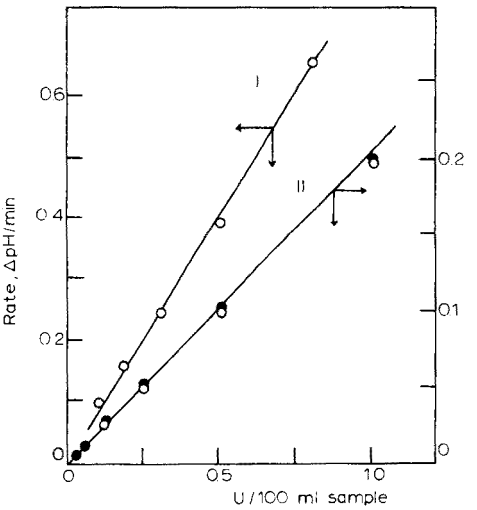

Fig. 6. Calibration curves for cholinesterase. 2 mM Tris buffer, pH 8.10, μ = 0.01. I. Cell 1. II. Cell 2. •Results obtained without nitrogen.

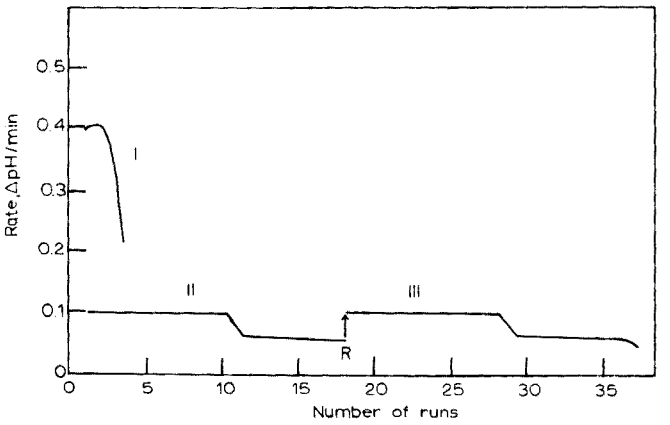

Fig. 7. Stability of immobilized substrate preparations. 2 mM Tris buffer, pH 8.10 ± 0.05, μ = 0.01, 0.5 U/100 μl cholinesterase added. I. Cell 1. II. Cell 2. III. Cell 2, after renewal of substrate layer, without nitrogen.

REFERENCES

1 H. O. Michel, J. Lab. Clin. Med., 34 (1949) 1566.
2 J. Chouteau, P. Rancien and A. Karamanicin, Bull. Soc. Chim. Biol., 38 (1956) 139.
3 K. L. Crochet and J. G. Montalvo, Anal. Chim. Acta, 66 (1973) 259.
4 K. Gibson and G. G. Guilbault, Anal. Chim. Acta, 76 (1975) 245.
5 G. G. Guilbault and M. Tarp, Anal. Chim. Acta, 73 (1974) 355.

Analytica Chimica Acta, 85 (1976) 301—307

INDIRECT POTENTIOMETRIC DETERMINATION OF ARSENITE, SULPHITE, ASCORBIC ACID, HYDRAZINE AND HYDROXYLAMINE WITH AN IODIDE-SELECTIVE ELECTRODE

R. CHRISTOVA, M. IVANOVA and M. NOVKIRISHKA

Department of Analytical Chemistry, University of Sofia, Sofia 26 (Bulgaria)

(Received 23rd February 1976)

SUMMARY

Reductants which react stoichiometrically with iodine can be determined under appropriate conditions by oxidation with a purified ethanolic solution of iodine and measurement of the iodide formed with an iodide-selective electrode. Arsenic(III), sulphite, ascorbic acid, hydrazine and hydroxylamine in concentrations ranging from $5 \cdot 10^{-7}$ to 10^{-3} M can be determined, the limits of determination being 33 ng $NaAsO_2$, 32 ng Na_2SO_3, 44 ng $C_6H_8O_6$, 13 ng $N_2H_4 \cdot 2$ HCl and 17 ng $NH_2OH \cdot HCl$ per ml. The reproducibility is similar to that of direct potentiometric methods, i.e. 2—3 % for 10^{-5}N solutions.

The method proposed for the determination of low concentrations of reductants is based on quantitative oxidation under appropriate conditions with a virtually iodide-free ethanolic solution of iodine, followed by measurement of the activity of the iodide ions formed with an ion-selective electrode.

The method is applicable to any reductant which reacts stoichiometrically with iodine. It is particularly appropriate for determining reductants that are unstable in contact with air. The method was tested in determinations of arsenite, sulphite, ascorbic acid, hydrazine and hydroxylamine in the concentration range between $5 \cdot 10^{-7}$ and $1 \cdot 10^{-3}$ N. The reproducibility was found to be similar to those of direct potentiometric methods based on ion-selective electrodes. At reductant levels above $1 \cdot 10^{-5}$ N, the errors do not exceed 1 mV, i.e., 2—3 % (relative). At lower levels the errors increase to about 5 %.

EXPERIMENTAL

Equipment

Two kinds of iodide-selective electrodes were used; a Radiometer F1032 electrode and a Crytur iodide-selective electrode (Czechoslovakia). A Seibold glass electrode and a Radiometer saturated calomel reference electrode (K 401) were also used. Measurements were made with a Radiometer PHM63 digital pH-meter and a Titrierautomat AT-2 (GDR).

All volumetric glassware was calibrated; micropipettes were used for volumes of less than 5 ml.

Reagents

Only p.a. reagents and twice-distilled water were used.

Preparation of an iodide-free iodine solution. The iodine solution used must be essentially free of iodide ions. Aqueous solutions are obviously unsuitable. When iodine is dissolved in organic solvents, the solvent itself is partly oxidized with a resulting release of iodide ions. When an ethanolic 0.1 M solution of iodine was used, a blank assay (prepared by diluting 0.05 ml of the solution to 50 ml with monochloroacetate buffer, pH 2) contained $5—8 \cdot 10^{-6}$ M iodide. Such a solution was suitable for oxidizing reductants at concentrations greater than $1 \cdot 10^{-5}$ N. In order to achieve full benefit from the electrode sensitivity (10^{-7} M) in determining reductants, it was necessary to remove the iodide from the iodine solution.

A strongly basic anion-exchange resin was used for this purpose. The anion-exchange resins Dowex 1 or Dowex 2 adsorbed 6 meq g^{-1}, i.e., almost double the usual capacity of those resins (3.5—4.5 meq g^{-1}). This can be explained by the formation of polyiodide complexes with the tetraalkylammonium ions of the resins; the complexes are of the type $—CH_2(CH_3)_3NI_x$, in which x can attain values of up to 9 [1, 2].

The iodine-saturated anion exchanger selectively adsorbed iodide ions from aqueous and ethanolic solutions alike. To prepare an iodide-free solution of iodine, 0.2—0.5 g of Dowex 1-X8 (chloride form; 100-200 mesh) was introduced into a small glass tube (4—5 mm i.d.) to form a small bed supported on glass wool. The resin was saturated with 12—30 ml of an ethanolic 0.1 M solution of iodine; the flow rate had no significance.

When the ethanolic solution passed through the column, the iodine concentration remained virtually unaltered, but there was an almost total adsorption of iodide. A blank assay prepared by passing the iodine solution through the column contained less than $1 \cdot 10^{-7}$ M iodide. Such columns could be used over a period of several weeks. The iodide content in the blank test is an indication of its fitness for use.

Choice of a suitable pH value

When an ethanolic solution of iodine is diluted with water, hydrolysis and the accompanying disproportionation cause the iodide concentration to rise

$$I_2 + H_2O = HIO + I^- + H^+ \qquad (1)$$

The iodide concentration can be calculated from the potentials of the two redox couples [3, 4]: $HIO + H^+ + e \rightleftharpoons \frac{1}{2} I_2 + H_2O$ ($E^\circ = 1.45$ V; E(formal) = 1.04 V at pH 7) and $\frac{1}{2} I_2 + e \rightleftharpoons I^-$ ($E^\circ = 0.6197$ V). At equilibrium, the potentials of the two couples are equal, and rearrangement of the appropriate Nernst relationships gives

$$0.4203/0.059 = -\log([HIO]\,[I^-]/[I_2]) \qquad (2)$$

Equation (1) indicates that $[I^-] = [HIO] = [H^+]$. In an aqueous solution

saturated with iodine, the iodine concentration is 0.0013 M; and substitution in eqn. (2) shows that $[I^-] = 10^{-5.05}$ M. In neutral media, the activity of iodide released by hydrolysis exceeds the electrode sensitivity by about two orders of magnitude. It was therefore of interest to establish the pH value at which the activity of released iodide would be less than 10^{-7} M, either by calculation from eqn. (2) or by measurement of iodide.

The hydrolytic equilibrium was investigated as follows: 0.1 ml of an iodide-free ethanolic 0.1 M iodine solution was added to 10 ml of 0.1 M acetic acid (pH 2.9), the iodide activity was measured, then 0.1 M sodium hydroxide was added to the solution in 1-ml increments, and the iodide was measured after each addition. Activity coefficients were calculated from the equation: $-\log f = 0.512\, z^2\, \mu^{\frac{1}{2}}/(1 + \mu^{\frac{1}{2}})$. The pH values were measured simultaneously. The experiment was repeated with differing volumes (0.05 and 0.5 ml) of the iodine solution added to acetic acid. The results obtained (Fig. 1) show that $[H^+]$ and $[I^-]$ become equal at pH 5.5. With such data it is possible to establish a suitable pH for the oxidations. It is obviously preferable to use a pH value below 3, and pH 2 is convenient; this can be maintained with a monochloroacetate buffer. The e.m.f. measured in a buffer solution of pH 2 containing 10^{-4} M iodine corresponded to that found with no iodine or iodide present.

The experimental values of $[I^-]$ are slightly lower than those of $[H^+]$ throughout the pH range (Fig. 1), obviously because of the slow rate of hydrolysis; the values of $[I^-]$, measured immediately after altering the pH, do not correspond to the equilibrium $[I^-]$ values at the same pH. This was

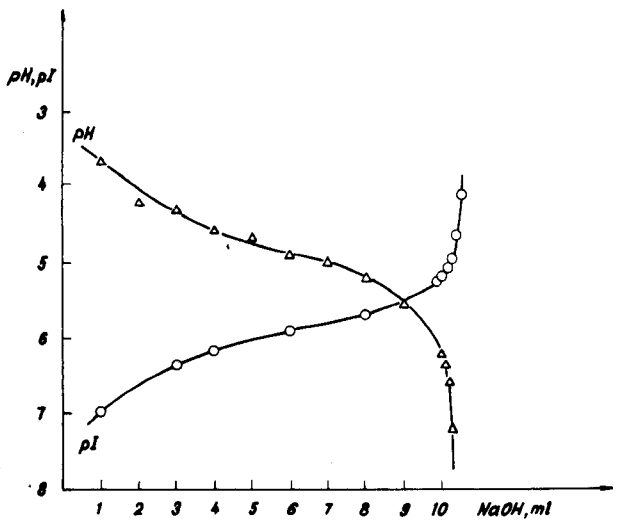

Fig. 1. Dependence of degree of hydrolysis on pH. pH and pI values were measured during the titration of 0.001 M iodine solution (in 0.1 M CH_3COOH) with 0.1 M NaOH.

established by measuring the e.m.f. at intervals of time after the ethanolic iodine solution had been diluted with buffer. The following data were obtained:

Time (min)	1	2	3	4	5	6	7
E.m.f. (mV)	133	120	108	94	78	60	43

The final value corresponded to $[I^-] = 10^{-7}$ M.

When the e.m.f. was measured at iodide levels of less than 10^{-5} M with intervals exceeding 10 min between the introduction of iodine into the aqueous solution and the measurement itself, the results were affected by the slow hydrolysis. For more than 10^{-5} M iodide, the measurements were not affected by hydrolysis even when the e.m.f. was measured 48 h after the introduction of iodine.

The experimentally determined values of $[I^-]$ coincided fairly accurately with the calculated ones. The experimental value of $[I^-]$ at pH 7 was $10^{-5.0}$ M (theoretical, $10^{-5.05}$ M).

Oxidations were done with an ethanolic 0.1 M solution of iodine flowing from the column. E.m.f. values were measured with moderate stirring at 20 ± 0.2 °C in solutions of pH 2 (monochloroacetate buffer).

When the electrode was immersed for a long period of time in solutions containing up to 10^{-4} M HIO, it was observed that the electrode sensitivity diminished by about two orders of magnitude. Polishing the membrane surface restored the initial sensitivity of the electrode.

DETERMINATIONS OF ARSENITE, SULPHITE AND ASCORBIC ACID

Stock 0.01 N solutions of $NaAsO_2$, Na_2SO_3 and $C_6H_8O_6$ were prepared. If the solutions were not exposed to light, their concentration remained unaltered for a week. Just before the determination, 10^{-4} N solutions were prepared by dilution. Then aliquots containing $5 \cdot 10^{-2}$, $5 \cdot 10^{-3}$, $5 \cdot 10^{-4}$, $2.5 \cdot 10^{-4}$, $5 \cdot 10^{-5}$, $2.5 \cdot 10^{-5}$ and $5 \cdot 10^{-6}$ meq of the reductants were transferred from the stock or dilute solutions to volumetric 50-ml flasks. Monochloroacetate buffer (2.5 ml) was added to each flask. For the four highest reductant concentrations, the ethanolic 0.1 M iodine solution was added dropwise from the column until a pale yellow colour unaffected by stirring, appeared. Some dexterity was needed to ensure that the excess of iodine added did not significantly exceed 10^{-4} M. If it does, iodide tends to combine into triiodide ions, and the iodide activity drops; otherwise the excess of iodine does not affect the iodide-selective electrode and need not be removed. For the three lowest reductant concentrations, the same volume (0.05 ml) of iodine solution was added to each flask, and to the blank assay. The solutions were then diluted to the mark with water and stirred.

E.m.f. measurements were made first in the blank assays, and then in the

solutions, beginning with the lowest concentrations, at intervals of 15 s. Values which remained steady for 1—2 min were considered correct; at concentrations above 10^{-6} N, steady values were achieved in 30 s. For comparison, the e.m.f. values in solutions with potassium iodide activities between 10^{-7} and 10^{-2} (μ = 0.05; KNO_3) were measured under identical conditions.

Standard curves were plotted with e.m.f. vs.pN_{red} and e.m.f. vs.pM_{kI} (Fig. 2). The response was 59 ± 1 mV per decade at reductant levels between 10^{-3} and 10^{-5} N. The characteristic curve remained usable down to $5 \cdot 10^{-7}$ N, but the response per decade diminished by a few mV.

For the reductants tested, the sensitivity of the method (in ng ml^{-1}) was as follows: $NaAsO_2$, 33; Na_2SO_3, 32; $C_6H_8O_6$, 44.

It is noteworthy that the standard curves for the reductants coincide fairly well with that for potassium iodide. This indicates that, under the conditions used, the oxidation of the reductants with iodine proceeds quantitatively. The effect of secondary reactions, such as iodine hydrolysis, is clearly slight.

To check the recommended conditions, in further experiments, the same reductants were oxidized in neutral media. The data are given in Fig. 3. At reductant concentrations above 10^{-5} N, the e.m.f. values coincided, within 1 mV, with those obtained at pH 2; at lower concentrations, the values in neutral media were higher. Accordingly, a pH of 2 is a necessary condition for quantitative oxidation at low reductant concentrations.

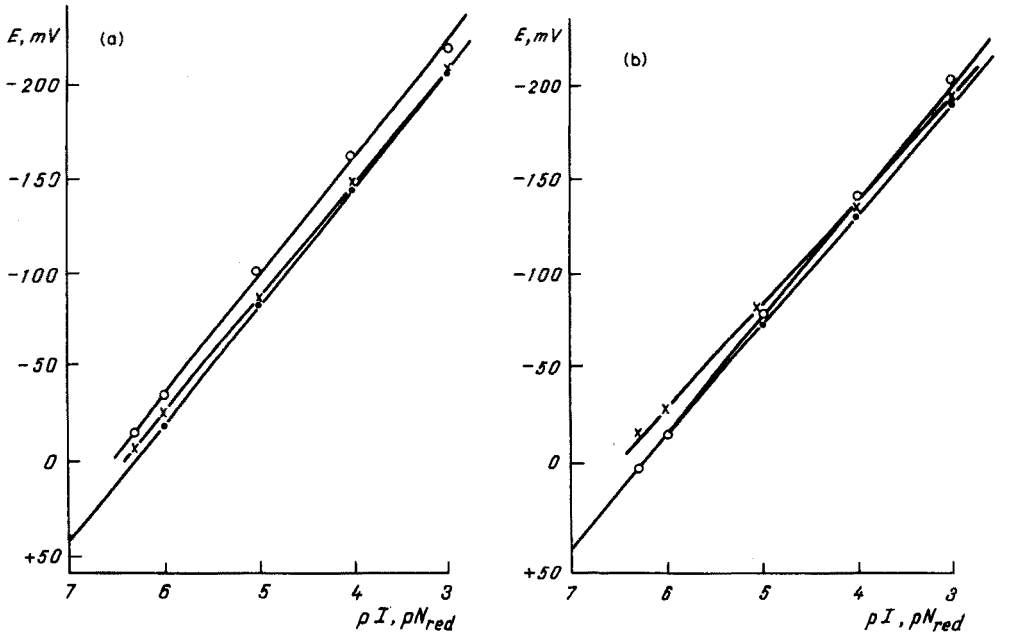

Fig. 2. Calibration plots for KI (•), arsenite (○), and ascorbic acid (×). (a) With the Crytur electrode. (b) With the Radiometer electrode.

Comparison of the two types of iodide-selective electrode

The Crytur electrodes do not differ in response and sensitivity from the Radiometer electrodes. However, certain discrepancies were observed when results obtained at different times were compared. Parallel tests carried out at different times over a period of six months, showed that the Radiometer electrode has a reproducibility of ±1 mV over the 10^{-5}—10^{-2} N range; with the Crytur electrode, there was a slightly greater discrepancy between the standard curves (Fig. 2), caused by drift in the E_0 value.

DETERMINATION OF HYDRAZINE AND HYDROXYLAMINE

The reactions with iodine of $N_2H_4 \cdot 2HCl$ [5] and $NH_2OH \cdot HCl$ [6] are

$$N_2H_4 + 2\,I_2 \rightarrow N_2 + 4\,H^+ + 4\,I^-$$
$$2\,NH_2OH + 2\,I_2 \rightarrow N_2O + 4\,H^+ + 4\,I^- + H_2O$$

Stock solutions (10^{-2} N) of the two reductants were prepared and 10^{-4} N solutions were prepared by dilution as required. Samples containing $5 \cdot 10^{-2}$ —$5 \cdot 10^{-6}$ meq of the reductants were transferred to volumetric 50-ml flasks, and 2.5 ml of buffer (pH 2) was added to each flask. The stronger solutions were heated for 5 min at 80 °C in a water bath, and then the purified solution of iodine was added dropwise until a pale yellow colour appeared. The flasks were then replaced in the water bath; if the colour persisted for 2 min, the solutions were allowed to cool to 20 °C and then diluted with water to the mark; if the colour disappeared, a further addition of iodine was followed by a further 2-min check in the water bath. For the solutions containing $5 \cdot 10^{-5}$ — $5 \cdot 10^{-6}$ meq of reductant, and for the blank assays, 0.05 ml of iodine solution was added and the flasks were kept for 2—3 min in the water bath; the solutions were then left to cool and diluted to the mark.

For hydrazine concentrations between 10^{-6} and 10^{-3} N, the response was 59 ± 1 mV per decade (Fig. 4). For hydroxylamine, the response failed, throughout the concentration range, to attain the theoretical value by some 10 mV/decade, but the calibration curve was linear and the results showed good reproducibility. The inadequate response is probably due to the difficulty of achieving quantitative oxidation of hydroxylamine according to the above equation [6]. The sensitivity of the method is 13 ng ml^{-1} for $N_2H_4 \cdot 2$ HCl and 17 ng ml^{-1} for $NH_2OH \cdot HCl$.

DISCUSSION

The indirect potentiometric method is superior in sensitivity to other methods for determining the above-mentioned reductants [6—9], except for the atomic absorption determination of arsenic [10].

Calculated from the mean blank assay and the confidence limit, the sensitivity of the method is $5 \cdot 10^{-7}$ N. The selectivity is the same as that of the direct iodimetric determination of these reductants. The excellent sensitivity

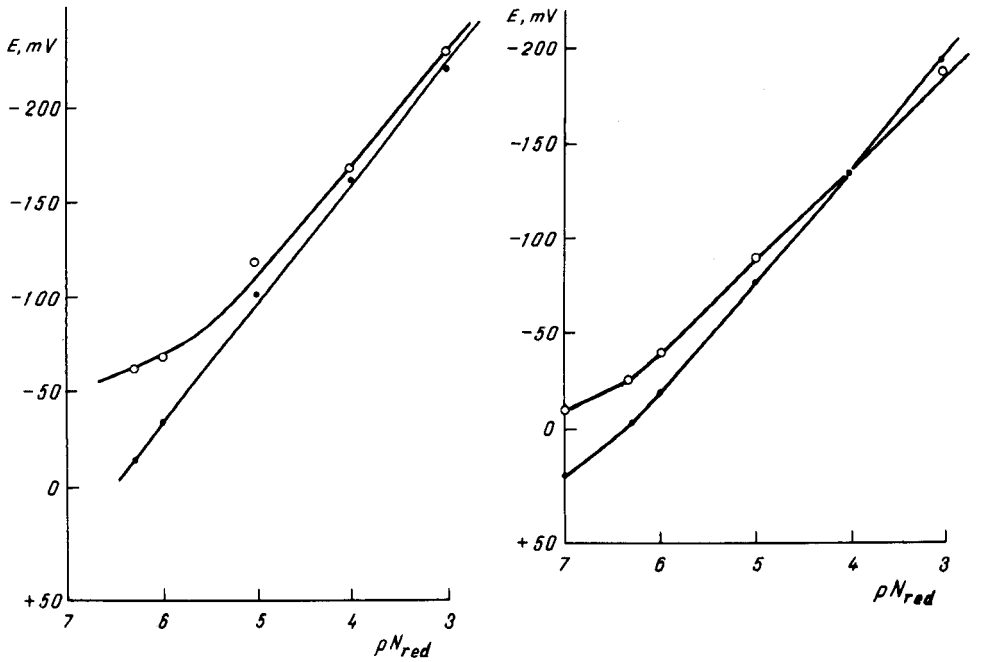

Fig. 3. Calibration plots for $NaAsO_2$ at pH 2 (•) and in a neutral KNO_3 solution (○) with the Crytur electrode.

Fig. 4. Plots for N_2H_4 (•) and NH_2OH (○) with the Radiometer electrode calibration.

is advantageous for the elimination of some interfering effects by dilution of the sample solutions. The proposed method has also the advantages of expeditious and simple application, and low cost. During the investigation, it was established that the iodide-selective electrode provides a convenient means of studying the equilibrium and kinetics of reactions involving the $I_2/2\ I^-$ couple.

REFERENCES

1 M. Heuterbise and W. J. Ross, Anal. Chem., 44 (1972) 596.
2 M. Novkirishka and R. Christova, Anal. Chim. Acta, 78 (1975) 63.
3 F. A. Cotton and G. Wilkinson, Advanced Inorganic Chemistry, Interscience, New York, 2nd edn., 1966.
4 I. M. Kolthoff, E. B. Sandell, E. J. Meehan and S. Bruckenstein, Quantitative Chemical Analysis, Macmillan, London, 4th edn., 1971.
5 I. M. Kolthoff, R. Belcher, V. A. Stenger and G. Matsuyama, Volumetric Analysis, Vol. III, Interscience, New York, 1957.
6 G. Charlot, Chimie Analytique Quantitative, Tome II, Masson, Paris, 1974.
7 Conference of the Heads of the Water Management Agencies of the Member Countries of the Council for Mutual Economic Aid, Unified Methods for Investigating Water Quality, Part I, Moscow, 1974.
8 R. Ammon und W. Dirscherl, Fermente-Hormone-Vitamine, III Auf., Band III/1. Vitamine, Georg Thieme, Stuttgart, 1974.
9 B. Jaselskis and J. Nelapaty, Anal. Chem., 44 (1972) 2,379.
10 H. R. Griffin, M. B. Hocking and D. G. Lowery, Anal. Chem., 47, N2, (1975) 229.

Analytica Chimica Acta, 85 (1976) 309—316

SOLID-STATE ION-SELECTIVE ELECTRODES AS END-POINT DETECTORS IN COMPLEXIMETRIC TITRATIONS
PART III. SELECTION OF SOME EXPERIMENTAL CONDITIONS FOR BACK-TITRATIONS IN ALKALINE MEDIUM

J. M. VAN DER MEER*, G. DEN BOEF and W. E. VAN DER LINDEN

Laboratory for Analytical Chemistry, University of Amsterdam, Nieuwe Achtergracht 166, Amsterdam (The Netherlands)

(Received 24th February 1976)

SUMMARY

The applicability of the copper(II) solid-state electrode in alkaline medium for complexiметric back-titrations of the alkaline-earth metals with EDTA and EGTA has been studied. Copper(II) is used as the back-titrant. Special attention is given to the use of ammonia and cyclohexylamine as the buffer substance.

In a previous paper [1] complexiметric back-titrations in acidic medium with end-point indication by means of a copper(II)-selective electrode have been discussed. In the present paper, the results obtained in alkaline medium are described. In alkaline medium the behaviour of the electrode proved to be less reproducible than in acidic medium, probably because of the increased solubility of the membrane material, leading to an ill-defined composition of the electrode surface. However, alkaline media are necessary for the determination of alkaline earth metals. In these media the conditional stability constants of complexes of these ions have their maximum values whereas the values for the complexes of other metals are generally rather low.

Theoretical curves

The equations for the calculation of the theoretical curves have already been given [1]. The theoretical titration curve, f vs. E, can be obtained [1,2] by means of the equation

$$E = E' + S \log \{[\mathrm{Cu}] + K'_{\mathrm{Cu,\,N}}\,[\mathrm{N}] + D_{\mathrm{Cu}}\} \qquad (1)$$

in which N is a divalent ion. If f vs. E curves do not produce satisfactory end-points, f vs. [M] curves may yield better results. The equation for these linearized curves is

*Present address: Institute for Animal Feeding and Nutrition Research, Runderweg 2, Lelystad (The Netherlands).

$$\text{antilog}\,[(E - E')/S] = [\text{Cu}] + K'_{\text{Cu, N}}[\text{N}] + D_{\text{Cu}} \quad (2)$$

EXPERIMENTAL

Reagents

All solutions were prepared from analytical-grade chemicals and redistilled water. Metal ions were added as nitrates. The buffer solutions were 0.25 M ammonia–ammonium nitrate buffer pH 10, and 0.25 M cyclohexylamine–CHA nitrate buffer pH 11.

Apparatus

All details have been described previously [1, 2]. An electronic device [3] producing a signal equal to antilog $[(E - E')/S]$ was applied. The electrodes were conditioned in 10^{-3} M EDTA and 0.25 M ammonia buffer pH 10. After each titration the electrode had to be kept in water for several hours before being used again. The procedure was the same as for the potentiometric titration in acidic medium [1].

Precipitate formation

The formation of a precipitate $M(OH)_n$ depends on the solubility constant $K_{so} = [M][OH]^n$ which is now recommended to be written as

$$*K_{so} = [M]/[H]^n \quad (3)$$

If eqn. (3) is combined with

$$[M']/[M] = \sum_n \beta_n [OH]^n \quad (4)$$

where $\beta_0 = 1$, an equation for the equilibrium for the precipitation of the hydroxide is obtained [4]:

$$pM'_{max} = -\log *K_{so} + n\text{pH} - \log \sum_n \beta_n [OH]^n \quad (5)$$

For freshly precipitated copper hydroxide, $Cu(OH)_2 \cdot nH_2O$, $\log *K_{so} = 8.1$ [5]. Substitution of this value and of $\log \beta_1 = 6.0$ and $\log \beta_2 = 13.2$ in eqn. (5) leads to the equilibrium line in Fig. 1. In the presence of complexing agents such as ammonia or EDTA, a value for the side-reaction coefficient α_M must be added to eqn. (5). In those cases new equilibrium lines will be found. To avoid precipitation of copper(II) hydroxide, the copper(II) concentration must remain above the equilibrium line for the medium under consideration.

The use of a pure 10^{-1} M copper(II) nitrate solution (pH 4.3, point A in Fig. 1) as the titrant caused difficulties in titrations at pH 10–11, because on delivery of titrant a precipitate of copper(II) hydroxide was formed at the burette tip. Erroneous end-points were thus obtained. Presumably the reaction between copper(II) and hydroxide is faster than the reaction between copper(II) and EDTA. At the burette tip the titrant is diluted and

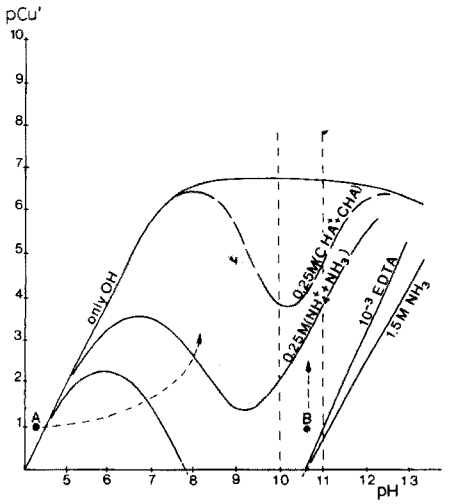

Fig. 1. Equilibrium lines (eqn. 5) for copper(II) hydroxide formation as a function of the pH in the absence and in the presence of NH_3, CHA and EDTA. The constants used are: log $^*K_{so}$ = 8.1 for $Cu(OH)_n$, log β_1 = 6.0, log β_2 = 13.2; for $Cu(NH_3)_n$, log β_1 = 4.3, log β_2 = 7.6, log β_3 = 10.5, log β_4 = 12.6; for $Cu(CHA)_3$, log β_3 = 11.5; $pK_b^{NH_3}$ = 4.6; pK_b^{CHA} = 3.4.

strongly increased in pH which results in the change suggested qualitatively by the dotted line. Precipitation can be avoided by making the titrant solution 1.5 M with respect to ammonia (pH 10.7, point B in Fig. 1). When the titration starts from B, no equilibrium line is crossed on dilution, and no precipitation occurs.

RESULTS AND DISCUSSION

Figure 2 gives the experimental and theoretical curves for the titrations of Trien, EDTA and EGTA with copper(II) in an ammonia buffer pH 10. The absolute values of the stability constants [5, 6] are: log $K_{CuTrien}$ = 20.4, log K_{CuEDTA} = 18.8 and log K_{CuEGTA} = 17.7. The relevant side-reaction coefficients log $\alpha_{L(H)}$ are 0.3 for Trien, 0.5 for EDTA and 0.1 for EGTA; log $\alpha_{CuEDTA(NH_3)}$ = 1.45 [7], log $\alpha_{CuEGTA(OH)}$ = 0.55 and log $\alpha_{Cu(NH_3)}$ = 9.98.

If there were no influence from the limit of detection of the electrode (D_{Cu}), the curves for $f < 1$ would be determined only by the values of the conditional stability constants. This is obviously the case for Trien and EGTA. The discrepancy between the theoretical and experimental curves for EDTA can be explained by the limit of detection of the electrode. The value of D_{Cu} in relation to the concentration of EDTA is given in Fig. 3. For values of $f > 1$, the three curves ought to coincide as these parts depend on C_L only. The differences observed can only be attributed to changes in the electrode behaviour depending on the nature of the ligand used in the titration.

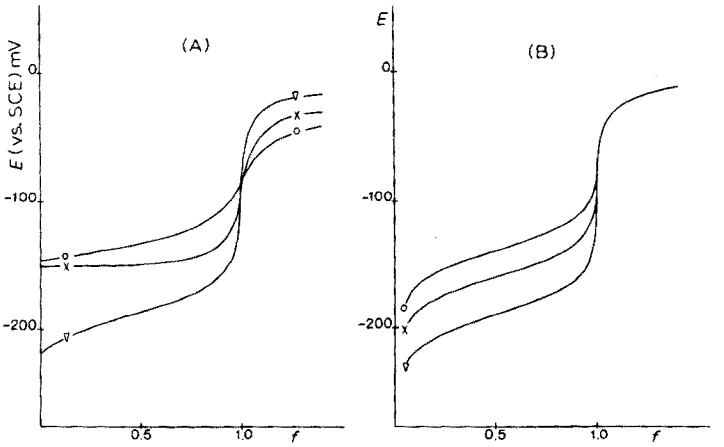

Fig. 2.(A). Experimental titration curves for 10^{-3} M Trien (▽), EDTA (×) and EGTA (○) with copper(II) in 0.25 M ammonia—ammonium nitrate buffer pH 10. (B). Theoretical curves.

Figure 4 gives the same titrations in cyclohexylamine buffer pH 11. As little information is yet available for this medium, no theoretical curves could be calculated. The steep part of the curves in Fig. 4 is larger than for the corresponding curves in Fig. 2. Most likely the conditional stability of the copper(II)—ligand complex is larger because of a change in the side-reaction coefficients; the increase in the pH from 10 to 11 will result

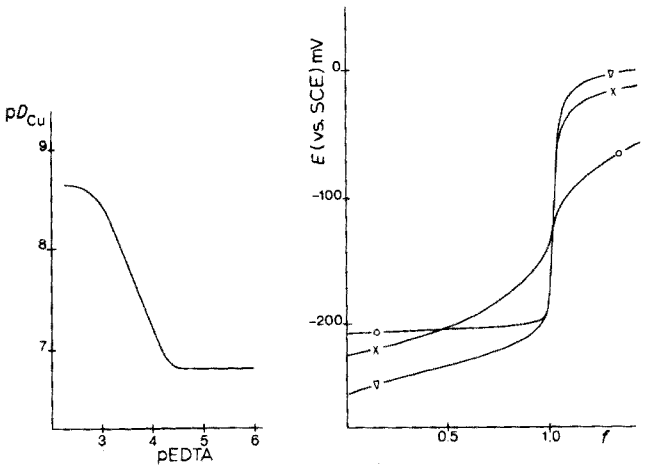

Fig. 3. The limit of detection of the electrode (D_{Cu}) as a function of the EDTA concentration at pH 10.

Fig. 4. Experimental titration curves in 0.25 M cyclohexylamine—CHA nitrate buffer pH 11, corresponding to Fig. 2.

in a small decrease of $\alpha_{L(H)}$ and an increase in $\alpha_{CuL(OH)}$. This means that for $f < 1$ more negative potentials are obtained.

If it is assumed that the liquid junction potential and the ionic strength are about the same for the two buffer systems, the observed increase of the potential for $f > 1$ may be caused by a decrease of α_M. The deviation in the case of EGTA can only be explained by a different electrode behaviour.

The experimental titration curves given in Figs. 5 and 6 for the determination of calcium(II) and magnesium(II) will be discussed in relation to the conditional stability constants of the chelates of these metals with EDTA and EGTA; the insets in Figs. 5 and 6 show these constants as functions of the concentration of ammonia and cyclohexylamine. The discussion is restricted to EDTA and EGTA as Trien does not form complexes with the alkaline earth metals. The experimental conditions (0.25 M ammonia or 0.25 M cyclohexylamine are given by the solid line (NH_3; pH 10) and the dotted line (cyclohexylamine; pH 11) perpendicular to the x-axis. The lines for cyclohexylamine media were calculated with $pK_b = 3.4$ and $\log \alpha_{Cu(CHA)} = 9.4$. The value of $\log \alpha_{Cu(CHA)}$ was obtained from the titration curves of EDTA and Trien with copper(II).

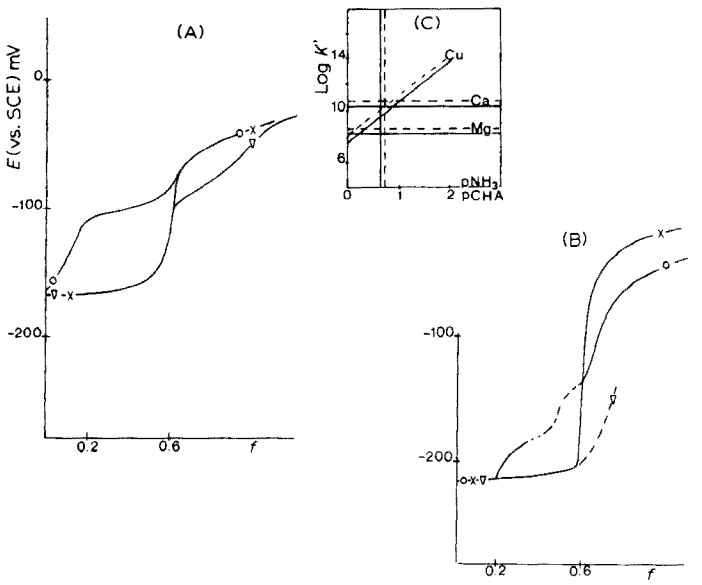

Fig. 5. Titration curves for the back-titration of $4 \cdot 10^{-4}$ M calcium(II) (×), $4 \cdot 10^{-4}$ M magnesium(II) (▽) and their sum (○) with copper(II). $C_{EDTA} = 10^{-3}$ M. (A). In 0.25 M ammonia buffer pH 10. (B). In 0.25 M cyclohexylamine buffer pH 11.

(C). The conditional stability constants of copper(II)—, calcium(II)— , and magnesium(II)— EDTA as a function of the buffer concentration. (———) In NH_3 buffer pH 10. (------) In CHA buffer pH 11.

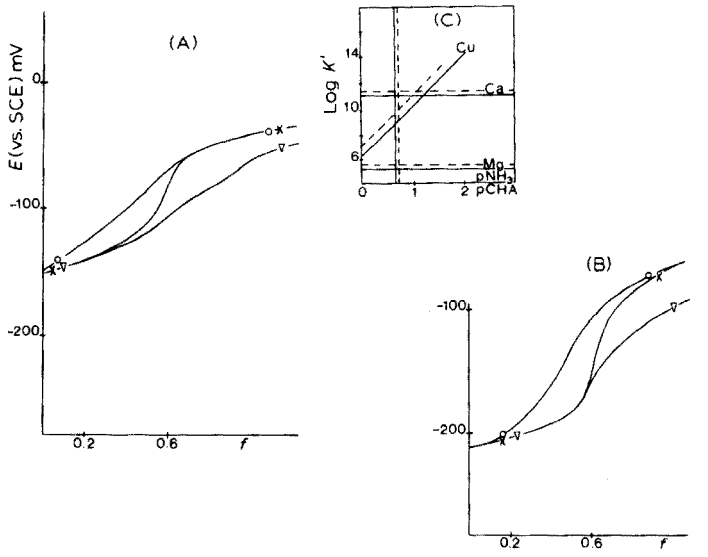

Fig. 6. The titration curves and conditional stability constants when EGTA is used as the ligand. All other conditions as for Fig. 5.

It should be kept in mind that back-titrations are only possible when $K' c \geqslant 10^2$ for both the back-titrant metal and the metal to be determined. The value 10^2 applies to linear end point indication; in the case of logarithmic indication this value has to be 10^5—10^6. The sum of the concentration of a number of metal ions can be determined when $K' c \geqslant 10^2$ for all the metal ions involved. When two metals have to be determined in an approximately equimolar mixture, then two end-points must occur, one for the sum and the other for the metal ion which forms the weaker complex. In that case, which is encountered here for mixtures of calcium and magnesium, with magnesium forming the weaker complex, two additional requirements have to be fulfilled, i.e. $K'_{CuL}/K'_{MgL} \geqslant 10^2$ and $K'_{CaL} \geqslant K'_{MgL}$. From Fig. 5(C) it can be seen that with EDTA as the ligand, back-titrations are possible for both calcium and magnesium with buffer concentrations smaller than 0.25 M. The buffer capacity may, however, be a limiting factor. These considerations are confirmed by the experiments (Fig. 5A, B). Because of the larger conditional stability constants, better results would be expected for the cyclohexylamine medium. The titration of calcium in this medium appears to be very sharp indeed, but when magnesium was present no useful end-points could be obtained.

A different situation exists in the case of EGTA. From Fig. 6(C), it is clear that magnesium cannot be determined whereas the determination of calcium(II) should be possible. This diagram indicates that the value of about 0.25 M for the free ammonia concentration in the buffer is almost an optimum one; when higher concentrations are used, the conditional stability constant for copper(II)—EGTA becomes too low to fulfil the

titration condition $K' c \geqslant 10^2$. Figure 6(A) shows that the shape of the titration curve for calcium(II) is worse than would be expected . The presence of magnesium(II) makes determinations impossible. As would be expected, the curve for calcium(II) is better when cyclohexylamine is used instead of ammonia (Fig. 6(B)).

The failure of the titrations with both EDTA and EGTA at pH 11 in cyclohexylamine buffer where magnesium(II) was present, can be explained by the fact that at this pH value magnesium(II) precipitates as magnesium(II) hydroxide even at 10^{-5} M. This concentration is reached almost immediately after the point at which the excess of EDTA has been titrated. With EGTA as the ligand this precipitation occurs at even smaller values of f than in the case of EDTA.

Some difficulties arise with the estimation of the end-points from the asymmetric titration curves. According to Whitfield and Leyendekkers [8], the point of maximum slope is taken as the end-point. When f—E curves do not produce satisfactory end-points, better results may be obtained from the f—[M] curves. In some cases, linearization of the upper bend of the titration curve will result in a better accuracy.

Table 1 gives some experimental results for the determination of calcium and magnesium with potentiometric and linear end-point indication.

TABLE 1

Back-titrations with copper(II)

Substance	Taken (μmol)[a]	Logarithmic			Linear		
		Found[b] (μmol)	Error (%)	s_r[c]	Found (μmol)	Error (%)	s_r
Ammonia							
EDTA	9.75	9.74	−0.1	0	9.79	+0.4	0.1
Calcium(II)	3.72	3.90	+4.8	0.1	4.02	+8.1	0.3
Magnesium(II)	4.00	4.02	+0.6	0.6	4.02	+0.5	0.1
EGTA	9.75	9.73	+0.2	0.5	9.93	+1.8	0.4
Calcium(II)	3.72	3.86	+3.8	0.9	3.88	+4.3	2.2
Magnesium(II)	4.00	—[d]	—[d]	—[d]	4.54	+13.5	7.3
Cyclohexylamine							
EDTA	9.75	9.75	0	0.4	9.75	0	0.4
Calcium(II)	3.72	3.73	+0.3	1.4	3.62	−2.7	1.1
Magnesium(II)	4.00	—[e]	—[e]	—[e]	—[e]	—[e]	
EGTA	9.75	9.54	−2.2	0.8	9.56	−1.9	0.2
Calcium(II)	3.72	3.76	+1.1	1.2	4.06	+9.1	3.0
Magnesium(II)	4.00	3.66	−8.5	0.8	4.21	+5.3	1.6

[a]In 10 ml. [b]Mean of 4 determinations. [c]Relative standard deviation (%). [d]No determination possible. [e]No reproducible curves could be obtained.

REFERENCES

1 J. M. van der Meer, G. den Boef and W. E. van der Linden, Anal. Chim. Acta, 76 (1975) 261.
2 J. M. van der Meer, G. den Boef and W. E. van der Linden, Anal. Chim. Acta, 79 (1975) 27.
3 J. M. van der Meer and J. C. Smit, Anal. Chim. Acta, 83 (1976) 367.
4 J. Kragten, Analyst (London), 99 (1974) 43.
5 L. G. Sillen and A. E. Martell, Stability Constants of Metal-ion Complexes, Chemical Society, Spec. Publ. No. 17, London, 1964.
6 A. Ringbom, Complexation in Analytical Chemistry, Interscience, New York, 1963.
7 D. Aikens, G. Schmuckler, F. Sadek and C. Reilly, Anal. Chem., 33 (1961) 1664.
8 M. Whitfield and J. V. Leyendekkers, Anal. Chim. Acta, 45 (1969) 383.

Analytica Chimica Acta, 85 (1976) 317—322

THE MICRO DETERMINATION OF COPPER(II) WITH A SOLID-STATE COPPER-SELECTIVE ELECTRODE

J. M. VAN DER MEER, G. DEN BOEF and W. E. VAN DER LINDEN

Laboratory for Analytical Chemistry, University of Amsterdam, Nieuwe Achtergracht 166, Amsterdam (The Netherlands)

(Received 24th February 1976)

SUMMARY

The standard addition and standard subtraction methods are discussed briefly. Both methods are applied to the determination of copper(II) in very small sample volumes. A microcell (25 μl) and a copper-selective micro-electrode are described for this purpose; a nanoliter burette was constructed for the addition of very small increments. The results are compared with those obtained in a 10-ml cell.

During the last two decades, much attention has been paid to the use of electrochemical methods in (ultra)microchemical analysis. The work of Alimarin et al. [1, 2] and Helbig [3] is of particular importance; for they were able to titrate nanogram amounts of metal ions with adequate accuracy in cell volumes down to 1 μl. All their experiments, including the potentiometric ones, were done with micro-electrodes with dimensions adapted to these extreme small cell volumes.

Apart from glass electrodes, it is rather difficult to scale down the size of ion-selective solid-state electrodes. An elegant solution to this problem was suggested by Durst and Taylor [4]; they cemented a small ring on the active membrane surface of an inverted fluoride electrode to form a microcell with a volume of about 10 μl, and determined $2 \cdot 10^{-6}$ M solutions of fluoride in this cell by linear null-point potentiometry [5]. For that purpose the micro-cell containing the sample was connected to a much larger cell to form a concentration cell; a standard solution of the test compound was then added to the solution in the larger cell until the concentration cell had an e.m.f. of zero.

The present paper describes the determination of copper in a 25-μl cell containing a copper-selective solid-state electrode. The electrodes used have an active membrane area at least 4 times smaller than those used before [6, 7]. These electrodes were also tested in larger cell volumes. Instead of potentiometric complexiметric titrations [6, 7], the methods of standard subtraction and standard addition were used; the former method corresponds to linearization of the initial part of a titration curve. This procedure has the

advantage that the condition $K'c \geqslant 10^6$, which must be fulfilled for logarithmic titration curves [8], is replaced by the less stringent condition $K'c \geqslant 10^2$. For the same medium and "titrant", this allows the determination of smaller concentrations. For very low concentrations, the standard addition is generally preferable. Results obtained with both procedures will be discussed.

THEORETICAL

The response of a copper-selective solid-state electrode can be represented in the general form [6]

$$E = E' + S \log \{[\mathrm{Cu}] + K'_{\mathrm{Cu,N}} [\mathrm{N}] + D_{\mathrm{Cu}}\} \quad (1)$$

where [Cu] is the actual concentration of Cu^{2+} in the original sample solution, and [N] is the concentration of an interfering ion N in this solution; $K'_{\mathrm{Cu,N}}$ is the selectivity factor, D_{Cu} the lower limit of detection of the electrode, and S and E' have their usual meanings.

If to V_0 ml of the sample solution is added ΔV ml of a standard copper(II) solution of concentration $[\mathrm{Cu}]_s$ or a complexing agent reacting with copper in a 1:1 ratio, eqn. (1) can be transformed to

$$\frac{V_0 [\mathrm{Cu}] \pm \Delta V [\mathrm{Cu}]_s}{V_0 + \Delta V} + K'_{\mathrm{Cu,N}} \frac{V_0}{V_0 + \Delta V} [\mathrm{N}] + D_{\mathrm{Cu}} = 10^{(E-E')/S} \quad (2)$$

It is assumed that D_{Cu} is not affected by the addition. The positive sign applies in the case of the standard addition procedure, whereas the negative sign is necessary for the subtraction method. Rearrangement of eqn. (2) leads to

$$[\mathrm{Cu}] + K'_{\mathrm{Cu,N}} [\mathrm{N}] + D_{\mathrm{Cu}} + \frac{\Delta V}{V_0} (\pm [\mathrm{Cu}]_s + D_{\mathrm{Cu}}) = \frac{V_0 + \Delta V}{V_0} 10^{(E-E')/S} \quad (3)$$

By plotting the right-hand side of eqn. (3) against ΔV, a straight line is obtained; this line intersects the abscissa at ΔV^* where

$$[\mathrm{Cu}] = \mp \frac{\Delta V^*}{V_0} [\mathrm{Cu}]_s - K'_{\mathrm{Cu,N}} [\mathrm{N}] - \frac{V_0 + \Delta V^*}{V_0} D_{\mathrm{Cu}} \quad (4)$$

A similar procedure was recommended by Liberti and Mascini [9], who pointed out that multiple additions (or subtractions) give better accuracy than single addition. Liberti and Mascini did not consider the last two terms on the right-hand side of eqn. (4); these terms determine the systematic error, and are caused by interfering ion N, and by the lower limit of detection of the electrode, D_{Cu}. The contribution of D_{Cu} to the systematic error will decrease, as the value of $V_0 + \Delta V^*$ is reduced. Because ΔV^* is negative for the addition method, $[(V_0 + \Delta V^*)/V_0] D_{\mathrm{Cu}}$ will vanish if the standard solution has about the same concentration as the sample solution; this concentration will generally be low in the region where D_{Cu} is of importance. For the subtraction method ΔV^* is positive, and the contribution of D_{Cu}

will be minimized if the standard solution is much more concentrated, i.e. $\Delta V^* \ll V_0$.

EXPERIMENTAL

Reagents

All solutions were prepared from analytical reagent-grade chemicals and redistilled water. The Ag_2S/CuS (1:1) precipitate was prepared by homogeneous precipitation from a solution containing the metal ions and thioacetamide as described by Růžička et al. [10].

Apparatus

A Philips pH-meter (PW 9408) in its mV-mode was used with a linearization device [11], the output of which was connected to a volume correction unit as described by Johansson [12]. The total device enables direct reading of the value $[(V_0 + \Delta V)/V_0]\, 10^{(E-E')/S}$.

Figure 1 shows the construction of the microcell and micro-electrode. The surface of the electrode is placed vertically to diminish the chance of scratching with the platinum wire used to mix the contents of the cell. Figure 2 shows the construction of the "nanoliter" burette. The total volume of the burette was 5 μl, readable to 1 nl. The nanoburette was calibrated against a standard 500-μl syringe burette by filling the burettes with 10^{-1} M or 1 M and 10^{-2} M copper(II) solutions, respectively. The two calibration lines (Fig. 3) show the good linearity of the nanoburette.

Conditioning of the electrode

To ensure proper functioning, freshly prepared electrodes must be conditioned by immersion in a 10^{-3} M solution of EDTA for at least 10 h to remove all traces of free metal ions. A calibration line obtained at this stage shows a discrepancy in the range pCu 5—6 (Fig. 4). When the electrode is then immersed in a 10^{-4} M copper(II) solution until a constant potential value is established, a correct calibration line is obtained (Fig. 4). The establishment of a constant potential never takes more than 10 min. The response of a micro-electrode prepared in this way was recorded after a stepwise change of the concentration from 10^{-4} M to $2 \cdot 10^{-4}$ M in 10-ml and 25-μl cells (Fig. 5). Probably because of the less adequate mixing, a larger response time t was found for the micro-cell (26 s for the 10-ml cell and about 47 s for the 25-μl cell). Therefore, in all experiments, waiting times of 2 min for the 10-ml cell and 3 min for the 25-μl cell were observed.

RESULTS AND DISCUSSION

Good results were found for the subtraction as well as the addition method in both the 10-ml cell and the 25-μl microcell (Table 1). For amounts smaller than about 10 nmol, only the standard addition method

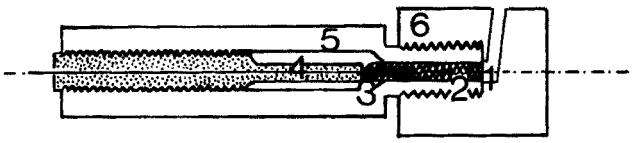

Fig. 1. Construction of micro-cell and micro-electrode. 1. CuS/Ag_2S-layer pressed on the surface of the Teflon-graphite. 2. Teflon-graphite (75 %/25 % w.w.; length 15 mm; diameter 3 mm). 3. Electrical contact (rustless steel wire hot soldered to a brass screw). 4. Teflon screw (hollow to press out the graphite rod for renewing the surface of the electrode. 5. Teflon holder. 6. Teflon cell screwed on the electrode holder; diameter 3 mm, bore for salt bridge and burette tip 2 mm.

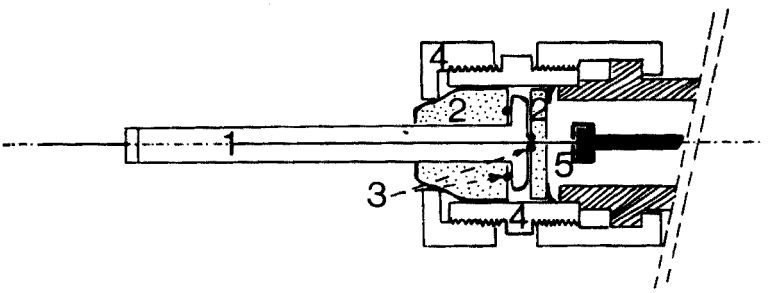

Fig. 2. Construction of the "nanoliter" burette. 1. Hamilton injection needle (10 μl). 2. Drilled Teflon holders. 3. Viton rings. 4. Metal holder screwed to a Metrohm E 457 micro-burette. 5. Connection of plunger head with micro-burette.

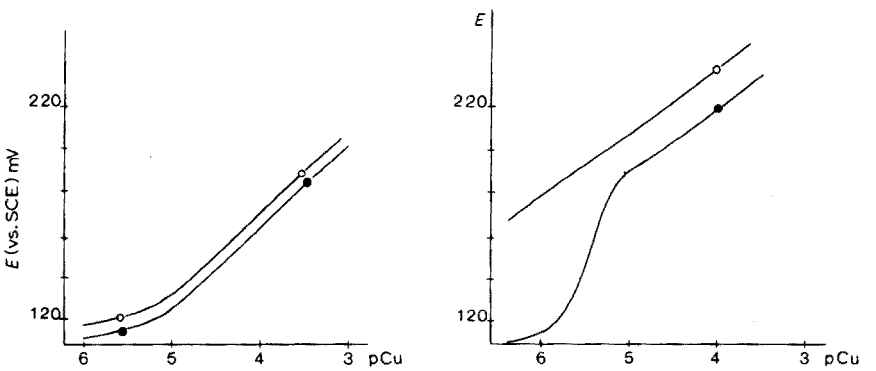

Fig. 3. Calibration lines by means of a micro-burette and the nanoliter burette. —●— 0.5 ml burette, —○— 5-μl burette.

Fig. 4. Influence of pretreatment of the electrode on the calibration line. —●— After at least 10 h in a 10^{-3} M EDTA solution. —○— After the treatment with EDTA and immersion in 10^{-4} M copper(II) solution until a constant reading was obtained.

was used. This amount corresponds to concentrations lower than 10^{-6} M in the 10-ml cell and about 10^{-4} M in the 25-μl cell. However, with such small amounts, large systematic errors occur. As the amounts of other chemicals introduced, e.g. buffer substances, appeared to have no effect, it was concluded that the major contribution to the systematic error was the limit of detection of the electrode. Because this limit depends on the solubility of the membrane, it might be possible to extend it by reducing the dielectric constant of the solvent, e.g. by addition of methanol [13]. This was partly confirmed by experiments in a 50 % methanolic medium (Table 2), but clearly there are other important factors which affect the accuracy. Possibly, by analogy with the result of Parthasarathy et al. [14] copper may be present in the chemicals used, or copper(II) may be released from the walls of the cell after previous adsorption, i.e. memory effects. Particularly in the micro cell, there exists an unfavourable volume-to-area ratio, which may increase the influence of adsorption equilibria. This may explain why the deviation from linear response starts at much higher copper concentrations in the case of this microcell (Fig. 6); the higher value of D_{Cu} will increase the systematic error according to eqn. (4).

TABLE 1

Determination of nanomolar amounts of copper(II) by the standard subtraction and standard addition methods

Cell volume	Increments[a] (n mol)	Cu(II) (n mol)		s[b]	s_r	n
		Taken	Found			
Subtraction						
10 ml	1990	10350	10300	13	0.13	4
10 ml	99.6	1035	1024	1.8	0.18	7
25 μl	2.49	25.88	24.77	1.17	4.7	4
Addition						
10 ml	103.5	103.5	102.8	2.7	2.6	5
25 μl	10.35	25.88	26.98	0.5	2.0	3
10 ml	20.70	10.35	14.28	0.3	2.9	4
10 ml	10.35	10.35	11.70	0.8	7.7	5
25 μl	2.59	2.59	2.57	0.35	12.8	5

[a] EDTA for the subtraction method and copper(II) for the addition method.
[b] Standard deviation (s) and relative standard deviation (s_r) are given for n determinations.

TABLE 2

Determination by the standard addition method in 50 % methanolic medium

Cell volume	Increments (n mol)	Cu(II) (n mol)		s	s_r	n
		Taken	Found			
10 ml	25.9	10.35	12.37	0.55	5.3	3
25 μl	2.59	2.59	2.05	0.2	7.8	4

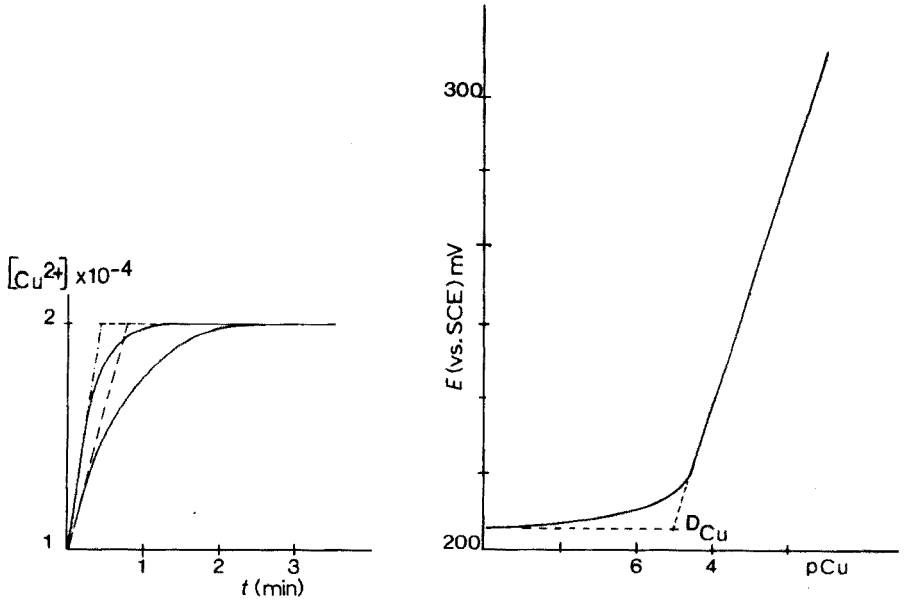

Fig. 5. Dynamic response on stepwise change of the copper concentration from $1 \cdot 10^{-4}$ M to $2 \cdot 10^{-4}$ M.

Fig. 6. Calibration line for the 25-μl cell.

REFERENCES

1 I. P. Alimarin and M. N. Petrikova, Zh. Anal. Khim., 14 (1959) 239; 21 (1966) 3, 1257; 23 (1968) 1042; 24 (1969) 333; 25 (1970) 213, 1008.
2 I. P. Alimarin and M. N. Petrikova, Anorganische Ultramikroanalyse, VEB Deutscher Verlag der Wissenschaften, Berlin, 1962.
3 W. Helbig, Z. Anal. Chem., 216 (1966) 280; 245 (1969) 359; 246 (1969) 169, 173, 225, 353.
4 R. A. Durst and J. Taylor, Anal. Chem., 39 (1967) 1483.
5 R. A. Durst, Anal. Chem., 40 (1968) 931.
6 J. M. van der Meer, G. den Boef and W. E. van der Linden, Anal. Chim. Acta, 76 (1975) 261.
7 J. M. van der Meer, G. den Boef and W. E. van der Linden, Anal. Chim. Acta, 79 (1975) 27; 00 (1976) 000.
8 U. Hannema and G. den Boef, Anal. Chim. Acta, 39 (1967) 479.
9 A. Liberti and M. Mascini, Anal. Chem., 41 (1969) 676.
10 J. Růžička, C. G. Lamm and J. Chr. Tjell, Anal. Chim. Acta, 62 (1972) 15.
11 J. M. van der Meer and J. C. Smit, Anal. Chim. Acta, 83 (1976) 367.
12 A. Johansson, Talanta, 21 (1974) 1269.
13 A. M. Elbakai, G. J. Kakabadse, M. N. Khayat and D. Tyas, Proc. Anal. Div. Chem. Soc., 12 (1975) 83.
14 N. Parthasarathy, J. Buffle and D. Monnier, Anal. Chim. Acta, 68 (1974) 185.

Analytica Chimica Acta, 85 (1976) 323—329

PROTON-INDUCED X-RAY EMISSION ANALYSIS FOR METALS EXTRACTABLE FROM SOILS WITH BUFFER SOLUTIONS

RUDY BAUM and WILLIAM F. GUTKNECHT*

Department of Chemistry, Duke University

ROBERT D. WILLIS and RICHARD L. WALTER

Department of Physics, Duke University and Triangle Universities Nuclear Laboratory, Durham, North Carolina 27706 (U.S.A.)

(Received 12th December 1975)

SUMMARY

The application of proton-induced x-ray emission analysis (p.i.x.e.a.) has been extended to soils and soil extracts. Studies of metal abundances for six elements (Mn, Fe, Cu, Zn, Sr and Pb) are given for three soil samples and for four extracts at different pH values for each sample. The p.i.x.e.a. method is described briefly and its value in soil analyses is indicated.

Some techniques for the determination of trace metals in soils provide for only a single metal per analysis. Any extraction and /or preconcentration steps necessary usually involve the removal and/or preconcentration of only the metal in question; the fate of other metals present is often ignored, unless they interfere in some way. A new technique, proton-induced x-ray emission analysis (p.i.x.e.a.), can determine all the elements from sulfur through uranium quantitatively in one analysis at levels as low as 1 p.p.m., depending on the particular metal and sample [1]. Any extraction and/or preconcentration technique to be used with p.i.x.e.a. must accordingly remove and/or preconcentrate a significant proportion of the elements determinable. The relationship of the trace metal content of plants to the metal content of their native soils is being investigated; [2] 0.5 M acetic acid was chosen as the extracting agent as this solution will extract those metals which are available to plants [3].

This report describes the results of an attempt to apply the p.i.x.e.a. technique to a more complete soil analysis; the amounts of metals extracted from various soil samples were determined as a function of the extracting buffer solution and its pH. The technique was also used to determine the total metal content of the soils before extraction, and comparisons of these data are presented. One of the long range aims is to relate the relative amounts of metals extractable at different pH levels to the relative metal contents of

*Author to whom correspondence should be addressed.

plants growing in the soil, in order to ascertain if there exists an optimum extraction pH which reflects the amounts of metal in the soil available to the plant.

EXPERIMENTAL

Extractions

Three soils from an earlier project [2] were chosen for extraction studies. Organic matter such as roots, etc. was removed and the soils were dried and finely ground.

The buffering extracting solutions were of the following composition: (a) pH 1.50, $3.11 \cdot 10^{-2}$ M Cl_3CCOOH; (b) pH 4.05, stock calcium phthalate buffer; (c) pH 6.65, $2.82 \cdot 10^{-2}$ M NaH_2PO_4 and $2.49 \cdot 10^{-2}$ M Na_2HPO_4; (d) pH 9.17, 10^{-2} M $Na_2B_4O_7 \cdot 10H_2O$.

The extractions were made by adding 10 g of soil to 50 ml of the buffer solution. These mixtures were agitated for 2 h and filtered twice through no. 41 paper. pH measurements were made on the final filtered solutions to ascertain that no substantial pH change had occurred during the extraction. Filtration did not remove all traces of sediment from the extracts at pH 6.65 and pH 9.17; these were left for 36 h to allow the sediment to settle, then portions were taken from the clear supernatant solution.

Target preparation

The extracted solutions were deposited with a micropipette on 8-μm pore diameter Nuclepore membrane filters, small pieces (11 mm × 25 mm) of which were mounted on an aluminum frame with glue [1]; about 17 pieces fit onto each of three aluminum target support frames. A total of 50 μl of extract solution was deposited on each Nuclepore backing. The deposit was restricted to an area of about 0.3 cm^2 by depositing 1 × 10 μl and 2 × 20 μl aliquots, each of which was allowed to dry before the next was applied. At least two replicates were prepared from each solution.

Soil samples were prepared by placing about 100 mg of soil in a 1-cm diameter die and compressing at about 30,000 lb/in^2. These pellets were sandwiched between two layers of mylar and this assembly was glued on to the aluminum target frame.

Instrumentation

The proton beam was generated with the Triangle Universities Nuclear Laboratory 4-MeV Van de Graaff accelerator at Duke University. The beam energy was approximately 3.0 MeV with a beam current at the target of 15—30 nA. The area of the beam striking the sample had a constant value of 0.4 cm^2. The target chamber and accelerator system were operated under a vacuum of ca. 10^{-5} torr.

The membranes were orientated so that the horizontal proton beam was incident at an angle of 35° with respect to the normal (vector) of the

membrane surface. Those x-rays generated perpendicularly downward from the sample passed through a 26-μm mylar window, through about 1.0 cm of air, and finally through the 25-μm beryllium window of a Si(Li) x-ray detector. For expediency in data collection, a 0.8-mm polyethylene absorber was placed in the air gap to absorb most of the low energy x-rays produced; this filter reduces the problems associated with high counting rates in the detector and analyzer systems, but makes it impossible to obtain valid abundances for the elements between sulfur and potassium normally observable. The normal data runs with only a 100-μm mylar filter in place were not obtained in this study; this filter permits the determination of the elements, from sulfur to potassium, whose characteristic x-rays are absorbed strongly by the polyethylene filter. For a more complete description of the accelerator, target, absorber and detection system, see ref. 1.

Analytical procedure

The data were recorded with a 512-channel pulse-height analyser interfaced to an on-line DDP-224 Honeywell computer. The data were also stored on magnetic tape for later off-line analysis on a second DDP-224 computer. The associated oscilloscope display and light pen were used to analyse the spectra. A program which fits a gaussian curve to the peaks and interprets inter-element interferences was utilized to determine the total number of counts in a peak. The program also relates these counts to the abundance of the individual elements in the specimens.

The spectrum from the extract of soil no. 1 at pH 1.5 (Fig. 1) shows the typical signal-to-noise ratios for the various elements. Approximately 40 such spectra were obtained for the present work. The two K-lines for the lighter elements (potassium to strontium) or the more complex set of three L-lines for heavy elements (barium, mercury, lead) were used for each metal under study.

RESULTS AND DISCUSSION

This report concentrates on the more abundant metals found in the extracts, i.e. Mn, Fe, Cu, Zn, Sr and Pb. The soil pellet analyses yielded abundances for about 20 elements from sulfur to lead, but for many of the extractions, most of the metals of interest other than Mn, Fe, Cu, Zn, Sr and Pb were found at levels less than the 3σ detectibility limit (see, e.g., Fig. 1). Potassium and calcium are easily seen with p.i.x.e.a. and were present in the extractions at determinable levels, but the intent of the present project was to concentrate on the observable metals heavier than chromium. The results ($\mu g\ g^{-1}$) for the six metals are listed in Table 1.

Some interesting trends become apparent on inspection of Fig. 2. The extraction of zinc and strontium appear to be relatively straightforward. A linear relationship between log (e.m.c.) and the pH of the extracting solution would be expected if a direct ion-exchange process occurs; the data indicate

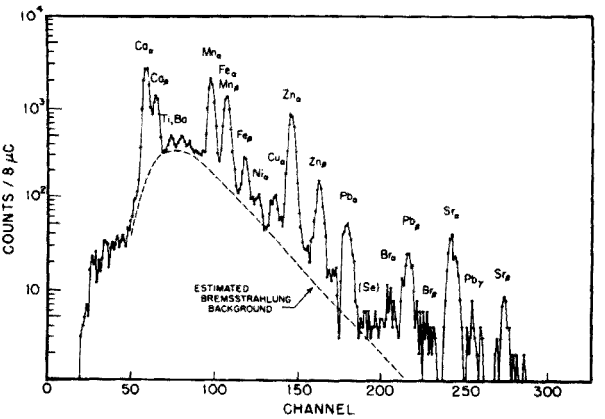

Fig. 1. A typical p.i.x.e.a. spectrum, wherein numbers of x-rays counted per 8 μC of proton beam are plotted versus channel number (channel number is proportional to x-ray energy). The spectrum was obtained for the extract from soil no. 1 at pH 1.5, at 3.0 MeV with a polyethylene absorber.

TABLE 1

Amount (μg g^{-1}) of metal extracted as a function of the pH of the extracting solution[a]

Element	pH 1.50	pH 4.05	pH 6.65	pH 9.17	Average sensitivity level
Soil no. 1					
Mn	390	32	2	2	4
Fe	106	14	49	87	3
Cu	8	3	8	4	2
Zn	250	45	7	3	2
Sr	70	18	3	0	2
Pb	73	6	15	1	5
Soil no. 2					
Mn	190	34	7	0	
Fe	240	32	88	480	
Cu	10	2	4	6	
Zn	14	2	6	6	
Sr	83	30	5	4	
Pb	14	3	7	2	
Soil no. 3					
Mn	130	12	4	5	
Fe	66	20	105	0	
Cu	6	1	2	1	
Zn	0	3	0	1	
Sr	117	56	6	4	
Pb	7	8	5	0	

[a] Amounts given are averaged values obtained from replicate deposits.

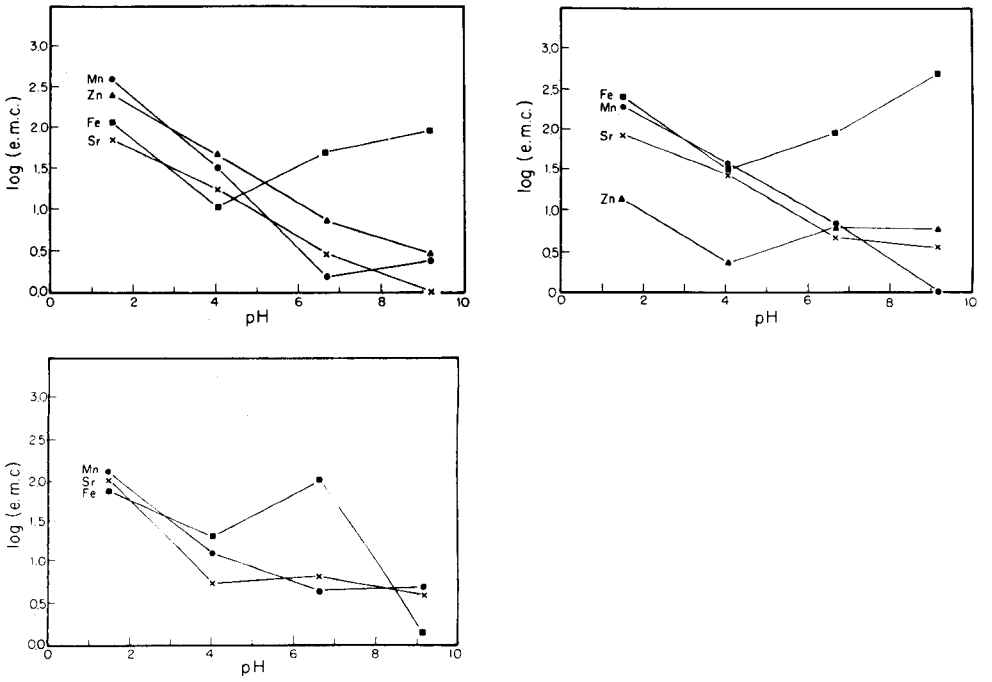

Fig. 2. Log (e.m.c.) (where e.m.c. is the extracted metal content) versus pH of the extracting solution for three different soils.

that this is the case. However, this does not imply that these figures are reliable estimates of the absolute quantities of metals available to the plant. (For relative comparisons between soil and plant metal content of the two metals, the acetic acid extraction technique probably will prove to be the most valid or realistic. The main complication is that the acetic acid is not as effective as some plants at removing the metal complexed to organic compounds.)

Manganese presents a more complex picture. Much of this element occurs in soils in the form of insoluble hydrous oxides; these are not generally available to the plant, but the acetic acid liberates them to the solution by contributing hydrogen ion to the negatively charged oxide. According to Mitchell [4], manganese at high pH and in the presence of suitable organic material forms organic complexes not accessible to plants. Soil no. 1 in this study was a black humus soil which seemed to have the greatest quantity of organic material. Inspection of Fig. 2 shows that only in soil no. 1 was the manganese extracted at pH 9.17 higher than that extracted at pH 6.65. Formation of these manganese(II)—organic complexes, and their contribution to the manganese content of the extract, provides a viable explanation of the increase from pH 6.65 to pH 9.17 observed for soil no. 1. In acidic media, the linear relationship expected is observed in the plots for all three soils.

Lead is difficult to release from soils. The rise in lead extracted from pH 4.05 to 6.65 probably results from the formation of lead phosphate, some of which passes through a filter.

Most of the iron in soils occurs in the form of $Fe_2O_3 \cdot H_2O$ (geothite) and Fe_2O_3 (hematite). The iron extracted with acidic solutions is primarily the result of the acid attacking these oxides. The rise in the quantity extracted at pH 6.65 over that extracted at pH 4.05 is due, in part, to the formation of iron phosphate, some of which passes through the filter. Soluble forms such as $Fe(OH)^{2+}$ and $Fe(OH)_2^+$ also form at the higher pH. In basic solution the sharp rise in the quantity of iron extracted results from the formation of $Fe(OH)_3$, some of which apparently passes through the filter, and $Fe(OH)_4^-$ [5]. The iron values tabulated for the pH 9.17 extract are probably low. In filtering the pH 9.17 extracts, the flow through the filter paper dropped almost to zero as soon as the filter paper was exposed to the solution; it seems reasonable to propose that the hydrated iron oxide was responsible and that much of the iron extracted from the soil was lost in the filter paper.

Table 2 presents the total metal content in the soils as obtained from p.i.x.e.a. analysis of soil pellets. Table 3 presents the percentages of the total content of a particular soil that were extracted; these figures show that acidic extraction liberates different percentages of metals from different soils.

TABLE 2

Metal content ($\mu g\ g^{-1}$) of soil pellets

Element	Soil 1	Soil 2	Soil 3
Mn	480	570	970
Fe	9300	28,400	47,000
Cu	53	22	20
Zn	150	57	102
Sr	72	110	240
Pb	210	52	46

TABLE 3

Percentage of total metal in soil extracted by pH 1.50 buffer

Element	Soil 1	Soil 2	Soil 3
Mn	82	33	14
Cu	16	44	30
Zn	(100)[a]	41	0
Sr	97	79	50
Pb	28	27	16

[a]This high value is apparently due to inhomogeneity in the soil pellet, which resulted in a low zinc value for the direct soil analysis.

CONCLUSION

These results confirm that the problems involved in the study of trace metals in soils are complex. A study such as that reported here yields useful data, and illustrates some of the problems that may be encountered.

It is evident that the p.i.x.e.a. technique works well for soil extraction analysis. The individual analyses are rapid; the total beam time per target was less than 3 min and analysis of a spectrum with the off-line computer requires a further 2 min. Since an entire range of metals is listed for each spectrum treated by the computer, the technique can be very economical, particularly if sufficient analyses are performed. In addition, the liquid deposits on Nuclepore membranes present very little interference from outside sources of metals. Enhancement of signals can be achieved by increasing the amount of sample deposited, as most of the background x-rays are produced by the Nuclepore membrane.

With the method now developed, other extractants will be tested, especially those which do not form insoluble compounds with some of the metals under study. A broader range of soil types and metals will also be examined to elucidate further the relation between the metal content of soils and plants.

We would like to acknowledge the help of Janette Stanford in collecting and grinding the soil samples, and conducting the analyses. This work was supported in part by the U.S. Atomic Energy Commission.

REFERENCES

1 R. L. Walter, R. D. Willis, W. F. Gutknecht and J. M. Joyce, Anal. Chem., 46 (1974) 843.
2 J. A. Stanford, R. D. Willis, R. L. Walter, W. F. Gutknecht and J. Antonovics, Radiat. Environ. Biophys., 12 (1975) 175.
3 M. Pinta, Detection and Determination of Trace Elements, Ann Arbor Science Publ., London, 1962, pp. 40—42.
4 R. L. Mitchell, Trace Elements in Soils, in F. E. Bear (Ed.), Chemistry of the Soil, Reinhold, New York, 1964.
5 W. Strumm and J. T. Morgan, Aquatic Chemistry, Wiley-Interscience, New York, 1970, Chap. 6.

Analytica Chimica Acta, 85 (1976) 331—340

EXTRACTION DU TITANE(IV) D'UNE PHASE AQUEUSE CHLORHYDRIQUE PAR DES MÉLANGES DE THÉNOYLTRIFLUOROACÉTONE–TRI-n-BUTYLPHOSPHATE ET D'OXYDE DE TRI-n-BUTYLPHOSPHINE EN SOLUTION DANS LE 1,2-DICHLOROETHANE

G. ROLAND, M. PONDANT et G. DUYCKAERTS

Laboratoire de Chimie analytique, Université de Liège au Sart Tilman, B-4000 Liège (Belgique)

(Reçu le 5 Mars 1976)

RÉSUMÉ

Nous avons étudié l'extraction du titane(IV) de phases aqueuses chlorhydriques par la thénoyltrifluoroacétone (HTTA) associée au tributylphosphate (TBP) ou à l'oxyde de tributylphosphine en solution dans le 1,2 dichloroéthane. Par dosages des ions Ti(IV) en phases aqueuse et organique, nous avons pu montrer qu'il y avait un effet synergique et que le complexe mixte a la stoechiométrie 1:1:1 (HTTA—TBP—Ti(IV)). Les valeurs des constantes de stabilité apparentes de ces complexes sont d'autant plus élevées que l'acidité de la phase aqueuse est grande.

SUMMARY

The extraction of titanium(IV) from hydrochloric acid solutions by thenoyltrifluoroacetone (HTTA) in the presence of tributylphosphate (TBP) or tri-n-butylphosphine oxide (TBPO) was studied in 1,2 dichloroethane. It is shown that there is a synergic effect because of the formation of a 1:1:1 HTTA—TBP (or TBPO)—Ti(IV) complex. The apparent stability constants of these complexes increase with the acidity of the aqueous phase.

Le titane(IV) peut être extrait d'une phase aqueuse par formation de complexes du type accepteur—donneur avec les bases de Lewis ou encore par formation de complexes de chélation.

Parmi les bases neutres employées jusqu'à présent, nous pouvons citer l'acétate d'amyle [1], l'acétate d'éthyle et de phényle [2], la n-propylcétone [1], le n-dibutyléther [1], le tributylphosphate, pur ou en solution [1, 3—6], l'oxyde de tri-n-butylphosphine [7—9]. En général, l'extraction du titane(IV) par ces composés n'est totale que pour des concentrations élevées en base ou pour des milieux fortement acides.

Les agents chélatants, par contre, permettent d'extraire le titane(IV) de solutions aqueuses de pH > 0, mais nécessitent la présence d'un complexant pour éviter l'hydrolyse du cation particulièrement acide. Les conditions

d'extraction du titane(IV) par les agents chélatants les plus courants sont résumées dans l'ouvrage de Stary [10].

Bien que le domaine d'utilisation des principaux agents chélatants se situe généralement en milieu peu acide, quelques travaux ont montré qu'il était possible d'extraire les cations du groupe IV b de phases aqueuses fortement acides. De et Rahaman [11] ont extrait le titane(IV) d'une phase aqueuse 11 M en acide chlorhydrique par la HTTA 0,15 M en solution dans un mélange d'alcool isoamylique et de benzène. Le Zr(IV) et le Hf(IV) peuvent aussi être extraits d'une phase aqueuse chlorhydrique, perchlorique [12] et nitrique [13].

L'utilisation simultanée de bases neutres et d'agents chélatants donnant souvent lieu à des effets synergiques importants [14], nous nous sommes demandé si cet effet s'observait lors de l'extraction du titane(IV) en associant la thénoyltrifluoroacétone (HTTA) au n-tributylphosphate (TBP) ou à l'oxyde de tri-n-butylphosphine en solution dans le 1,2 dichloroéthane.

L'emploi de ces mélanges d'extractants a déjà fait l'objet de nombreux travaux [14, 15] mais, à notre connaissance, ceux-ci n'ont jamais été utilisés pour l'extraction du titane(IV) en milieu fortement acide.

PARTIE EXPÉRIMENTALE

Le 1,2-dichloroéthane de qualité "pour analyse" a été distillé avant l'emploi. Le TBP commercial a été traité par une solution aqueuse de Na_2CO_3 à 10 % puis lavé à l'eau distillée. Après séchage, il a été distillé sous vide. Les solutions de TBP ont été préparées soit par pesée directe du TBP en ballon jaugé, soit par dilution d'une solution stock.

Les solutions de TBPO (préparé par réaction de synthèse $(C_4H_9)_3P + H_2O_2 \rightleftarrows (C_4H_9)_3PO + H_2O$) ont été préparées de la même manière que les solutions de TBP.

La thénoyltrifluoroacétone (Aldrich) a été distillée sous vide puis recristallisée dans l'éther éthylique.

L'extraction du Ti(IV) a été réalisée en agitant vigoureusement 5 ml de solution aqueuse et 5 ml de solution organique pendant 10 min.

Les concentrations en Ti(IV) en phase aqueuse ont été déterminées en mesurant l'absorbance à 410 nm du complexe Ti(IV)–H_2O_2 en milieu H_2SO_4 1 M. Les concentrations en phase organique ont été obtenues soit par réextraction du Ti(IV) dans le réactif colorimétrique, soit par différence lorsque la réextraction du Ti(IV) en phase aqueuse était trop lente (cas des solutions concentrées en Ti(IV) dans la phase organique).

Les spectres visibles et ultra-violets ainsi que les mesures colorimétriques ont été obtenus au spectrophotomètre Cary 17, le trajet optique des cellules variant de 1 à 50 mm suivant les concentrations.

Les spectres infra-rouges ont été enregistrés à l'aide d'un spectrophotomètre Perkin-Elmer 125 équipé de cellules dont l'armature était recouverte de téflon pour éviter tout contact entre les solutions et l'acier des porte-cellules.

RESULTATS EXPÉRIMENTAUX

Extraction du titane(IV) par la HTTA seule

Sur la Fig. 1 nous avons porté, en fonction de la molarité en HCl dans la phase aqueuse, le pourcentage d'extraction du Ti(IV) entre une phase aqueuse chlorhydrique et le TBPO, le TBP et la HTTA dans le 1,2-dichloroéthane. Les courbes montrent que l'extraction par le TBP et la HTTA est loin d'être totale et que pour le TBPO, base nettement plus forte que le TBP et HTTA, il faut des milieux très acides pour que l'extraction devienne appréciable.

Si les complexes formés entre le TBP [6] ou les oxydes de phosphine [9] d'une part et le Ti(IV) extrait d'une phase aqueuse chlorhydrique d'autre part, ont pour formule D_2TiCl_4 (D ≡ TBPO ou TBP), nous ne connaissons pas la stoechiométrie des complexes HTTA—Ti(IV) formés en milieu fortement chlorhydrique.

Nous avons déterminé cette stoechiométrie en travaillant à concentrations initiales en acide et en Ti(IV) en phase aqueuse constantes mais en faisant varier la concentration totale en HTTA dans la phase organique. Les valeurs des coefficients de partage obtenues pour un milieu 11,2 M en HCl et 0,1 M en Ti(IV) figurent au Tableau 1. En portant log E en fonction de log $\{[HTTA]_{t\,o} - 2[Ti(IV)]_{t\,o}\}$ on obtient une droite de pente 2,04 (Fig. 2) indiquant, semble-t-il, la formation d'un complexe de stoechiométrie 2:1. Remarquons que ces conclusions ne sont valables que si les complexes du HTTA avec l'eau et l'acide chlorhydrique sont peu stables ou si une seule molécule de HTTA entre dans ces complexes car, dans ces conditions, on peut montrer facilement que la concentration en HTTA libre est proportionnelle à $\{[HTTA]_{t\,o} - 2[Ti(IV)]_{t\,o}\}$. La formation d'un complexe 2:1 pour-

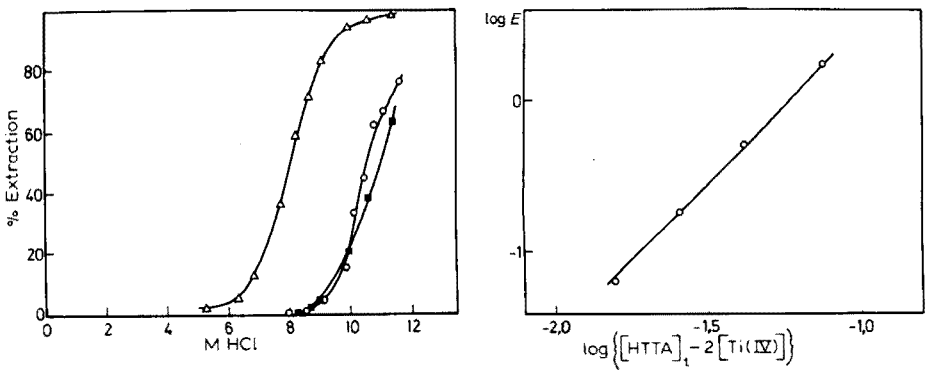

Fig. 1. Pourcentage d'extraction du Ti(IV) en fonction de la molarité en HCl dans la phase aqueuse. Δ $[TBPO]_t$ = 0,1 M; $[Ti(IV)]_{initiale}$ = 0,020 M. ○ $(TBP)_t$ = 0,1 M; $[Ti(IV)]_{initiale}$ = 0,004 M. ■ $(TTA)_t$ = 0.1 M; $[Ti(IV)]_{initiale}$ = 0,020 M. Solvant: 1,2-dichloroéthane.

Fig. 2. Log E en fonction de log $\{[HTTA]_{t\,o} - 2[Ti(IV)]_{t\,o}\}$.

TABLEAU 1

Variation des coefficients de partage pour un milieu 11,2 M en HCl et 0,1 M en Ti(IV)

$\log\{[HTTA]_{to} - 2[Ti(IV)]\}_{to}$ [a]	$\log E$
−1,126	0,231
−1,373	−0,276
−1,589	−0,724
−1,806	−1,196

[a]Le symbole o signifie que l'on considère l'entité en phase organique.

rait s'expliquer par une réaction entre $TiCl_4$, probablement présent en très faible proportion en phase aqueuse, et HTTA, réaction de type analogue à celui observé avec les β-dicétones [16]

$$TiCl_4 + 2HTTA \rightleftarrows (TTA)_2TiCl_2 + 2HCl$$

La présence de complexes du type $(TTA)_4Ti$ ou $(HTTA)_2TiCl_4$ semble exclue car la valeur du rapport $[Cl^-]/[Ti(IV)]$ dans les complexes obtenus par extraction du Ti(IV) de solutions 12 M en HCl est voisine de 2 et, en outre, les spectres infra-rouges de ce complexe présente les bandes caractéristiques des complexes chélatés de HTTA [17].

Détermination de la stoechiométrie et des constantes de stabilité des complexes mixtes

Nous avons déterminé la stoechiométrie des complexes mixtes par la méthode des variations continues [18]. Pour chaque série d'expériences, nous avons maintenu la composition initiale de la phase aqueuse constante et nous avons fait varier le rapport $[HTTA]_t/[D]_t$ en phase organique tout en maintenant la somme des concentrations en HTTA et en base neutre constante et égale à 0,1 M. Les Fig. 3 et 4 où nous avons porté le coefficient de partage en fonction de la fraction molaire en HTTA (*m* HTTA) reprennent partiellement les résultats expérimentaux.

DISCUSSION

Les courbes obtenues pour le système HTTA—TBP présentent toutes un seul maximum pour une fraction molaire en HTTA voisine de 0,5 (Fig. 3), ce qui signifie que le complexe mixte contient un nombre égal de molécules de HTTA et de TBP.

Dans le cas des complexes TBPO—Ti(IV), la valeur du coefficient de partage, maximum lorsque *m* HTTA est compris entre 0,2 et 0,4 (Fig. 4), pourrait suggérer la présence d'un complexe mixte où le rapport HTTA/TBPO serait 1:2. Cette conclusion n'est cependant pas valable, car l'extraction du Ti(IV) par le TBPO en excès est relativement importante et les courbes $E = f(m\ \text{HTTA})$ ne permettent plus de déduire la stoechiométrie des complexes.

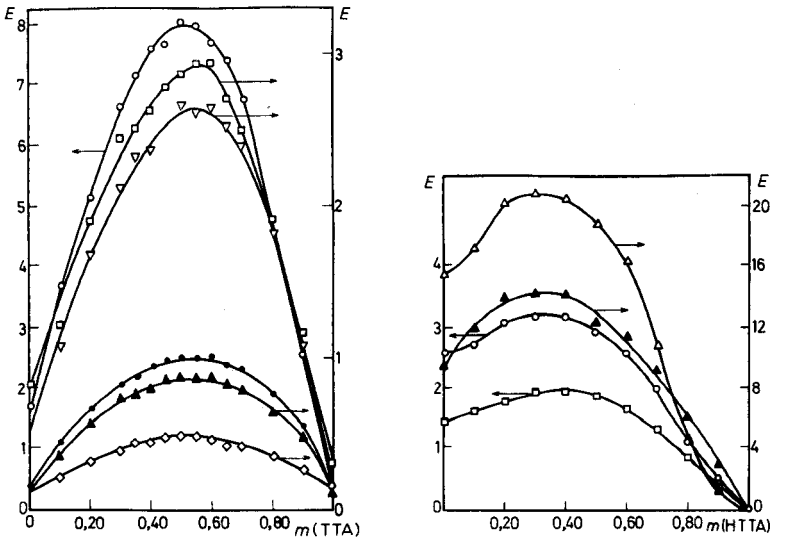

Fig. 3. Système HTTA—TBP—Ti(IV), $[HTTA]_{to} + [TBP]_{to} = 0{,}10$ M dans le 1,2-dichloroéthane
$[Ti(IV)]_{initiale}$, M, ◇ $2 \cdot 10^{-2}$; ▲ $2 \cdot 10^{-2}$; ● $4 \cdot 10^{-3}$; ▽ $4 \cdot 10^{-3}$; □ $2 \cdot 10^{-2}$; ○ $4 \cdot 10^{-3}$.
[HCl], M, ◇ 9,5; ▲ 9,9; ● 9,83; △ 10,17; □ 10,50; ○ 10,80.

Fig. 4. Système HTTA—TBPO—Ti(IV), $[HTTA]_{to} + [TBPO]_{to} = 0{,}10$ M dans le 1,2-dichloroéthane
$[Ti(IV)]_{initiale}$, M, □ $2 \cdot 10^{-2}$; ○ $2 \cdot 10^{-2}$; ▲ $4 \cdot 10^{-3}$; △ $2 \cdot 10^{-2}$.
[HCl], M, □ 8,27; ○ 8,70; ▲ 9,0; △ 9,98.

Celle-ci peut être établie d'une manière beaucoup plus certaine par le calcul de la constante de stabilité des complexes mixtes. En effet, aux erreurs de mesures près, la valeur de la constante de formation du complexe ne sera "constante" que si les calculs sont effectués à partir de la stoechiométrie réelle du complexe.

En nous basant sur les résultats obtenus pour le système HTTA—TBP, nous avons supposé que le complexe mixte formé avec les deux bases étudiées (représentées par D) avait la stoechiométrie 1:1:1 et répondait vraisemblablement à la formule TTA—TBPO—$TiCl_3$.

Puisque le titane(IV) forme des complexes de stoechiométrie 2:1 avec la HTTA et les deux bases dans la phase organique, nous pouvons écrire les réactions suivantes; où D et HTTA correspondent respectivement à $\{[D]_{to} - 2[Ti(IV)]_o\}$ et à $\{[HTTA]_{to} - 2[Ti(IV)]_o\}$

$$2D + TiCl_4 \overset{K_1}{\rightleftarrows} D_2TiCl_4; \quad K_1 = \frac{[D_2TiCl_4]_o}{[D]_o^2 \cdot [TiCl_4]_o} \tag{1}$$

$$2HTTA + TiCl_4 \overset{K_2}{\rightleftarrows} (TTA)_2TiCl_2 + 2HCl; \quad K_2 = \frac{[(TTA)_2TiCl_2]_o \cdot [HCl]_o^2}{[HTTA]_o^2 \cdot [TiCl_4]_o} \tag{2}$$

$$D + HTTA + TiCl_4 \overset{K_3}{\rightleftarrows} TTA.D.TiCl_3 + HCl; \quad K_3 = \frac{[TTA.D.TiCl_3]_o\ [HCl]_o}{[D]_o . [HTTA]_o . [TiCl_4]_o} \tag{3}$$

Si E_0 représente le coefficient de partage du $TiCl_4$ entre la phase aqueuse et le solvant seul, on peut écrire

$$E_0 = [TiCl_4]_o / [Ti(IV)]_{aq}$$

où Ti(IV) représente la concentration analytique du Ti(IV) en phase aqueuse.

En ne tenant compte ni de la valeur de E_0 ni de $[HCl]_o$, ni des complexes formés entre la HTTA, le TBP ou le TBPO d'une part et l'eau et l'acide chlorhydrique d'autre part, nous obtiendrons les constantes de stabilité apparente dont les valeurs dépendront essentiellement de l'acidité de la phase aqueuse.

$$K_1' = K_1 . E_0 = \frac{[D_2TiCl_4]_o}{[D]_o^2 . [Ti(IV)]_{aq}} \tag{4}$$

$$K_2' = \frac{K_2 . E_0}{[HCl]_{aq}^2} = \frac{[(TTA)_2TiCl_2]_o}{[HTTA]_o^2 . [Ti(IV)]_{aq}} \tag{5}$$

$$K_3' = \frac{K_3 E_0}{[HCl]_{aq}} = \frac{[TTA.D.TiCl_3]_o}{[HTTA]_o . [D]_o . [Ti(IV)]_{aq}} \tag{6}$$

Les valeurs de K_1' et de K_2' peuvent se calculer, pour chaque série d'expériences, à partir des résultats d'extraction obtenus lorsqu'on a 100 % de D et 100 % de HTTA respectivement. Ainsi, si on extrait le Ti(IV) par la base seule

$$[D]_{to} = [D]_o + [D_2TiCl_4]_o$$

$$[Ti(IV)]_{to} = [D_2TiCl_4]_o + [TiCl_4]_o$$

où $[D]_{to}$ et $[Ti(IV)]_{to}$ représentent respectivement les concentrations analytiques en D et en Ti(IV) dans la phase organique. Comme $TiCl_4$ est toujours négligeable vis-à-vis de D_2TiCl_4, on obtient directement la valeur de K_1'

$$K_1' = \frac{[Ti(IV)]_{to}}{([D]_{to} - 2[Ti(IV)]_{to})^2 . [Ti(IV)]_{aq}} \tag{7}$$

où toutes les concentrations sont soit des données, soit le résultat des mesures. K_2' peut être obtenu par le même raisonnement (en considérant que la HTTA passée dans la phase aqueuse ne modifie que très peu la valeur de $[HTTA]_{to}$).

La valeur de K_3' a été calculée comme suit: si nous écrivons les bilans des différents complexes en phase organique, nous obtenons

$$[Ti(IV)]_{to} = [D_2TiCl_4]_o + [(TTA)_2TiCl_2]_o + [DTTATiCl_3]_o$$

$$[D]_{to} = [D]_o + 2[D_2TiCl_4]_o + [DTTATiCl_3]_o$$

$[HTTA]_{to} = [HTTA]_o + 2[(TTA)_2TiCl_2]_o + [DTTATiCl_3]_o$

En remplaçant les concentrations en complexes en fonction de leur constante de stabilité apparente et en posant

$[Ti(IV)]_{to} = A$; $[D]_{to} = B$; $[HTTA]_{to} = C$; $[Ti(IV)]_{aq} = k$; $K_1' = a$; $K_2' = b$; $[D]_o = x$; $[HTTA]_o = y$ et $K_3' = z$, les équations précédentes deviennent

$$A = kax^2 + kby^2 + kxyz \tag{11}$$

$$B = x + 2kax^2 + kxyz \tag{12}$$

$$C = y + 2kby^2 + kxyz \tag{13}$$

En combinant ces équations de la manière suivante (12) + (13) − 2.(11), nous obtenons

$$B + C - 2A = x + y \tag{14}$$

Or, à partir des éqns. (11) et (12), on a

$$A - B = kby^2 - kax^2 - x \tag{15}$$

et en y remplaçant x par sa valeur tirée de la relation (14), on aboutit à une équation du second degré en y

$y^2(kb - ka) + y\,\epsilon + \gamma = 0$ où $\epsilon = 1 + 2\,ka(B + C - 2A)$ et $\gamma = A - C - ka(B + C - 2A)^2$.

La valeur de $x = [D]_o$ est tirée de la relation (14)

$x = B + C - 2A - y$

On peut alors calculer les concentrations des complexes simples à partir des définitions de leur constante de stabilité

$[D_2TiCl_4]_o = K_1'.[D]_o^2.[Ti(IV)]_{aq} = kax^2$

$[(TTA)_2\,TiCl_2]_o = K_2'.[HTTA]_o^2.[Ti(IV)]_{aq} = kby^2$

La concentration en complexe mixte s'obtient par une des équations de bilan (8), (9) ou (10), par exemple

$[TTA.D.TiCl_3]_o = [D]_{to} - [D]_o - 2[D_2TiCl_4]_o$

Finalement, K_3' est calculé à partir de sa définition

$$z = K_3' = \frac{B - x - 2kax^2}{kxy}$$

Le Tableau 2 rassemble les résultats des calculs effectués en donnant à l'ordinateur les données expérimentales correspondant à des fractions molaires en HTTA comprises entre 0,1 et 0,9. Les valeurs de K_3' renseignées sont les valeurs moyennes et s est l'écart type.

TABLEAU 2

Valeurs de K'_3 pour les deux systèmes

$[Ti(IV)]_tM$	HCl (M)	K'_1 (M/l)$^{-2}$	K'_2 (M/l)$^{-2}$	K'_3 (M/l)$^{-2}$	s
Système TBP—HTTA—Ti(IV)					
4.10^{-3}	8,84	$1,9_6$	2,9	35	4
	9.83	14,6	11,2	416	28
	10,17	52,0	19,3	1112	89
	10,80	188,0	40,4	3410	168
2.10^{-2}	9,50	15,8	11,0	212	13
	9,90	20,8	20,4	496	42
	10,50	126,0	55,0	2360	416
Système TBPO—HTTA—Ti(IV)					
4.10^{-3}	7,01	51	0,27	244	27
	9,02	1095	4,0	4890	280
2.10^{-2}	8,27	250	$1,1_6$	1127	45
	8,70	509	2,6	2010	46
	9,98	3970	22,8	17550	800

Ces valeurs permettent de calculer les constantes de stabilité apparente pour la réaction synergique dans la phase organique

$$HCl + D + (TTA)_2TiCl_2 \overset{K_{syn}}{\rightleftarrows} D.TiCl_3.TTA + HTTA \qquad (16)$$

En effet, à partir des éqns. (5) et (6), on voit immédiatement que

$$K'_{syn} = K'_3/K'_2 = K_{syn}\,[HCl]_o = \frac{[D.TiCl_3.TTA]_o.[HTTA]_o}{[D]_o.[(TTA)_2TiCl_2]_o}$$

Les valeurs de K'_{syn} sont reprises dans le Tableau 3.

Les valeurs plus élevées de K'_{syn} lorsqu'on effectue l'extraction du Ti(IV) avec le TBPO confirment les résultats obtenus par Healy [15] d'une part et par Bok et al. [19] d'autre part qui ont montré que la formation du complexe mixte de la HTTA avec les dérivés phosphorés et quelques β-dicétones est d'autant plus aisée que la molécule neutre est plus basique.

Les courbes de répartition des différents complexes en solution organique permettent de suivre les variations des concentrations relatives des différentes entités en fonction de m HTTA (Fig. 5). Dans le cas des complexes TBP—HTTA—Ti(IV) les complexes $(TBP)_2TiCl_4$ et $(TTA)_2TiCl_2$ sont relativement peu abondants et le complexe mixte prédomine nettement pour $0,9 < m$ HTTA $< 0,1$. Par contre, le TBPO, base plus forte que le TBP, forme des complexes plus stables avec $TiCl_4$ et le complexe mixte se forme par conséquent plus difficilement aux faibles valeurs de m HTTA. Pour les faibles concentrations en TBPO, (m HTTA élevé), la HTTA est déplacée de son complexe suivant la réaction (16) et l'entité mixte prédomine nettement.

TABLEAU 3

Valeurs de K'_{syn} pour les deux systèmes

$[Ti(IV)]_t$ (Ml^{-1})	HCl (M)	K'_{syn}	$[Ti(IV)]_t$ (Ml^{-1})	HCl (M)	K'_{syn}
Système TBP—HTTA—Ti(IV)			Système TBPO—HTTA—Ti(IV)		
4.10^{-3}	8,84	12	2.10^{-2}	8,27	900
	9,83	37		8,70	770
	10,17	58		9,98	770
	10,80	85			
2.10^{-2}	9,50	19	4.10^{-3}	7,01	903
	9,90	24		9,02	1225
	10,50	43			

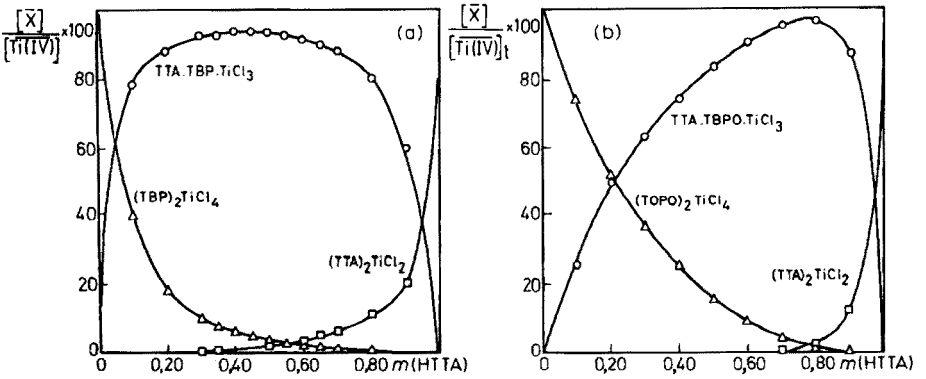

Fig. 5. Les variations des concentrations relatives des différentes entités en fonction de m HTTA. $[HTTA]_t + [TBP \text{ ou } TBPO]_t = 0{,}10$ M dans 1,2-dichloroéthane. $[Ti(IV)]_{initiale} = 2 \cdot 10^{-2}$ M. (a) TBP; [HCl] = 9,9 M. (b) TBPO; [HCl] = 9,98 M.

En conclusion, ce travail nous a permis de montrer que l'extraction du titane(IV) de phases aqueuses fortement chlorhydriques par des mélanges HTTA—TBP ou HTTA—TBPO donne lieu à un effet synergique.

Du point de vue pratique, l'extraction est maximum lorsque la fraction molaire en HTTA est voisine de 0,5 (pour les mélanges HTTA—TBP) et de 0,3 (pour les mélanges HTTA—TBPO) et elle augmente régulièrement lorsque la molarité de l'acide chlorhydrique en phase aqueuse croît.

BIBLIOGRAPHIE

1 Y. G. Sevast'yanov, B. Z. Iofa, A. N. Nesmeyanov et V. G. Vinogradova, Radiokhimiya, 12 (1970) 33.
2 E. A. Mari, Anal. Chim. Acta, 29 (1963) 303.
3 V. N. Startsev, E. I. Krylov et Y. U. Koz'min, Russ. J. Inorg. Chem., 10 (1965) 1285.
4 V. N. Startsev, E. I. Krylov et Y. U. Koz'min, Russ. J. Inorg. Chem., 11 (1966) 1239.
5 V. N. Startsev, Y. I. Sannikov, G. N. Ben'yash et E. I. Krylov, Russ. J. Inorg. Nucl. Chem., 13 (1968) 586.

6 G. Roland et B. Gilbert, Anal. Chim. Acta, 50 (1972) 57.
7 J. C. White et W. J. Ross, Nat. Acad. Sci. Nucl. Sci., N.A.S.-N.S., (1961) 3102.
8 J. O. Hibbits, S. Kallmann, W. Giustetti et H. K. Oberthin, Talanta, 11 (1964) 1464.
9 G. Roland, M. C. Blandiaux et G. Duyckaerts, Anal. Chim. Acta, 00 (1976) 000.
10 J. Stary, The Solvent Extraction of Metal Chelates, Pergamon Press, Oxford, 1964.
11 A. K. De et M. S. Rahaman, Anal. Chim. Acta, 31 (1964) 81.
12 J. Hala, J. Inorg. Nucl. Chem., 29 (1967) 187.
13 J. Hala, J. Inorg. Nucl. Chem., 29 (1967) 1317.
14 Y. Marcus et A. S. Kertes, Ion Exchange and Solvent Extraction of Metal Complexes, Wiley-Interscience, New York, 1969.
15 T. V. Healy, Nuclear Science and Engineering, 16 (1963) 413.
16 N. Serpone et R. C. Fay, Inorg. Chem., 6 (1967) 1835.
17 K. Ohwada, J. Inorg. Nucl. Chem., 29 (1967) 833.
18 I. J. Gal et R. M. Nikolic, J. Inorg. Nucl. Chem., 28 (1966) 563.
19 L. D. C. Bok, G. F. C. Wessels et I. G. Leipoldt, Z. Anorg. Allg. Chem., 404 (1974) 76.

Analytica Chimica Acta, 85 (1976) 341—349

APPLICATION OF THE THEORY OF KUBELKA AND MUNK TO DENSITOMETRY

F. A HUF, H. J. DE JONG and J. B. SCHUTE*

Department of Pharmaceutical Analysis, University of Leiden, Gorlaeus Laboratoria, Wassenaarseweg 76, Leiden (The Netherlands)

(Received 12th January 1976)

SUMMARY

It is argued that the Kubelka—Munk relations cannot be generally applied to quantitative t.l.c. densitometry carried out with an apparatus which utilizes a source of collimated light since the angular distribution of the radiant flux may change by passing through the layer in such a way that the conditions upon which the Kubelka—Munk equations are based, are not met. In addition, a true blank absorbance value of the thin layer, which plays an important part in these relationships, cannot be measured with such a source. These difficulties can be avoided with a source of diffuse scattered light, the angular distribution of which approximates to the Lambert cosine distribution. A flying spot densitometer with such a source has been constructed, and absorbance measurements with spots of Sudan Yellow, developed with chloroform on a silica layer, have been evaluated in terms of the theory and integrated over the spot area. Excellent results were obtained.

The theory of light transmission and reflection in scattering media was developed in the first half of this century by several authors. Kubelka and Munk derived a number of equations relating several properties of scattering layers and these are generally applicable to densitometry. One of these equations relates the transmittance T of a layer of light-absorbing material in a scattering medium to the coefficient of scatter s, the coefficient of absorption k, and the thickness of the layer X by

$$T = b/(a \sinh bsX + b \cosh bsX) \quad (1)$$

with $a = (s + k)/s$ and $b = (a^2 - 1)^{\frac{1}{2}}$.
In the particular case where $k = 0$ (scatter with no absorption) eqn. (1) reduces to

$$T_0 = 1/(sX + 1) \quad (2)$$

Now kX is proportional to the amount of absorbing compound in the light beam. For quantitative measurements with absorption densitometry the

*This paper was presented in part at the 35th International Congress of Pharmaceutical Sciences, Dublin, September 1975.

inverse of function (1) i.e. $kX = f(T, sX)$ is required. Goldman and Goodall [1] derived such a function:

$$0.434\,kX = 2\exp[-2A_0]\,(A + 0.4A^2) \tag{3}$$

and this is approximately valid in the range $0.7 < A_0 < 1.3$ and $A < 1$ when $A_0 = -\log T_0$ = absorbance of the thin layer blank, and $A = \log T_0/T$ = absorbance of the compound at one point of the t.l.c. spot. The amount m of absorbing compound present in the spot is found by integration [2] over the area O of the spot

$$m = \frac{2}{\epsilon}\int \exp[-2A_0]\,(A + 0.4A^2)\mathrm{d}O \tag{4}$$

where ϵ is the absorptivity of the compound. For this integration a "flying spot" densitometer is needed.

A previous article [2] described quantitative in situ determinations on t.l.c. plates with a commercial flying spot densitometer which could not, however, integrate according to eqn. (4) and yielded values proportional to the integrated absorbance. The theory was therefore applied only to non-developed spots for which A could be regarded as constant over the area of the spot.

In later investigations, the apparatus was provided with an analog computing unit to integrate according to eqn. (4). The results obtained in this way with developed spots were, however, disappointing since the plot of m versus the integral of eqn. (4) was often poorly linear or crossed the axes too far from the origin. This unsatisfactory performance had two major causes; both resulted from the fact that the apparatus utilized a collimated light beam which was partly scattered in passing through the thin layer. First, the angular distribution in the layer is not constant; thus an essential requirement for the applicability of the theory of Kubelka and Munk is not met. Secondly, true values of A_0 are not measured since only part of the transmitted light beam falls on the detector, and the higher the scatter the smaller the part. Both difficulties can be avoided with a source emitting diffuse scattered light, as discussed below.

Influence of the angular distribution of the radiant flux

Kubelka and Munk used the following differential equations

$$\begin{aligned} \mathrm{d}I &= -(k + s)\,I\mathrm{d}x + sJ\mathrm{d}x \\ \mathrm{d}J &= (k + s)\,J\mathrm{d}x - sI\mathrm{d}x \end{aligned} \tag{5}$$

where x is the distance from the illuminated surface of the layer, I the radiant flux in the positive x-direction, and J the radiant flux in the negative x-direction.*

*The x-direction is defined in the opposite sense to that used by Kortüm [3]. The symbols I and J are taken for the flux in accordance with Kortüm, even though the symbol I is generally used for the luminous intensity, i.e. the flux per unit solid angle or per unit surface area.

At first it was considered that the light travels only in a direction perpendicular to the plane of the layer, i.e. k and s are constants and eqn. (1) can be found as a solution of eqn. (5). This presumption is not a realistic one: the light is scattered in all directions during its travel; k and s should be replaced by $K = 2\,k$ and $S = 2\,s$ respectively if the light in and outside the layer has an angular distribution according to the Lambert cosine law. In the latter case I and J represent the total flux travelling forward and backward, respectively, through the layer dx. The derivation is reviewed by Kortüm [3]. K and S, the effective coefficients of absorption and of scatter respectively, are constants if diffuse light with a Lambert angular distribution is used for absorbance and reflectance measurements, and in eqn. (1) k and s can be replaced by the effective coefficients.

The use of collimated light leads to other effective coefficients because the beam becomes more and more diffuse on passing through the layer. Furthermore, the coefficients now depend on X and differ for the light in forward and backward directions. As a result, eqn. (1) is no longer valid and a substantially more complex solution is found [4].

The role of the blank absorbance

When a scanning system such as a densitometer is used, it is not possible to collect all the light that passes through the layer. With a constant aperture, an increase in the scattering power of the layer decreases the measured radiant flux. Since $A_0 = \log I_1/I_2$, where I_1 is the flux outside the layer (no scatter) and I_2 is the flux transmitted through the blank layer (scatter), the blank absorbances measured with collimated light are substantially too high.

True A_0-values are needed for the application of eqn. (3). Errors in A_0 have a great influence on the results, since A_0 appears in the exponent. Moreover, the value of A_0 determines the validity of eqn. (3).

True A_0-values can be measured with light of an angular distribution which does not change on passing through the layer. Values obtained in this way (see below) for prefabricated t.l.c. plates (Camag 30179) used in this laboratory appeared to fall in the range $0.5 < A_0 < 0.8$. Since eqn. (3) could not be applied for these plates, another approximation was derived by the method of Goldman and Goodall, who arrived at eqn. (3) by assuming that kX is determined by two independent functions of A_0 and A

$$0.434\,kX = F(A_0).G(A) \tag{6}$$

in which $F(A_0) = (dkX/dA)_{A=0}$ and $G(A) = A + \alpha A^2$ $(A < 1)$

From eqn. (1)

$$F(A_0) = 3/(1 + 2\cosh 2.303\,A_0) \tag{7}$$

It was shown by plotting $\log F(A_0)$ versus A_0 that in the range $0.7 < A_0 < 1.3$ eqn. (7) approximated to $F(A_0) = 2\exp[-2\,A_0]$. Furthermore α varied from 0.33 to 0.46 in this range for A_0 and its value was taken to be 0.4.

The best fitting linear substitution of $\log F(A_0)$ was calculated for the

range $2 \leqslant SX \leqslant 5$, which corresponds to $0.45 \leqslant A_0 \leqslant 0.80$ according to eqn. (2). The calculation, by the method of least squares, was based on four points calculated with the SX values 2, 3, 4 and 5. The result, $\log F(A_0) = -0.7247\ A_0 + 0.1891$, leads to

$$F(A_0) = 1.55 \exp[-1.67\ A_0] \tag{8}$$

Now α is calculated as a function of SX and KX with eqns. (1), (2), (6) and (7), giving the values shown in Figs. 1(a) and 1(b). It appears that α depends rather strongly on SX, and thus on A_0, in this range of low SX values.

In Fig. 1(b), α is presented as a function of SX, with KX values such that the value of A is approximately 0.8*. This value of A was chosen since A should be smaller than 1.0 whilst the correction term αA^2 will only be important if A is not too small. In a restricted range of values of SX, α depends linearly on

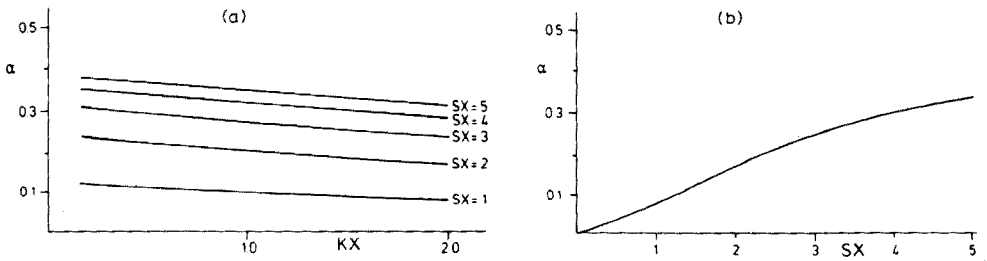

Fig. 1. Dependence of the coefficient α of eqn. (10) (a) on KX at given values of SX; (b) on SX when $A = 0.8$.

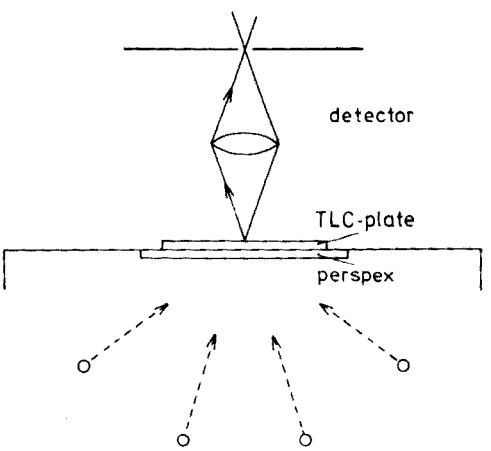

Fig. 2. Light source used for illuminating with diffuse light.

*These values of KX were found by linear interpolation between the values of A calculated from (1), taking suitable values of KX and the desired value of SX.

A_0 to a good approximation. The least-squares method yields $\alpha = 0.53\,A_0 - 0.06$; substituting this value and $F(A_0)$ according to eqn. (8) in eqn. (6) gives

$$0.434\,KX = 1.55\exp[-1.67\,A_0]\,(A + [0.53\,A_0 - 0.06]\,A^2) \qquad (9)$$

which is valid for $0.45 \leqslant A_0 \leqslant 0.80$ and $A < 1$.

For higher values, up to $A_0 = 1.3$, eqn. (3) can be used.

When A_0 exceeds the value 1.3, $F(A_0)$ approximates to $F(A_0) = 3 \cdot 10^{-A_0}$ since eqn. (8) can be written as $F[A_0] = 3/(1 + 10^{A_0} + 10^{-A_0})$. At high values of A_0, α appears to reach a maximum value of 0.46, and a further approximation $0.434\,KX = 3\exp[-2.30\,A_0]\,(A + 0.46\,A^2)$ is valid for $A_0 > 1.3$ and $A < 1$. Generally, the inverse of function (1) can be expressed by

$$0.434\,KX = \beta\,[\exp - \gamma A]\,(A + \alpha A^2) \qquad (10)$$

The coefficients α, β and γ and their dependence on A_0 are summarized in Table 1.

EXPERIMENTAL

Instrumentation

Starting with the requirements mentioned above a new densitometer was built. The light source consists of four d.c. neon discharge tubes mounted within a mat white painted box, the upper side of which is closed with a light-scattering perspex plate (see Fig. 2).

The discharge tubes are placed in a cylindrical array; the intensity of the light leaving the center of the perspex plate is therefore proportional, within a good approximation, to the cosine of the angle with the normal. Consequently, a perspex plate of very high diffusing power (which would lead to a poor light source efficiency) is not necessary. T.l.c. plates are placed on the light source in such a way that the spot to be measured lies in the center of the perspex plate.

By means of two lead screws (driven by stepping motors) a photomultiplier head scans an adjustable area of the chromatogram in a zig-zag pattern (Fig. 3). The photomultiplier contains an interference filter (as monochromator); a circular aperture of 0.1-mm diameter was used. The signal from the photomultiplier is transformed to absorbance values by a voltage

TABLE 1

Values of the coefficients of equation (10) for varying ranges of SX and corresponding ranges of A_0 ($A < 1$)

SX	A_0	α	β	γ
2— 5	0.45—0.80	$0.53\,A_0 - 0.06$	1.55	1.67
4—19	0.70—1.30	0.40	2.00	2.00
>19	>1.30	0.46	3.00	2.30

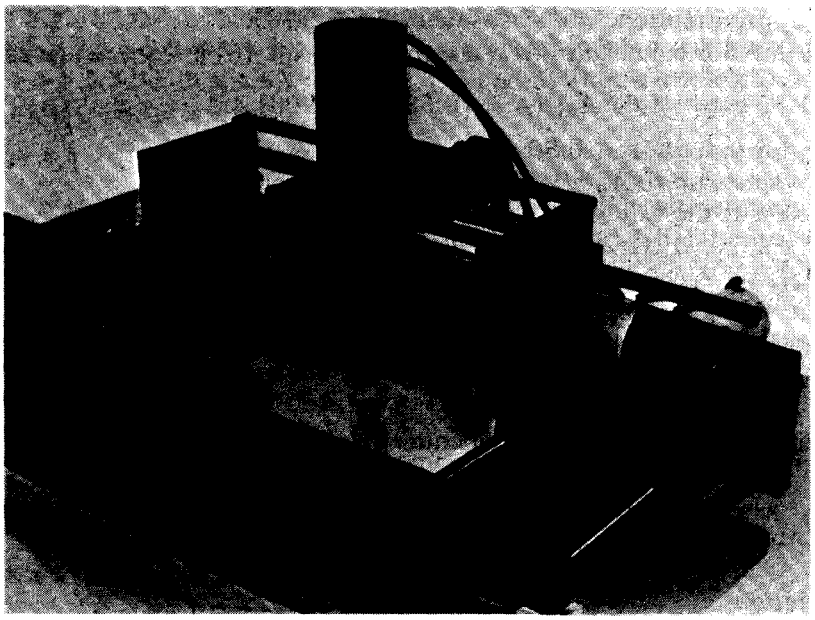

Fig. 3. Scanning part of the densitometer.

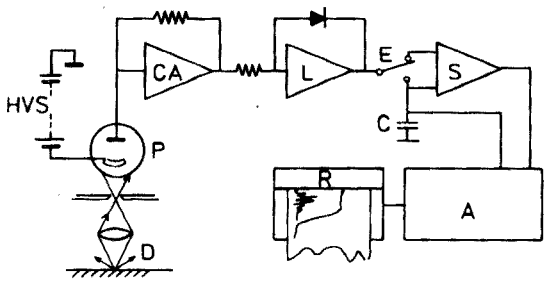

Fig. 4. Electronic diagram. HVS: High voltage supply (Keithley). P: Photomultiplier (RCA 6099). CA: Current amplifier (Keithley). L: Logarithmic converter. E: Electronic switch. S: Subtractor. C: Capacitor. A: Analog computer. R: Integrating recorder (Kipp BD 12). D = Diffuse light.

follower and a lin/log converter (Fig. 4). By electronic switching, A_0 is stored in capacitor C at every turning point of the zig-zag movement. During the zig-zag movement the stored A_0 value is subtracted from the total absorbance to obtain the net absorbance of the spot.

Signals for A_0 and A are fed to an analog computing unit, which performs the transformation according to eqn. (3). The coefficients α and γ are adjustable and are adapted to the measured absorbance of the t.l.c. blank. The transformed signal is recorded and integrated by a two-pen recorder (Kipp BD 12).

Methods

Solutions containing different concentrations of Sudan yellow in ethyl acetate were applied to t.l.c. plates (Camag 30179) as 4-μl spots. A polyethylene pipet was used, as described previously [2]. The chromatogram was developed with chloroform over a distance of 10 cm (R_F = 0.7). After drying for 1 h, the spots were measured with a 499-nm filter.

To check the theory, it was sufficient to measure the value of

$$P = g \int A_{corr}\, dO \tag{11}$$

where $A_{corr} = \exp[-\gamma A_0]\ (A + \alpha A^2)$ and g is a proportionality factor depending on the unit of integration of the apparatus. According to eqns. (4) and (10), P should be proportional to the amount of Sudan yellow applied, provided that g and the absorptivity ϵ are constant.

The α- and γ-values corresponding to the range 0.45—0.80 for A_0 were used (Table 1). The value of α was calculated with a value for A_0 averaged over the plate.

The value of A_0 in the exponent should, ideally, be measured at every point of the spot together with the total absorbance. A is then found by subtracting A_0 from the total absorbance and A_0 is further used to find A_{corr}. Since a double-beam instrument was not available, A_0 was measured on both sides of the spot during the zig-zag movement. The values measured in this way are, generally, not equal and this gives rise to a positive or negative sloping base line in the integral on which P is superimposed.

In order to avoid serious errors arising from the base-line correction, it is important that A_{corr} is large compared with the difference of A_0 on both sides of the spot. The quantity measured was therefore not the absolute value of A_0 but its difference, ΔA_0, from the value A'_0 of a reference point on the plate i.e. $\Delta A_0 = A_0 - A'_0$, with A'_0 chosen so that ΔA_0 is always positive. In this way the integral

$$P' = g \int A'_{corr}\, dO \tag{12}$$

where $A'_{corr} = \exp[-\gamma \Delta A_0]\ (A + \alpha A^2)$ is obtained. Obviously, P and P' are related by

$$P = P' \exp[-\gamma A'_0] \tag{13}$$

RESULTS AND DISCUSSION

Table 2 presents the slopes (Sl') and the intercepts of the plot of P' versus m calculated by the least-squares method for six sets of chromatograms. On each plate four different concentrations giving m-values from 0.10 to 0.52 μg of Sudan yellow per spot were applied. The regression is calculated including zero as a point of the line. In addition, the correlation coefficients and the (residual) standard deviation of each line are given. Intercepts and standard deviations are expressed in μg (i.e. the value in integration units is divided by

TABLE 2

Parameters of regression lines obtained by plotting P' of equation (12) versus μg of Sudan yellow applied

Plate number	1	2	3	4	5	6
Slope SI'[a]	174	152	155	146	176	122
Intercept (μg)	0.000	−0.007	0.001	−0.002	−0.001	−0.000
S.d. (μg)	0.000	0.011	0.004	0.005	0.008	0.005
Correlation coefficient	1.0000	0.9990	0.9999	0.9998	0.9995	0.9998
A'_0 of reference point	0.59	0.52	0.52	0.47	—[b]	0.36
$SI = SI' [\exp -1.67 A'_0]$	65	64	65	67	—	67

[a] Integration units per μg.
[b] Not measured.

the slope SI'), in order to allow a comparison between different plates. For the same reason the slopes are multiplied by $\exp[-1.67 A'_0]$. The corrected slopes (SI) obtained in this way should all have the same value, as follows from eqn. (13).

The results presented in Table 2 are in good agreement with the theory. The agreement between the response of the apparatus and the amount of substance applied is satisfactory, as shown by the correlation coefficients, the small values of the intercepts, and the standard deviations. The best linearity is shown by the results for plate number 1, the worst by those for plate number 2. Taking into account the inaccuracy of the determination of A'_0, the equality of the corrected slopes is also satisfactory. The measurements on different plates are thus directly comparable and, theoretically, there is no need for the use of reference spots on every plate for quantitative evaluation.

The theory of Kubelka and Munk can thus provide a satisfactory model for the theoretical treatment of transmission densitometry. According to this model, the densitometer should integrate the corrected absorbance according to eqn. (11) or (12) and should use a source of diffuse scattered light. No commercial densitometer appears to meet these conditions. Spots of Sudan yellow have been measured with several commercial densitometers, including flying spot densitometers, but the relationships between the amount of substance applied and the response of the apparatus were not good.

Several authors [5—11] have described densitometric experiments with equipment incorporating collimated light, and have obtained linear regression lines or even a proportionality between response and concentration. In those experiments reflectance or transmittance, or a combination of both, was used. The results were obtained by an empirical transformation of the measurements or by a transformation based partly or wholly on the Kubelka—Munk relationships.

The theory of Kubelka and Munk can also be applied to measurements obtained with a collimated light beam, but it is considered that special condi-

tions should be met in this case. For instance, when thin layers with a constant SX-value are used, A_0 need not be measured since, in eqn. (12), $\exp[-\gamma\Delta A_0] = 1$. Furthermore, a constant fraction of the transmitted light is measured and the effective values of s and k can be considered as constants. The value of SX may, however, vary substantially over the plate. The layers used here showed variations up to 40 %.

Apparently, for a more general application of the theory of Kubelka and Munk to densitometry it is important to measure true A_0 or ΔA_0 values and to use conditions which give a good approximation to constant values of the effective coefficients of scatter and absorption, regardless of severe fluctuations in the thickness of the layer. This can be realized by the use of a diffuse scattered light source. Similar considerations will hold if the theory is applied to reflectance and fluorescence densitometry.

The authors are indebted to J. H. G. Janmaat and J. A. v.d. Spek for their contributions in the development of the apparatus, and to M. A. Span for experimental help.

REFERENCES

1 J. Goldman and R. Goodall, J. Chromatogr., 40 (1969) 345.
2 J. B. Schute, H. J. de Jong and H. Dingjan, Pharm. Weekbl., 105 (1970) 1025.
3 G. Kortüm, Reflexionsspektroskopie, Springer, Berlin, 1969, p. 111.
4 S. Q. Duntley, J. Opt. Soc. Am., 32 (1942) 61.
5 L. R. Treiber and B. Örtengren, J. Chromatogr., 73 (1972) 151.
6 H. Jork, J. Chromatogr., 82 (1973) 85.
7 J. M. Owen, J. Chromatogr., 79 (1973) 165.
8 L. R. Treiber, J. Chromatogr., 100 (1974) 123.
9 R Goodall, J. Chromatogr., 103 (1975) 265.
10 S. Ebel and J. Hocke, Z. Anal. Chem., 277 (1975) 105.
11 H. Yamamoto, T. Kwita, J. Suzuki, R. Hira, K. Nakano, H. Makabe and K. Shibata, J. Chromatogr., 116 (1976) 29.

Analytica Chimica Acta, 85 (1976) 351—355

THIN-LAYER CHROMATOGRAPHY OF COORDINATION COMPOUNDS. FACTORS AFFECTING THE RETENTION OF COMPLEXES ON SILICA GEL*

R. H. OKSALA, Jr. and R. A. KRAUSE

Department of Chemistry, University of Connecticut, Storrs, Conn. 06268 (U.S.A.)

(Received 9th January 1976)

SUMMARY

Thin-layer chromatography of a group of transition-metal acetylacetonates on silica gel has established a structure—R_F correlation for the complexes. Several mechanisms of adsorption of complexes on silica gel are considered and the results are correlated with these mechanisms.

Thin-layer chromatography has become a very useful laboratory technique but there has been little systematic work dealing with the interaction of complexes with adsorbents, although Galik [1] considered the effects of solvent composition and air humidity on the t.l.c. behavior of some complexes and Bradley and Pantony [2] considered the mechanism of adsorption of some chelates, concluding it to be of the chemisorption type.

The pentan-2,4-diones or acetylacetonates (acac) of di- and trivalent transition metals have been studied extensively; paper chromatography has been used for the identification of metal ions, e.g. Co(III), Co(II), Ni(II), in solution [3] and the use of D-lactose hydrate in column chromatography [4] led to a partial resolution of the cobalt(III) and chromium(III) tris(acac) complexes into optically active fractions. Chromatographic studies [5] of several acacs have been made with both silica gel and alumina on thin-layer plates; the results indicated pronounced differences in the chromatographic behavior of the acac complexes (R_F value, shape of spot), but these differences were not explained adequately. The purpose of the present research is to correlate the chromatographic behavior of the acac complexes of several transition metals with their respective structures, and to consider the mechanism of adsorption on thin layers of silica gel in various solvents.

*Presented to the Graduate School of the University of Connecticut by R. H. O., Jr. in partial fulfilment of the requirements for the degree Master of Science.

EXPERIMENTAL

Silica gel GF (Brinkman Instruments, Westbury, N.Y.) was spread to a wet thickness of 0.25 mm on 5 × 20 cm glass plates by means of a Reeve-Angel apparatus (Quickfit and Quartz Ltd., England). The plates were air-dried for about 15 min, activated in a drying oven at 110 °C for 1 h and stored over Drierite in a drying cabinet until required.

Acetylacetonates, prepared by literature methods [6—8], were recrystallized at least once. The infrared absorptions were in agreement with the accepted values [9]. About 10 μl of solutions of the acac complexes (ca. $1.5 \cdot 10^{-2}$ M) were applied and elution was carried out in closed glass jars until the solvent front had travelled 12 cm. Visualization was by ultraviolet light; a fluorescent indicator was incorporated in the silica gel, and dark spots on a pale green background were obtained.

RESULTS AND DISCUSSION

Different mechanisms are important in the adsorption of substances on silica gel, including: (a) physical entrapment of adsorbed species, (b) bonding to an active site on the silica gel, (c) dipole—dipole or charge—dipole attractions, (d) ion exchange (charge—charge attractions).

Ion-exchange effects should not be appreciable in the chromatography of neutral species such as metal acetylacetonates, but (a), (b) and (c) above are of varying importance, depending on the complex under investigation. Burwell et al. [10] have proposed negative surface sites, $\equiv SiO^-$ and possibly $=Si(OH)_2^-$, as the active components in silica gel. These negative centers can attract the positive end of a dipole, or coordinate to a metal ion through displacement of a ligand or through expansion of the coordination sphere.

The acac complexes studied were those of Cu(II), Cr(III), Co(III), Fe(III), Co(II), and Ni(II). These complexes represent three different types of structure, and a solvent was sought to elucidate these differences. The solvents employed were: benzene, toluene, carbon tetrachloride, diethyl ether, chloroform, acetone, methanol, ethanol, acetonitrile and water (listed in order of increasing dielectric constant) [11]. Benzene, toluene, and carbon tetrachloride were ineffective as solvents but the acac complexes began to move from the origin with the solvents of higher dielectric constant, and noticeable differences in the chromatograms became apparent. It will be shown how these differences may be related to the structures of the complexes and to some extent to the mechanism of adsorption.

The use of solvents of high dielectric constant (methanol, ethanol, and acetonitrile) masked any differences in chromatographic behaviour and all compounds moved with essentially the same high R_F value. As is well-known, a solvent of intermediate dielectric constant should be chosen. Diethyl ether met the requirement of distinguishing between the compounds studied, which fall into three major structural classes: square planar,

octahedral monomeric, and octahedral polymeric. A relationship between structure and R_F is seen in Table 1.

The compounds consisting of discrete monomeric species, e.g. Cu(II), Cr(III) and Co(III), moved extremely well along the t.l.c. plate and appeared to suffer little hindrance from the silica gel. The exception to this, Fe(III)—acac, will be discussed below. Co(II)—acac and Ni(II)—acac, a tetramer and trimer respectively, show no movement; this suggests some physical entrapment by the silica gel. By employing a more polar solvent, such as methanol, the less polymeric species, the nickel trimer, should be less hindered and exhibit more movement on the silica gel than the cobalt tetramer. This was found to be the case; $[Ni(acac)_2]_3$ gave R_F 0.63 (discrete spot), and $[Co(acac)_2]_4$ gave R_F 0—0.51 (broad band).

The movement of the monomeric iron(III)—acac on silica gel is anomalous; behaviour similar to that of the chromium(III) and cobalt(III) complexes would be expected, but tailing is observed. Kluiber [18] studied the exchange of coordinated acac with ^{14}C-labeled acetylacetone and found that, in chloroform, iron(III)—acac exhibited 90 % exchange within 10 min, indicating a labile species; for chromium(III) or cobalt(III)—acac, exchange was negligible in the same time. A high exchange rate indicates a weakly held ligand, readily displaced from the metal ion by a coordinating site on the silica gel. Such a displacement would account for the tailing on the iron (III)—acac spot and the low R_F value. Evidence supporting this concept was found with a solvent system containing a small amount of the ligand, acetylacetone; any displacement equilibrium will be shifted toward the octahedral tris—acac species, and a chromatogram similar to that of the Co(III) and Cr(III) would be expected for Fe(III). The results (Table 2) supported this concept.

The square planar copper(II) complex also shows a relatively low R_F value in ether (Table 1). Two mechanisms are possible for the strong adsorption: (a) dissociation of ligand acac, as occurs with iron(III), (b) expansion of coordination number by bonding to the silica gel. A coordination number exceeding four is not unusual for copper(II). Either of these mechanisms should cause a much stronger retention of the compound, and consequently a lower R_F value, than is observed with the cobalt(III) or chromium(III) complexes, where retention is likely to be of the charge—dipole attraction type.

TABLE 1

R_F values of acac complexes in diethyl ether (silica gel substrate)

Compound	Structure	R_F	Structure ref.
$Cu(acac)_2$	Square planar	0.30	12
$Cr(acac)_3$	Octahedral monomer	0.93	13
$Co(acac)_3$	Octahedral monomer	0.63	14
$Fe(acac)_3$	Octahedral monomer	0—0.25	15
$[Co(acac)_2]_4$	Octahedral polymer	0.0	16
$[Ni(acac)_2]_3$	Octahedral polymer	0.0	17

TABLE 2

Chromatogram of octahedral monomers with benzene—diethyl ether—acetylacetone eluent (50:50:1) (silica gel substrate)

Compound	R_F	Compound	R_F
$Fe(acac)_3$	0.80	$[Co(acac)_2]_4$	0—0.11
$Cr(acac)_3$	0.77	$[Ni(acac)_2]_3$	0—0.12
$Co(acac)_3$	0.70	$Cu(acac)_2$	0.08—0.65

With the mixed eluent of Table 2, the copper complex exhibits a greater R_F value than in ether, but the area of the spot also increases; this is difficult to rationalize. The increased R_F value is taken as confirmation of a coordination adsorption mechanism, but the exact choice of mechanism is difficult. Considering the difference in behaviour between the copper(II) and iron(III) complexes, both modes may operate. In the latter compound, where expansion of coordination number is unexpected but dissociation highly likely, the effect of added ligand has already been seen and the adsorption mechanism is unambiguous. But in the former complex added ligand does not serve to move the compound to the same extent as iron(III), cobalt(III) and chromium(III). The increase in R_F over that given by ether is evidence for the elimination of part of the adsorption mechanism (probably ligand dissociation), while the greater retention than that of the simple octahedral complexes implies that a stronger adsorption still exists.

Tables 1 and 2 show that the effect of added ligand on the chromium(III) and cobalt(III) complexes is negligible, as predicted. The differences that occur may be attributed primarily to the less polar benzene—ether eluent.

If the silanol sites were deactivated to some extent by protonation, then retention by negative sites should be reduced. The addition of aqueous hydrochloric acid to the eluent serves to accomplish this (Table 3). When a plate eluted with the acidic eluent was sprayed with indicator, the plate was found to be acidic up to R_F 0.57—0.72, i.e. the acid did not follow the solvent front. The complexes moved approximately the same distance as the acid under these conditions, showing very little retention (if any) in the acidic region.

TABLE 3

Protonation of the silanol sites

Compound	Ethanol	Ethanol + 1 % HCl (aq.)
$Cu(acac)_2$	0.39 (broad)	0.65
$Cr(acac)_3$	0.67	0.75
$[Ni(acac)_2]_3$	0.48 (broad)	0.72

This interpretation of the retention of acetylacetone complexes on silica gel should extend to a wide variety of systems and assist the development of separations. Non-labile, coordinately saturated complexes should move with large R_F values on elution with solvents of moderate polarity, provided that a large permanent dipole is not present in the compounds. Labile complexes which are coordinately saturated should show less retention on elution with excess of ligand. Complexes capable of undergoing a ready expansion of coordination number are expected to show greater retention under similar elution conditions.

REFERENCES

1 A. Galik, Anal. Chim. Acta, 67 (1973) 357.
2 M. P. T. Bradley and D. A. Pantony, Talanta, 16 (1969) 473.
3 E. Berg and J. Strassner, Anal. Chem., 27 (1955) 127.
4 T. Moeller and E. Gulyas, J. Inorg. Nucl. Chem., 5 (1958) 248.
5 Y. Tsunoda, T. Takeuchi and Y. Yoshine, Sci. Pap. Coll. Gen. Educ., Univ. Tokyo, 14 (1964) 63.
6 W. C. Fernelius and J. E. Blanch, Inorg. Synth., 5 (1957) 130.
7 B. E. Bryant and W. C. Fernelius, Inorg. Synth., 5 (1957) 188.
8 R. G. Charles and M. A. Pawlikowski, J. Phys. Chem., 62 (1958) 440.
9 K. Nakamoto, Infrared Spectra of Inorganic and Coordination Compounds, Wiley, New York, 1963.
10 R. L. Burwell, Jr., R. G. Pearson, G. L. Haller, P. B. Tjok and S. P. Chock, Inorg. Chem., 4 (1965) 1123.
11 J. Bobbitt, Thin-Layer Chromatography, Reinhold, New York, 1963.
12 H. Shibata, Bull. Chem. Soc., Jpn, 29 (1956) 852.
13 B. Morosin, Acta. Crystallogr., 19 (1965) 131.
14 J. P. Fackler, Jr., in R. F. Gould (Ed.), Werner Centennial, American Chemical Society Publications, Washington, D.C., 1963.
15 R. B. Roof, Acta. Crystallogr., 9 (1956) 781.
16 F. A. Cotton and R. C. Elder, J. Am. Chem. Soc., 86 (1964) 2294.
17 F. A. Cotton and J. P. Fackler, Jr., J. Am. Chem. Soc., 83 (1961) 2818.
18 R. W. Kluiber, J. Am. Chem. Soc., 82 (1960) 4839.

Analytica Chimica Acta, 85 (1976) 357—373

ELECTRONIC ABSORPTION OF CARBOXYLIC ACIDS AND THEIR ANIONS

M. SZYPER and P. ZUMAN

Department of Chemistry, Clarkson College of Technology, Potsdam, New York 13676 (U.S.A.)

(Received 3rd November 1975)

SUMMARY

Electronic spectra of formic, acetic, mono-, di-, trichloro- and trifluoroacetic, glycolic, cyanoacetic, pivalic, α-methoxyacetic, lactic, oxalic, tartaric and citric acids and betaine and of corresponding anions were recorded. The acid forms of all the carboxylic acids studied show a medium-strong $\pi \rightarrow \pi^*$ and a weak $n \rightarrow \pi^*$ absorption band, the latter in the 220—250-nm region. The corresponding anions (or the completely dissociated forms of polybasic acids) show the $\pi \rightarrow \pi^*$ absorption bands, but no indication of a shoulder corresponding to a $n \rightarrow \pi^*$ transition. Changes in the absorbance in the wavelength region corresponding to the $n \rightarrow \pi^*$ transition with addition of alkali metal hydroxides can be used for end-point detection in titrations. Changes of these absorbances in solutions of buffers or strong acids can be used for pK determinations. A pK value of 0.89 (at $\mu = 0.5$) was found for dichloroacetic acid; approximate pK values were established by means of the H_0 acidity scale for trichloroacetic acid (—0.80) and trifluoroacetic acid (—0.92). Finally, absorbances in the 220—250-nm region can be used for determination of carboxylic acids in solutions of strong acids, and some buffers, like phosphate or borate.

In the course of an investigation of electronic absorption by inorganic and organic anions, it was considered of importance to compare the absorption of species containing only σ-bonds with those bearing both σ- and π-bonds. Scrutiny of the literature showed that surprisingly little has been reported on the electronic absorption even of carboxylates, which can be considered to be the commonest representative of anions containing both single and double bonds. As even the absorption of the corresponding acids has not received much attention, information on the behavior of carboxylic acids on interaction with u.v. radiation is included in this paper. Information on the u.v. spectra of acids in the vapor state, where vacuum spectroscopy can be used and measurements can be carried out at low wavelengths, unaffected by absorption by solvent and oxygen, is presented first, followed by a discussion of the behaviors of the acids in solutions.

Absorption of carboxylic acids in the vapor state

The vacuum spectra of aliphatic carboxylic acids in the vapor state show absorption maxima [1—6] in the vicinity of 200 nm with molar absorptivities

of about 50. These absorption bands are attributed to the $n \rightarrow \pi^*$ transition and are considered to correspond to the same electronic transition as the absorption band of aldehydes and ketones observed in the region of 260—280 nm. The $n \rightarrow \pi^*$ transition involving the carbonyl group has been proved [7] to occur in a plane which is perpendicular to the single C—O bond [7, 8]. Such transitions are — according to the selectivity rules — forbidden and this explains the observed low molar absorptivity.

Another, much stronger, absorption band is observed in the vapor-phase spectra of carboxylic acids at about 160 nm. This absorption band has a much higher molar absorptivity [4] — of the order of 2500—4200 l mol^{-1} cm^{-1} — than the band at 200 nm, and is most frequently [4] attributed to a $\pi \rightarrow \pi^*$ transition. Nevertheless, Lyuts et al. [9] attributed the band at 160 nm to an $n \rightarrow \sigma^*$ transition involving the electrons of the carbonyl group. He explained the high probability of the studied transition, as reflected by the very intense absorption band, by an overlap of the $n \rightarrow \sigma^*$ transition corresponding to C=O electrons with a transition in which the electrons of the C—OH bond are transferred to excited σ^* orbitals of the carbonyl group.

Quantum chemical calculations [4] of the energy levels for formic acid indicate that the processes involved in the transitions at 160 nm are of mixed character. They have been interpreted as being due to contributions of the local excitation within the C=O group and a charge-transfer type of excitation resulting in an electron transfer from the OH group to the C=O group. The band in the far ultraviolet, at 109 nm, has been attributed [10] to the ionization of the acid, resulting from a removal of a 2*p*-electron from the carbonyl oxygen. Several diffuse bands between 225 and 250 nm have been reported for formic acid in the gas phase [10].

Spectra of thin solid films of amino acids [11—17] show absorption bands at 120 nm ($\epsilon \approx 10^3$ l mol^{-1} cm^{-1}), 158 nm ($\epsilon \approx 10^4$), 180 nm ($\epsilon \approx 10^3$) and 200—210 nm ($\epsilon \approx 10^2$), attributed to transitions involving the carboxylic group.

Absorption of carboxylic acids in solution

Investigation of the spectra in the liquid phase is complicated by the absorption of the solvents used and by interactions of carboxylic acids with such solvents. As none of the solvents commonly used has negligible absorbance below 190 nm, the required information is usually obtained in one of two ways: either the absorbance of the acids compared is followed at a chosen wavelength, or the wavelength of the absorption maximum and the molar absorptivity are estimated. Extrapolation or curve-fitting techniques have been adopted for this purpose. The absorption bands followed are those at about 180 nm (corresponding to $\pi \rightarrow \pi^*$ transitions) and at about 200—210 nm (attributed to $n \rightarrow \pi^*$ transitions). Frequently, the small band at 200 nm is so overlapped by the intense band at 180 nm that the two processes cannot be distinguished and only one absorption peak enveloping both bands, is observed.

For neat acids, e.g. glacial acetic acid, the absorption band [18] at 204 nm (ϵ = 44.9 l mol^{-1} cm^{-1}) is similar to that observed in the gas phase. The n → π* transition is little affected in nonpolar solvents [3] (e.g., in petrol ether λ_{max} = 200 nm, ϵ = 30 l mol^{-1} cm^{-1}) and seems to be similar even in aqueous solutions [18, 19]. This was interpreted as indicating that the hydrated acid molecules are similar in structure to the associates which exist in nonpolar solvents and neat acids. With increasing polarity of the solvent, the n → π* band is shifted to longer wavelengths and its intensity decreases [20—22], e.g., for myristic acid in heptane and isoctane λ_{max} = 205 nm and ϵ = 63 l mol^{-1} cm^{-1}, and in 95 % ethanol λ_{max} = 210 nm and $\epsilon \approx$ 50 l mol^{-1} cm^{-1}.

Apart from the effect of solvent polarity on the solvation of the ground and excited states, the solvent effect on association of the carboxylic acid has been considered [20, 23, 24], as well as the role of hydrogen bonding [1].

For the forms of amino acids with undissociated carboxylic groups, the n → π* bands observed [15, 25—29] were of similar intensity in the same 200—210 nm region as for unsubstituted carboxylic acids.

The n → π* bands of dicarboxylic acids are more intense and occur at longer wavelengths than those of monocarboxylic acids [9, 21], e.g., for aqueous solutions of oxalic acid, λ_{max} = 250 nm. Similarly, an increase has been postulated for the intensity of the π → π* bands [21].

The use of the absorbance corresponding to the n → π* transition for analytical purposes has been considered [30].

Substituent effects on spectra of carboxylic acid solutions

Discussion of substituent effects is restricted to those substituents which do not themselves possess chromophoric properties.

Increase in chain length in RCOOH has been reported [11, 15, 23, 31] to result in small shifts of the n → π* band to longer wavelengths accompanied by a slight increase in molar absorptivity. An exception is formic acid, where the n → π* band is observed [16, 20] at somewhat longer wavelength than for acetic acid.

Introduction of halogen, as in acid chlorides and bromides [32], results in a shift to longer wavelengths and an increase in band intensity. Direct participation of halogen electrons in the excitation process is possible.

Similarly, introduction of an electronegative group on the α-carbon results [33] in a shift of the absorption band to longer wavelengths. The shift increases with increasing number of electronegative substituents, e.g., chlorine atoms [34, 35]. The effect of an α-hydroxy group is difficult to evaluate, since the experimental evidence [36—43] is unreliable. The effect of an ammonium group, as indicated above, is small.

Absorption of anions of carboxylic acids

It has been assumed [2, 3] that for carboxylate ions the intensity of the n → π* band is much smaller than for the free acid, and that the observed absorption can be attributed predominantly to π → π* transition. Experimental

evidence is very meager and mostly concerned with spectra of unbuffered aqueous solutions [16, 19, 44, 45] where the concentrations of individual species are uncertain. Thus an increase of absorbance at 200 nm has been reported for aqueous solutions of sodium acetate compared with acetic acid [19, 46]. For aqueous solutions of sodium propionate, λ_{max} occurs at 188 nm with ϵ = 1410 l mol^{-1} cm^{-1} [47]. Similarly, there is an increase in absorbance intensity in the far-u.v. region for alkaline solutions of glycine compared with acidic or unbuffered aqueous solutions [26]. In contrast, for oxalic acid, absorption of the monoanion occurs [16] in the same region and with equal molar absorptivity as for the free acid. For tartrate, the absorption intensity at 240 nm has been said to be lower than that for the free acid [40], but the data seem not to be reliable.

Absorbance at a given wavelength has been shown to increase with the number of carboxylate groups, e.g., at 210 nm the following molar absorptivities have been reported [45]; acetate 45.4, tartrate dianion 417, oxalate dianion 667, and citrate trianion 500 l mol^{-1} cm^{-1}.

The present study

The present study was designed to investigate how the spectra of simple carboxylic acids change with pH, adjusted either by titration of the acid or by addition of the acid to a buffered solution or to a solution of a strong acid. The changes in the spectra were followed in order to attribute the observed bands to n → π^* and π → π^* transitions, and to use the spectra for the determination of pK values. The change in absorbance on addition of a base can be applied to spectrophotometric titrations, and the absorption spectra can be utilized for the determination of weak acids in strong acids and buffers.

EXPERIMENTAL

All spectral measurements were done with a Pye-Unicam SP800 recording spectrophotometer in 10-mm silica cells. The cells were thermostated with an Ultrathermostat Haake FJ at 25.00 ± 0.01 °C using water pumped into metallic cell holders.

The acids were of analytical grade from the following sources: Aldrich Chemical Company (chloroacetic, trichloroacetic, nitriloacetic, lactic, tartaric, and citric acids, glycine and betaine); Eastman Kodak Company (dichloroacetic, pivalic, methoxyacetic, and trifluoroacetic acids); J. T. Baker Chemical Co., (formic, acetic and oxalic acids); and City Chemical Corp., N.Y. (glycolic acid).

Stock 0.1—0.01 M solutions of these acids were prepared. Standard solutions of sodium hydroxide were prepared carbonate-free from J. T. Baker Dilut-it. The concentration of sulfuric acid solutions was determined titrimetrically. Phosphate and borate buffers were prepared from analytical-grade reagents.

To follow the changes of spectra with addition of sodium hydroxide, constant volumes of the stock solution (usually to give final concentration of the order of 10^{-3}—10^{-2} M) were mixed with varying amounts of standard sodium hydroxide solution, and the solutions were diluted with water to a volume (usually 10 ml) constant in the series.

Alternatively, the same volume of stock solution was added to a constant volume of a buffer or diluted strong (sulfuric, hydrochloric, perchloric) acid, the ionic strength was adjusted, and the spectrum recorded. When strong acids such as trichloro- and trifluoroacetic acids were studied, the spectra were recorded in solutions of sulfuric acid of varying concentrations and known acidity function H_0. No attempts were made to add neutral salts to sulfuric acid more concentrated than about 1.0 M.

Finally, varying concentrations of a weak acid studied were added to solutions of sulfuric, perchloric, hydrochloric and phosphoric acid or to phosphate or borate buffers (most other buffer anions also absorb), and the spectra were recorded.

RESULTS

Formic acid

Free formic acid shows an absorption band at 210 nm (Fig. 1) accompanied by a weak shoulder at 228 nm; however, it is possible that the maximum observed has been partly cut off, and the real maximum may be at lower wavelength. The anion shows a stronger absorption band at 205 nm, but no shoulder at 228 nm. Hence in titration of the formic acid by sodium hydroxide the band at 205—210 nm increases whereas absorbance at 228 nm decreases. An isosbestic point at 213 nm is observed.

The absorbance at 225 nm is a linear function of the analytical formic acid concentration from $2 \cdot 10^{-3}$ M to $6 \cdot 10^{-2}$ M in aqueous solutions in 0.5 M sulfuric acid, 1 M hydrochloric acid, 1 M phosphoric acid (Fig. 1), and 1 M perchloric acid. Standard deviations of absorbance are given in Table 1. The wavelength used in obtaining the calibration curves — here and in experiments described subsequently — were selected so as to achieve highest sensitivity and accuracy, and are not in general identical with the wavelength of any absorption maximum.

The concentration of free formic acid (HCOOH) was calculated from the analytical concentration of this acid and (a) the tabulated [48] value of K_a ($1.77 \cdot 10^{-4}$) and the known concentration of sodium hydroxide added, and (b) from the absorbance measured at 225 nm and the molar absorptivity. The values obtained by these two methods were in good agreement.

The absorbance at 225 nm for solutions containing $1.6 \cdot 10^{-2}$ M formic acid plotted against sodium hydroxide concentration gave a V-shaped curve. The decrease in the absorbance before the equivalence point was linear (except for the first point which deviated because of self-dissociation of the acid); the increase after the equivalence point was due to absorption caused

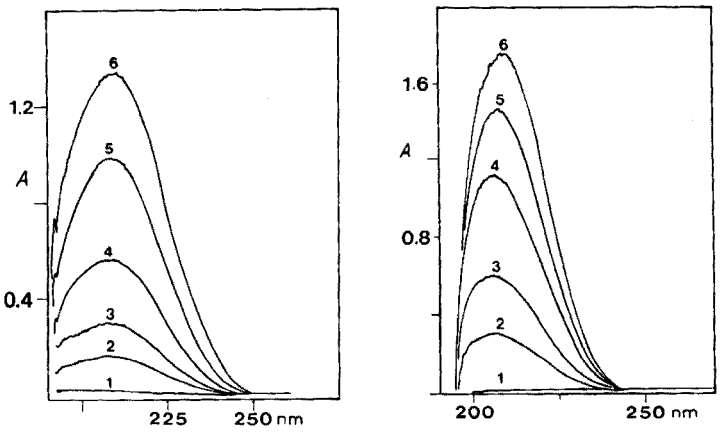

Fig. 1. Dependence of absorption spectra of formic acid on concentration in 1 M phosphoric acid solutions at 25 °C. Concentration of formic acid: (1) 0; (2) 0.4; (3) 0.8; (4) 1.6; (5) 3.2; (6) $4.5 \cdot 10^{-2}$ M.

Fig. 2. Dependence of absorption spectra of acetic acid on concentration in 0.5 M sulfuric acid solutions at 25 °C. Concentration of acetic acid: (1) 0; (2) 0.8; (3) 1.6; (4) 3.2; (5) 4.5; (6) $6.0 \cdot 10^{-2}$ M.

TABLE 1

Standard deviations (±) of absorbance of carboxylic acids from linear absorbance—concentration relationships in various media

Carboxylic acid	HCl (1 M)	$HClO_4$ (1 M)	H_2SO_4 (0.5 M)	H_3PO_4 (1 M)	Borate buffer pH 9.3
HCOOH	0.024	0.011	0.010	0.014	—
CH_3COOH	0.018	0.012	0.016	0.017	0.066

by hydroxide ions [49], which show continuously increasing absorption in this range, with a molar absorptivity similar to that of formic acid — about 18 l mol^{-1} cm^{-1}.

Acetic acid

Free acetic acid shows an absorption band at 205 nm (probably partial cut-off) with a weak shoulder at 230 nm (Fig. 2). The anion shows a stronger absorption at 205 nm, but no shoulder at 230 nm. In the titration of acetic acid by sodium hydroxide, the band at 205 nm increases, and the absorbance at 230 nm decreases, resulting in an isosbestic point at 214 nm.

The absorbance at 225 nm is a linear function of acetic acid concentration over the range $5 \cdot 10^{-3}$—10^{-1} M in aqueous solutions and in 0.5 M sulfuric acid (Fig. 2), 1 M hydrochloric acid, 1 M perchloric acid and 1 M phosphoric acid. In borate buffer pH 9.3, the absorbance at 230 nm is a linear function

of acetic acid concentration (i.e., of acetate ion) from $2 \cdot 10^{-2}$—$3 \cdot 10^{-1}$ M. Standard deviations are summarized in Table 1.

The concentration of free acetic acid calculated from the known analytical concentration of acetic acid and the tabulated value of K_a ($1.76 \cdot 10^{-5}$) was a strictly linear function of the added sodium hydroxide concentration, and agreed well with values obtained from the absorbance measured at 225 nm and the molar absorptivity. The titration curve was V-shaped for the same reasons as for formic acid.

Monochloroacetic acid

Free monochloroacetic acid shows a strong absorption band just below 200 nm, accompanied by a shoulder at 225 nm and a very weak shoulder at 247 nm. The anion shows an even stronger absorption band below 200 nm which overlaps the shoulder at 225 nm; there is no shoulder at 247 nm.

In the titration of chloroacetic acid with sodium hydroxide, the absorbance at 210—225 nm increases, and the shoulder at 247 nm decreases, with an isosbestic point at 233 nm. Absorbance at 260 nm in 0.5 M sulfuric acid proved to be a linear function of monochloroacetic acid concentration over the range $5 \cdot 10^{-3}$—1.10^{-1} M. The difference between the absorbance of the acid and its anion at about 260 nm was small and not suitable for spectrophotometric titration.

Dichloroacetic acid

Free dichloroacetic acid shows a strong absorption band at 225 nm accompanied by a weak shoulder at 240 nm. Spectra of dichloroacetic acid were recorded in solutions of hydrochloric acid of varying concentration and in phosphate buffers pH 1—3. With increasing pH the absorbance at 225 nm increased, and the shoulder at 240 nm decreased, with an isosbestic point at 233 nm. Addition of potassium chloride to 1 M hydrochloric acid up to μ = 2.0 increased the absorbance at 220 nm, but there was practically no change above 235 nm.

The pK value of dichloroacetic acid was determined in solutions of hydrochloric acid and in phosphate buffers at constant ionic strength (μ = 0.5). As the concentration of the dichloroacetic acid was in all instances smaller than $1 \cdot 10^{-2}$ M, correction for self-dissociation was unnecessary. For determination of the pK value, the absorbance at 215 nm (A^{215}) was measured and the following expression used

$$pK = pH + \log (A^{215}—A_0^{215})/(A_R^{215}—A^{215})$$

where A_0^{215} is the absorbance measured in 2.5 M hydrochloric acid, and A_R^{215} the absorbance obtained in a phosphate buffer pH 2.5. Values of pH were measured by a glass electrode. At μ = 0.5 the pK value was found to be 0.89 ± 0.05, independent of dichloroacetic acid concentration in the range $2.5 \cdot 10^{-3}$—$1.0 \cdot 10^{-2}$ M. The plot of $\log (A^{215}—A_0^{215})/(A_R^{215}—A^{215})$ against pH was linear with unit slope. The absorbance A_R^{215} was found to be independent of ionic strength.

Trichloroacetic acid

Free trichloroacetic acid has a strong absorption band at 215 nm and a shoulder at 240 nm. The anion absorbs strongly at 220 nm and shows no shoulder at 240 nm.

Spectra of trichloroacetic acid in sulfuric acid solutions of varying concentration indicated half-titration in about 2.0 M sulfuric acid corresponding to $H_0 = -0.85$. If the Hammett acidity function (which is, nevertheless, obtained for systems $ArNH_3^+ \rightleftharpoons ArNH_2 + H^+$ rather than $RCOOH \rightleftharpoons RCOO^- + H^+$) were applicable, the p$K$ value would be about −0.80 with a standard deviation of ±0.04. With increasing sulfuric acid concentration, absorbance at 220 nm decreases and that at 240 nm increases, with an isosbestic point at 226 nm. The plot of the logarithmic concentration ratio of the acid and base forms as a function of H_0 had a slope of 0.91 ± 0.03. This seems to be sufficiently close to unity and the conditions for application of the H_0 function seem to be fulfilled, at least approximately.

Trifluoroacetic acid

The free acid shows a strong absorption below 195 nm, and two shoulders: one stronger at 210 nm, and one weaker at 225 nm. The anion shows strong absorption below 195 nm and a shoulder at 210 nm, but no shoulder at 225 nm.

When spectra were recorded in sulfuric acid solutions of decreasing concentration, the shoulder at 210 nm remained almost unchanged, the absorbance below 195 nm increased, and the shoulder at 225 nm decreased. Half-titration was reached in about 2.5 M sulfuric acid and the half-titration point corresponded to a pK value of about −0.92 on the H_0 acidity scale, but the slope of the dependence of $\log (A^{230}-A_R^{230})/(A_0^{230}-A^{230})$ [where $A_0^{230} = 1.07$ was measured in 7.0 M H_2SO_4 and $A_R^{230} = 0.48$ in 0.01 M H_2SO_4] on H_0 function was 0.70 ± 0.02, which clearly indicates that the H_0 function cannot be assumed to provide even a rough approximation.

Glycolic acid

The free acid shows a medium strong band at 206 nm and a shoulder at 220 nm, whereas the anion shows strong absorption at 202 nm and no shoulder at 220 nm.

Spectra recorded in dilute solutions of sulfuric acid and phosphate and borate buffers show an increase in the absorbance at 206 nm and a decrease at 220 nm with an isosbestic point at 215 nm. The change of the absorbance is in good agreement with the value of $pK_2 = 3.83$ reported in the literature [49].

Cyanoacetic acid

The free acid shows a medium strong band below 200 nm and a shoulder at 220 nm. The anion absorbs in a strong band at 205 nm with no shoulder at 220 nm.

When the acid is titrated with sodium hydroxide, the absorbance at 200—210 nm increases, and the shoulder at 220 nm decreases, with an isosbestic point at 216 nm. In 0.5 M sulfuric acid, the absorbance at 240 nm is a linear function of the concentration of cyanoacetic acid from $5 \cdot 10^{-3}$—$1 \cdot 10^{-1}$ M. The difference in the absorbances of the acid and the anion at 230 nm is small, so that spectrophotometric titrations are inaccurate.

Pivalic acid

The free acid shows a moderately strong band at 210 nm, accompanied by a shoulder at 225 nm; the anion absorbs strongly at 205 nm with no shoulder above 220 nm.

Titration with sodium hydroxide causes an increase of absorbance at 205 nm, and a decrease of the shoulder at 225 nm with an isosbestic point at 215 nm (Fig. 3). In 0.5 M sulfuric acid, absorbance at 225 nm is a linear function of pivalic acid concentration from $2 \cdot 10^{-3}$—$5 \cdot 10^{-2}$ M.

The concentration of free pivalic acid (calculated for $1 \cdot 10^{-2}$ M analytical concentration of the acid and the tabulated value of $K = 8.9 \cdot 10^{-6}$) was a strictly linear function of concentration of added sodium hydroxide, and agreed well with values obtained from the absorbance measured at 225 nm and the molar absorptivity.

The titration curve (Fig. 4) shows the expected decrease in the absorbance at 230 nm before the equivalence point is reached. Measurement at 230 nm is preferred for the titration to that at 225 nm, as at the former absorption from hydroxide ions plays a smaller role. After the equivalence point the absorbance becomes practically constant, as the absorbance of hydroxide ions [48] at 230 nm is small.

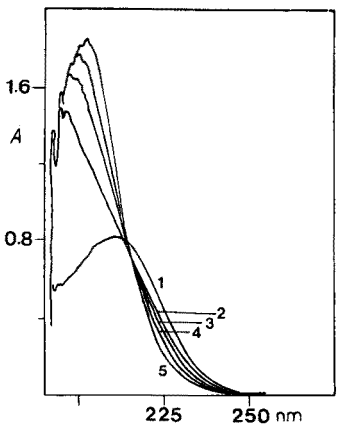

Fig. 3. Dependence of absorption spectra of $1 \cdot 10^{-2}$ M pivalic acid solution on sodium hydroxide concentration at 25 °C. Concentration of sodium hydroxide: (1) 0; (2) 3; (3) 5; (4) 7; (5) $10 \cdot 10^{-1}$ M.

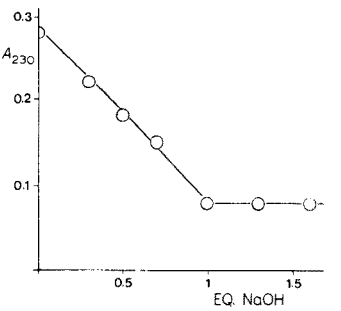

Fig. 4. Plot of absorbance at 230 nm of pivalic acid ($1 \cdot 10^{-2}$ M) as a function of sodium hydroxide concentration.

α-Methoxyacetic acid

The free acid shows a moderately strong absorption band at 206 nm with a very weak shoulder at 220 nm; the anion shows strong absorption at 205 nm and no shoulder at 220 nm.

On titration with sodium hydroxide, α-methoxyacetic acid shows an increase in the absorbance at 205 nm and decrease in the shoulder at 220 nm, but as the shoulder is very weak, the changes are indistinct and so is the isosbestic point.

Glycine

The completely protonated form of glycine $\overset{+}{N}H_3CH_2COOH$ gives an absorption band below 200 nm with a weak shoulder at 220 nm. The zwitterion $^+NH_3CH_2COO^-$ shows strong absorption below 205 nm and no shoulder at 220 nm. The anion $NH_2CH_2COO^-$ shows strong absorption with a maximum below 200 nm; this absorption band may be accompanied by a shoulder at 215 nm, but absorption of hydroxide ions makes the distinction difficult.

Spectra of glycine were recorded in phosphate and borate buffers from pH 1.9 to 12. The changes below pH 3 are not very pronounced because of the weakness of the shoulder at 220 nm, and are therefore unsuitable for titrations or pK determinations. Spectral changes in the pH range (8—10.5) of the second dissociation constant, are more marked and might be used for pK determination and spectrophotometric titration.

Betaine hydrochloride

The acid form shows strong absorbance below 195 nm accompanied by two shoulders: a strong one at 210 nm and a weak one at 230 nm. The zwitterion shows an even stronger absorption below 195 nm, and no change in the shoulder at 210 nm, but no shoulder at 230 nm.

When the spectra of betaine hydrochloride were recorded for sulfuric acid solutions of varying concentration and in phosphate buffers, the absorbance below 205 nm increased, and the shoulder at 230 nm decreased with increasing pH. The corresponding isosbestic point was observed at 220 nm. The small difference between the molar absorptivities of the acid and the anion at 230 nm limits the utility of spectrophotometric titrations.

Lactic acid

The free acid shows a strong absorption below 195 nm, a band of medium intensity at 210 nm and a shoulder at 225 nm; the anion shows strong absorption below 200 nm and no shoulder at 225 nm.

When 0.01 M lactic acid in 0.0033 M phosphoric acid was titrated with 0.1 M sodium hydroxide, the absorbance below 210 nm increased, and the shoulder at 225 nm decreased with an isosbestic point at 213 nm. The pK value found from this titration (pK 3.73) differs from the literature value [50] of 3.86. The discrepancy might be due to a difference in ionic strength and its change in the course of the titration.

Oxalic acid

Both free oxalic acid and its monoanion ($HOOC—COO^-$) show practically identical spectra with a well developed absorption band at 203 nm which does not seem to be affected by the cut-off. This maximum is accompanied by a weaker, but well developed maximum at 250 nm. The dianion ($^-OOCCOO^-$), however, gives an intense maximum at a short wavelength (< 200 nm) and a small shoulder at 260 nm (Fig. 5).

Hence little change of spectra is observed in the course of titration of oxalic acid by the first equivalent of sodium hydroxide. During titration by the second equivalent, absorbance decreases both in the 215—220 nm region and at 250 nm, until it reaches a constant value. Simultaneously, the weak absorption band at 260 nm becomes apparent.

In 0.5 m sulfuric acid the absorbance at 250 nm is a linear function of oxalic acid concentration.

The concentration of free oxalic acid in solutions containing more than one but less than two equivalents of sodium hydroxide was calculated from the known analytical concentration and the value [51] of the second dissociation constant $K_2 = 5.4 \cdot 10^{-5}$; this value agreed well with values obtained from absorbance measured at 260 nm and molar absorptivity. The plot of this concentration against concentration of added sodium hydroxide was linear (Fig. 6); the effect of the first dissociation step was neglected, which caused deviations of the first point.

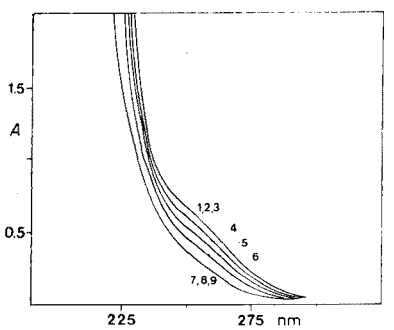

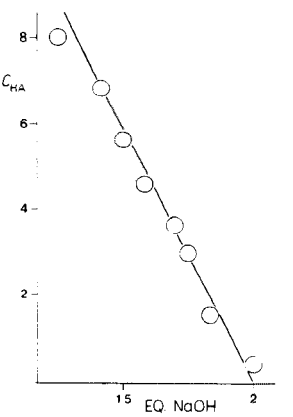

Fig. 5. Dependence of absorption spectra of oxalic acid ($1.2 \cdot 10^{-2}$ M) on sodium hydroxide concentration at 25 °C. Concentration of sodium hydroxide: (1) 0; (2) 0.6; (3) 1.2; (4) 1.5; (5) 1.8; (6) 2.1; (7) 2.4; (8) 3.0; (9) $3.8 \cdot 10^{-2}$ M.

Fig. 6. Plot of theoretical curve and experimental points for concentration of the free monoanion of oxalic acid as a function of sodium hydroxide concentration. Analytical concentration of oxalic acid (C), $1.2 \cdot 10^{-2}$ M. Theoretical curve was calculated assuming for the second dissociation constant value $K_2 = 5.4 \cdot 10^{-5}$, and for the molar absorptivity of the monoanion $\epsilon_{HA^-} = 26.3$. Concentration of the acid (C_{HA}) given in mmol l^{-1}.

The titration curve shows three linear sections (Fig. 7): pH-independent portions for concentrations of sodium hydroxide below one equivalent and in excess of two equivalents, and a decreasing linear portion between the first and second equivalent, corresponding to the decrease in monoanion concentration.

Tartaric acid

The acid absorbs at about 210 nm and shows a shoulder at 230 nm. The monoanion absorbs also at 210 nm and shows a shoulder at 230 nm only slightly weaker than that of the free acid. The dianion shows little change in the absorbance at 210 nm, but practically no shoulder at 230 nm.

Hence in the course of titration by sodium hydroxide, only a small change in absorbance at 230 nm is observed during addition of the first equivalent, but a considerable decrease during addition of the second. Consequently, a non-linear titration curve is observed.

In these titrations, the pH values were measured after each successive addition of sodium hydroxide and the absorbance at 230 nm was calculated from the expression

$$A_{230} = C[H^+]\,(\epsilon_{H_2A}\,[H^+] + \epsilon_{HA} - K_1)/([H^+]^2 + K_1\,[H^+] + K_1K_2)$$

where $\epsilon^{230}_{H_2A} = 64$ and $\epsilon^{230}_{HA^-} = 32$; the dissociation constants [52] used were $K_1 = 9.2 \cdot 10^{-4}$ and $K_2 = 4.3 \cdot 10^{-5}$. Data calculated by means of this equation and the experimental data show good agreement (Fig. 8).

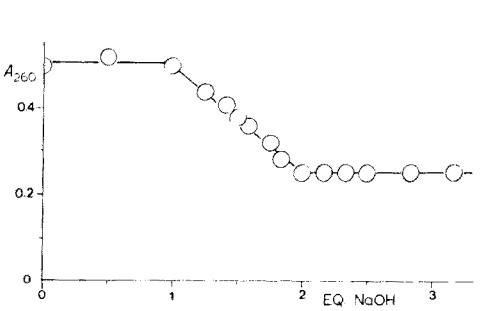

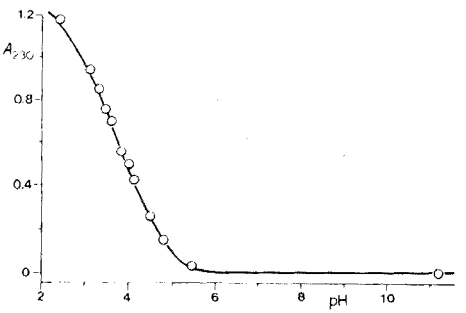

Fig. 7. Dependence of absorbance at 260 nm on the sodium hydroxide concentration added to a solution containing $1.2 \cdot 10^{-2}$ M oxalic acid.

Fig. 8. Plot of theoretical curve and experimental points for the dependence of absorbance of tartaric acid at 230 nm on pH in the course of titration with sodium hydroxide. Theoretical curve was calculated for $2 \cdot 10^{-2}$ M tartaric acid assuming $pK_1 = 3.00$, $pK_2 = 4.39$. The molar absorptivities used were $\epsilon_{H_2A} = 64$ for the free acid and $\epsilon_{HA^-} = 32$ for the monoanion.

Citric acid

All four forms of citric acid absorb strongly at 210 nm and the absorptivities are similar. The free acid shows a shoulder at 235 nm, which is weaker for the monoanion and dianion and practically absent for the trianion.

Consequently, in titrations of citric acid with sodium hydroxide, the absorbance shows a negligible decrease during the addition of the first equivalent, a small — about 20 % — decrease during the addition of the second, and sharp decrease during the addition of the third equivalent.

DISCUSSION

The acid forms of all the carboxylic acids studied show a short-wave absorption band of medium intensity, which can be attributed to the $\pi \rightarrow \pi^*$ absorption. In many cases, the intensity of the band, expressed by molar absorptivities in Table 2, may be larger than that given, as the maximum of the band may be in the cut-off region. This absorption band is accompanied by a weak absorption band in the 220—250-nm region, which usually appears as a shoulder, obvious only when the absorption of the acid is compared with that of the anion. This absorption band may be attributed to a forbidden $n \rightarrow \pi^*$ transition.

The corresponding anions (or the completely dissociated forms of polybasic acids) show either an increased or unchanged $\pi \rightarrow \pi^*$ absorption band, but no indication of the shoulder corresponding to an $n \rightarrow \pi^*$ transition. Either the $n \rightarrow \pi^*$ transition occurs at shorter wavelengths than for the free acid and is overlapped by the absorption corresponding to the $\pi \rightarrow \pi^*$ transition, or the probability of the $n \rightarrow \pi^*$ transition in the anion is considerably smaller than in the free acid. The latter explanation would be in agreement with the greater stabilization of π-electrons in the anion because of resonance, than is possible in the free acid.

The relationship between the intensity of the $n \rightarrow \pi^*$ absorption band and structure of the acid seems to be complex, as is the relationship between structure and the separation of the $\pi \rightarrow \pi^*$ and $n \rightarrow \pi^*$ absorption bands. The introduction of substituents seems to exert more than one type of effect. Particularly well separated $\pi \rightarrow \pi^*$ and $n \rightarrow \pi^*$ absorption bands can be observed for pivalic and oxalic acid.

For the polyvalent acids studied, the spectral behavior of the monoanions (and for the tribasic acids even of the dianions) resembles more closely that of the acid than that of the conjugate base.

Changes in the absorbance in the wavelength region corresponding to the $n \rightarrow \pi^*$ transition of the free acid (or the incompletely dissociated form of a polybasic acid) with addition of alkali metal hydroxides can be used for detection of end-points in titrations of most of the acids studied. The difference between the absorbance before titration and after reaching the equivalence point must be substantial. In practice it was shown that sharp equivalence points can be obtained, if the change is at least 30 % of the original absorbance

TABLE 2

Molar absorptivities and wavelengths of maximum absorption for various carboxylic acids and their anions

Acid	RCOOH				$RCOO^-$	
	$\pi \rightarrow \pi^*$		$n \rightarrow \pi^*$[a]		Maximum[g]	
	λ[f]	ϵ[c]	λ[b]	ϵ[c]	λ[f]	ϵ[c]
HCOOH	210	45	228	13	205	100
CH_3COOH	205	33	230	4	205	45
$CH_2ClCOOH$	200	150[d]				
	225[e]	30[e]	247	1	<215	≈200
$CHCl_2COOH$	225	85	240	12	225	>200
CCl_3COOH	215	>230	240	36	220	>300
$CH_2OHCOOH$	206	52	220	10	202	130
$CH_2CNCOOH$	198	>80	220	5	205	>100
$(CH_3)_3CCOOH$	210	82	225	25	205	220
CH_2COOH | OCH_3	206	58	220	3	205	170
CH_2COOH | NH_3^+	<195	>200	220	6	<205	200
CH_2COO^- | NH_3^+	<205	>200	—	—	<200	>200
CH_2COOH | $N(CH_3)_3^+$	<195	>100			<195	>200
	210[e]	30[e]	230	2	210[e]	≈30[e]
CH_3CCOOH | OH	<195	>150	225	10	<200	>200
	210[e]	92[e]				
CF_3COOH	<195	>100	225	10	<195	>200
	210[e]	≈30[e]			210[e]	≈30[e]
COOH | COOH	203	1500	250	25	200	1500
					250	25
COOH | COO^-	200	1500	250	25	<200	>1500
					260[e]	4[e]
$CH(OH)COOH$ | $CH(OH)COOH$	210	≈250	230	64	210	≈250
					230[e]	≈40[e]
$CH(OH)COO^-$ | $CH(OH)COOH$	210	≈250	230	≈40	210	≈250

[a]Corrected for $\pi \rightarrow \pi^*$ absorbance at this wavelength.
[b]Wavelength of the absorption maximum in nm.
[c]Molar absorptivity in l mol^{-1} cm^{-1}.
[d]Probably due to excitation of electrons of the C—Cl bond.
[e]Shoulder.
[f]Wavelength of highest measured absorption, affected by cut off.
[g]Apparent maximum.

TABLE 3

Suitability of spectrophotometric titration of carboxylic acids based on comparison of total molar absorptivities of the free acid and at the equivalence point

Acid	Wavelength used (nm)	ϵ (l mol^{-1} cm^{-1}) NaOH added		% Change	Suitability
		None	Equiv.		
HCOOH	225	21	7	66.6	+
CH_3COOH	225	12	6	50	+
$CH_2ClCOOH$	250	2.5	1.4	44	+
$CH_2CNCOOH$	220	21	16	24	—
$(CH_3)_3CCOOH$	230	28	10	64	+
$CH_2(OCH_3)COOH$	220	33	30	9	—
$CH_2(NH_3^+)COOH$	220	16	10	27.5	±
$CH_2(NH_3^+)COO^-$	215	28	58	52	+
$CH_2(N(CH_3)_3^+)COO^-$	235	5.5	4.0	27	±
$CH_2OHCOOH$	225	46	34	26	±
$(COOH)_2$	250	25	25	0	—
$COOHCOO^-$	260	42	21	50	+

(Table 3). If the change is below 25 % the location of the end-point is unsatisfactory. For acids where the decrease is in the range 25—30 % (denoted by ± in Table 3), the accuracy of the location of the end-point is a borderline case, and the use of the titration will be governed by requirements on accuracy and concentration range. Such spectrophotometric titrations can, in most cases, be carried out in millimolar or more concentrated solutions. The possibility of working in more dilute solutions is limited by the low molar absorptivities at wavelengths suitable for titration.

Spectrophotometric titrations of 50-ml samples of $2.423 \cdot 10^{-2}$ M oxalic acid at 250 nm with standard sodium hydroxide from a 50-ml burette gave the theoretical value within ± 0.104 % with a standard deviation of ±0.074 %. With more sophisticated volumetric instrumentation there would undoubtedly be an improvement in accuracy.

Changes in the absorbance with acidity can also be used for determination of the pK values of individual carboxylic acids. For acids with pK values above 2, this method does not seem to offer advantages over the conventional electrometric methods. Because in most instances absorbances are measured on the rising portion of the absorption maximum, the accuracy of the measurements is less than the accuracy that can be achieved in pH measurements. However, the situation is different for strong carboxylic acids with pK values smaller than about 2, where potentiometric methods can be used only with difficulty or not at all. Here the proposed spectrophotometric method competes with conductometric methods and seems to be preferable.

The value measured for dichloroacetic acid (pK = 0.89 at μ = 0.5) differs from the value reported in the literature [53] (pK = 1.23, at $\mu \rightarrow 0$) measured

conductometrically, possibly because of the difference in ionic strength. Similarly, the values for trichloroacetic acid (approximate $pK = -0.80$) and trifluoroacetic acid (approximate $pK = -0.92$) differ considerably from literature reports ($pK = 0.23$ for trichloroacetic acid [54] and $pK = 0.58$ for trifluoroacetic acid [55]). Here comparison is much more difficult. The data reported in the literature seem not to be reliable and are undoubtedly too high. However, the use of the acidity function H_0 cannot be considered to be more than a first approximation. An acidity scale based on dissociation of strong acids of the type RCOOH would be necessary for obtaining thermodynamic values of pK.

Finally, measurements of the absorbances of the acid form can be exploited for determinations of weak carboxylic acids in solutions of strong acids, like sulfuric, perchloric, or hydrochloric acid. Moreover, the absorption of the acid or the carboxylate forms can be used for determinations of carboxylic acids and their ionized forms in some buffers, like phosphate or borate buffers.

M. S. thanks the Rochester Research Center, Xerox Corporation, for financial support of this research.

REFERENCES

1 G. Briegleb and W. Strohmeir, Naturwissenschaften 33 (1946) 344.
2 B. Hiroaki and S. Nagakura, J. Chem. Soc., Jpn Pure Chem. Sect., 73 (1951) 214.
3 S. Nagakura, Bull. Chem. Soc. Jpn., 25 (1952) 164.
4 J. C. D. Brand, J. Chem. Soc., 1956, 858.
5 J. A. Pople and J. W. Sidman, J. Chem. Phys., 27 (1957) 1270.
6 S. Nagakura, K. Kaya, and H. Tsubomura, J. Mol. Spectrosc., 13 (1964) 1.
7 E. E. Barnes and W. T. Simpson, J. Chem. Phys., 39 (1963) 670.
8 H. Basch, M. B. Robin, and N. A. Kuebler, J. Chem. Phys., 49 (1968) 5007.
9 A. E. Lyuts, A. E. Cherkashin, and Yu. A. Kushnikov, Izv. Akad. Nauk. Kaz. SSR Ser. Khim, 18 (1968) 55.
10 B. Sugarman, Proc. Phys. Soc., (London) 55 (1943) 429.
11 T. Inagaki, Biopolymers, 12 (1973) 1353.
12 J. P. Vinogradov and N. Ya. Dodonova, Opt. Spektrosk., 30 (1971) 27.
13 J. W. Preiss and R. Setlow, J. Chem. Phys., 25 (1956) 138.
14 G. Scheibe, F. Povenz, and C. F. Lindstrom, Z. Physik. Chem., B20 (1933) 283.
15 L. J. Saidel, A. R. Goldfarb, and S. Waldman, J. Biol. Chem., 197 (1952) 285.
16 H. Ley and B. Arends, Z. Physik. Chem., B17 (1932) 177.
17 Yu. P. Morozova and T. N. Kopylova, Izv. Vyssh. Uckebn. Zaved. Fiz., 16 (1973) 141.
18 A. Hantzsch and E. Scharf, Ber. Dtsch. Chem. Ges., 46 (1913) 3570.
19 H. Ley and B. Arends, Ber. Dtsch. Chem. Ges. B: 61 (1928) 212.
20 M. Grunfeld, Ann. Chim., 20 (1933) 304.
21 Yu. P. Morozova, in N. A. Prilezhaeva, (Ed.), Spektrosk. Tr. Sib. Soveshch., 4th edn., (Pub. 1969) Nauka, Moscow, USSR, 1965, p. 89.
22 I. I. Rusoff, J. R. Platt, H. B. Klevens, and G. O. Burr, J. Am. Chem. Soc., 67 (1945) 673.
23 P. J. Orenski, Ph.D. Thesis, Columbia University, New York (1967).
24 N. A. Izmailov and V. A. Kremer, Fak. Moskov. Gosudarst. Univ. Trudy Soveshchanija, Moscow 1958 (1959) 22.
25 G. A. Anslow, M. L. Foster, and C. Klingler, J. Biol. Chem., 103 (1933) 81.

26 E. Abderhalden and E. Rossner, Z. Physiol. Chem., 176 (1928) 249.
27 A. Castille and M. E. Ruppol, Bull. Acad. Roy. Med. Belg., 6 (1926) 263.
28 R. B. Setlow and W. R. Guild, Arch. Biochem. Biophys., 34 (1951) 223.
29 E. Abderhalden and E. Rossner, Z. Physiol. Chem., 178 (1928) 156.
30 B. Miličević and S. Dj. Janković, Glas. Hem. Drus., 22 (1957) 363.
31 J. Bielecki and V. Henri, Ber. Dtsch. Chem. Ges, 46 (1913) 1304.
32 P. Borrel, Nature, 184, Suppl. No. 25 (1959) 1932.
33 M. Kobayashi and K. Nakamoto, J. Chem. Soc. Jpn, Pure Chem. Sect. 70 (1949) 243.
34 H. Ley and H. Hünecke, Ber. Dtsch. Chem. Ges. B: 59 (1926) 510.
35 F. Leuthardt and M. Pfister, Helv. Chim. Acta, 16 (1933) 228.
36 G. Bruhat and R. Legris, Compt. Rend., 189 (1929) 745.
37 G. Bruhat and J. Terrien, Compt. Rend., 191 (1930) 37.
38 G. Bruhat and J. Terrien, Compt. Rend., 191 (1930) 125.
39 G. Bruhat, Compt. Rend., 192 (1931) 489.
40 G. Bruhat, Trans. Faraday Soc., 26 (1930) 400.
41 H. Ley and B. Arends, Z. Phys. Chem. Abt. B, 17 (1932) 177.
42 L. I. Katzin and E. Gulyas, J. Am. Chem. Soc., 90 (1968) 247.
43 J. Schurz, D. Kaempgen, M. Schlor, and K. Windisch, Papier, 17 (1963) 556
44 H. R. Wright, J. Chem. Soc., 105 (1914) 669.
45 R. P. Buck, S. Singhadeja, and L. B. Rogers, Anal. Chem., 26 (1954) 1240.
46 S. Hoshino, H. Hosoya, and S. Nagakura, Can. J. Chem., 44 (1966) 1961.
47 I. T. Edward and I. C. Wang, Can. J. Chem., 40 (1962) 966.
48 P. Zuman and W. Szafranski, Angew. Chem., in print.
49 A. Albert and E. P. Serjeant, The Determination of Ionization Constants, Chapman and Hall, London, 1971.
50 A. W. Martin and H. V. Tartar, J. Am. Chem. Soc., 59 (1937) 2672.
51 G. D. Pinching and R. G. Bates, J. Res. Natl. Bur. Stand., 40 (1948) 405.
52 R. G. Bates and R. G. Canham, J. Res. Natl. Bur. Stand., 47 (1951) 343.
53 L. J. Minnick and M. Kilpatrick, J. Phys. Chem., 43 (1939) 259.
54 M. v. Halban and R. Klockmann, Z. Phys. Chem., Abt. A: 157 (1931) 209.
55 A. L. Henne and C. J. Fox, J. Am. Chem. Soc., 73 (1951) 2325.

Analytica Chimica Acta, 85 (1976) 375—381

STABILITY OF FLAVONOID COMPLEXES OF COPPER(II) AND FLAVONOID ANTIOXIDANT ACTIVITY

M. THOMPSON* and C. R. WILLIAMS

Department of Chemistry, University of Technology, Loughborough LE11 3TU (England)

G. E. P. ELLIOT

Department of Physical Sciences, The Trent Polytechnic, Nottingham (England)

(Received 3rd March 1976)

SUMMARY

Certain flavonoids inhibit the oxidation of ascorbic acid; this behaviour has been attributed to the ability of flavonoids to act as free radical acceptors and also to remove catalytic metal ions by complexation. To place the latter property on a quantitative footing, protonation constants and copper(II) chelate formation constants of several flavonoids have been determined by potentiometric titration and computation by the program SCOGS. The constants are discussed in terms of previous studies of antioxidant activity.

The vitamin L-ascorbic acid is relatively stable in acid solution but is oxidized rapidly to dehydroascorbic acid in neutral or alkaline solution in the presence of oxygen. The aerobic oxidation is catalyzed by copper(II) ions and thought to proceed through a free radical mechanism [1, 2]. Khan and Martell [3] proposed that the reaction involves an unstable copper—ascorbic acid—oxygen complex which decomposes to copper(I), dehydroascorbic acid and an oxygen free radical.

The ability of flavonoids to inhibit the oxidation has long been recognized [4], and is known to be important in the protection of ascorbic acid present in natural fruit juices [5, 6]. Also, antioxidant protection of flavonoids may be significant in the alkaline medium of the jejenum of normal individuals and in patients suffering from achlorhydria [7]. The mechanism of the protective effect has been the subject of debate for some time. Davidek [8] studied the antioxidant activity of several flavonoid glycosides in aqueous solution with and without the presence of copper(II) ions. No activity was found in the absence of metal ions. Furthermore, in view of the increasing antioxidant effect with pH in the presence of copper(II), it was suggested that abolishment of the catalytic effect of the metal through chelation with flavonoid is the major mechanism. Clemetson and Andersen [7] came to a

*Present address: Department of Chemistry, University of Toronto, 80 St. George Street, Toronto M5S 1A1, Canada.

similar conclusion from an extensive study at neutral pH. However, other workers [9—13] have suggested that the primary inhibitory effect is associated with the ability of flavonoids to act as free radical trapping agents.

Much of the previous discussion has involved comments which are based on seriously inadequate experiments involving the copper(II)-complexing ability of flavonoids. In the present paper the stabilities of copper(II) complexes are measured and related to previous work.

EXPERIMENTAL

Reagents

The flavonoids listed in Table 1 were obtained from commercial sources. Their purity was checked by paper chromatography according to the appropriate standard procedure [14]. A copper(II) solution (0.10 M) was prepared from copper(II) perchlorate hexahydrate and standardized against EDTA and sodium thiosulphate. 1,4-Dioxane was purified by refluxing over sodium for 24 h followed by fractional distillation. The hydrogen ion concentration of an 0.01 M solution of perchloric acid which contained sodium perchlorate (0.21 M) was determined titrimetrically with standard sodium hydroxide.

Apparatus

The potentiometric titration apparatus consisted of a Corning-E.E.L. Model 110 pH meter fitted with glass and calomel electrodes, titration cell, burettes, and constant-temperature water bath. The system was protected from carbon dioxide with soda-lime guard tubes.

Proton magnetic resonance

The p.m.r. spectra of the flavonoids were recorded, at the same molar concentration in a mixture of $CDCl_3$ and dimethylsulphoxide-d_6 as solvent, with a Perkin-Elmer R32 spectrometer. The reference standard was TMS.

Procedure

The potentiometric titration of the flavonoids to obtain protonation constants, and with copper(II) to obtain formation constants, was carried out in the usual manner at ionic strength 0.1, temperature 25.0 ± 0.1 °C, a metal-to-ligand molar ratio of 1:5, and in 50 % (v/v) aqueous 1,4-dioxane. The Van Uitert and Haas parameter was 0.1 ± 0.01 and pK_w 15.27. The constants were calculated by means of a modified version of the program SCOGS [15—17] on an ICL 1904A computer. Protonation constants are given as log K. The overall metal—chelate stability constants are given either as log β_{pqn} for species $Cu_pH_qL_n$ (L = flavonoid anion) or as log β'_{pqn} for species in which undissociated hydroxyl groups are assumed for convenience in computation.

Precipitation of copper complexes during titration of 5-hydroxyflavone, techtochrysin, and chrysin prevented the calculation of log $\beta_{1,0,2}$ for these compounds. Values are not reported for 7-hydroxyflavone because of insuf-

TABLE 1

Summarized proton magnetic resonance spectra of flavonoids

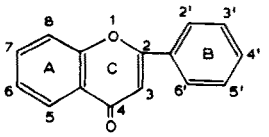

Flavonoid	Chemical shift (p.p.m.)					
	H_3	H_5	H_6	H_7	H_8	B-ring
Techtochrysin[a] (5-OH, 7-OMe flavone)	6.78	—	6.37	—	6.62	7.5—7.7 H_2', H_4', H_6', 7.8—8.1 H_3', H_5',
Chrysin (5,7-di OH flavone)	6.72	—	6.28	—	6.49	7.5—7.7 H_2', H_4', H_6', 7.8—8.1 H_3', H_5',
Apigenin (5,7,4'-tri OH flavone)	6.58	—	6.23	—	6.46	6.95 H_3', H_5', 7.81 H_2', H_6',
Quercetin (3,4,7,3',4'-penta OH flavone)	—	—	6.21	—	6.44	6.94 H_5', 7.63 H_6', 7.78 H_2',
5-OH flavone	6.85	—	(6.7—7.2)			7.5—7.7 H_2', H_4', H_6', 7.9—8.1 H_3', H_5',
7-OH flavone	6.73	(6.7—7.1 without H_7)				7.5—7.7 H_2', H_4', H_6', 7.9—8.1 H_3', H_5',
3-OH flavone	7.3—7.8 H_6, H_7, H_8, H_2', H_4', H_6', 8.1—8.4 H_5, H_3', H_5',					

[a]Methoxy CH_3 at 3.92 p.p.m.

ficient chelation. Also, values are not given for quercetin constants since the decomposition of the molecule at approximately pH 9 prevented the computation of the necessary protonation constants.

RESULTS AND DISCUSSION

P.m.r. and protonation constants

Although the flavonoids appear to have been well-characterized by p.m.r., previous studies have generally involved TMS ethers and various solvents because of solubility problems [14]. The results of the present work on the parent molecules in the same solvent are given in Table 1. The protonation constants reported in Table 2 can be correlated with the p.m.r. results in

TABLE 2

Protonation constants of flavonoids (25 °C, ionic strength 0.1 and 50 % (v/v) 1,4-dioxane)

Flavonoid	Log K	SCOGS σ	Proton
3-OH flavone	10.34	0.01	3-OH
5-OH flavone	11.44	0.01	5-OH
7-OH flavone	8.48	0.01	7-OH
Techtochrysin	11.79	0.01	5-OH
Chrysin	12.37	0.03	5-OH
	8.37	0.04	7-OH
Apigenin	13.14	0.02	5-OH
	8.54	0.03	7-OH
	9.93	0.03	4'-OH
Quercetin	8.46	0.02	7-OH

terms of the +M effect of the hydroxyl substituents (and methoxy group in the case of techtochrysin) in the A, B and C-rings of the molecules. For example, the increasing donation of electron density into the molecule as a whole in the series 5-hydroxyflavone, techtochrysin, chrysin, and apigenin results in increasing shielding of the H_3-proton (6.85—6.58 p.p.m.) and increase in basicity of the 5-hydroxyl protonation constants (11.44—13.14). Similar correlations are exhibited by the chemical shifts of the H_6- and H_8-protons.

The protonation constant of 7-hydroxyflavone is significantly lower than that of the 3- and 5-monohydroxylated flavones. The higher values of the latter may be explained in terms of the stabilization of the protonated structure by intramolecular hydrogen bonding through interaction of the 3- and 5-hydroxyl protons with the keto group [18]. The decrease in shielding of the H_3 proton in the 5-hydroxy derivative (6.85 p.p.m.) relative to that in the 7-substituted compound (6.72 p.p.m.) is consistent with this argument. Furthermore, the higher value of the 5-hydroxyl protonation constant compared with that for the 3-substituted compound is consistent with the suggested greater strength of the hydrogen bond in the former [18].

Stability constants and antioxidant activity

Chelate stability constants of several copper(II) complexes of flavonoids are reproduced in Table 3. Titration curves associated with these data (not shown) indicate, with the sole exception of quercetin, that chelation occurs only to a minor extent (e.g. $\alpha_{CuH_qL} < 0.1$ and Fig. 1) at pH values of 2—3. Thus, these results support the argument of Clegg and Morton [11] who pointed out that the antioxidant effect at the low pH conditions found in natural fruit juices is likely to be of a free radical trapping nature especially in view of the presence of relatively high concentrations of sequestering natural acids. However, the situation may be different in near neutral or alkaline media where metal—flavonoid complexation does occur as suggested by Davidek [8] and Letan [9].

TABLE 3

Stability constants of copper(II) complexes of flavonoids (25 °C, ionic strength 0.1, 50 % 1,4-dioxane)

Flavonoid	Stability Constant		SCOGS σ
3-OH flavone	9.03	$\beta_{1,0,1}$	0.02
	17.49	$\beta_{1,0,2}$	0.07
5-OH flavone	9.21	$\beta_{1,0,1}$	0.03
7-OH flavone	Insufficient chelation for determination		
Techtochrysin	9.83	$\beta_{1,0,1}$	0.08
Chrysin	10.64	$\beta'_{1,0,1}$ [a]	0.06
Apigenin	11.39	$\beta'_{1,0,1}$ [b]	0.06
	21.44	$\beta'_{1,0,2}$	0.11
	29.86	$\beta_{1,2,1}$	0.06
	58.38	$\beta_{1,4,2}$	0.11

[a] Equilibrium at 7-OH ignored.
[b] Equilibrium at 7-OH and 4′-OH ignored.

As expected, the $\beta_{1,0,1}$ or $\beta'_{1,0,1}$ constants for the complexes of the series 5-hydroxyflavone, techtochrysin, chrysin, and apigenin increase linearly with log K for the 5-hydroxyl group in the compounds. On the basis of an estimated protonation constant for 5-hydroxyl in quercetin, a value of $\beta'_{1,0,1} \approx 12$ can be calculated for the quercetin—copper complex. Therefore, of the compounds investigated this ligand forms the most stable chelate with copper(II). The constants of the 1:1 chelates of the 3- and 5-hydroxyflavones are in the reverse order of the protonation constants. The slightly higher constant for the latter is probably associated with the stability of the six-membered chelate ring over that of the five-membered ring. In the light of the values it is surprising that Letan [10] from antioxidant behaviour and Harper et al. [13] considered the 3-hydroxy-4-keto system to form "stronger" complexes with copper(II) than the 5-hydroxy-4-keto grouping. Undoubtedly stability has been confused with degree of complexing of copper which is, of course, related to ligand basicity. Clearly, on considering the metal complexing mechanism of antioxidant behaviour the degree of complexation under the same ligand concentration conditions should be compared with activity.

Probably the most useful comparisons of activity versus complexation can be made with Clemetson and Andersen's work [7], although, unfortunately, in their experiments suspensions of flavonoids were used where the concentrations of ligand varied according to solubility. The results apparently suggest that the 3-hydroxy-4-keto coupling is a prerequisite for activity and for high antioxidant behaviour an additional 3′,4′-dihydroxy system in the B-ring, such as is present in quercetin, is important. Certainly, the potent activity of quercetin can be associated at least in part with the large degree of complexation exhibited by the molecule. Moreover, the more modest activity of both the 3-hydroxy-4-keto and 5-hydroxy-4-keto systems of such derivatives as

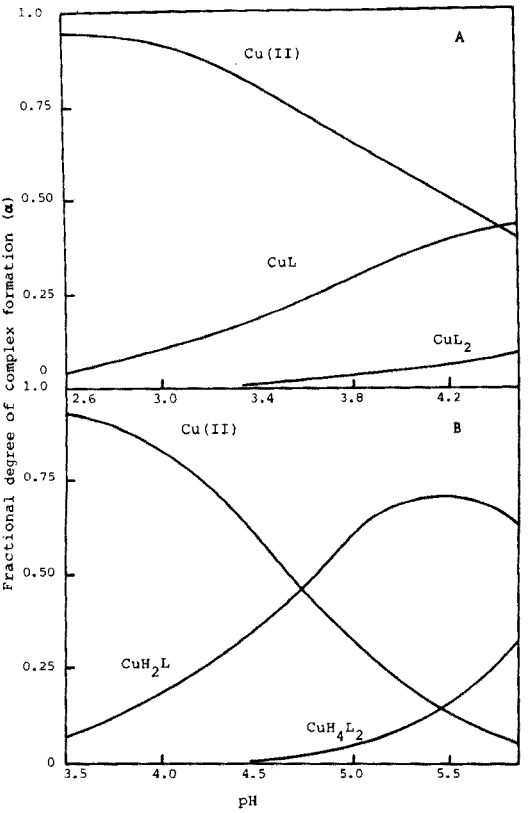

Fig. 1. Degree of formation (α) of copper(II) complexes of 3-hydroxyflavone (A) and apigenin (B) as a function of pH.

3-hydroxyflavone and apigenin correlates with the complexation behaviour of these ligands (Fig. 1). Therefore, it appears that the former system has no particular virtue over the latter as indicated by the present work.

Many in vivo experiments (see ref. 7) have confirmed the protection of ascorbic acid by flavonoids. The mechanism of the behaviour may be influenced by the pH (6.5—7.6) [19] of the contents of the lower intestine. Under such conditions, the bioflavonoids, although only a small fraction of the diet, could protect ascorbic acid by complexation of catalytic metal ions such as copper(II). There will be other competing ligands, viz. the sulphydryl groups of some amino acids, nevertheless because of the relatively high stability of some flavonoid complexes, it seems that the compounds could minimize the loss of dietary ascorbic acid by acting as antioxidants.

We wish to thank The Trent Polytechnic, Nottingham, for financial support (to C. R. W.). Helpful discussion with Professor W. F. Reynolds of the University of Toronto concerning the p.m.r. results is gratefully acknowledged.

REFERENCES

1 N. G. Levandoski, E. M. Baker and J. E. Canham, Biochemistry, 3 (1964) 1465.
2 C. Lagercrantz, Acta Chem. Scand., 18 (1964) 562.
3 M. Khan and A. E. Martell, J. Am. Chem. Soc., 89 (1967) 4176.
4 G. G. Kelley and B. M. Watts, Food Res., 22 (1957) 308.
5 A. D. Morton, J. Food Technol., 3 (1968) 269.
6 A. J. Shrikhande and F. J. Francis, J. Food Sci., 39 (1974) 904.
7 C. A. B. Clemetson and L. Andersen, Ann. Rev. N.Y. Acad. Sci., 136 (1966) 339.
8 I. Davidek, Biokhimiya, 25 (1960) 1105.
9 A. Letan, J. Food Sci., 31 (1966) 395.
10 A. Letan, J. Food Sci., 31 (1966) 518.
11 K. M. Clegg and A. D. Morton, J. Food Technol., 3 (1968) 277.
12 K. A. Harper, A. D. Morton and E. J. Rolfe, J. Food Technol., 4 (1969) 255.
13 K. A. Harper, J. Food Technol., 4 (1969) 405.
14 T. J. Mabry, K. R. Markham and M. B. Thomas, The Systematic Identification of Flavonoids, Springer-Verlag, New York, 1970.
15 I. G. Sayce, Talanta, 15 (1968) 1397.
16 I. G. Sayce, Talanta, 18 (1971) 653.
17 I. G. Sayce and V. S. Sharma, Talanta, 19 (1972) 831.
18 T. H. Simpson and L. Gardner, J. Chem. Soc., (1952) 4638.
19 G. H. Bell, J. N. Davidson and E. Emslie-Smith, Textbook of Physiology and Biochemistry, Churchill Livingstone, Edinburgh, 1972, p. 291.

Analytica Chimica Acta, 85 (1976) 383—391

SOLVENT EFFECTS IN THE DISTRIBUTION OF BENZOYLACETONE BETWEEN APOLAR SOLVENTS AND WATER

Y. YOSHIMURA and N. SUZUKI*

Department of Chemistry, Faculty of Science, Tohoku University, Sendai (Japan)

(Received 12th December 1975)

SUMMARY

The distribution coefficients of benzoylacetone between aqueous 0.001 M hydrochloric acid and eight apolar solvents have been determined at 25 °C. The distribution coefficients into n-hexane, cyclohexane, carbon tetrachloride, benzene, chlorobenzene, ethylene chloride, methylene chloride and chloroform were 96.4, 128.6, 546.7, 1070, 1336, 1824, 2998 and 4711, respectively. A linear correlation was observed between the free energy change associated with the distribution of keto or enol tautomer of benzoylacetone and the solvent property, $(\epsilon - 1)/V(2\epsilon + 1)$, involving the dielectric constant ϵ and the molar volume V of the solvent.

Because β-diketones are useful chelating agents in liquid—liquid extraction systems, the extractability of a number of metal ions from aqueous solutions has been studied. Acetylacetone and thenoyltrifluoroacetone have been widely used; although benzoylacetone has been used for the extraction of metals [1] few studies of the distribution of benzoylacetone itself have been reported. Generally, β-diketones are capable of exhibiting keto—enol tautomerism in a given system; this has been studied by n.m.r., i.r., u.v., and other spectroscopic measurements. Lintvedt and Holtzclaw [2] reported a correlation between the formation constants of metal β-diketonates and the stability of the enol tautomer of β-diketones. Celiano [3] investigated the kinetics of reactions between copper(II) and β-diketones in methanol; the rate of first complex formation decreased with increasing stability of the enol tautomer of the β-diketones. The stability of the enol tautomer of β-diketones is therefore important; although a little attention has been given to the keto—enol tautomerization in a distribution system involving β-diketones, the rôle of the solvent has been less thoroughly studied [4, 5]. To clarify the distribution behavior of β-diketones, the distribution coefficients of each tautomer must be determined. The purpose of the present study was to determine the distribution coefficients of each tautomer of benzoylacetone between non-polar solvents and water, and to discuss the effect of solvents on the distribution of each tautomer.

*To whom correspondence should be addressed.

EXPERIMENTAL

Materials

Reagent-grade benzoylacetone, purified by recrystallization three times from methanol, and dried in vacuo, gave m.p. 57.8—58.5 °C, and its i.r. and n.m.r. spectra in carbon tetrachloride agreed well with those reported [6, 7].

Organic solvents (reagent grade) were purified, dried [8], and distilled. No impurities were detected by gas chromatography. Redistilled water was used, and all other materials were reagent grade.

Determination of molar absorptivity of benzoylacetone

Because benzoylacetone has low solubility in water, three replicate measurements were performed to minimize experimental error. The aqueous stock solution of benzoylacetone (ca. $6.0 \cdot 10^{-4}$ M) was prepared just before use by accurate weighing. In each run, the concentration of benzoylacetone in sample solutions ranged from 2 to $12 \cdot 10^{-5}$ M by diluting the stock solution, and the concentration of hydrochloric acid was brought to 0.001 M. The absorbance of the enol tautomer [9] at 310 nm was measured at 25 ± 0.1 °C with a Hitachi 356 spectrophotometer. The absorbances obeyed Beer's law in each run, and least-squares analysis was applied to obtain the molar absorptivity. The results from three separate determinations agreed satisfactorily within a relative range of 1 %. The molar absorptivity of benzoylacetone at 310 nm was 5150 ± 23 l $mole^{-1}$ cm^{-1}.

Determination of the distribution ratio of benzoylacetone

The distribution ratios were obtained with the apparatus shown in Fig. 1,

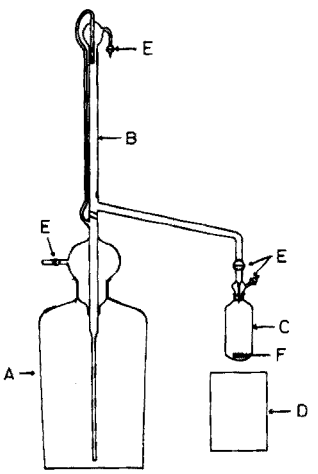

Fig. 1. Apparatus for determination of distribution ratio. A Bottle, about 500-ml capacity. B 10-ml buret. C Centrifuge tube, about 30-ml capacity. D Magnetic stirrer. E Teflon stop-cock.

designed to minimize the error associated with the vaporization of volatile solvents during the experiment. A centrifuge tube with a volume of about 30 ml (C) was connected directly to a buret (B). A known amount of benzoylacetone was placed in a 250-ml volumetric flask, and an organic solvent was added to the mark. This solution was kept at about 5 °C to minimize vaporization. Immediately after the transfer of this solution to the bottle (A), the buret (B) was connected. The apparatus, covered with a black cloth to exclude light, was allowed to stand for about 24 h at 25 ± 0.3 °C. Then the buret was fitted with the centrifuge tube containing 10 ml of 0.001 M hydrochloric acid, and 10 ml of the organic solution of benzoylacetone, added to the aqueous phase from the buret, was equilibrated by magnetic stirring. With all the solvents, distribution equilibrium was attained within 1—2 h. To minimize the error from the volume change arising from the mutual solubility, the organic and aqueous phases were pre-saturated with each other before the organic solution of benzoylacetone was prepared. The centrifuge tube was then removed from the buret and stoppered. After the two phases had been separated with a centrifuge, a portion of the aqueous phase was transferred to an absorption cell and the absorbance at 310 nm was measured against a reference blank. The aqueous phase was diluted, if necessary. The equilibrium concentration of benzoylacetone in the aqueous phase was calculated from the molar absorptivity, and the distribution ratio, D, was given by

$$D = (C^{o}_{org} - C_{aq})/C_{aq} \quad (1)$$

where C^{o}_{org} and C_{aq} denote the initial concentration of benzoylacetone in the organic phase and its equilibrium concentration in the aqueous phase, respectively. To check the reproducibility of this procedure, ten determinations of the distribution ratio of benzoylacetone between benzene and water were performed; the relative deviation from the mean did not exceed 2 %. The distribution ratios of benzoylacetone for other organic aqueous systems were obtained as the average of five separate determinations.

Determination of the keto—enol tautomerism constant of benzoylacetone in organic solvents

To determine the keto—enol tautomerism constant (defined as the ratio of the concentrations of the keto and enol tautomers), the n.m.r. spectrum of benzoylacetone was measured at 30 ± 1 °C with a JEOL JNM PS-100 spectrometer in a pure organic solvent and in that organic phase equilibrated with the aqueous phase. The concentration of benzoylacetone ranged from 0.1 to 0.2 M in each case. The tautomerism constant was determined as the ratio of the signal area of the methyl type protons of the keto tautomer to that of the enol tautomer.

RESULTS AND DISCUSSION

A preliminary experiment showed the distribution ratios of benzoylacetone between various organic solvents and water to depend on the concentration and nature of the electrolyte (hydrochloric acid, sodium chloride, perchloric acid and sodium perchlorate) in the aqueous phases. When the concentration of these electrolytes was limited to 0.001 M, however, the distribution ratios were independent of the electrolyte. Hence, distribution ratios were measured between organic and aqueous 0.001 M hydrochloric acid phases. The effect of the electrolytes on the distribution will be discussed elsewhere.

Figure 2 shows the influence of the initial concentration of benzoylacetone on the distribution ratio. Because of the experimental limitation resulting from the very high distribution ratio of benzoylacetone and the spectrometrically measurable concentration limit, this influence could not be studied over a wide range of benzoylacetone concentration. Figure 2 shows that, within the concentration range studied, the distribution ratios were approximately constant for all the solvents except chloroform. The distribution ratios obtained are shown in Table 1 along with the literature data available. The differences between the present results and the literature values [10, 11] shown in Table 1 may be ascribed to differences in the experimental conditions such as ionic strength and temperature etc., and also in the purities of the materials.

TABLE 1

Distribution ratio of benzoylacetone in apolar solvent—aqueous 0.001 M hydrochloric acid systems and the tautomerism constant (k_{org}) in the organic phase

No.	Solvent	ϵ[a]	V_{org}[a] (ml mol^{-1})	C^o_{org} (M)	D (at 25 °C)[b]	log D[c]	k_{org} X (at 30
1	n-Hexane	1.8799	131.6	0.01	96.4 ± 0.4	1.984 ± 0.002 (2.03)	0
2	Cyclohexane	2.023[d]	108.7	0.01	128.6 ± 0.9	2.109 ± 0.003	0
3	Carbon tetrachloride	2.238[d]	97.1	0.05	546.7 ± 4.5 (661)	2.737 ± 0.003 (2.81)	2.4 ±
4	Benzene	2.275	89.4	0.07	1070 ± 12 (1395)	3.029 ± 0.005 (3.02)	6.8 ±
5	Chloroform	4.806[d]	80.7	0.2	4711 ± 54 (4003)	3.673 ± 0.005 (3.64)	9.8 ±
6	Chlorobenzene	5.621	101.7[d]	0.1	1336 ± 15	3.126 ± 0.005	4.7 ±
7	Methylene chloride	8.93	64.5	0.2	2998 ± 32	3.477 ± 0.005	12.1 ±
8	Ethylene chloride	10.36	79.4	0.2	1824 ± 13	3.261 ± 0.003	11.2 ±

[a] Dielectric constant (ϵ) and molar volume (V_{org}) of solvent at 25 °C [8].
[b] Literature values [10] are given in parentheses.
[c] Literature values [11] are given in parentheses
[d] Value at 20 °C.

Table 1 also includes the tautomerism constants of benzoylacetone in organic phases equilibrated with the aqueous phase, k_{org}, and some physical properties which are of use in the discussion below.

Because of its small apparent acid dissociation constant (pK_a 8.69 [12]), the dissociation of benzoylacetone is negligible in aqueous 0.001 M hydrochloric acid. Thus the distribution ratio of benzoylacetone is given by

$$D = \{(C_e)_{org} + (C_k)_{org}\}/\{(C_e)_{aq} + (C_k)_{aq}\} \quad (2)$$

where C denotes molar concentration, and the subscripts e, k, org and aq refer to the enol tautomer, keto tautomer, organic phase, and aqueous phase, respectively. The distribution coefficient of the enol tautomer, P'_e, and that of the keto tautomer, P'_k, (each defined as the ratio of the molar concentrations of the species in two phases) can be calculated by the following equations, derived from eqn. (2).

$$P'_e = (C_e)_{org}/(C_e)_{aq} = D(1 + k_{aq})/(1 + k_{org}) \quad (3)$$

$$P'_k = (C_k)_{org}/(C_k)_{aq} = D\{k_{org}(1 + k_{aq})\}/\{k_{aq}(1 + k_{org})\} \quad (4)$$

In eqns. (3) and (4), k indicates the keto—enol tautomerism constant of benzoylacetone defined as $k = C_k/C_e$. The value 1.94 [13, 14] was used for k_{aq}. Although the thermodynamic distribution coefficient must be defined as the ratio of the activities of the species distributed between two phases, the observed distribution ratios are independent of the concentration of benzoylacetone within certain limits (cf. Fig. 2), and so the ratio of the molar concentrations may be used instead of the activity ratio.

Powling and Bernstein [15] estimated a difference in the internal energy, E, of a species A between the gas state and a dilute solution in apolar solvents by

$$E_{A(gas)} = E_{A(soln)} - \delta E \quad (5)$$

where δE, the electrostatic interaction energy between A and the solvent, is given by

$$\delta E = -\{(\epsilon - 1)/V(2\epsilon + 1)\}_{solvent} \times \mu_A^2 \quad (6)$$

where ϵ and V denote the dielectric constant and molar volume of the solvents, respectively, and μ_A is the dipole moment of species A. Assuming that the enthalpy change, ΔH, is approximately equal to ΔE, the change in the heats of tautomerization of acetylacetone in apolar solvents, $\Delta H_{T(soln)}$, may be represented by the equation [16].

$$\Delta H_{T(soln)} = E_{k(soln)} - E_{e(soln)} = \Delta H_{T(gas)} - \{(\epsilon - 1)/V(2\epsilon + 1)\}_{solvent} \times (\mu_k^2 - \mu_e^2) \quad (7)$$

On the assumption that the entropy change, ΔS, is a linear function of ΔH,

the above treatment was extended to the free energy change accompanying tautomerization, ΔG_T, and the distribution between apolar solvents and water, ΔG_D, of benzoylacetone. The following equations were obtained.

$$\Delta G_{T(\text{soln})} = \Delta G_{T(\text{gas})} - \{(\epsilon - 1)/V(2\epsilon + 1)\}_{\text{solvent}} \times (\mu_k^2 - \mu_e^2)(1 - \alpha_1) \quad (8)$$

$$\Delta G_{D,e} = -\{(\epsilon - 1)/V(2\epsilon + 1)\}_{\text{solvent}} \times \mu_e^2 (1 - \alpha_2) + W_1 \quad (9)$$

$$\Delta G_{D,k} = -\{(\epsilon - 1)/V(2\epsilon + 1)\}_{\text{solvent}} \times \mu_k^2 (1 - \alpha_3) + W_2 \quad (10)$$

where α_1, α_2 and α_3 are proportional constants between ΔS and ΔH accompanying each process, and W_1 and W_2 are terms representing interaction energies between each of the tautomers of benzoylacetone and water, respectively. ΔG_T and ΔG_D were calculated from the equations

$$-\Delta G_T = RT \ln k_{\text{org}} \quad (11)$$

$$-\Delta G_D = RT \ln P \quad (12)$$

In eqn. (12), P denotes the thermodynamic distribution coefficient defined as the ratio of the mole fractions and, in dilute solutions, is related [17] to the distribution coefficient in terms of molarity by

$$P = P' \times V_{\text{solvent}}/V_{\text{water}} \quad (13)$$

Figure 3 shows a plot of the free energy change of tautomerism, ΔG_T, against the solvent property, $(\epsilon - 1)/V(2\epsilon + 1)$; the value of ΔG_T in both the pure solvents and the organic phases equilibrated with the aqueous phase agreed approximately with each other. For n-hexane and cyclohexane, the tautomerism constants of benzoylacetone could not be determined by n.m.r. spectroscopy. In accordance with eqn. (8), the linear relationship between ΔG_T and this solvent property held, except for benzene and chloroform. Therefore, it can be concluded that the change in the keto–enol tautomeric equilibrium of benzoylacetone may also be accounted for by a difference in the electrostatic interaction energies of each tautomer with its surrounding medium. For $\Delta G_{T(\text{gas})}$, a value of 2.67 ± 0.03 was obtained from the intercept on the ΔG_T axis in Fig. 3 by least-squares analysis. This value corresponds to an enol content of about 99 % in the gaseous state.

Figures 4(a) and (b) show plots of the free energy change accompanying the distribution of each tautomer, $\Delta G_{D,e}$ and $\Delta G_{D,k}$, against the solvent property, $(\epsilon - 1)/V(2\epsilon + 1)$. The relationships expressed by eqns. (9) and (10) held approximately. For n-hexane and cyclohexane, the distribution coefficients of the keto tautomer could not be calculated by eqn. (4) because the accurate determination of very small tautomerism constants is difficult in these solvents. In the calculation of the distribution coefficients of the enol

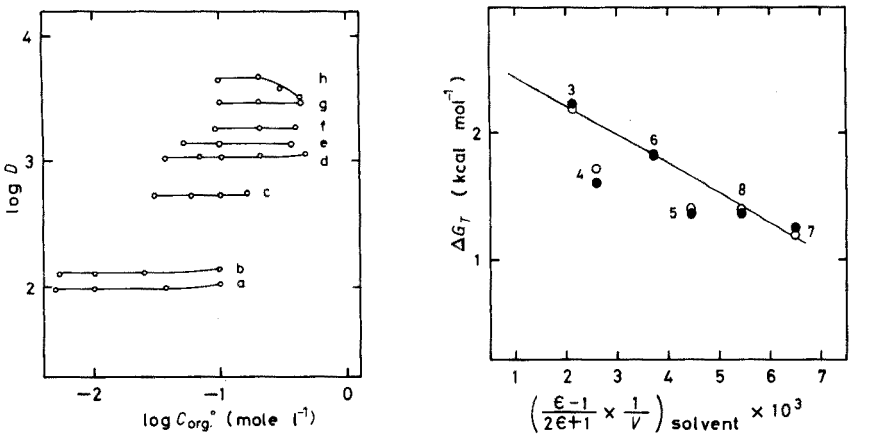

Fig. 2. Influence of the initial concentration of benzoylacetone in the organic phase (C^{o}_{org}) on the distribution ratio (D). (a) n-hexane, (b) cyclohexane, (c) carbon tetrachloride, (d) benzene, (e) chlorobenzene, (f) ethylene chloride, (g) methylene chloride, (h) chloroform. Aqueous phase: 0.001 M HCl.

Fig. 3. Plot of free-energy change accompanying tautomerization (ΔG_T) vs. the solvent property, $(\epsilon - 1)/V(2\epsilon + 1)$. ○ In pure solvent. ● In organic phase equilibrated with aqueous 0.001 M HCl. See Table 1 for key to the numbers.

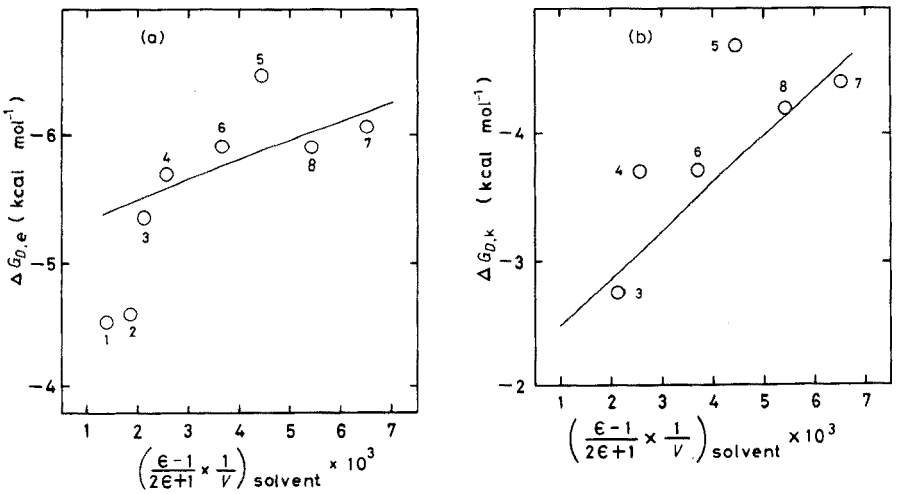

Fig. 4. Plot of free-energy change accompanying distribution of the benzoylacetone tautomer between organic solvent and aqueous 0.001 M HCl solution: $\Delta G_{D,e}$ or $\Delta G_{D,k}$ vs. the solvent property, $(\epsilon - 1)/V(2\epsilon + 1)$. (a) Enol tautomer. (b) Keto tautomer. See Table 1 for key to the numbers.

tautomer by eqn. (3) for these solvents, however, the uncertainty in very small tautomerism constants is not a serious source of error. The deviations for n-hexane and cyclohexane from the line in Fig. 4(a) do not appear to be an experimental error but may imply that the electrostatic interaction is not the predominant mode of interaction of benzoylacetone with these solvents. As expressed by eqns. (9) and (10), the slopes of the straight-line plots of ΔG_D vs. the solvent property, $(\epsilon - 1)/V(2\epsilon + 1)$, for each tautomer must give some measure of the dipole moments of each of the two tautomers. From the slopes of the lines in Fig. 4, the keto tautomer apparently has a higher dipole moment than the enol tautomer, but the values of the dipole moments cannot be estimated because α_2 and α_3 are not known. The enol tautomer has an intramolecular hydrogen-bonded ring structure and the electrons in this ring are delocalized [18], while the keto tautomer has two polar carbonyl groups and acts almost as a purely ketonic compound. Accordingly, it appears reasonable to assume that the keto tautomer will have a higher dipole moment than the enol tautomer.

Figure 5 shows plots of the distribution coefficient, $\log P$, against tautomerism constant, $\log k_{org}$, for both the tautomers of benzoylacetone. This simple correlation shows that a solvent with a large tautomerism constant favors the keto tautomer content in this system. Since a higher content of the keto tautomer in a given solvent can be related to stronger electrostatic interaction between the keto tautomer and the solvent molecules, this solvent will give a higher distribution coefficient for the keto tautomer. Thus, the distribution coefficient of the keto tautomer increases with an increase in the

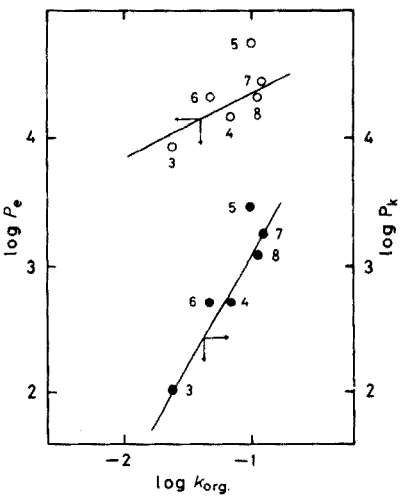

Fig. 5. Correlations between the distribution coefficients of keto (P_k) and enol tautomers (P_e) of benzoylacetone and tautomerism constant in the organic phase (k_{org}). ○ Enol tautomer. • Keto tautomer. See Table 1 for key to the numbers.

tautomerism constant. The correlation between the distribution coefficient of the enol tautomer and the tautomerism constant shown in Fig. 5 may also be explained as follows. As shown in Fig. 3, the tautomeric equilibrium in a solvent depends on the difference in the electrostatic interaction between each of two tautomers and the solvent molecules. Even with an increase in the solvent property, $(\epsilon - 1)/V(2\epsilon + 1)$, both the tautomers have increased energy of electrostatic interaction with the solvent molecule but the keto tautomer has much the higher interaction energy because of its higher dipole moment. Thus, the distribution coefficient of the enol tautomer also increases with an increase in the tautomerism constant.

As shown in Figs. 3—5, the experimental values for benzene and chloroform deviate from the lines. Kondo et al. [7] also found that the keto tautomer content was higher in benzene than that expected from its dielectric constant, and ascribed this discrepancy to the high polarizability of benzene. This consideration is not sufficient to explain the deviation, because the induction effect related to polarizability is taken into account in eqn. (6), but no immediate explanation is apparent. Johansson and Rydberg [19] investigated the temperature dependence of the distribution ratio of acetylacetone between chloroform and water and the chemical shift for the hydroxyl proton of the enol tautomer in chloroform; they concluded that the enol tautomer of acetylacetone interacts with chloroform by hydrogen bonding, but the n.m.r. spectrum obtained in this study for benzoylacetone in chloroform showed no distinct evidence of hydrogen bonding.

REFERENCES

1 J. Starý and E. Hladký, Anal. Chim. Acta, 28 (1963) 227.
2 R. L. Lintvedt and H. F. Holtzclaw, Jr., Inorg. Chem., 5 (1966) 239.
3 A. V. Celiano, J. Phys. Chem., 66 (1962) 1132.
4 N. Suzuki and K. Akiba, J. Inorg. Nucl. Chem., 33 (1971) 1169.
5 H. M. N. H. Irving, In Y. Marcus, (Ed.) Solvent Extraction Reviews, Vol. 2, M. Dekker, New York, 1972 p. 139.
6 S. Bratož, D. Hadži and G. Rossmy, Trans. Faraday Soc., 52 (1956) 464.
7 K. Kondo, Y. Kondo, T. Takemoto and T. Ikenoue, Kogyo Kagaku Zasshi, 68 (1965) 1404.
8 J. A. Riddick and W. B. Bunger, Techniques of Chemistry, Vol. VII, Organic Solvents, Wiley-Interscience, New York, 3rd edn., 1970.
9 R. A. Morton, A. Hassan and T. C. Calloway, J. Chem. Soc., (1934) 883.
10 J. Starý and N. P. Rudenko, Nauchn. Dokl. Vyssh. Shk. Khim. Teknol., (1958) 624, (Chem. Abstr., 53 (1959) 5828g).
11 T. Sekine, Y. Hasegawa and N. Ihara, J. Inorg. Nucl. Chem., 35 (1973) 3968.
12 M. L. Eidinoff, J. Am. Chem. Soc., 67 (1945) 2072.
13 M. L. Eidinoff, J. Am. Chem. Soc., 67 (1945) 2073.
14 M. Bergon and J. P. Calmon, Bull. Soc. Chim. Fr., (1972) 1020.
15 J. Powling and H. J. Bernstein, J. Am. Chem. Soc., 73 (1951) 1815.
16 J. Powling and H. J. Bernstein, J. Am. Chem. Soc., 73 (1951) 4353.
17 P. D. Cratin, Ind. Eng. Chem., 60 (1968) 14.
18 R. Grinter, J. Mol. Spectrosc., 17 (1965) 240.
19 H. Johansson and J. Rydberg, Acta Chem. Scand., 23 (1969) 2797.

Analytica Chimica Acta, 85 (1976) 393—397

LOSS OF IRIDIUM, OSMIUM AND RUTHENIUM FROM AQUEOUS SOLUTIONS DURING STORAGE

E. S. GLADNEY and K. E. APT

Los Alamos Scientific Laboratory, P.O. Box 1663, Los Alamos, New Mexico 87545 (U.S.A.)

(Received 16th December 1975)

SUMMARY

Aqueous solutions of iridium are stable (within 3 %) over a four-month storage period in a variety of container types and over a range of acid concentrations. Standard solutions of water-soluble iridium compounds at pH 7 can be employed reliably. Rapid loss of osmium and ruthenium from aqueous solutions at pH 7 means that standard solutions must be used within 1 day of preparation. Nitric acid solutions of osmium and ruthenium should also be avoided. The six plastics studied are unacceptable containers for 0.1 M hydrochloric acid solutions of osmium; 1 M hydrochloric acid is an adequate preservative for osmium solutions for up to two months and for ruthenium solutions for up to four months in glass, quartz or polyethylene containers.

The adoption of noble metal-based catalytic exhaust convertors for automobiles, and research involving noble organometallic compounds in cancer therapy [1, 2], has stimulated interest in the detection of trace quantities of noble metals in various media. Recent research at this laboratory into sensitive techniques for the measurement of noble metals in environmental materials has prompted the examination of the stability of aqueous noble metal solutions used as trace elemental standards. The loss of metallic species from aqueous solutions has been documented for cadmium [3, 4], lead [4, 5], mercury [6—8], zinc [4, 8], chromium [9], and selenium [10]. Solutions of gold and silver have been studied and serious losses [4, 11—14] have been observed under certain conditions. Limited information concerning the adsorption of ruthenium as a function of pH and container type has been reported [15, 16].

The present study was undertaken to determine the losses of iridium, osmium, and ruthenium from dilute aqueous solutions stored in various container types. The losses from solutions of different concentrations and pH were measured as a function of time; ^{192}Ir, ^{191}Os and ^{103}Ru were employed as tracers.

EXPERIMENTAL

The bottles used were of 500-ml capacity, with screw caps. Standard borosilicate glass and quartz bottles and six different plastic bottles (low-density polyethylene, high-density linear polyethylene, teflon, polyvinyl chloride, polypropylene, and polycarbonate) were investigated: the bottles were soaked for approximately 12 h in concentrated nitric acid and then rinsed with distilled water. Aliquots were taken with microliter pipets, and two-dram polyethylene vials were used for sample counting

The radiotracers were counted at a distance of 5 cm from a 55-cm^3 Ge(Li) detector (FWHM = 1.8 keV at 1332 keV) coupled with a linear amplifier and 4096-channel analyzer. A special constant-geometry counting system which provided counting reproducibilities of ±0.2 % was constructed. Samples were counted until a minimum of 10,000 counts in the γ-ray peak of interest was obtained.

Two different water-soluble forms of each element were employed: iridium tetrachloride, osmium trichloride, ruthenium trichloride, ammonium chloroiridate, ammonium chloro-osmate and ammonium chlororuthenite. The latter three compounds are non-hygroscopic standard materials commonly used in noble metal analysis [17, 18]. Analytical reagent-grade hydrochloric and nitric acids were used in solution preparations, and distilled water was employed for all dilutions. Radioactive ^{192}Ir, ^{191}Os and ^{103}Ru were produced by 3—8 h neutron bombardments of the six noble metal compounds at the Los Alamos Scientific Laboratory Omega West Reactor with a neutron flux of $7 \cdot 10^{12}$ n cm^{-2} s^{-1}.

Noble metal solutions were prepared from each of the six irradiated standards at two different concentrations (1000 μg ml^{-1} and 1 μg ml^{-1}) in distilled water, in 1 M nitric acid, and in four different concentrations of hydrochloric acid (0.1, 1.0, 3.0 and 6.0 M). Each solution (500 ml) was stored in glass, quartz, and low-density polyethylene containers at room temperature in a lighted area for up to four months. The other plastic containers mentioned above were studied for each tracer at the 1 μg ml^{-1} level in 0.1 M hydrochloric acid only. Counting aliquots of 1 ml were taken daily during the first week and at weekly intervals thereafter for four months, or, in the case of osmium, until the tracer became too weak to measure accurately (ca. 2 months).

RESULTS

Iridium

No measurable losses were observed in any of the iridium solutions during the four-month period of study.

Osmium

Osmium losses were not observed for solutions in which the hydrochloric acid concentration was at least 1 M. Glass and quartz containers gave

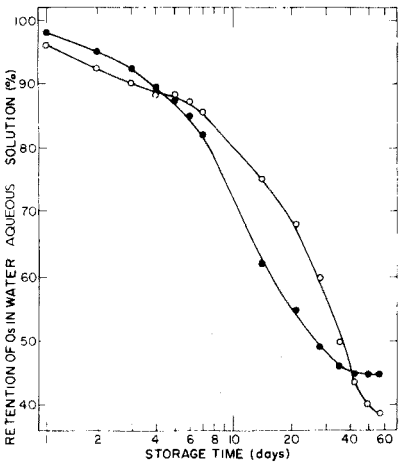

Fig. 1. Osmium loss from aqueous solutions (1 μg Os ml^{-1}) stored in glass (•) and polyethylene (○) containers.

satisfactory results for hydrochloric acid concentrations as low as 0.1 M. Adsorption from distilled water solutions was observed at both the 1000 μg ml^{-1} and 1 μg ml^{-1} levels for all containers. Typical loss rates are shown in Fig. 1. The loss curve for quartz (not shown) was similar to that for glass. As much as half of the total osmium was removed from solution during a period of two months, with most of this occurring during the first two weeks. The aqueous solutions appeared stable (within the accuracy of the γ-ray counting statistics) for only 1 d, with losses of up to 10 % by the end of 3 d. None of the plastics provided a suitable storage container for 0.1 M hydrochloric acid osmium solutions, as shown in Fig. 2 (A and B). Losses could not be detected during the first day, but 5 % changes occurred within 3 d, and losses as great as 20 % were evident over two months. All losses from

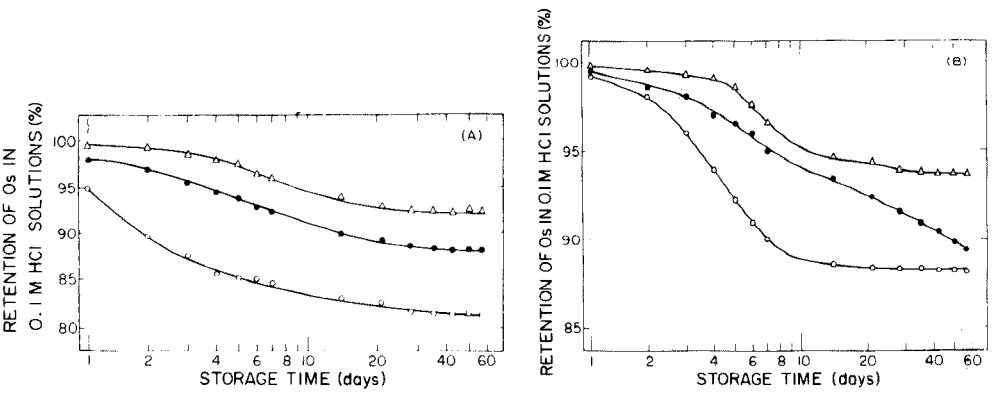

Fig. 2. Osmium loss from 0.1 M hydrochloric acid solutions (1 μg Os ml^{-1}) stored in (A) polycarbonate (△), linear polyethylene (•) and polyvinylchloride (○). (B) teflon (△), polypropylene (•) and low-density polyethylene (○).

hydrochloric acid and water solutions seemed to be due to adsorption only, since tracer activity could be detected only on container surfaces that had been in direct contact with the solutions.

The 1 M nitric acid solutions of osmium behaved somewhat differently (Fig. 3). Solutions contained in glass and quartz showed no statistically significant evidence for adsorption or volatilization of osmium. However, osmium losses from plastic containers were as high as 40 % from 1 M nitric acid, and tracer was detected on the lids of the containers as well as on the inside surfaces, suggesting that oxidation to the volatile tetroxide had occurred. Addition of hydrochloric acid retarded but did not prevent these losses (Fig. 3). The osmium concentration or compound used seemed to have little effect on preventing adsorption and volatilization.

Ruthenium

Adsorption of ruthenium was observed for distilled water solutions in glass and polyethylene (Fig. 4). The loss curve for quartz (not shown) is similar to that for glass. Up to 25 % loss of ruthenium from 1 M nitric acid over four months was also detected for the polyethylene container. No losses were detected in glass, quartz or polyethylene containers for the four hydrochloric acid concentrations studied nor for any of the plastic containers studied at 0.1 M hydrochloric acid. These observations are in general agreement with the 35 % adsorption at pH 7 reported for borosilicate glass [14]. Ruthenium loss to both glass and polycarbonate surfaces, with maximum loss at pH 4.5, was reported by Belloni et al. [15], but the percentage loss was not given; adsorption of ruthenium on polycarbonate in 0.1 M hydrochloric acid was not observed in the present study.

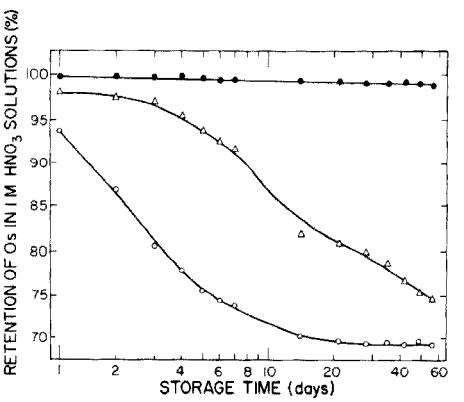

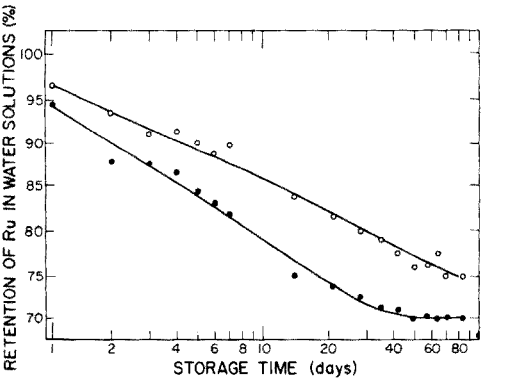

Fig. 3. Osmium loss from 1 M nitric acid solutions (1 μg Os ml^{-1}) stored in glass (•) and polyethylene (○), and from 3 M hydrochloric acid solutions stored in polyethylene (△).

Fig. 4. Ruthenium loss from aqueous solutions (1 μg Ru ml^{-1}) stored in glass (•) and polyethylene (○).

We thank James Gilmore, who provided the $OsCl_3$, and ths staff of the Omega West Reactor, who performed the irradiations. This work was supported by the U.S. Energy Research and Development Administration.

REFERENCES

1 B. Rosenberg, L. Van Camp, J. Trosko and V. Mansour, Nature (London), 222 (1969) 385.
2 A. Leroy, National Institute of Health, private communication, 1974.
3 W. G. King, J. M. Rodriguez and C. M. Wai, Anal. Chem., 46 (1974) 771.
4 A. W. Stuempler, Anal. Chem., 45 (1973) 2251.
5 H. J. Issaq and W. L. Zielinski, Anal. Chem., 46 (1974) 1328.
6 P. Benes and I. Rajman, Collect. Czech. Chem. Commun., 34 (1969) 1375.
7 R. V. Coyne and J. A. Collins, Anal. Chem., 44 (1972) 1093.
8 Y. Dokiya, H. Ashikawa, S. Yamazaki and K. Fuwa, Spectrosc. Lett., 7 (1974) 551.
9 A. D. Shendrikar and P. W. West, Anal. Chim. Acta, 72 (1974) 91.
10 A. D. Shendrikar and P. W. West, Anal. Chim. Acta, 74 (1974) 189.
11 P. Benes, Radiochim. Acta, 3 (1964) 159.
12 P. Benes and J. Smetana, Radiochim. Acta, 6 (1966) 1966.
13 F. K. West, P. W. West and F. A. Iddings, Anal. Chim. Acta, 37 (1967) 112.
14 G. K. Schweitzer and W. N. Bishop, J. Am. Chem. Soc., 75 (1953) 6330.
15 J. Belloni, M. Haissinsky and H. N. Salama, J. Phys. Chem., 53 (1959) 881.
16 F. Kepak, Chem. Rev., 71 (1971) 357.
17 F. E. Beamish and J. C. Van Loon, Recent Advances in the Analytical Chemistry of the Noble Metals, Pergamon Press, Oxford, 1972.
18 R. A. Nadkarni and G. H. Morrison, Anal. Chem., 46 (1974) 232.

Analytica Chimica Acta, 85 (1976) 399—402

Short Communication

GENERATION OF STANDARD METAL OXIDE PARTICULATES IN THE RESPIRABLE RANGE

V. DHARMARAJAN and P. W. WEST

Environmental Science Institute, Chemistry Department, Louisiana State University, Baton Rouge, Louisiana 70803 (U.S.A.)

(Received 2nd February 1976)

One of the most fundamental requirements for research and development in the field of air pollution is the availability of reliable standards. The ambient air is a complex mixture containing both gaseous and particulate pollutants, and therefore standard pollutant gases and particulates are needed. Significant progress has been made in the generation standards in the laboratory. Almost all of the gaseous species are readily available in high purity, and primary standards can be obtained, therefore, by simply diluting with clean air to obtain the desired concentration. Alternatively, a pollutant species can be diluted and its concentration determined by appropriate analytical procedures to provide a secondary standard [1].

In recent years, permeation tubes for generating standard amounts of gaseous pollutants have gained wide popularity because of their simplicity and ease of application [2]. Permeation tubes can easily be made for most of the inorganic and organic gaseous pollutants. In contrast, particulate standards have presented difficult problems because, unlike the gases, they are seldom homogeneous nor can they be diluted or otherwise manipulated readily. For laboratory studies, particulates have to be generated in situ and transported by means of pumps or blowers. Moreover, in the case of particulates, size is an important parameter to be considered. The major focus of air pollution studies is the determination of particulates in the "respirable" range of 0.5—5 μm in size.

Recently a convenient method was reported [3] for the generation of metal oxide particulates. Preliminary investigations with microscopic techniques have indicated the size of the particulates to be within the range 0.1—5 μm. This communication reports a critical study of the size of the particulates generated using the Anderson sampler.

Experimental

Apparatus and materials. The dust generator described previously [3] was utilized, except that a new glass stack (3 in. i.d.) was used. An Anderson

air sampler (Model No. 20-2000; Anderson 2000 Inc., Atlanta, Georgia, 30320) having glass plates for eight-stage classification was utilized for determination of size of the generated particulates. In addition, a pump capable of pulling 1 cu. ft. min^{-1} of air was used with the Anderson sampler, and gas flows were measured with a dry test meter (Model DTM 115; American Meter Company). Metal determinations were made with a Perkin-Elmer Model 403 atomic absorption spectrometer.

Solutions (1000-p.p.m.) of Zn, Pb and Cu were prepared by dissolving 1.000 g of the respective metal in a minimum amount of nitric acid and diluting to 1 l. Appropriate dilutions were made to obtain a mixture containing 50 p.p.m. of each metal. Individual standards of Pb, Zn and Cu, containing 0.1, 0.5, 1.0 and 5.0 p.p.m. were obtained by appropriate dilutions. All chemicals used were of analytical grade.

Procedure. The experimental set up is shown in Fig. 1. The sampling probe was connected to the Anderson sampler with Tygon tubing, which in turn was connected in series to a meter valve and pump. Before the start of each experiment, the dry test meter was connected upstream to the Anderson sampler and a flow rate of 1 cu. ft. min^{-1} was established by the meter valve. Once the flow rate was adjusted, the dry test meter was disconnected and the sampler attached to the sampling probe. The burner in the generator was operated with oxygen at 15 psi and acetylene at 1.0 psi. A solution containing 50 p.p.m. each of Pb, Cu and Zn was separated into the flame. The aspiration rate under these conditions was 1.5 ml min^{-1}. After about 5 min (time for reaching steady state), the pump was started and samples were collected for 2 h. Isokinetic sampling was unnecessary since most of the particulates were less than 5 μm in diameter. The residue on each sampler stage plate was

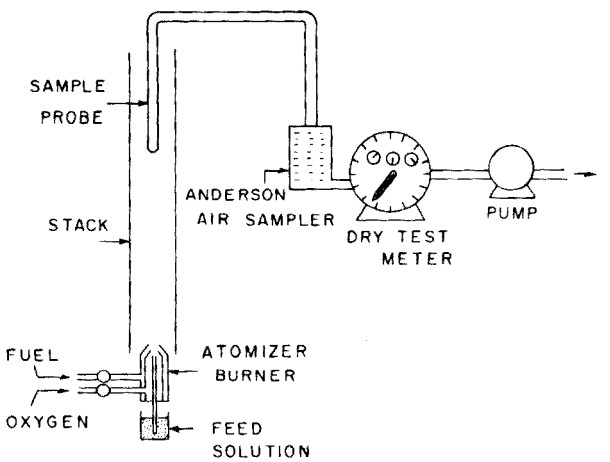

Fig. 1. Equipment used for measurement of particulates.

first dissolved with a hot mixture of (1 + 9) HNO_3 and (1 + 9) HCl and then evaporated to complete dryness. The dried residue was redissolved in 2 ml of (1 + 9) HNO_3 and diluted to 10 ml with deionized water. The amount of Pb, Cu and Zn in each of the solutions was determined by standard atomic absorption spectrometric procedures.

Results and discussion

Table 1 summarizes the amount of each metal found on different plates (stages) and also show the particle size range of each stage. Figure 2 shows the distribution of the particles generated by this method. It is clear from Fig. 2 that more than 94 % of the particles generated are distributed within the respirable range with a maximum in stage 5 (i.e. 1.1—2.1-μm range). This study clearly demonstrates the potential of this method of generation for provided complex mixtures of various metal particulates, for applications in toxicological and industrial hygiene investigations.

TABLE 1

Amount of each metal found on the different plates of the Anderson sampler

Stages	Size range (μm)	Total			Mean (μg)	% Metal in each stage
		Cu	Pb	Zn		
0	>11	5.1	4.5	5.9	5.2	4.68
1	7—11	1.5	1.5	2.1	1.7	1.5
2	4.7—7	1.5	1.5	2.1	1.7	1.5
3	3.3—4.7	2.84	3.0	3.5	3.1	2.8
4	2.1—3.3	14.1	13.5	14.2	13.9	12.4
5	1.1—2.1	50.2	52.5	57.0	53.2	47.3
6	0.65—1.1	23.0	22.5	22.2	22.6	20.1
7	0.43—0.65	10.8	10.2	12.5	11.2	9.9
				Total=	112.6	

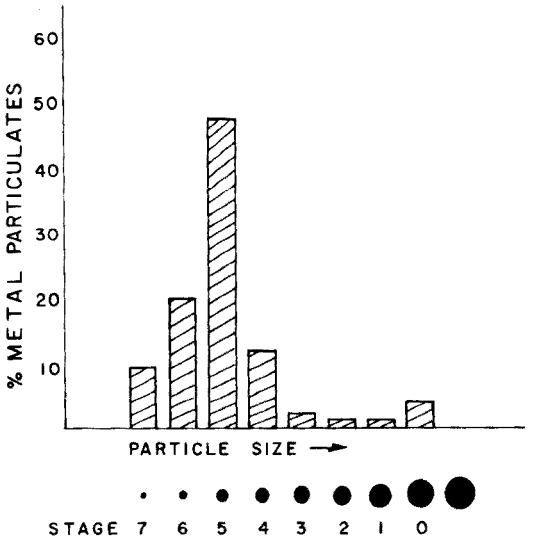

Fig. 2. Particle size distribution of the particulates generated with the Anderson sampler. See Table 1 for the size ranges of the different stages.

REFERENCES

1 J. P. Lodge, Production of Controlled Test Atmospheres, in Arthur C. Stern (Ed.), Air Pollution, 2nd edn., Chap. 27, Vol. II, Academic Press, New York, 1968, p. 466.
2 A. E. O'Keefe and G. C. Ortman, Anal. Chem., 38 (1966) 760.
3 V. Dharmarajan and P. W. West, Anal. Chim. Acta, 69 (1974) 43.

Analytica Chimica Acta, 85 (1976) 403—406

Short Communication

DETERMINATION OF LEAD IN CONFECTION WRAPPERS BY ATOMIC ABSORPTION SPECTROMETRY

DAWN WATKINS, THOMAS CORBYONS, JOHN BRADSHAW and JAMES WINEFORDNER*
Department of Chemistry, University of Florida, Gainesville, FL 32611 (U.S.A.)
(Received 2nd January 1976)

Recently, Hankin et al., [1] briefly reported the presence of concentrations of lead to up to 30,000 p.p.m. in food wrappers and colored magazine pages [1, 2], but no essential details of their procedures (sampling and measurement) were given. Because extraordinarily large concentrations of lead were reported, with no apparent corroborative determinations, the lead content of several food wrappers has been studied by wet and dry ashing techniques with different atomic absorption measurements. One sampling method involved digestion of the paper by hot concentrated nitric acid and the digested sample was aspirated directly into the flame of an atomic absorption spectrometer. A second sampling procedure involved dry ashing of the paper, dissolution in nitric acid, and aspiration of this solution; ammonium nitrate and aluminium nitrate were used as dry ashing aids, and the ashing conditions were carefully controlled to minimize lead loss by volatilization [2].

Experimental

Apparatus. A Unicam SP-90 atomic absorption spectrometer was used. The experimental conditions were: air/acetylene flame, 6.5 l min^{-1}/1.4 l min^{-1}; sample aspiration rate, 2.7—3.3 ml min^{-1}; monochromator slit width, 0.10 mm; burner top 0.8—1.2 cm below light beam hollow-cathode lamp current, 8.0 mA; measurement at 283.3 nm (resonance line) and 280.2 nm (non-resonance line).

Reagents. Stock solutions prepared from reagent-grade lead nitrate and demineralized water, were stored in polyethylene bottles. More dilute solutions were prepared by successive dilution. Standards containing less than 10 p.p.m. Pb were prepared fresh daily.

Concentrated reagent-grade nitric acid was used in the ashing procedure. Ammonium nitrate—aluminium nitrate ashing acid contained the reagent-grade materials at concentrations of 0.1 M for each.

*Author to whom reprint requests should be sent.

General sample preparation. All wrappers were wiped clean with a damp Kimwipe. The colored portions were cut up into approximately 0.5 mm × 0.5 mm sections and dried at 110 °C for 2 h. Plastic wrappers were dried at 80 °C for 1 h.

Wet chemical dissolution. Approximately 0.5 g of sample, accurately weighed, was placed in a 100-ml volumetric flask to which 20 ml of concentrated nitric acid was added. This mixture was heated for about 30 min in a water bath at 70—80 °C. The mixture was allowed to stand for 3—4 h (this time was not critical). The mixture was then diluted to give a lead content of 2—35 $\mu g\ ml^{-1}$ (the linear working range for lead on the instrument used). The volume of undissolved sample remaining in the flask was less than 1 ml and taken as being negligible. In the standard addition calibration, the standards were added in the nitric acid step.

Dry ashing method. Approximately 0.5 g of sample, accurately weighed, was added to a 30-ml Vycor crucible. To this 1.0 ml of concentrated nitric acid was added, and the mixture was heated on a hot plate at 90—100 °C until a partial digest was formed (10—20 min). By adding small amounts of deionized water the mixture was not allowed to become dry. To this mixture, 1 ml of the 0.1 M ammonium nitrate—aluminium nitrate solution was added. The mixture, heated in an oven at 110 °C for 2 h to dry the sample, was ashed for 12 h at 450—460 °C in a muffle furnace. The ash was dissolved in 1 ml of hot nitric acid, transferred quantitatively, and diluted to give a final lead concentration in the range 2—35 $\mu g\ ml^{-1}$. In the crucible retention—volatilization studies, the lead was added with the initial nitric acid before partial digestion. In the addition standard calibrations, the lead was added after the ashing was completed.

Results and discussion

About 20 different food wrappers were surveyed initially by the wet digestion method. In general, lead was found most frequently in wrappers with yellow and/or orange pigments. The object of this study was to determine the lead in food wrappers reliably by several sample preparation techniques (wet vs. dry methods) and by two atomic absorption standardization methods (analytical curve vs. standard addition). Atomic absorption spectrometry is an accepted measurement method for lead, and reliable results are obtained if light scatter in the flame is minimal (or is corrected for) and if sample matrix effects are negligible. Although correction for light scatter can be made by optical—electronic means, it was not necessary here as scatter was negligible in both the wet- and dry-ashed samples. Since similar results were obtained by both the analytical calibration curve and standard addition methods, matrix effects were also negligible.

The wet procedure gave the more reliable results. In the dry ashing procedure, appreciable losses (see Table 1) resulted for the plastic bread wrapper samples only; other wrappers gave similar results by both wet and dry methods. The losses may arise from volatilization of the lead despite the efforts made to minimize this, or of lead in the Vycor vessel.

Table 1 shows the results obtained for four different food wrappers prepared in two ways (wet vs. dry ashing) with the lead determined by both the analytical curve and the standard addition methods of calibration. Many other food wrappers were studied; in confirmation of the earlier reports [1], some had lead concentrations greater than 30,000 p.p.m. although others had essentially negligible lead contents. The presence of lead was frequently associated with the presence of yellow (30,700 p.p.m.) or orange (39,100 p.p.m.) pigments although all orange and yellow pigments did not contain lead. The reproducibility of the sampling and measurement procedures is given in Table 2. Standard additions of lead to the samples before the wet chemical dissolution indicated that the lead recoveries were excellent.

This work was supported by AF-AFOSR-74-2574.

TABLE 1

Lead content of food wrappers by different atomic absorption spectrometric methods

Product	Preparation[a]	Standardization	Pb found[b] ($\mu g\ g^{-1}$)	
Bread wrapper X	Wet	Standard addition	30,200	(1)
	Wet	Analytical curve	28,700	(4)
	Dry	Analytical curve	11,200	(1)
Ice cream bar wrapper X	Wet	Analytical curve	1,400	(2)
	Wet	Standard addition	1,380	(1)
	Dry	Analytical curve	1,350	(1)
	Dry	Standard addition	1,400	(1)
Bubble gum wrapper 1	Wet	Analytical curve	5,140	(3)
	Wet	Standard addition	4,590	(3)
	Dry	Analytical curve	4,980	(3)
	Dry	Standard addition	4,910	(1)
Raisin wrapper 1	Wet	Analytical curve	22,400	(3)
	Wet	Standard addition	18,700	(1)

[a]Blanks for both the wet and dry ashing procedures were negligible. Blanks were taken through the entire procedure.

[a]( ) gives the number of determinations; the average result is quoted if more than one determination was made.

TABLE 2

Reproducibility of sampling and measurement procedure, with standardization by the analytical curve method

Product	Preparation	No. of detns.	Av. Pb found ($\mu g\ g^{-1}$)	s	s_r (%)
Bread wrapper	Wet	4	28,700	650	2.3
Bubble gum wrapper 1	Wet	3	5,130	160	3.1
Bubble gum wrapper 1	Dry	3	4,920	280	5.7
Raisin wrapper	Wet	3	22,350	1,200	5.4

REFERENCES

1 L. Hankin, G. H. Herchel and R. A. Botsford, Clin. Pediatr., 12 (1974) 654; 13 (1974) 1064.
2 T. T. Gorsuch, Analyst (London), 84 (1959) 135.

Analytica Chimica Acta, 85 (1976) 407—410

Short Communication

NICHT KOMPENSIERBARER UNTERGRUND ALS SYSTEMATISCHER FEHLER BEI DER ATOMABSORPTIONS-SPEKTROMETRIE

R. HÖHN und E. JACKWERTH

Institut für Spektrochemie und angewandte Spektroskopie, 4600 Dortmund 1, Bunsen-Kirchhoff-Str. (B.R.D.)

(Eingegangen am 16. März 1976)

Bei der Bestimmung von Spurenverunreinigungen in Indium durch Atomabsorptions-Spektrometrie haben wir bei einigen Elementen systematische Fehler beobachtet, die nur schwer zu korrigieren sind. In Lösungen hoher $InCl_3$-Konzentration erhält man Signale, die durch Untergrundabsorption verfälscht und daher zu gross sind. Werden dieselben Lösungen unter Verwenden eines Untergrundkompensators analysiert, so erhält man bei geringen Spuren-Konzentrationen negative Messwerte (Abb. 1). Der durch den Untergrund verursachte systematische Fehler kann also über die übliche Korrektur der Messignale mit einem Kontinuum-Strahler nicht eliminiert werden. Störungen dieser Art treten besonders stark bei der Bestimmung von Gold auf, wenn bei 267,59 nm gemessen wird. Die Grösse des Fehlers hängt dabei in gewissem Umfang von den Arbeitsbedingungen ab (Ansaugrate des Zerstäubers, Zusammensetzung der Flamme, Beobachtungshöhe in der Flamme etc.).

Nähere Untersuchungen ergaben, dass die bei der Gold-Bestimmung beobachtete Störung auf die Besonderheit des Untergrundes zurückzuführen ist, der im Bereich 260—275 nm vor allem auf Molekülabsorption durch InCl beruht. Die bereits seit längerer Zeit bekannten Absorptionsspektren [1] sind kürzlich auch im Zusammenhang mit atomabsorptions-spektrometrischen Arbeiten beschrieben worden [2—4]. Um den durch die Molekülabsorption verursachten Fehler deuten zu können, haben wir den Untergrund bei hoher spektraler Auflösung untersucht. Dies erschien uns sinnvoll, da nach Arbeiten von Massmann und Mitarbeitern mit nicht kompensierbaren Untergrundstörungen immer dann zu rechnen ist, wenn die Analysenlinien in einem strukturierten Untergrund liegen [5, 6].

Experimentelle Angaben

Die analytischen Bestimmungen wurden mit den Atomabsorptions-Spektrometern Varian Modell 1000 sowie Perkin—Elmer Modell 300 durchgeführt. Beide Geräte waren mit einem Untergrund-Kompensator ausgerüstet.

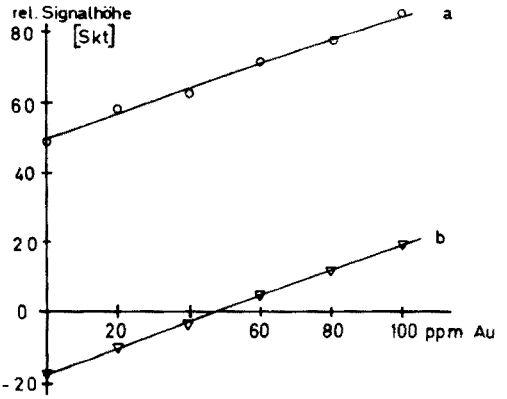

Abb. 1. Bestimmung von Au in $InCl_3$ nach dem Additionsverfahren (0,1 g In ml^{-1}). (a) Messung ohne Untergrundkompensation. (b) Messung mit Untergrundkompensation.

Die hochaufgelösten Absorptions-Spektren wurden mit einem 3,5-m Ebert-Spektrographen bei photographischer Strahlungsmessung aufgenommen und anschliessend mit einem registrierenden Photometer gezeichnet (Deuterium-Lampe als Hintergrundstrahler, Messung in der 2. Ordnung, Auflösung $\lambda/\Delta\lambda > 100\,000$). Die Spektren wurden in der Luft—Acetylen- bzw. in der Luft—Propan-Flamme gemessen. Für die Untersuchungen wurde $InCl_3$-Lösung (0,1 g In ml^{-1}) verwendet, zu deren Herstellung Indium-Metall (99,9995 % In) in Salzsäure aufgelöst wurde.

Ergebnisse und Diskussion

Für die InCl-Absorption sind drei Bandensysteme bekannt [7, 8]. Einen Ausschnitt mit hoher Auflösung aus dem die Goldbestimmung störenden System zeigt Abb. 2. Die Absorptionslinie von Gold bei 267,59 nm fällt dabei in die intensivste Bande mit der kurzwelligen Kante bei 267,21 nm; dieser Bande wird der Übergang 0—0 zugeordnet [7, 8]. Abbildung 3 enthält einen Teil dieser Bande in grösserer Spreizung.

Anhand von Abb. 3 kann der systematische Fehler bei der Untergrundkorrektur leicht erklärt werden. Man erkennt, dass die Bande fein strukturiert ist; die einzelnen Linien besitzen etwa die gleiche Breite wie die Absorptionslinie des Goldes. Bei Messungen mit der elementspezifischen Hohlkathodenlampe wird allein der Untergrund unmittelbar unter der Goldlinie, d.h. ein nur schmaler Spektralbereich erfasst. Wegen der relativ grossen Bandbreite des Monochromators im Atomabsorptions-Spektrometer wird mit einem Kontinuumstrahler jedoch auch der Untergrund in der Umgebung der Analysenlinie gemessen. Nach Abb. 3 fällt die Au-Linie bei 267,59 nm nicht mit einer Linie des Untergrundes zusammen. Dies bedeutet, dass die Untergrundabsorption bei Anregung mit der Au-Hohlkathodenlampe geringer ist als mit

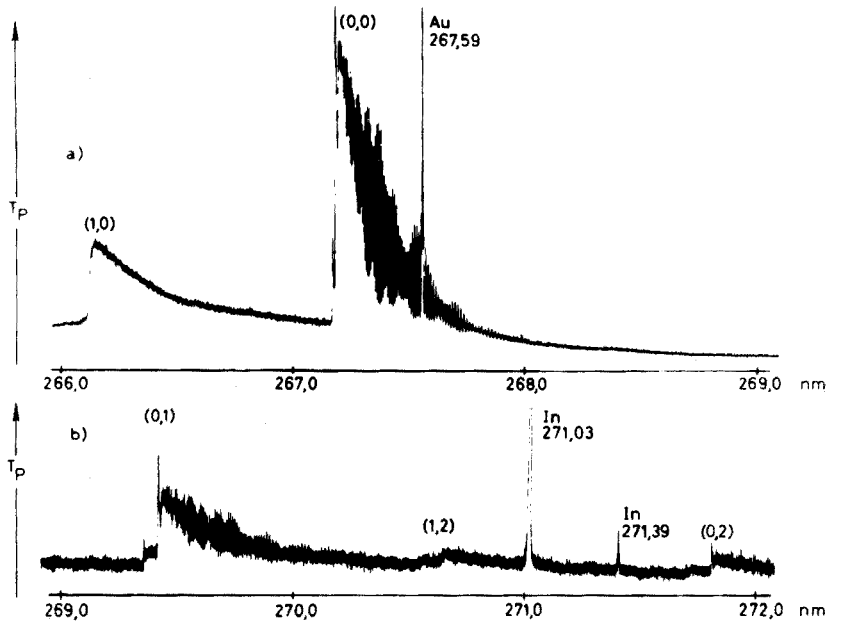

Abb. 2. Absorptionsspektrum von InCl und Absorptionslinie für Au in der Luft—Propan-Flamme. (T_p = Transparenz Photoplatte) Auflösung $\lambda/\Delta\lambda > 100\,000$. Teil (b) des Spektrums wurde mit 5-facher Verstärkung registriert.

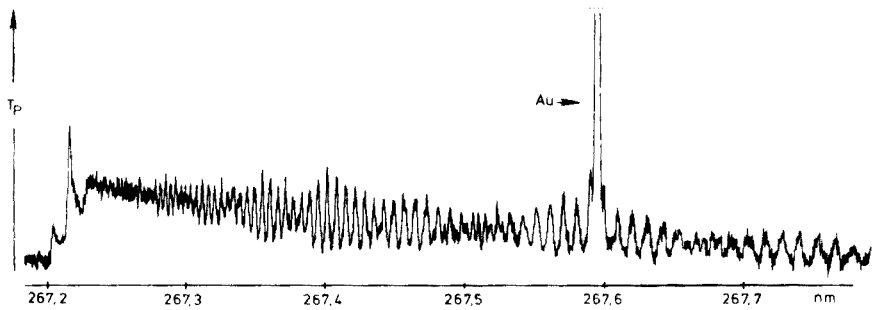

Abb. 3. Absorptionsspektrum von InCl und Absorptionslinie für Au in der Luft—Acetylen-Flamme (T_p = Transparenz Photoplatte) Auflösung $\lambda/\Delta\lambda > 100\,000$.

dem Kontinuumstrahler. Bei Differenzbildung wird demnach ein zu grosser Wert für den Untergrund abgezogen; man erhält damit zu kleine, u. U. sogar negative Signale.

Wir danken Herrn Dr. H. Massmann für anregende Diskussionen sowie Frau B. Mergler für die Messung der hochaufgelösten Spektren.

LITERATUR

1 A. Petrikaln und J. Hochberg, Z. Physik., 86 (1933) 214.
2 R. Höhn, Dissertation Bochum, 1975.
3 H. Haraguchi und K. Fuwa, Spectrochim. Acta, Part B, 30 (1975) 535.
4 T. Nakahara und S. Musha, Anal. Chim. Acta, 80 (1975) 47.
5 H. Massmann und Z. El Gohary, CSI XVIII, Grenoble, 1975, S. 557.
6 H. Massmann, Z. El Gohary und S. Güçer, Spectrochim. Acta, Part B, im Druck.
7 B. Rosen, Spectroscopic Data Relative to Diatomic Molecules, Pergamon, Oxford, 1970, S. 227.
8 R. W. B. Pearse und A. G. Gaydon, The Identification of Molecular Spectra, Chapman & Hall, London, 1950, S. 151.

Analytica Chimica Acta, 85 (1976) 411—414

Short Communication

EPITHERMAL NEUTRON ACTIVATION ANALYSIS OF ELEMENTS PRESENT IN TRACE QUANTITIES IN BIOLOGICAL MATERIALS

D. BRUNE and B. BIVERED
AB Atomenergi, Studsvik (Sweden)
(Received 29th January 1976)

In neutron activation analysis with a reactor, activation of the nuclide on which the analytical determination is based, is most often achieved with thermal neutrons. When biological materials such as blood and tissue specimens are analyzed in this way, the activity of ^{24}Na normally dominates the γ-spectrum for a period of several days after the end of irradiation [1]. The production of ^{24}Na is, however, small when epithermal rather than thermal neutrons are used. Accordingly, the use of epithermal neutrons facilitates the determination of a nuclide that possesses a high resonance cross-section in such organic materials. The same consideration applies to water, especially sea water, in which the ^{24}Na activities predominate.

The application of epithermal neutron activation analysis (e.n.a.a.) to rock samples has been studied extensively [2]. The technique has also found applications in the biological field [3—5]. The present study indicates how this technique can be applied to the multielemental assay of trace elements in biological materials such as liver tissue.

Epithermal neutrons at selected energies

In a complex reactor spectrum practical use is made of the resonance neutrons by placing thin cadmium shields around the sample to remove thermal neutrons.

The performance of e.n.a.a. with a high-intensity neutron beam, having a narrow energy range which corresponds to a major resonance in the excitation function of a specific reaction, provides the "ideal case" for analytical purposes. A close approach to these conditions can be made by using beams transmitted through resonance window filters of resonance scatterers inserted in a reactor channel. If the filter for the neutron beam is chosen to correspond to a selected energy, the γ-background can be lowered considerably. The technique seems promising, therefore, for application in prompt analysis [6]. A list of epithermal neutron intensities at selected energies is given in Table 1.

TABLE 1

Epithermal neutron intensities at selected energies

Energy	Intensity ($n\ cm^{-2}\ s^{-1}$)	Energy resolution	Filter, scatterer	Ref.
19 eV	$2 \cdot 10^4$	0.6 eV	W — Scatterer	7
139 eV	$3 \cdot 10^4$	6.0 eV	Co — Scatterer	7
2 keV	$5 \cdot 10^6$	0.7 keV	Sc — Filter	6
2.8 keV	$1 \cdot 10^4$	0.5 keV	NaF — Scatterer	7
24.5 keV	$6 \cdot 10^5$	1.8 keV	Fe — Filter	6
144 keV	$1 \cdot 10^7$	30—50 keV	Si — Filter	6

It should be stressed that epithermal neutrons of selected energy intervals can also be produced in accelerators such as the van de Graaff, by reactions of the type $^7Li\ (p,n)^7Be$. The neutron beams indicated in Table 2 can be produced [8]. Currents of about 20 μA can be obtained by such techniques. The neutron beams formed are focussed in a forward direction [9]. Below 50 keV, however, the energy resolution is poor. These high-energy epithermal neutrons might be applied to in vivo analysis of elements located at various depths in the human or animal body, after being moderated to appropriate energies by hydrogen and carbon present in tissues and biological fluids.

Present investigation. Neutron activation analysis for elements present in biological samples and water at trace levels is now well established. With group separation methods, it is possible to achieve the simultaneous characterization of about 30 elements [10]. After irradiation, biological materials such as blood and tissue specimens require handling by remote control or behind radiation shielding during the chemical treatment in order to minimize the dose to which the chemist is exposed.

In this study, thermal and epithermal n.a.a. were used, and their feasibility was compared for the trace element analysis of liver tissue containing As, Br, Cd, Cu, Fe, Mn, Mo, Na, Se and Zn.

TABLE 2

Neutron beams in accelerators

Energy (keV)	Intensity ($n\ cm^{-2}\ s^{-1}\ \mu A^{-1}$)	Resolution (keV)
50	$2 \cdot 10^6$	15
100	$5 \cdot 10^6$	25
200	$2 \cdot 10^7$	25

Experimental

The samples were dried samples of human liver tissue (wet weight about 1 g). They were irradiated in a central position in the MTR reactor R2 at Studsvik at a thermal flux of $4 \cdot 10^{13}$ n cm^{-2} s^{-1}. The cadmium ratio for gold (^{198}Au) was 10 in the irradiation position. The samples were enclosed in cadmium sheet (0.5-mm thick).

The various radionuclides were separated by the group separation system developed by Samsahl [10].

Results and discussion

The results of the measurements of As, Br, Cd, Cu, Fe, Mn, Mo, Na, Se and Zn in liver tissue by thermal or epithermal n.a.a. are given in Table 3. This Table also lists values of the "advantage factor" [11] for e.n.a.a. compared with thermal n.a.a. when ^{24}Na is considered as the main interfering nuclide. The activity levels of the various nuclides generated by e.n.a.a. and thermal n.a.a. are also included. When the present irradiation technique is used the following nuclides can suitably be determined by e.n.a.a.: ^{76}As, ^{82}Br, ^{115}Cd, ^{64}Cu, ^{56}Mn, ^{99}Mo, ^{75}Se, ^{65}Zn and ^{69m}Zn. The "advantage factors" for these nuclides range from 1.79 to 77.7.

TABLE 3

Analysis of liver tissue

Element (nuclide measured)	Ratio Cd		Content[a] ($\mu g\ g^{-1}$)	Liver activity[b]		"Advantage" factor
	Calcd.	Measured (liver)		With Cd	Without Cd	
As (^{76}As)	10.9	10.4	0.46	349	3636	22.1
Br (^{82}Br)	9.5	14	4.0	3513	48454	25.4
Cd (^{115}Cd)	3.1	5.8	4.3	516	3018	77.7
Cu (^{64}Cu)	125	154	14.7	3034	467059	1.93
Fe (^{59}Fe)	135	72	176.0	5.8	415	1.79
Mn (^{56}Mn)	135	120	0.5	75	8998	1.79
Mo (^{99}Mo)	3.6	2.2	0.4	1032	2297	66.9
Na (^{24}Na)	241	102		177900	18060000	1
Se (^{75}Se)	16.5	19.6	0.3	13.4	223	14.6
Zn (^{65}Zn)	73	43	75.8	72.4	3114	3.3
Zn (^{69m}Zn)	42	36	75.8	4021	142859	5.7

[a]From ref. 12 (referred to wet weight).

[b]Pulse number in full-energy peak/g of dried sample after end of irradiation.

When a quartz container was used, the total activity of the sample was reduced from about 2 R for thermal n.a.a. to 100 mR for e.n.a.a. (3 days cooling).

The e.n.a.a. technique seems also suitable for the analysis of sea water samples. The enormous ^{24}Na activities induced in such samples can be reduced by a factor of more than an order of magnitude by using e.n.a.a. rather than the thermal activation technique. In a preliminary study, the nuclides ^{76}As, ^{82}Br and ^{99}Mo were optimized in water samples from the Baltic sea by the e.n.a.a. method.

REFERENCES

1 D. Comar, in Advances in Activation Analysis, Vol. I, Academic Press, London, 1969, p. 171.
2 See, e.g., E. Steinnes, Inaugural Dissertation, Oslo University, 1972, IFA, 1972.
3 D. Brune and P. O. Wester, Anal. Chim. Acta, 52 (1970) 372.
4 N. V. Bagdavadze and L. M. Mosulishvili, J. Radioanal. Chem., 24 (1975) 65.
5 B. Maziere, J. Gros and D. Comar, J. Radioanal. Chem., 24 (1975) 279.
6 R. M. Brugger and O. D. Simpson, Symposium Proceedings, Teheran, Nov., 1972, IAEA, Vienna, 1973, p. 131.
7 W. Dilg and H. Vonach, Nucl. Instrum. Methods, 100 (1972) 83.
8 R. O. Bergman, Symposium Proceedings, Neuherberg, Oct., 1973, IAEA, Vienna, 1974, p. 83.
9 J. L. Fowler and J. E. Brolly, Jr., Rev. Mod. Phys., 28 (1956) 103.
10 See, e.g., K. Samsahl, Sci. Total Environ., 1 (1972) 65.
11 D. Brune and K. Jirlow, Nukleonik, 6 (1964) 242.
12 E. I. Hamilton and M. J. Minski, Sci. Total Environ., 1 (1973) 375.

Analytica Chimica Acta, 85 (1976) 415—419

Short Communication

GAS CHROMATOGRAPHY OF SOME VOLATILE METAL DIETHYLDITHIOCARBAMATES

TERENCE J. CARDWELL and DOMINIC J. DESARRO

Department of Inorganic and Analytical Chemistry, La Trobe University, Bundoora, Victoria 3083 (Australia)

PETER C. UDEN

Department of Chemistry, University of Massachusetts, Amherst, Massachusetts 01002 (U.S.A.)

(Received 10th March 1976)

Until about 1970, much of the emphasis in the gas chromatography of metal chelates centered on the β-diketonates and their fluorinated derivatives. In general, these complexes proved valuable for the determination of trivalent metal ions (Cr, Al, Sc, Rh and lanthanides) but rarely for divalent metal ions (except Be) [1, 2]. More recently, major efforts have been directed towards the investigation of other metal chelate systems, basically for the determination of divalent transition metals. Monothio-β-diketones proved useful for several metal ions [3], the most notable being nickel which could be determined down to 10^{-11} g as its monothiotrifluoroacetylacetonate [4]; in general, this system suffers from the disadvantage that many complexes are difficult to prepare. Bidentate and tetradentate β-aminoketonates have also found favour for some elements (Cu, Ni, Pd and Pt) [5, 6]; the tetradentates show excellent stability and chromatographic behaviour, and have been investigated [7] for the determination of copper and nickel at the picogram level, with fluorinated derivatives and electron capture detection. Other systems include the dialkyldithiophosphates for zinc, nickel, palladium and platinum [8] and the salicylaldimines for copper, nickel and zinc [9].

D'Ascenzo and Wendlandt [10] have established that some metal dithiocarbamates are volatile. It was therefore considered of interest to study such chelates thoroughly to determine their suitability for gas chromatographic analysis. During this work, Daughtrey et al. [11] reported the use of diethyldithiocarbamate for the gas chromatographic determination of arsenic.

Experimental

The diethyldithiocarbamates of Ni, Cu(II), Pd(II), Zn, Cd, Hg(II), Pb, Pt(II), Ag(I), Fe(III) and Co(III) were prepared by the general procedure of mixing warm aqueous solutions of the metal salt (sulphate or nitrate, except

for Pd and Pt where the chlorides were used) and sodium diethyldithiocarbam ate so that a ligand/metal ratio of 4:1 was established. The isolated complexes were purified by vacuum sublimation or recrystallization from chloroform—ether solution, and were characterized by melting point and mass spectroscopy.

Gas chromatographic studies were carried out on two instruments, a Perkin-Elmer F30 and a Varian 2440, both with flame ionization detectors. U-shaped pyrex glass columns (6.5 mm o.d., 2.8 mm i.d., length 35 cm) were fitted to the Perkin-Elmer F30, and coiled stainless steel columns (3.2 mm o.d., 2.16 mm i.d., length 1 m) were used with the Varian 2440. The packing material was acid-washed Chromosorb W (60-80 mesh) which was exhaustively silanized by refluxing with a 5 % dimethyldichlorosilane (DMCS) solution in ether, before it was coated with 5 % OV-101. Eluted samples were collected and identified by mass spectrometry.

Thermal analyses (TGA and DTA) of the metal chelates were done under nitrogen with a Rigaku-Denki Thermal Analysis System. Sample masses of 5—10 mg were run at a heating rate of 20 °C min^{-1} from ambient to 500 °C. Mass spectra were obtained on a Perkin-Elmer RMU-6L spectrometer with a direct solids probe.

Results and discussion

Thermal analysis. The diethyldithiocarbamates of nickel, zinc, iron(III) and cobalt(III) showed complete volatility under the conditions used for the thermal analyses; the remaining complexes were less volatile and decomposed slightly. In all cases, the TGA curves showed one-step weight losses. In general all of the complexes investigated proved to be highly thermally stable, with the initial inflection on the TGA curves (Fig. 1) appearing in the range 240 °C (Cu and Ag) to about 300 °C (Ni, Co, Pd and Pt).

These results clearly indicate that the complexes of nickel, zinc, iron and cobalt have the properties of volatility and thermal stability required for gas chromatography. The remaining metal chelates also possess reasonable thermal stability and some volatility, so that chromatography is possible if the operating temperatures are selected carefully so that volatilization is rapid and decomposition minimal.

Gas chromatography. From a wide range of liquid phases and solid supports tested, the most satisfactory chromatographic results were obtained with 5 % OV-101 on a highly deactivated diatomaceous earth support, acid-washed Chromosorb W pretreated with DMCS. It is imperative that the support be exhaustively silanized before being coated with the liquid phase; this is in agreement with the conditions found by Daughtrey et al. [11] for the chromatography of arsenic diethyldithiocarbamate.

All the complexes, except for those of Fe(III) and Ag(I), could be eluted successfully at column temperatures in the range 220—245 °C, with injector and detector temperatures of 250 °C. Glass and stainless steel were equally

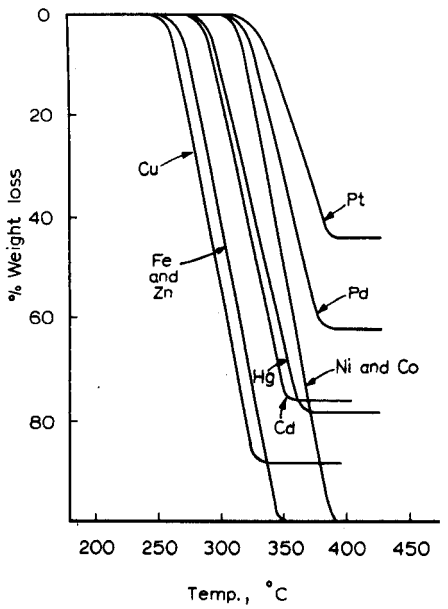

Fig. 1. Thermograms of the diethyldithiocarbamates of Cu(II), Fe(III), Zn(II), Hg(II), Cd(II), Ni(II), Co(III), Pd(II) and Pt(II).

effective for column construction and well defined peaks were obtained with no chromatographic evidence of decomposition taking place. Eluted samples were analysed by mass spectrometry, which confirmed that elution was effected without decomposition; e.g. when a sample was collected after injection of the nickel chelate, the major ions observed in the mass spectrum occurred at *m/e* 355, 323, 229 and 207, identical to the spectrum of the pure chelate. Column efficiencies of up to 1000 theoretical plates were achieved with the narrower bore stainless steel columns.

It is of interest that this is the first chelate system found to be suitable for the gas chromatographic elution of cadmium and mercury. Figure 2 shows an example of the separation of zinc, cadmium and lead at 220 °C. The order of elution is in close agreement with the volatilities of the complexes observed in thermal analysis.

Until recently [9], it has proved difficult to separate zinc and nickel chelates. Figure 3 shows a separation of zinc from nickel, palladium and platinum; as in the previous example, the order of elution agrees with the order of volatility observed in thermal analysis.

Table 1 summarizes the chromatographic data for the metal chelates examined. Although the survey is by no means complete, the metal dithiocarbamates clearly show considerable promise for metal analysis by gas chromatography. There is considerable scope for variation of alkyl substituents which may lead to improved resolution of metals which have similar

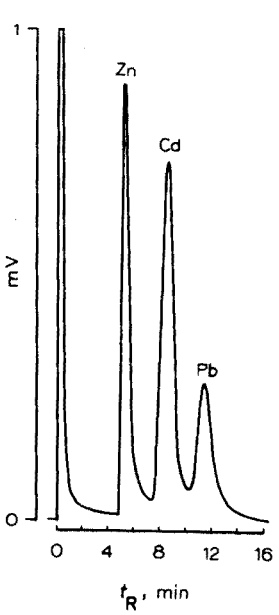

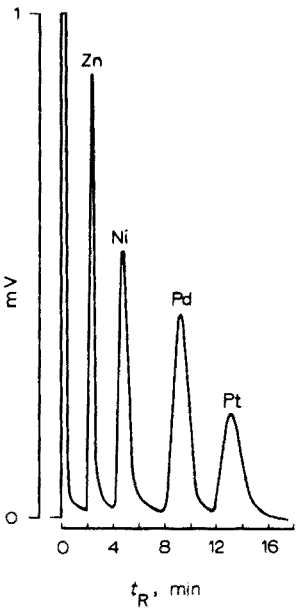

Fig. 2. Gas chromatographic separation of zinc, cadmium and lead diethyldithiocarbamates from a pyrex glass column (35 cm × 2.8 mm i.d.) packed with 5 % OV-101 on DMCS-treated Chromosorb W. Conditions: oven 220 °C; injector/detector, 250 °C; carrier gas flow, 20 cm^3 min^{-1}. The chloroform solution injected (1.0 μl) contained 0.5 % (w/v) of each complex. Attenuation, 64 × 1.

Fig. 3. Gas chromatographic separation of zinc, nickel, palladium and platinum diethyldithiocarbamates from the glass column described in Fig. 2. Conditions: oven, 225 °C; injector/detector, 250 °C; carrier gas flow, 45 cm^3 min^{-1}. The chloroform solution injected (1.3 μl) contained 0.4 % (w/v) of the Ni and Zn chelates and 0.6 % (w/v) of the Pd and Pt chelates. Attenuation, 128 × 1.

TABLE 1

Gas chromatographic data
(Injector/detector, 250 °C; carrier gas flow, 60 cm^3 min^{-1}; glass column, 35 cm × 2.8 mm i.d.)

Chelate	Ni	Pd	Pt	Zn	Cd	Cu	Pb	Hg	Co
Oven temp (°C)	230	235	245	205	225	230	220	220	24
Retention time (min)	2.81	4.63	4.17	4.00	3.00	2.36	3.01	5.80	

retention times for the diethyl derivatives. The range of metals could also be extended to include some non-transition metals such as As, Sb and Bi. Other advantages of the dithiocarbamate system are the ready availability of chelating agents, the simplicity of chelate preparation, and the wealth of information available on extraction conditions and physical properties of the chelates.

Note added in proof: After this communication had been submitted, our attention was drawn to two papers on the gas chromatography of nickel and zinc diethyldithiocarbamates:
J. Krupcik, J. Garaj, S. Holotik, D. Oktavek and M. Kosik, J. Chromatogr., 112 (1975) 189; and J. Masaryk, J. Krupcik, J. Garaj and M. Kosik, J. Chromatogr., 115 (1975) 256.

We wish to thank the National Science Foundation (U.S.A.) for support through Grant NSF 41168X.

REFERENCES

1 R. W. Moshier and R. E. Sievers, Gas Chromatography of Metal Chelates, Pergamon, Oxford, 1965.
2 J. A. Rodriguez-Vásquez, Anal. Chim. Acta, 73 (1974) 1.
3 R. Belcher, W. I. Stephen, I. J. Thomson and P. C. Uden, J. Inorg. Nucl. Chem., 33 (1971) 1851; 34 (1972) 1017.
4 R. S. Barratt, R. Belcher, W. I. Stephen and P. C. Uden, Anal. Chim. Acta, 59 (1972) 59.
5 R. Belcher, K. Blessel, T. J. Cardwell, M. Pravica, W. I. Stephen and P. C. Uden, J. Inorg. Nucl. Chem., 35 (1973) 1127.
6 R. Belcher, R. J. Martin, W. I. Stephen, D. E. Henderson, A. Kamalizad and P. C. Uden, Anal. Chem., 45 (1973) 1197.
7 P. C. Uden, D. E. Henderson and A. Kamalizad, J. Chromatogr. Sci., 12 (1974) 591.
8 T. J. Cardwell and P. S. McDonough, Inorg. Nucl. Chem. Lett., 10 (1974) 283.
9 P. C. Uden and B. A. Waldman, Anal. Lett., 8 (1975) 91.
10 G. D'Ascenzo and W. W. Wendlandt, J. Therm. Anal., 1 (1969) 423; J. Inorg. Nucl. Chem., 32 (1970) 2431.
11 E. H. Daughtrey, Jr., A. W. Fitchett and P. Mushak, Anal. Chim. Acta, 79 (1975) 199.

Analytica Chimica Acta, 85 (1976) 421—424

Short Communication

GAS CHROMATOGRAPHY—ATOMIC ABSORPTION SPECTROMETRY FOR THE DETERMINATION OF TETRAALKYLLEAD COMPOUNDS

Y. K. CHAU, P. T. S. WONG and P. D. GOULDEN

Canada Centre for Inland Waters, Burlington, Ontario L7R 4A6 (Canada)

(Received 2nd February 1976)

The combination of gas chromatography and atomic absorption spectrometry has proved to be an excellent system for the determination of volatile organometallic compounds such as tetraalkyllead [1, 2] and dimethyl selenide [3] compounds. In a previous method for tetraalkyllead compounds [2], the g.c.—flame a.a.s. combination showed a detection limit of about 0.1 μg Pb. Recent investigations have shown that by using a silica furnace in the a.a.s. unit, the sensitivity can be enhanced by three orders of magnitude. The present communication describes the use of the furnace in analysis for tetraalkyllead compounds. This method was developed for the study of conversion of lead compounds to tetramethyllead in sediment systems. It can be applied readily to the determination of these compounds in the atmosphere.

Experimental

The g.c.—a.a.s. system. The system consisted of a Microtek 220 gas chromatograph and a Perkin-Elmer 403 atomic absorption spectrophotometer. These instruments were connected by means of stainless steel tubing (2 mm o.d.) connected from the column outlet of the gas chromatograph to the silica furnace of the a.a.s. (Fig. 1). A 4-way valve was installed between the carrier gas inlet and the column injection port so that a sample trap could be mounted, and the sample could be swept into the g.c. column by the carrier gas. The recorder (10 mV) was equipped with an electronic integrator to measure the peak areas, and was simultaneously actuated with the sample introduction so that the retention time of each component could be used for identification of peaks.

The furnace was constructed from silica tubing (7 mm i.d., 6 cm long) with open ends (Fig. 2). The lead compounds separated by g.c. were introduced to the center of the furnace through a side-arm. Hydrogen gas was introduced at the same point at a flow rate of 135 ml min^{-1}; the burning of hydrogen improved the sensitivity. The furnace was wound with 26-gauge Chromel wire to give a resistance of about 5 ohms. The voltage applied to the

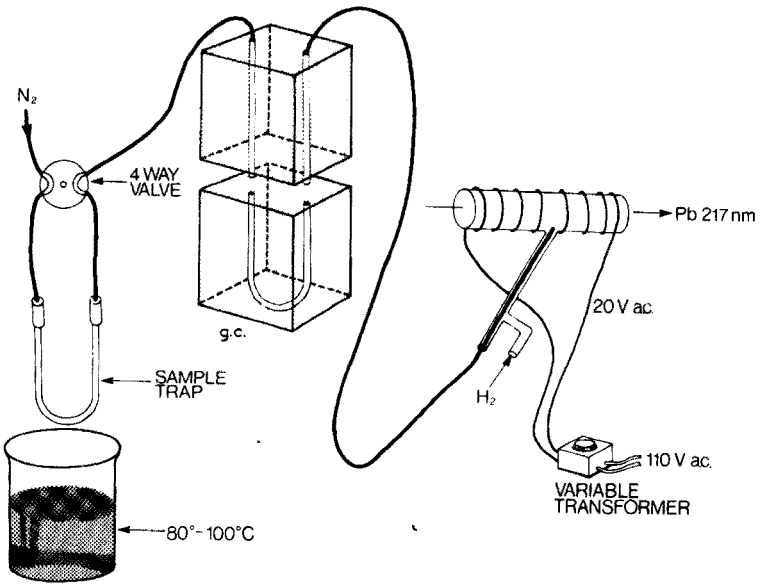

Fig. 1. Schematic diagram showing the interfacing of the g.c.—a.a.s. system.

furnace was about 20 V a.c. regulated by a variable transformer so that the furnace temperature with the hydrogen burning was about 1000 °C. The silica furnace was mounted on top of the a.a.s. burner and aligned to the light path.

The sample trap was a glass U-tube (6 mm diam., 26 cm long) packed with 3 % OV-1 on Chromosorb W, which was immersed in a dry ice—methanol bath at ca. −70 °C. A known amount of gaseous sample was drawn through the trap by a peristaltic pump operated at 130—150 ml min^{-1}. After sampling, the trap was mounted to the 4-way valve and heated to ca. 80—100 °C by a beaker of hot water, and the adsorbed compounds were swept into the g.c. column.

Liquid samples can be directly injected to the column through the injection port, without a sample trap.

Instrument parameters. Glass column, 1.8 m long, 6 mm diam., packed with 3 % OV-1 on Chromosorb W 80—100 mesh; carrier gas, 70 ml N_2 min^{-1}; injection port temperature, 150 °C; temperature program, initial 50 °C for 2 min, programmed at 15 °C min^{-1}, until 150 °C; sample trap temperature, 80—100 °C.

Lead line, 217 nm; lamp current, 8 mA; spectral band width, 0.7 nm; scale expansion 4× (0.25 A full scale); furnace gas, 135 ml H_2 min^{-1}. The deuterium background corrector was used.

Reagents

Tetramethyl- and tetraethyl-lead (Alfa Chemicals, Beverly, Mass.), and mixed alkyllead compounds (Me_3EtPb, Me_2Et_2Pb, $MeEt_3Pb$; Ethyl Corporation. Ferndale, Mich.) were used. Benzene was used as solvent to prepare dilute standards. The purities of these compounds were assessed by gas chromatography; standardization was done by atomic absorption determination of the lead content as described previously [2].

Results and discussion

The use of a silica furnace in the atomic absorption spectrometer achieved a 1000× enhancement of sensitivity over the flame technique [2]. Furthermore, as the conventional flame is not used, the hollow-cathode energy can be operated at lower amplifier gain, which gives very steady baselines at higher scale expansion. The lower limit of measurement of the method depended on the scale expansion of the instrument. Under the present instrumental conditions, 0.1 ng Pb could be detected with certainty.

The cold trap technique for collection of volatile organometallic compounds has been discussed previously [2]. The precision of the method was evaluated by replicate (5) analyses of a synthetic sample containing ca. 5 ng (as Pb) of each of the five tetraalkyllead compounds. The relative standard deviation was in the range 10—15 %. When the absorbances were plotted against lead concentrations, each of the five tetraalkyl compounds gave similar calibration curves; the response was linear up to at least 200 ng Pb, above which overlapping of the peaks occurred. If only one compound was present (e.g. tetramethyllead), the plot was linear up to at least 2000 ng. For determinations at the microgram level, the flame a.a.s. technique [2] is more suitable. Figure 3 illustrates a typical recorder tracing of a mixture of the five tetraalkyllead compounds.

Solvents such as chloroform, carbon tetrachloride, hexane and benzene gave absorption signals because of their non-specific absorption at the lead resonance line. Although these solvent peaks generally emerged well before the lead compounds, the use of the background corrector is recommended to eliminate these potential interferences.

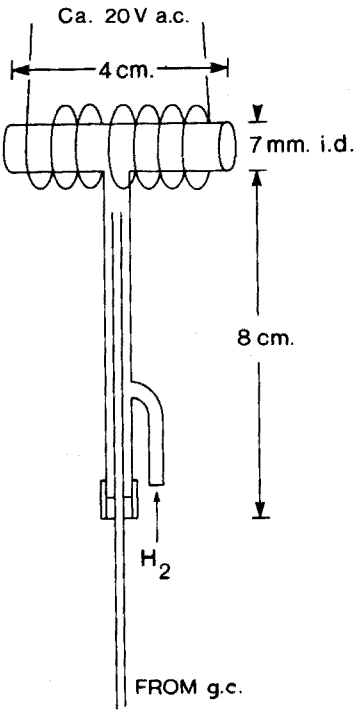

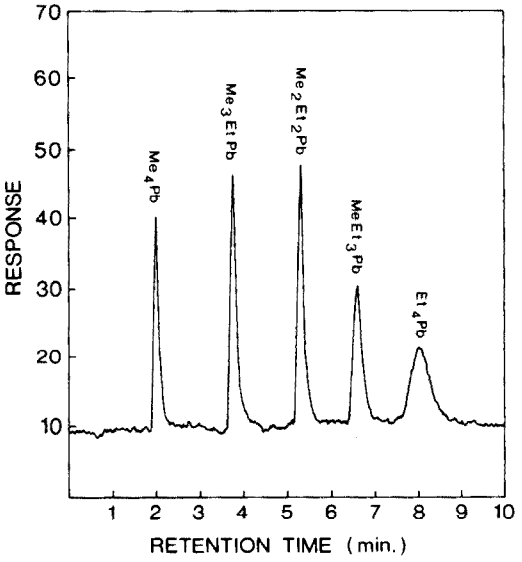

Fig. 2. Silica furnace.

Fig. 3. Recorder tracings for a mixture of five tetraalkyllead compounds. Each peak represents ca. 5 ng of the compound expressed as lead.

REFERENCES

1 D. A. Segar, Anal. Lett., 7 (1974) 89.
2 Y. K. Chau, P. T. S. Wong and H. Saitoh, J. Chromatogr. Sci., 14 (1976) 162.
3 Y. K. Chau, P. T. S. Wong and P. D. Goulden, Anal. Chem., 47 (1975) 2279.

Analytica Chimica Acta, 85 (1976) 425—428

Book Reviews

Joseph I. Goldstein and Harvey Yakowitz (Eds.), *Practical Scanning Electron Microscopy*, Plenum Press, New York, 1975, xviii + 582 pp., price $59.40.

The multiple author approach to compiling works of reference is fraught with hazards. If the end result is to exhibit the consistency of approach and clarity of presentation achievable in a single author text, the burden falling upon the editors is indeed a heavy one. Signs that they have faltered under this load are readily detected. Topics which might logically be expected to have a chapter to themselves, appear fragmented among different chapters prepared by the separate authors. Contradictory opinions or emphases are expressed in different parts of the book, which only help to confuse those new to the field.

At the price (£27) this book cannot be recommended to the individual as a source of information on scanning electron microscopy in which the important aspects are logically presented and easy of access. Like the curate's egg, it is very good in parts, the chapters on image formation and contrast mechanisms being particularly useful. The book has a sub-title, however, "Electron and Ion Microprobe Analysis", and chapters are included on these techniques, which in general, are not as well treated as the scanning electron microscopy; the book might have been better value for money without them.

Comment is made in the Introduction on the 23 years that elapsed between the first published description of a scanning electron microscope by Zworykin, Hillier and Snyder and the first successful commercial instrument. This is not contrasted, however, with the brief incubation period of the scanning electron probe microanalyser which, from the first description by Cosslett and Duncumb, took only 5 years to become available commercially.

As a general rule, work in this field carried out outside the USA is not well represented. There are also minor irritations. Comparisons between energy-dispersive and wavelength-dispersive spectra are, for example, made more difficult for the reader by printing one spectrum back to front with respect to the other. Errors also occur in the indexing.

Altogether, this is not the most efficient text for up-dating oneself in this field, but full of helpful information for those that are prepared to mine for it.

D. A. Melford

Roland S. Young, *Chemical Phase Analysis*, Charles Griffin, London, 1974, vii + 138 pp., price £4.50.

Chemical phase analysis, sometimes referred to as speciation, is essentially the determination of each of several phases, compounds or species containing

a common element (H_2S, SO_2 and SO_3, in gases for example). Although such analyses are commonplace in organic chemistry, and are not considered worthy of separate comment, their appreciation in inorganic analyses has largely been restricted to metallurgical and geological analysis. This small but delightfully informative book presents, for the first time, an account of chemical phase analysis for a wide range of samples, arranged by element. Most of the methods emanate from the analysis of metals, slags, ores, flue gases and deposits, but the chemistry involved is of much wider implication. Adequate experimental details are widely incorporated in the text, and each section is fully referenced. Subject and author indexes are included. This book will be valuable to all who are awakening to the value of chemical phase analysis.

A. Townshend

K. Bauer and C. Haller in, *Organometallic Compounds: Methods of Synthesis, Physical Constants and Chemical Reactions, Vol. 1, Compounds of the Transition Metals*, 2nd edn., *First Supplement*, M. Dub (Series Ed.), Springer-Verlag, Berlin, 1975, xxvi + 1171 pp., price DM 114.70 (U.S. $49.40).

The explosive growth of organometallic chemistry is nowhere better illustrated than in this compendium which covers methods of synthesis, physical constants and chemical reactions of transition metal compounds for the period 1965—1968. Over 2,500 references are cited, together with nearly 200 review publications and monographs which are listed separately. As with previous volumes in this series, its use is enhanced by the inclusion of references to commercial applications and to physiological data.

The contents are arranged as in previous volumes. The work is splendidly produced and will be a valuable addition to the literature.

E. J. Forbes

K. Müller, *Functional Group Determination of Olefinic and Acetylenic Unsaturation*, (Analysis of Organic Materials, Vol. 6), Academic Press, London, 1975, xii + 334 pp., Price £9.20.

The use of olefinic and acetylenic compounds in industry is widespread. In the plastics field, polymerizable monomers such as vinyl compounds and butadiene are used in large quantities, and methods for the determination of the purity of the monomers and the monomeric content of polymers usually depend on the determination of the double bond content of the material. Conversion of acetylene to acetylene alcohols, which serve as the intermediates for a wide range of compounds, and the determination of the crude products or small amounts of acetylene derivatives in other materials, are obviously of

importance. The book is divided into 2 parts, one dealing with the determination of double bonds and the other with triple bonds.

Although the book is entitled "Functional Group Determination", the first two chapters deal with identification of double bonds, and separation of compounds containing double bonds. At first this may seem to be a contradiction, but the inclusion of these chapters is of undoubted benefit. The equivalent section dealing with triple bonds is equally relevant.

There is extensive coverage of the methods available for functional group determination, and the details given are generally sufficient for access to the original research papers to be unnecessary. This is very useful, but adequate reference to original work is always made.

This is a worthwhile book, the value of which has been enhanced by the excellent translation by Professor Ashworth. For the many analytical chemists who have frequent need to analyse compounds containing these functional groups, this will be a good handbook; for those who have only occasional need, this book should be a standard reference.

L. S. Bark

N. K. Mathur and C. N. Narang, *Determination of Organic Compounds with N-Bromosuccinimide and Allied Reagents*, (Analysis of Organic Materials, Vol. 8) Academic Press, London, 1975, ix + 166 pp., price £5.20.

The use of positive bromine-containing compounds, such as N-bromosuccinimide, as synthetic reagents in organic chemistry, is widespread. The selectivity of these reagents, and the variety of experimental conditions under which addition, oxidation and substitution reactions can be made to occur, make the reagents of prime importance to the synthetic chemist. The high yields of the products obtained in the reactions, and the relative ease with which excess of the reagent may be determined, endow the reagents with analytical usefulness.

Although N-bromosuccinimide is by far the best known of the N-haloamides and N-haloimides, other related compounds possess desirable properties, and are occasionally more useful than N-bromosuccinimide. The authors have rightly recognised this, and have devoted an excellent chapter to the preparation and properties of these amides and imides, and to their applications; this should serve as a useful guide in critical investigations of reactions with positive bromine compounds, with their particular systems.

There is a good catalogue of the reactions and methods used for the determination of various classes of compounds, based essentially on functional group determinations. The six chapters devoted to these methods are well presented, and make the book a useful laboratory aid. The chapters dealing with structure and the determination of miscellaneous compounds

are perhaps somewhat sparse, but even here, sufficient detail or references to the original work are given.

Physically the book is well presented, and is well priced for the material it contains.

L. S. Bark

A. Zlatkis (Ed.), *Advances in Chromatography, 1975*, Elsevier, Amsterdam, 1975, xvi + 736 pp., price DFl. 180.00; U.S. $74.95.

This special volume, reprinted from Volume 112 of the Journal of Chromatography, contains the texts of the 61 papers presented at the Tenth International Symposium on Advances in Chromatography, held at Munich on November 3—6, 1975. Like the 1974 volume, this volume has appeared with admirable speed; perhaps the only adverse criticism is that the price, inexorably, has increased by about 10% for slightly fewer pages.

The volume opens with a splendid review, by L. S. Ettre, of "The Development of Chromatography"; this is a most readable account of the outstanding developments over the past 20 years, and gives a lot of critical comment and insight, together with personal details of many of those most closely involved. For students — and for those not sufficiently interested to have followed these developments at the time — this review should make fascinating reading.

The main text is subdivided into the same headings that were used in the 1974 volume: New Horizons (6 papers); Chromatographic Columns and Stationary Phases (8 papers); Theoretical and Practical Aspects of Chromatography (23 papers); Biomedical Applications (20 papers); and Environmental Applications (3 papers). Are these headings to continue unchanged for yet another year, and do the relative numbers of papers in the different sections bear any real relationship to the actual utilization of chromatography today? For there to be no apparent applications other than in the biomedical and environmental areas is ludicrous, although it is conceivable that workers in these areas are advantageously placed at present in obtaining financial support to attend meetings in expensive conference centres. There is therefore scope for change here.

D. M. W. Anderson

ANALYTICA CHIMICA ACTA, VOL. 85 (1976)

AUTHOR INDEX

ANALYTICA CHIMICA ACTA, VOL. 85 (1976)

SUBJECT INDEX

Detectors in Gas Chromatography

by JIŘÍ ŠEVČÍK, *Department of Analytical Chemistry, Charles University, Prague.*

JOURNAL OF CHROMATOGRAPHY LIBRARY, Vol. 4

1976. 192 pages. US $23.95/Dfl. 60.00. ISBN 0-444-99857-8

This publication is devoted to the function and optimal working conditions of gas chromatographic detectors. The first systematic treatment of gas chromatographic detection techniques, it devotes special attention to so-called specific detectors and working conditions which strongly influence results (e.g. gas flow, effect of additives in gases, working temperature, detector form and dimensions). Anomalous detector responses are explained and the form and size of a response under various working conditions are indicated. The problems presented are illustrated by experimental data which are summarized in numerous tables and figures. The book should be of interest to all who use gas chromatography in research and who would like to explore the possibilities and working conditions of different detector systems.

ELSEVIER SCIENTIFIC PUBLISHING COMPANY

P.O. Box 211, Amsterdam, The Netherlands

Distributed in the U.S.A. and Canada by:
AMERICAN ELSEVIER PUBLISHING COMPANY, INC.,
52 Vanderbilt Ave., New York, N.Y. 10017

The Dutch guilder price is definitive. US $ prices are subject to exchange rate fluctuations.

Advances in Chromatography 1975

Proceedings of the Tenth International Symposium, held in Munich, November 3-6, 1975

Special volume: Reprinted from the Journal of Chromatography, Vol. 112
edited by **A. ZLATKIS.**

associate editors: E. BAYER, L.S. ETTRE and I. HALÁSZ.

1975. 752 pages. US $74.95/Dfl. 180.00. ISBN 0-444-41382-0.

This volume represents the proceedings of the Tenth International Symposium on the Advances in Chromatography. All aspects of chromatography are covered by the 61 papers presented by scientists from 15 different countries. The increased importance of combined techniques such as GC-MS is evidenced by more than a dozen papers describing various advanced systems and their application in biochemical-clinical and environmental analysis. Following the renaissance of liquid column chromatography, a similar upsurge is appearing in thin-layer chromatography. The papers on further advances in selective detectors, high-performance open tubular colomns and special techniques such as head-space analysis demonstrate the still-continuing development of gas chromatography.

CONTENTS: **Foreword** (A. Zlatkis). **Winners of the M.S. Tswett Chromatography Medal. The development of gas chromatography** (L.S. Ettre). **New Horizons.** *Main Contributors:* I. Halász, J.E. Lovelock, C.S.G. Phillips, V. Pretorius, J.H. Purnell and J. Ripphahn. **Chromatographic columns and stationary phases.** *Main Contributors:* J. Garaj, E. Gil-Av, E. Grushka, J.K. Haken, H. kelker, J.H. Knox, R.D. Schwartz and A. Zlatkis. **Theoretical and practical aspects of chromatography.** *Main Contributors:* W.A. Aue, V.G. Berezkin, W. Bruening, S.P. Cram, S.N. Deming, H. Engelhardt, D.C. Fenimore, G. Guiochon, J.F.K. Huber, B.V. Ioffe, R.E. Kaiser, J.J. Kirkland, B. Kolb, E. Küllik, J.N. Little, C. Merritt Jr., J. Novák, B.A. Rudenko, G. Schomburg, R.P.W. Scott and A. Zlatkis. **Biomedical applications of chromatography.** *Main Contributors:* C.J.W. Brooks, P.R. Brown, H.Ch. Curtius, A. Frigerio, E. Grushka, E.C. Horning, M.G. Horning, E. Jellum, A. Karmen, H.M. Liebich, B.F. Maume, C.W. Moss, M. Novontny, C.D. Pfaffenberger, K. Tsuji, W.J.A. Van den Heuvel, W. Voelter and A. Zlatkis. **Environmental applications of chromatography.** *Main Contributors:* W. Bertsch, J.L. Monkman and W.D. Ross.

Advances in Chromatography 1974

Proceedings of the Ninth International Symposium held in Houston, Texas, November 4-7, 1974.
Special volume: Reprinted from the Journal of Chromatography, Vol. 99.

edited by **A. ZLATKIS,** and **L.S. ETTRE.**

1974. 789 pages. US $66.75/Dfl. 160.00. ISBN 0-444-41267-0

ELSEVIER SCIENTIFIC PUBLISHING COMPANY
P.O. Box 211, Amsterdam, The Netherlands

Distributed in the U.S.A. and Canada by:
AMERICAN ELSEVIER PUBLISHING COMPANY
52 Vanderbilt Ave., New York, N.Y. 10017, U.S.A.

The Dutch guilder price is definitive. US $ prices are subject to exchange rate fluctuations.

(continued from page 4 of cover)

Short Communications

Printed in The Netherlands

VOL. 85 NO. 2 ANALYTICA CHIMICA ACTA SEPTEMBER 1976

CONTENTS

(continued on inside page of the cover)